PROFILING THE EARLY MOLECULAR RESPONSE OF THE HUMAN BRONCHIAL EPITHELIUM TO *ASPERGILLUS FUMIGATUS* USING A MULTI-OMICS APPROACH

by

AMREEN TOOR

B.Sc., Western Washington University, December 2014

A THESIS SUBMITTED IN PARTIAL FULFILLMENT OF
THE REQUIREMENTS FOR THE DEGREE OF

MASTER OF SCIENCE

in

THE FACULTY OF GRADUATE AND POSTDOCTORAL STUDIES

(Experimental Medicine)

THE UNIVERSITY OF BRITISH COLUMBIA

(Vancouver)

August 2018

The following individuals certify that they have read, and recommend to the Faculty of Graduate and Postdoctoral Studies for acceptance, a thesis/dissertation entitled:

Profiling the early molecular response of the human bronchial epithelium to *Aspergillus fumigatus* using a multi-omics approach

submitted by Amreen Toor in partial fulfillment of the requirements for the degree of Master of Science

in Experimental Medicine

Examining Committee:

Dr. Scott Tebbutt
Supervisor

Dr. Margo Moore
Supervisory Committee Member

Dr. Delbert Dorscheid
Supervisory Committee Member

Dr. Pascal Lavoie
Additional Examiner

Additional Supervisory Committee Members:

Supervisory Committee Member

Supervisory Committee Member

Abstract

Aspergillus fumigatus (A. fumigatus) is an opportunistic fungal pathogen that is widely distributed in nature through the release of conidiospores (conidia). Upon inhalation, fungal conidia (2-3 μm) are capable of reaching the bronchial and alveolar epithelia. This interaction between conidia and airway epithelial cells may result in the development of allergic, chronic or invasive aspergillosis in susceptible hosts. Characterization of the early molecular response of host using a multi-OMICs molecular approach is an important first step for better understanding the host-pathogen interaction.

The aim of my research was to investigate the early molecular response of host upon interaction with *A. fumigatus* using an *in-vitro* model that closely recapitulates the *in-vivo* bronchial epithelium, and assess the applicability of this model to study host-pathogen interactions. A multi-OMICs approach utilizing NanoString and shotgun proteomics was applied to primary human bronchial epithelial cells (HBECs) grown for 21-28 days as differentiated air-liquid interface (ALI) cultures. Comparative analyses were conducted to compare the gene expression profiles of ALI cultures to submerged monolayer cultures of human airway epithelial cell line (1HAEo-) upon conidial exposure. In addition, transcriptional profiles of ALI cultures upon exposure to wild-type (WT) conidia of *A. fumigatus* were compared to Kdnase mutant strain (Δ*kdnase*) of *A. fumigatus* and to Respiratory Syncytial Virus (RSV).

Unlike submerged monolayer cultures, ALI cultures of primary HBECs internalized less than 1% of bound conidia 6 hours post-exposure. Transcriptomic and proteomic analyses of primary HBECs in ALI revealed that exposure to the fungus enriched the expression of genes related to cell cycle regulation, apoptosis/autophagy, iron homeostasis, calcium metabolism,

complement and coagulation cascades, endoplasmic stress and the unfolded protein response. Comparative analyses to submerged monolayer cultures of 1HAEs indicated that the host molecular response in each model is different. The immune response in differentiated ALI cultures upon exposure to Δ*kdnase A. fumigatus* conidia and RSV was pathogen-specific. Hence, ALI cultures of primary HBECs can provide novel insights into the mechanisms involved in the early molecular response associated with this opportunistic fungal pathogen.

Lay Summary

Humans inhale more than one hundred conidiospores (spores) of the fungus *Aspergillus fumigatus (A. fumigatus)* every day. In healthy individuals, these are effectively cleared from the lung; however, in some individuals with immune defects, exposure of airway cells to these spores can result in a variety of diseases. The aim of this study was to better understand the early molecular response of airway cells when they are exposed to *A. fumigatus* spores. We used a cell culture model that closely mimics the structure of the cells in the airway and assessed the molecular response of these cells by measuring changes in RNA and protein expression after adding fungal spores. To evaluate the model, the molecular response was compared to a different cell-culture model, and RNA expression in the presence of *A. fumigatus* spores was compared to that of other pathogens. Genes and pathways were identified using this cell culture model.

Preface

Chapter 3 and 4 contain material that is currently under preparation for submission. Luka Culibrk assisted in the ALIs experiment #1 (Chapter 3) and 1HAEs experiment (Chapter 4). Fresh conidia for these experiments was provided by Alison Hadwin in Dr. Margo Moore's laboratory. Dimethyl labeling for shotgun proteomics experiments was performed by Dr. Leonard Foster's group. Cells cultures of ALIs and 1HAEs for all experiments were provided by Dr. Gurpreet Singhera in Dr. Del Dorscheid's laboratory. I conducted all the other experiments and did the corresponding data analyses.

Table of Contents

List of Tables

List of Figures

Acknowledgments

I would like to thank my supervisor and mentor Dr. Scott Tebbutt for supporting and guiding me throughout my graduate studies. He has provided me with enormous opportunities to learn and grow, and his valuable feedback has been very essential in all aspects of my project. I have enjoyed working on this project under his supervision. Thanks for always being so generous of your time and knowledge.

I would like to thank my committee members, Dr. Margo Moore and Dr. Del Dorscheid for the support, guidance and feedback. They have gone far beyond the role of committee members and been available for feedback at all times. Thanks for supervising me on experiment protocols, conference abstracts and manuscripts; you were always only an email away.

Thanks to all the Tebbutt lab graduate and Co-op students who I have had the pleasure of working with over the last two years. Thanks to Dr. Amrit Singh, Dr. YoungWoong Kim, Yolanda Yang and Daniel He for all the valuable feedback and advice. I am very grateful for all the support, guidance and memories. Thanks to Luka Culibrk and Karen Tam for assisting me on this project.

Thanks to all the Moore and Dorscheid lab members. Specially, thanks to Alison Hadwin and Dr. Gurpreet Singhera for their valuable support and guidance in the lab at all times. Thanks for being there for everything, Gurpreet.

I want to acknowledge everyone at the Centre for Heart Lung Innovation. Thanks to Anna Siedlecki, Daniela Castillo-Saldana, Basak Sahin, Jasmine Yang, Beth Whalen, Amrit Samra, Dean English, Aaron Barlow and Ivan Leversage for their continued support and guidance.

TO MY PARENTS

for raising me to believe that with hard work and perseverance anything is possible. Thanks, Mom and Dad.

TO MY BROTHERS

for inspiring me to become stronger, more resilient and chase those gains every day. Thanks, Daman and Kanwar.

&

TO ALL THE AMBITIOUS WOMEN

For always supporting, inspiring and feeding me. Thanks, Nani, Bibi, Pua, Kamal Massi, Raji Massi, Deepa Massi, Ginder Massi and Devin.

Chapter 1 Introduction

1.1 *Aspergillus fumigatus*

Aspergillus fumigatus (*A. fumigatus*) is a filamentous, saprotrophic, ubiquitous fungal pathogen. It plays an important role in recycling environmental carbon and nitrogen, and is widely distributed in nature through the release of asexually produced conidia, also known as conidiospores (Latgé 1999). These fungal conidia are 2-3 μm in size and are typically grey-green in color and echinulate (Figure 1.1). They can disseminate in high concentrations in the atmosphere by air currents, and exist in the air both indoors and outdoors (1-100 conidia m^{-3}) (Latgé 1999, 2001).

The genus *Aspergillus* consists of >250 different species. The defining characteristic of these species is a spore-bearing structure in the asexual reproductive cycle that resembles an aspergillum, a device used in the Roman Catholic Church to sprinkle holy water (Figure 1.1). These saprotrophic species belong to the phylum Ascomycota and some species are used for industrial processes to produce enzymes, food products and commodity chemicals (Bennett 2010). The sexual reproduction cycle was recently characterized in *A. fumigatus* and results in the production of cleistothecia containing ascospores (Figure 1.2) (O'Gorman, Fuller, & Dyer, 2009) . Parasexual reproduction is also recognized in *A. fumigatus*, and involves nuclear fusion of genetically different, but compatible hyphae (Figure 1.2) (Verweij et al. 2016; Pontecorvo 1956).

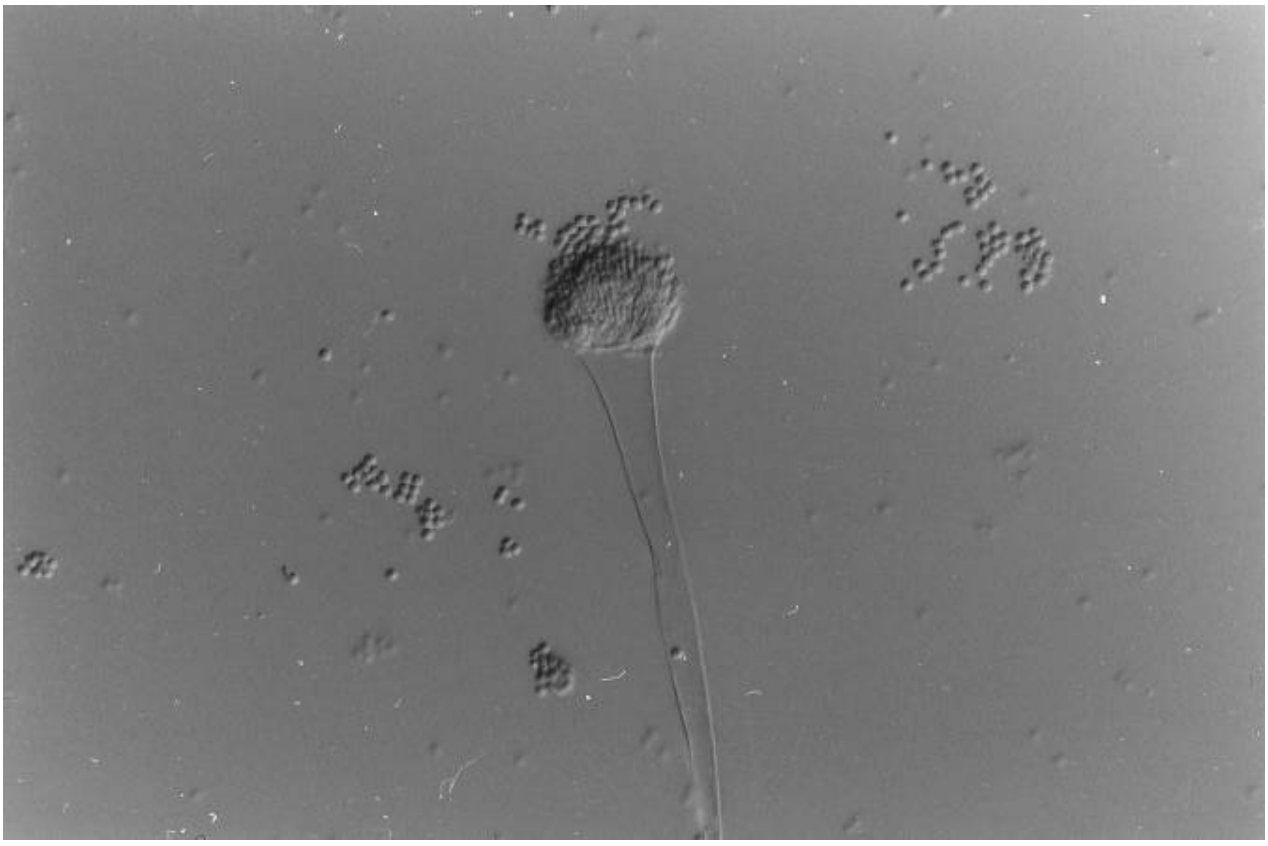

Figure 1.1 Sporulating structure of *A. fumigatus* in asexual reproduction.
Light microscopy of *A. fumigatus* spore-bearing structure, called a conidiophore. (Figure adapted from Latgé, 1999)

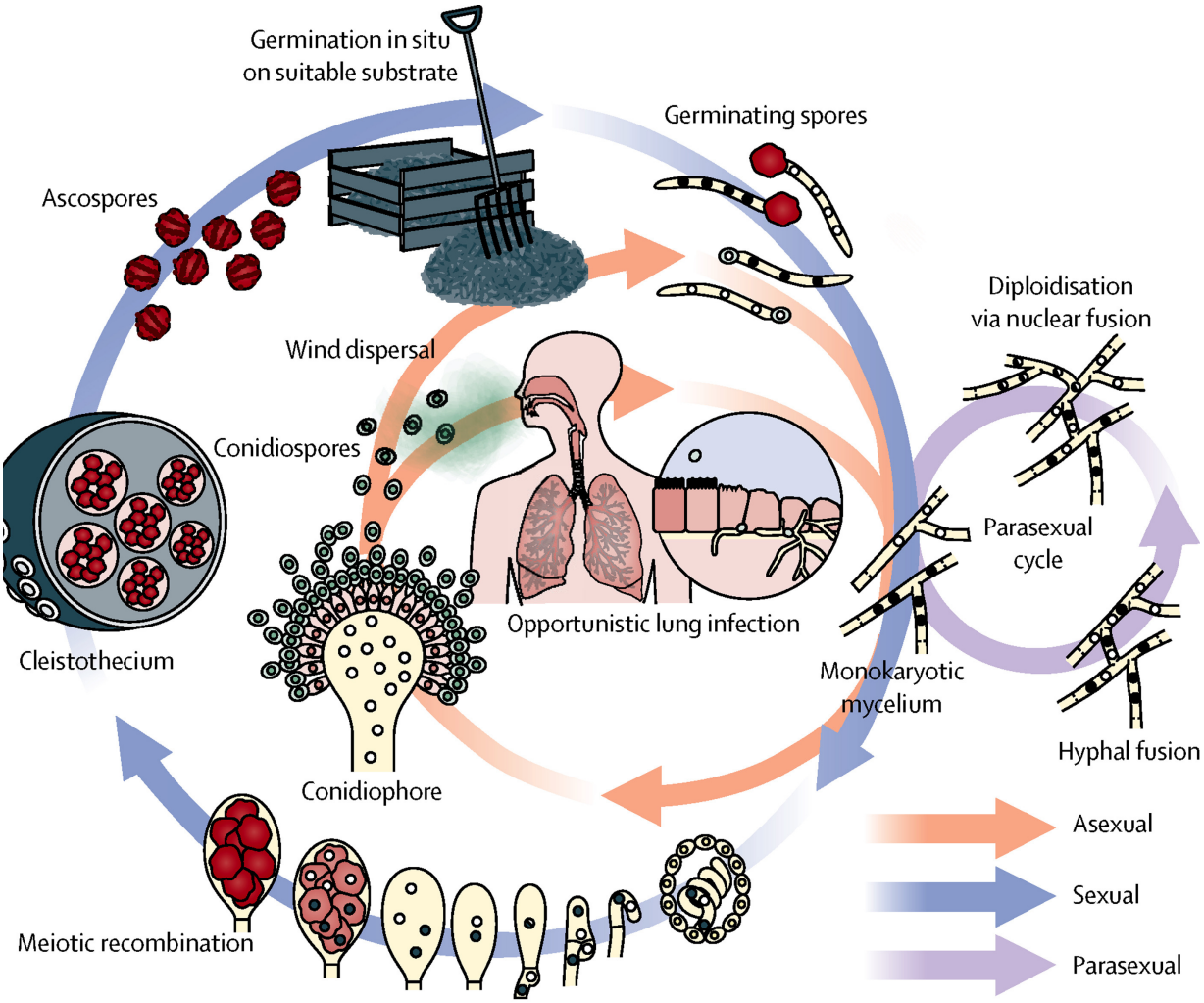

Figure 1.2 Three processes of reproduction are recognized in *A. fumigatus*.
A. fumigatus reproduces by asexual (orange), sexual (blue) and parasexual (purple) reproduction. (Figure adapted from Verweij et al. 2016)

Most humans inhale several hundred conidia every day. Inhalation of these airborne conidia in immunocompromised individuals or those with certain risk factors can result in a range of illnesses, collectively known as aspergillosis. *A. fumigatus* is also a major respiratory pathogen in birds (Arné et al. 2011). In addition to *A. fumigatus*, there are other *Aspergillus* species that are opportunistic pathogens as well, such as *A. nidulans, A. niger, A. terrus* and *A. flavus* (Latgé 1999).

1.1.2 Virulence factors of *A. fumigatus*

The virulence of *A. fumigatus* is multifactorial and has been challenging to elucidate. Upon reaching the host environment, the fungus is presented with different conditions than its normal niche in decaying organic matter. The structural features of conidia that allow it to survive inside the host as well as fungal proteins that promote conidial growth in the lung comprise the virulence of *A. fumigatus.* In addition, both the immune status of the host and the biological characteristics of the fungus contribute to the virulence of *A. fumigatus* (Latgé 2001; Sales-Campos et al. 2013).

Despite being technically challenging, mostly single-gene deletion studies have been conducted to study the virulence of *A. fumigatus* so far. For example, loss-of-function mutants have been difficult to generate. This is because genes contributing to virulence of the fungus are also important for its growth and in some cases, *A. fumigatus* can compensate for a loss of specific gene through a different pathway due to redundancy in number of its pathways (Croft et al. 2016). Some features that contribute to growth under specific conditions have been identified and include nutrient uptake, thermotolerance, secreted toxins and proteases, and features of the conidial surface. These features have been the focus of several studies conducted over the past decades (Sales-Campos et al. 2013; Latgé 2001; Rhodes 2006).

Within the host environment, *A. fumigatus* is presented with various stress conditions during the course of infection. In particular, it must be able to adapt to the host-derived sources of nutrients; e.g., *A. fumigatus* has shown to acquire amino acids from the host by secreting proteases (Sales-Campos et al. 2013). Ferric iron is another essential nutrient for cellular processes and virulence in *Aspergillus* species as it plays an important role in the redox

reactions of both the host cell and the fungus (Canessa and Larrondo 2013). However, excess iron can cause harm via the formation of reactive oxygen species (ROS) and result in oxidative stress. Since the host environment restricts availability of free iron by producing iron-binding proteins, such as transferrin and lactoferrin, the ability to obtain iron from host is important for the survival of *A. fumigatus* (Parrow, Fleming, and Minnick 2013). Specifically, *A. fumigatus* acquires iron through high affinity uptake, either by reductive iron assimilation or siderophore biosynthesis (Schrettl et al. 2004; Moore 2013). In reductive iron assimilation, a plasma membrane bound reductase reduces ferric iron into a more soluble ferrous form. However, genetic disruption of reductive iron assimilation did not affect *A. fumigatus* virulence (Schrettl et al. 2004). *A. fumigatus* also secretes iron-chelating siderophores, such as fusarinine C, triacetylfusarinine C, and produces intracellular siderophores such as ferricrocin and hydroxyferricrocin (Brown and Goldman 2016). *A. fumigatus* was avirulent in a mouse model of invasive aspergillosis when siderophore biosynthesis was abolished by gene deletion (Schrettl et al. 2004; Hissen et al. 2005). Hence, adaptation to iron limitation by siderophore production is essential for *A. fumigatus* virulence and can be considered as a true virulence factor of the fungus.

A. fumigatus is also more thermotolerant than any other *Aspergillus* species. It can efficiently grow between 37 °C and 50 °C, allowing it to survive within mammalian lung at temperatures 37 °C or above (Rhodes 2006; Bhabhra and Askew 2005). Stresses such as elevated temperatures within the host have been shown to increase the production of Heat shock protein 90 (Hsp90) by *A. fumigatus*. Hsp90 is an essential ATP-dependent molecular chaperone involved in protein folding, transport, maturation and degradation (Cowen and

Lindquist 2005). Repression of Hsp90 resulted in decreased spore viability and hyphal growth as well as major defects in germination and conidiation *in-vitro*; it plays an important role in cell wall integrity as inhibition of Hsp90 increased susceptibility to heat stress and caspofungin (Lamoth et al. 2012; Lamoth, Juvvadi, and Steinbach 2016). Hence, the ability of *A. fumigatus* to survive in elevated temperatures is important for its growth *in-vitro*.

A. fumigatus produces a number of toxic secondary metabolites, proteases and other fungal products that contribute to its virulence. Toxic secondary metabolites include gliotoxin, trypacidin and verruculogen (Frisvad et al. 2009). Gliotoxin has been shown to slow ciliary beat frequency and damage human respiratory epithelium *in-vitro*; damage to the mechanical barrier respiratory epithelium can allow *A. fumigatus* to establish in the airways (Amitani et al. 1995). In addition, gliotoxin has immunosuppressive activity *in-vivo*, indicating that these metabolites may result in immunosuppression in the host (Sutton et al. 1994; Tomee and Kauffman 2000). *A. fumigatu*s also produces proteases which have been shown to cause cell detachment and induce expression of pro-inflammatory cytokines in airway epithelial cells *in-vitro*. Production of pro-inflammatory cytokines may cause local inflammation, which combined with desquamation of cells, can allow fungal attachment and penetration (Tomee et al. 1997). For example, fungal serine proteases (Alp) induced expression of Interleukin-8, resulted in neutrophil recruitment and inflammation (Chotirmall et al. 2014) .

The conidial surface also possesses features that may contribute to the virulence of *A. fumigatus.* Conidia contain a gray-green pigment, 1, 8-Dihydroxynaphthalene (DHN)-melanin, which functions to protect the conidia from ultraviolet light, enzymatic lysis and oxidation. It also protects *A. fumigatus* from phagocytosis as phagocytes have been shown to internalize

non-melanized conidia in greater numbers than melanized conidia (Thywißen et al. 2011; Volling et al. 2011). The outer layer of the conidial cell wall is called the rodlet layer that is composed of hydrophobin proteins such as RodA. The rodlet layer can prevent conidial detection by masking pathogen-associated molecular patterns (PAMPs) such as β-1,3-glucan and α-mannose on the cell wall (Lee and Sheppard 2016). RodA is covalently bound to the conidial cell wall through glycosylphosphatidylinositol-remnants. The presence of this hydrophobin layer prevents recognition of dormant fungal conidia by the host immune system and consequently, prevents an inflammatory response. Upon conidial swelling and germination, the rodlet layer is rapidly shed, resulting in exposure of the underlying cell-wall PAMPs (Aimanianda et al. 2009).

Sialic acids have been detected on the surface of conidia (Julie A. Wasylnka and Moore 2000). They are a family of more than 50 substituted derivatives of a nine-carbon monosaccharide (neuraminic acid) that have been shown to play important roles in bacterial and viral pathogenesis (Varki and Schauer 2009). In *A. fumigatus*, adhesion to the extracellular matrix components in the host such as fibronectin, a component of basal lamina, is mediated by negatively-charged carbohydrates (Julie A. Wasylnka and Moore 2002). *A. fumigatus* conidia have sialic acids on their surface, and pathogenic *Aspergillus* species had greater amounts of sialic acids than non-pathogenic species (J. A. Wasylnka, Simmer, and Moore 2001). In cultured macrophages and type II pneumocytes, removal of sialic acid residues decreased binding of conidia to fibronectin as well as phagocytosis of conidia by cultured murine macrophages (Julie A. Wasylnka and Moore 2003; Warwas et al. 2007). There are two naturally occurring sialic acids, *N*-acetylneuraminic acid (Neu5Ac) and 2-keto-3-deoxy-D-*glycero*-D-*galacto*-nononic acid

(Kdn), with substitution at carbon 5 with an *N*-acetyl or an -OH group, respectively (Varki and Schauer 2009). These sialic acids can be released from the glycans on the cell wall by glycoside hydrolase enzymes, called sialidases. An *exo*-sialidase that prefers Kdn as a substrate (hence, it is a Kdnase) was recently identified in *A. fumigatus* (Telford et al. 2011) .The *A. fumigatus* Kdnase was shown to be important for fungal cell wall integrity and to contribute to virulence in the mouse model of invasive aspergillosis (Nesbitt et al. 2018).

1.1.3 Cell wall of *A. fumigatus*

The cell wall of *A. fumigatus* mediates contact with the host and acts as a protective barrier important for survival (Chotirmall et al. 2014). In addition, the dynamic and versatile structure of the cell wall plays an important role in fungal growth and protects the fungus against environmental stresses. The composition of the wall varies during different stages of fungal life cycle and in response to different growth conditions (Latgé, Beauvais, and Chamilos 2017).

In conidia, the wall consists of two layers composed of various polysaccharides: the inner cell wall (alkali-insoluble) contains 38% β-1,3-glucan, 26% galactomannan and 5.6% chitin/chitosan. These polymers provide structure and rigidity to the cell wall. The outer cell wall (alkali-soluble) consists of 14% α-1,3-glucans, 13% galactomannan, 5% β-1,3-glucan, and 0.5% chitin/chitosan. These polysaccharides are non-covalently attached and form a looser network of macromolecules. In contrast, the alkali-insoluble cell wall of hyphae (the fungal filaments) contains 30% β-1,3-glucans, 17% chitin/chitosan, 5% galactomannan, 4% galactosaminogalactan (GAG) and β-1,3;1,4-glucans. The alkali-soluble outer cell wall contains 42% α-1,3-glucans, 2.3% GAG, 1.4% galactomannan. Unlike conidia, hyphae produce an

extracellular matrix (ECM), composed of GAG (Mouyna and Fontaine 2009). Secretion of GAG has immunosuppressive properties as it can induce apoptosis in neutrophils (Robinet et al. 2014). The absence of GAG from the host makes them potential targets for novel anti-fungal treatments (Lee and Sheppard 2016).

1.1.4 Human diseases caused by *A. fumigatus*

A. fumigatus can cause a range of diseases, referred to as aspergillosis. The symptoms and clinical outcomes depend on the immune status of the host, and three forms of the disease are recognized: allergic, chronic and invasive aspergillosis.

The most common form of allergic aspergillosis is known as allergic bronchopulmonary aspergillosis (ABPA). ABPA is characterized by a severe allergic reaction which is triggered due to the secretion of toxins and allergens from prolonged fungal exposure (Margalit and Kavanagh 2015; Dewi, van de Veerdonk, and Gresnigt 2017). ABPA individuals usually have defects in their airway mucosal defenses; specifically, impaired mucociliary clearance and epithelial cell function. It is estimated that ABPA occurs in 1-2% of asthmatic subjects and 7-9% cystic fibrosis patients (Knutsen and Slavin 2011). Genetic predisposition to developing ABPA also exists (Tracy et al. 2016). The global burden of patients with ABPA is estimated to exceed 4.8 million patients (Soubani and Chandrasekar 2002). ABPA is likely to be under-diagnosed; e.g., in developing countries, it has been reported that ~ 1/3 of patients with ABPA are misdiagnosed as having pulmonary tuberculosis (Agarwal et al. 2013).

In cystic fibrosis patients, impaired mucociliary clearance along with immune dysfunction promotes fungal establishment and hinders clearance (Balloy and Chignard 2009). Bronchoalveolar lavage (BAL) of ABPA patients have shown the presence of eosinophils,

neutrophils, lymphocytes and often fungal hyphae as well (Agarwal et al. 2013; Wark and Gibson 2001). In addition, *A. fumigatus* antigens can elicit a polyclonal antibody response, resulting in elevated total IgE and *A. fumigatus* -specific IgE and IgG antibodies. The immune response of patients with ABPA is generally associated with immune deviation towards a hyperactive T_H2 response and is characterized by the production of IL-4, IL-5, IL-13 and IL-10 (Moss 2005; Agarwal et al. 2013). These cytokines also drive differentiation of B cells to secrete IgE antibodies specific to *A. fumigatus* and activation of eosinophils (by IL-5). The T_H2 inflammatory response from continuous airway sensitization activates mast cell degranulation and results in airway mucus production, hyper-responsiveness, inflammation and bronchiectasis, symptoms that characterize ABPA. Increased mucus production in the airways can result in biofilm formation, which can assist in fungal growth (Dewi, van de Veerdonk, and Gresnigt 2017). The symptoms of ABPA patients are a consequence of the immune response to *A. fumigatus* and include wheezing, productive cough, low-grade fever, hemoptysis, malaise, weight loss as well as worsening of asthma or CF. Diagnostic tests include *Aspergillus* skin test to check for the presence of IgE antibodies specific to *A. fumigatus*, total serum IgE levels, serum IgE and IgG antibodies specific to *A. fumigatus*, peripheral eosinophilia, sputum cultures, pulmonary function tests and radiological investigations (Agarwal et al. 2013). Following diagnosis, corticosteroids are used to suppress the inflammatory pathways to further prevent lung damage with corticosteroids, and antifungal agents are given to eradicate fungi from the airways (Soubani and Chandrasekar 2002).

In patients with pre-existing lung cavities formed due to tuberculosis, sarcoidosis, chronic obstructive pulmonary disease or other cavitary lung diseases, exposure to *A. fumigatus*

can cause chronic pulmonary aspergillosis (CPA) (Kawamura et al. 2000; Soubani and Chandrasekar 2002). CPA may be associated with an aspergilloma (fungal ball) that forms as a non-invasive fungal growth within the lung cavity. The majority of CPA patients are asymptomatic or experience mild hemoptysis. Severe hemoptysis may occur due to local invasion or mechanical damage of blood vessels lining the cavity from toxins released by the fungus (Soubani and Chandrasekar 2002). More severe symptoms associated with the underlying chronic lung disease include weight loss, profound fatigue, chronic productive cough and shortness of breath (Denning et al. 2003). After diagnosis, disease progression is observed in most patients; however, the fungal mass may also be surgically removed in patients who have more significant hemoptysis (Schweer et al. 2014). Various antifungal agents, such as azoles, have also been used for treating CPA patients; however, there is no consistent evidence that aspergilloma responds to antifungal drugs (Schweer et al. 2014).

The most severe form of aspergillosis is called invasive aspergillosis (IA) which affects individuals who have impaired immune defenses (Dagenais and Keller 2009). In IA, inhaled conidia penetrate the epithelial and endothelial barriers, resulting in germination and proliferation of the fungus within lung tissue. The infection can also spread to other organs, particularly to the brain via the bloodstream (Espinosa and Rivera 2016) (Figure 1.3).

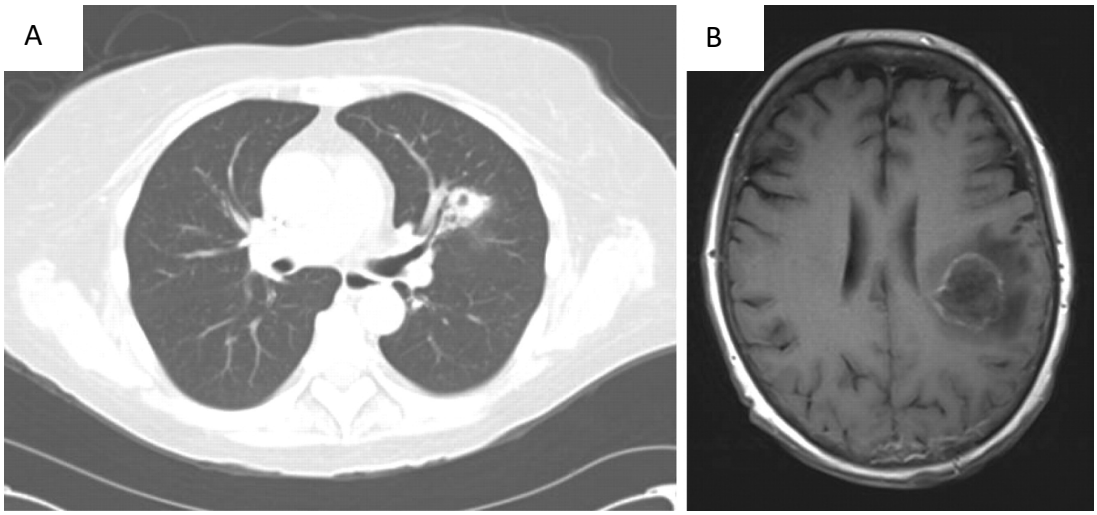

Figure 1.3 Chest computed tomography and brain magnetic resonance image showing invasive pulmonary aspergillosis.
A) Chest computed tomography image showing cavitary lesion in the left upper lobe in an allogenic hematopoietic stem-cell transplantation recipient. B) Brain magnetic resonance image from the same patient showing a lesion due to disseminated IPA. (Figure adapted from Kousha, Tadi, and Soubani, 2011)

Symptoms of IA include cough, fever, chest pain, dyspnea and hemoptysis (Cadena, Thompson, and Patterson 2016). The major risk factors for developing IA include neutropenia secondary to allogeneic hematopoietic stem cell transplant or solid organ transplant, and hematological malignancy. IA is estimated to occur in 5-25% of acute leukemia patients, 5-10% of patients with allogenic bone marrow transplantation, and in 0.5-5% of individuals after cytotoxic treatment of blood diseases or solid-organ transplantation (Latgé 1999). Patients infected with human immunodeficiency virus, those with undergoing high-dose corticosteroid therapy, or those with a genetic immunodeficiency such as chronic granulomatous disease (CGD) are also at risk (Ben-Ami, Lewis, and Kontoyiannis 2010). Mortality rates for IA range from 40 to 90% in high risk populations, even with drug treatment, and depend on multiple factors such as host immune status, the site of infection and the treatment (Dagenais and Keller 2009).

The diagnosis of IA remains challenging, and the gold standard is histopathological examination of lung tissue obtained by thoracoscopic or open-lung biopsy. Other diagnostic methods include the detection of *Aspergillus* antigens in body fluids. PCR detection of fungal DNA has not yet proven to be clinically useful (R. A. Barnes and White 2016) but detection of galactomannan in serum using ELISA has been approved by US Food and Drug Administration (FDA) for the diagnosis of IA (Verdaguer et al. 2007). Other antifungals can be used as alternatives or as salvage or in adjunct, including liposomal amphotericin B, and echinocandin derivatives such as caspofungin, micafungin and anidulafungin (Panackal, Bennett, and Williamson 2014). The treatment duration depends on patient's response and often lasts from several months to >1 year (Kousha, Tadi, and Soubani 2011).

1.2 Airway Epithelium

The primary point of contact with fungal conidia is the airway epithelium which initiates the immune response (Paris et al. 1997). The airway epithelium has numerous functions: it regulates lung fluid balance, attracts and activates inflammatory cells in response to injury, and regulates airway smooth muscle function by secreting mediators (Knight and Holgate 2003). Since they are an initial point of contact between the host and the fungus, and because the host immune response determines the outcome, a better understanding of how airway epithelial cells respond to conidia will shed light on the unique pathogenesis of the various *Aspergillus*-related disease.

1.2.1 Function of airway epithelium in aspergillosis

The bronchial epithelium of the conducting airways consists of a pseudostratified epithelium consisting of columnar epithelial cells; these include mucus-secreting goblet cells,

ciliated cells and basal cells (Knight and Holgate 2003). Ciliated cells are the predominant cell type within the airways, accounting for 50% of all epithelial cells. Ciliated cells arise from either basal or secretory cells (Spina 1998; Ayers and Jeffery 1988) and each cell is estimated to possess 300 cilia/cell with multiple mitochondria under the apical surface (Knight and Holgate 2003). Goblet cells protect the airway epithelial surface by producing mucus that traps inhaled particles; ciliated cells aid in removal of these trapped particles by moving mucus toward the throat where it can be swallowed or expectorated. Producing correct amounts of mucus is important for efficient mucociliary clearance, and goblet cell hyperplasia and metaplasia is commonly observed in chronic airway inflammatory diseases such as chronic bronchitis and asthma (Jeffery 1991). In immunocompetent hosts, most of *A. fumigatus* conidia are eliminated by mucociliary clearance (Rogers 1994; Balloy and Chignard 2009). As noted above, in ABPA patients, inhaled conidia cause a T_H2 mediated inflammatory response resulting in enhanced mucus production as well as production of cytokines, growth factors and chemokines. Airway damage and hyper-responsiveness is accompanied by production of T-cells, eosinophils, basophils and other immune cells (Osherov 2012).

Due to their small size (2.5 µm diameter), *A. fumigatus* conidia that escape the physical barrier can reach the lower bronchial airways to the terminal bronchioles and alveoli (P. D. Barnes and Marr 2006). Alveoli consist of type I and type II alveolar epithelial cells, and alveolar macrophages. Type I are thin, non-dividing squamous cells that enable rapid gas exchange. They cover 95% of the alveolar surface but are the least common of all major cell classes present in the lungs. Type II alveolar cells are cuboid and differentiate into type I cells (Crapo et al. 1982). They also secrete surfactant proteins, Surfactant Protein A (SP-A) and Surfactant

Protein D (SP-D). SP-A and SP-D are collectins, calcium-dependent lectins (with collagenous region and carbohydrate recognition domain) that opsonize conidia and enhance killing by neutrophils and macrophages (Madan et al. 1997). Type-II epithelial cells also secrete cytokines, chemokines and antimicrobial peptides. Airway epithelial cells can phagocytose conidia that are then trafficked to acidic organelles. However, it has been demonstrated that conidia can survive and germinate in the acidic organelles of epithelial cells *in-vitro* (Paris et al. 1997; Julie A. Wasylnka and Moore 2002, Wasynka and Moore, 2003).

In an immunocompetent host, alveolar macrophages are able to phagocytose dormant or swollen conidia, and kill them within 30 hours (Schaffner et al. 1983). Macrophages secrete chemokines to recruit neutrophils for elimination of conidia and germinating hyphae (Balloy and Chignard 2009); however, in immunocompromised patients, inhaled *A. fumigatus* conidia can enter the alveoli, germinate and penetrate the epithelial barrier to cause IA. This is due to the dysfunction of immune defenses that are necessary for recruitment of alveolar macrophages and neutrophils (Osherov 2012).

1.2.2 Pattern recognition receptors

Professional and non-professional phagocytes in the airways recognize pathogen-associated molecular patterns (PAMPs) on the cell wall of *A. fumigatus* by pattern recognition receptors (PRRs) (Sales-Campos et al. 2013*)*. These PAMPs on conidial cell wall include β-glucan, chitin, mannan or galactomannan. PRRs recognizing these components can be separated into two categories, soluble and cell surface PRRs. More details are presented below.

1.2.2.1 Soluble PRRs

The soluble PRRs act as opsonins, and include the acute-phase proteins, complement proteins, anti-microbial peptides and cytokines (Wong and Aimanianda 2017). Acute-phase proteins are proteins whose plasma concentrations increase or decrease by at least 25% during infection or inflammation. These include cytokines, C-reactive proteins and several components of complement proteins such as C3, C4 and mannose-binding lectin (Gabay and Kushner 1999).

The complement system consists of the classical, lectin pathway and alternative pathways, and upon activation, C3 convertase is formed by binding of pathogen-associated molecular patterns (PAMPs) (Walport 2001). C3 convertase cleaves C3 into opsonins, C3b and iC3b to result in 1) opsonization by C3b and iC3b; 2) recruitment of immune cells by production of anaphalytoxins C3a and C5a; and 3) direct lytic killing of the pathogen by formation of membrane attack complex (MAC). Due to the thick fungal cell wall, MAC is unlikely to kill the fungus by membrane lysis. Hence, complement system enhances immune recognition by conidia opsonization (Wong and Aimanianda 2017). All three forms of the complement system are known to be activated by different forms of fungus (Kozel et al. 1989).

The alternative pathway is activated by the resting conidia; however, classical pathway is known to be activated as conidia mature, exposing conidia to the innate immune system and resulting in C1q interacting with surface bound IgG and IgM (Kozel 1996; Aimanianda et al. 2009). In contrast, the lectin pathway is known to be activated by the binding of mannose-binding lectin (MBL) or ficolin with serine proteases on the pathogen surface, resulting in formation of a complex that cleaves C4 to form C3 convertase, and activates C3. (Fujita 2002). MBL opsonizes dormant conidia by binding to mannose in a calcium-dependent manner, and

directly activates C3 without the formation of C3 convertase. Similarly, ficolin-2 opsonizes conidia by recognizing N-acetylglucosamine (GlcNAc) and activates C3. Hence, the lectin pathway is not activated by dormant conidia; instead, C3 is activated directly to opsonize the conidia (Dumestre-Pérard et al. 2008; Bidula et al. 2013; Wong and Aimanianda 2017).

Ficolin-3 (FCN3) is another soluble PRR secreted by type II alveolar epithelial cells that binds to *A. fumigatus* in calcium-dependent manner (Bidula et al. 2013). Pentraxin-related protein 3 (PTX3) is also a soluble PRR and an acute-phase protein that binds to *A. fumigatus* conidia through the N-terminal domain and recognizes galactomannan. Similarly, C-reactive protein enhances conidial recognition in neutrophils through the Fcγ Receptor II *in-vitro* (Moalli et al. 2010). Phagocytic cells also recognize conidia through complement receptors (CR1, CR3, and CR4) and Fcγ receptors (Wong and Aimanianda 2017). Opsonized conidia are recognized through calreticulin-CD91 complex in macrophages as well (Ogden et al. 2001; Vandivier et al. 2002).

1.2.2.2 Cell surface PRRs

Cell surface PRRs allow binding to the pathogen before phagocytosis. These include dectin-1, a transmembrane C-type lectin receptor (CLR) that recognizes β-1,3-glucans, found on swollen and germinating conidia. In macrophages, dectin-1 recognizes swollen conidia both at the cell surface as well as in phagolysosomes (Faro-Trindade et al. 2012; Bercusson, de Boer, and Armstrong-James 2017). Increased expression of dectin-1 was observed in human bronchial epithelial cells upon exposure to *A. fumigatus* as well (W.-K. Sun et al. 2012). Dectin-1 can interact with signaling receptors to activate downstream signaling pathways via both spleen tyrosine kinase (Syk)-dependent and Syk-independent signaling cascades. Upon ligation of

extracellular domain in Syk-dependent signaling, cytoplasmic immunoreceptor tyrosine-based activation motif (ITAM)-like is phosphorylated, resulting in recruitment of Syk and caspase recruitment domain-containing protein 9 (CARD9). This results in the activation of transcription factors, including NF-κB, production of reactive oxygen species (ROS) and pro-inflammatory cytokines such as TNF-α and IL-12. These cytokines promote T_H1/T_H17 differentiation to recruit neutrophils and macrophages in response to the fungus (Drummond et al. 2011). Dectin-2 is another CLR expressed on dendritic cells and macrophages that recognizes α-mannans on the outer layer of conidia (H. Sun et al. 2013). Detection of swollen conidia by Dectin-2 results in the production of IL-1β, IL-10, IL-23p19 and TNFα via NF-κB mediated by Syk. In macrophages differentiated from human monocytic cell line, blocking of Dectin-2 results in reduced conidial killing (Sun et al. 2013, 2014).

Other signaling PRRs include the Toll-Like Receptors (TLRs). TLRs are membrane receptors consisting of a leucine-rich extracellular domain that recognizes PAMPs and an intracellular Toll/Interleukin-1 Receptor (TIR) domain for downstream signaling (Kawai and Akira 2006). Upon recognition of pathogen, signaling cascade results in activation of transcription factors such as NFκB, which leads to the production of cytokines and chemokines (Kawai and Akira 2006; Kawasaki and Kawai 2014). TLRs 1, 2, 4, 5 and 6 are found on the cell membrane, and TLRs 3, 7, 8 and 9 are found on the intracellular compartments. All TLRs are expressed by epithelial cells, alveolar macrophages and neutrophils (except for TLR3 which is not expressed in neutrophils) (Balloy and Chignard 2009). Both TLR2 and TLR4 play an important role in recognizing *A. fumigatus* conidia; however, the PAMPs with which they interact remain to be identified. TLR2 recognizes ligands on conidia and hyphae whereas TLR4

only recognizes ligands on conidia (Netea et al. 2003). TLR3 has been shown to be localized to the endosomal compartments in dendritic cells and epithelial cells, and detects double-stranded RNA released from the conidia as it enters the endosomal pathway (Beisswenger, Hess, and Bals 2012). TLR9 has also been shown to recognize unmethylated CpG DNA on *A. fumigatus* and is primarily found on dendritic cells and B cells (Ramirez-Ortiz et al. 2008).

1.2.3 Host innate immune response to *A. fumigatus*

Upon recognition, the innate immune system removes *A. fumigatus* conidia using the mechanical and anatomical barriers of the respiratory tract, professional and non-professional phagocytes and antimicrobial peptides. As previously mentioned, inhaled conidia are trapped in the mucus and removed by ciliated cells. However, when conidia bypass this anatomical barrier and reach the alveoli, cells encounter phagocytic cells such as neutrophils and alveolar macrophages (AM).

The AM are the first line of defense against conidia within the alveoli (Morton et al. 2012). Internalization of conidia by AM involves actin polymerization and endocytosis into endosomes that then fuse with lysosomes to form phagolysosomes (Wasynka and Moore, 2003). In the phagolysosome, fungal killing is achieved by both oxygen-dependent and oxygen-independent processes. Upon swelling of conidia, oxidative killing involves activation of Nicotinamide Adenine Dinucleotide Phosphate (NADPH) oxidase system that produces reactive oxygen species (ROS) that kill fungal conidia. In non-oxidative killing, acidification of the phagolysosome results in conidial degradation by hydrolytic enzymes, such as cathepsin D and chitinase (Brakhage et al. 2010). Upon phagocytosing conidia, AM release cytokines and chemokines, such as TNFα, MIP-α, IL-1β, IL-1α, IL-6, G-CSF and GM-CSF, which recruit innate

immune cells, including neutrophils, dendritic cells, monocytes, mast cells, eosinophils and natural killer (NK) cells (Espinosa and Rivera 2016) (Figure 1.4).

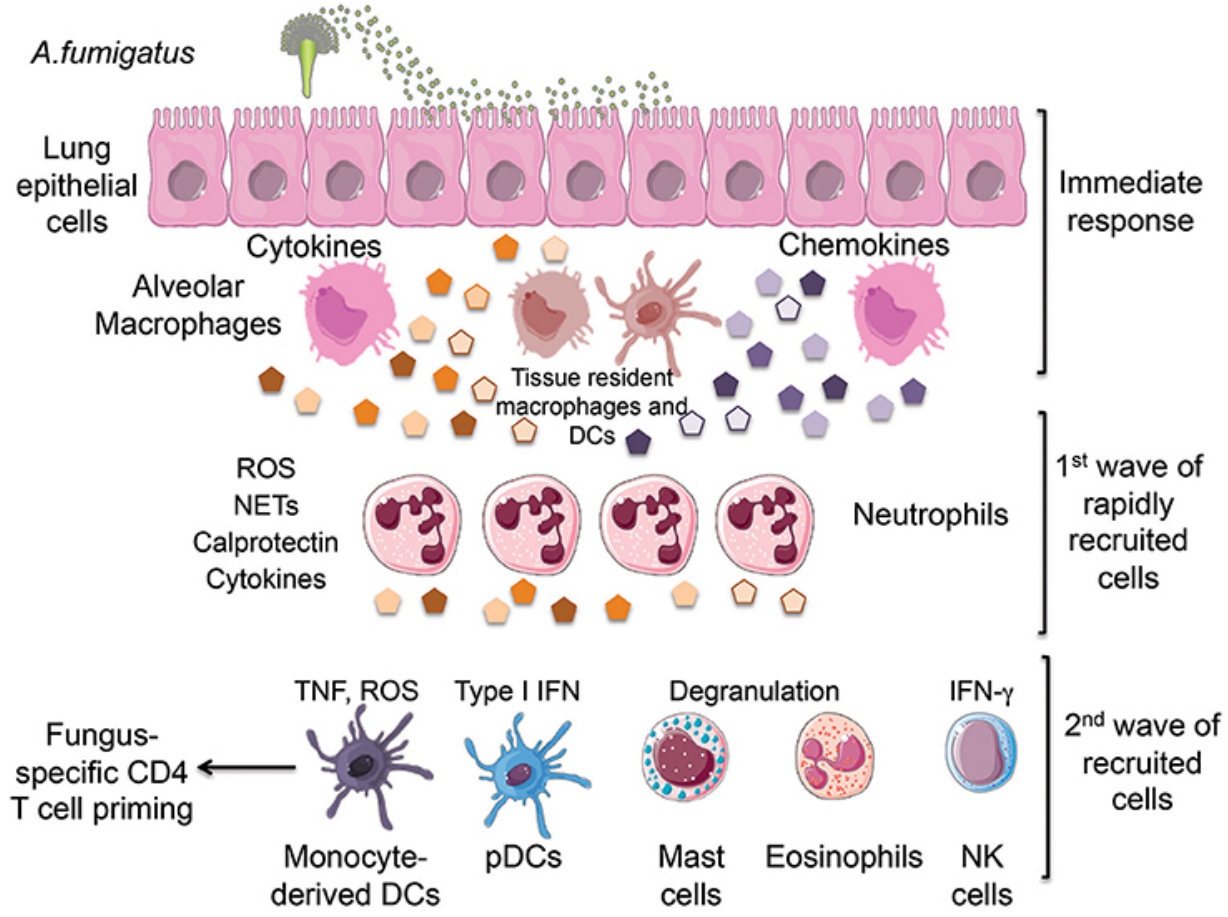

Figure 1.4 Inhalation of *A. fumigatus* conidia leads to initiation of immune response by lung epithelial cells and tissue-resident innate cells.
Upon recognition of conidia by lung epithelial cells, chemokines and cytokines are produced, resulting in recruitment of neutrophils and subsequent recruitment of monocytes, dendritic cells, mast cells, eosinophils and NK cells. (Figure adapted from Espinosa and Rivera, 2016)

Along with AM, neutrophils can also engulf and kill conidia via NADPH oxidase-mediated oxidative killing (Figure 1.4). Other mechanisms employed by neutrophils in elimination of *A. fumigatus* include production of lactoferrin and release of antimicrobial proteases by degranulation (Feldmesser 2006; Espinosa and Rivera 2016). The two predominant types of granules released during degranulation include azurophil granules and specific granules.

Azurophil granules are the primary granules and consist of fungicidal hydrolytic enzymes such as myeloperoxidase, cathepsin G, elastase and proteinase 3. Specific granules are the secondary granules and consist of lactoferrin, transcobalamin II etc. Hence, NADPH oxidase promotes activation of hydrolytic enzyme as well as degranulation (Segal 2005; Espinosa and Rivera 2016). Neutrophils also produce mesh-like extracellular traps (NETs), which are extracellular structures made of chromatin with proteins from neutrophilic granules attached (Brinkmann et al. 2004). These may inhibit fungi, however the role of NETs in killing *A. fumigatus* hyphae is controversial (P et al. 2016).

Dendritic cells (DCs) have been shown to play an important role in host defense against *A. fumigatus* as well (Figure 1.4). Three major subtypes of DCs in the lung include conventional DCs (cDCs), plasmacytoid DCs (pDCs) and monocyte-derived DCs (moDCs) (Kushwah and Hu 2011). They can phagocytose opsonized or unopsonized conidia and hyphae upon recognition by PRRs, such as Dectin-1, Dendritic Cell-Specific Intercellular adhesion molecular-3-Grabbing Non-integrin (DC-SIGN), complement receptor 3 (CR3) and FcγRIII (Bozza et al. 2002; Mezger et al. 2008; Charles O. Morton et al. 2011). Neutrophils are known to express CCL3/MIP-1α and CCL4/MIP-1β, which can recruit DCs to the site of infection (Scapini et al. 2000). In response to *A. fumigatus,* DCs produce proinflammatory cytokines such as TNFα, IL-6, IL-12, IL-1α and IL-1β (Bozza et al. 2002; Mezger et al. 2008; Charles O. Morton et al. 2011). In addition, infection of human DCs by *A. fumigatus* conidia *in-vitro* results in secretion of chemokines for recruitment of neutrophils and AM (CXCL8/IL8, CCL3, CCL4 and CCL5) as well as effector memory T cells and naïve T cells (CCR6 and CCR7) (Gafa et al. 2007; Charles O. Morton et al. 2011). This indicates

that DCs play an important role in both innate and adaptive immune responses against *A. fumigatus* (Espinosa and Rivera 2016; Margalit and Kavanagh 2015).

Other immune cells involved in host response against *A. fumigatus* include eosinophils, mast cells and NK cells (Figure 1.4). Eosinophils consist of granules that have been shown to consist antimicrobial proteins with fungicidal activity (Patterson and Strek 2014). There is evidence that they play a role in defense against *A. fumigatus* as mice deficient in eosinophils have been shown to have increased fungal burden and impaired production of pro-inflammatory cytokines and chemokines, compared to wild-type mice (Lilly et al. 2014). In contrast, in ABPA patients, recruitment of eosinophils can contribute to epithelial damage (Espinosa and Rivera 2016). Exposure to *A. fumigatus* can also result in degranulation of mast cells; however they cannot inhibit fungal growth (Urb et al. 2009; Bradding, Walls, and Holgate 2006).

Antimicrobial peptides also play an important role in the innate immune response to fungal infection. These include defensins and cathelicidins, which permeabilize fungal membranes and result in nonoxidative killing of fungi. Human β-defensin 2 is the most commonly expressed defensin in the lung (Smet and Contreras 2005; Alekseeva et al. 2009). In addition, LL-37 (or CAMP (Cathelicidin Antimicrobial Peptide) is the only human cathelicidin antimicrobial peptide expressed by neutrophils and airway epithelial cells, and is found to be highly expressed during inflammation (Bals et al. 1998; Chotirmall et al. 2013).

1.2.3 Host adaptive response to *A. fumigatus*

Along with innate immune response, adaptive immune response is essential in host defense against *A. fumigatus* as well. Specifically, T-helper responses are activated during

interaction of host with *A. fumigatus* (Dewi, van de Veerdonk, and Gresnigt 2017). Innate effector cells, such as dendritic cells, have been shown to be involved in activating and differentiating naïve $CD4^+$ T-helper cells into different effector cells (Ramirez-Ortiz and Means 2012). In addition, binding of T-cell receptor to major histocompatibility complex (MHC) class II, interaction of co-stimulatory molecules present on the surface of T-cells and antigen presenting cells, and autocrine production of IL-2 and other cytokines from different innate immune cells allows T-helper cell proliferation and differentiation into T_H1, T_H17, T_H22, T_H2, T_H9, Treg and Tr1 cells (Barrios et al. 2005; Dewi, van de Veerdonk, and Gresnigt 2017; Bozza et al. 2002) (Figure 1.5).

Upon infection with *A. fumigatus*, human DCs produce significant amounts of IL-12, a T_H1 cells inducing cytokine (Gafa et al. 2007). These T_H1 cells are characterized by transcription factor TBET and production of IFN- γ, and promote clearance of fungus from the lungs. An IFN- γ deficient mice has been shown to have impaired protective antifungal immunity and robust T_H2 responses (Cenci et al. 1999).

T_H2 cells are characterized by the transcription factor GATA3 and the production of IL-4, IL-5, IL-10 and IL-13, which mediate anti-inflammatory responses, allergy and fungal persistence in the lungs (Moss 2005; Dewi, van de Veerdonk, and Gresnigt 2017). Production of IL-10 by T_H2 cells suppresses production of pro-inflammatory cytokines and chemokines as well as inhibits T-cell activation and IFN- γ production (Del Sero et al. 1999). A T_H9 subset of cells has been shown to responses closely associated to T_H2 responses, and are characterized by production of IL-9 (Kaplan, Hufford, and Olson 2015). These T_H9 subset of cells play a role in the allergic responses to *A. fumigatus* in cystic fibrosis as well (Moretti et al. 2017).

Unlike T_H2 responses, T_H17 responses are important for fungal clearance in the host. They are characterized by the expression of transcription factor, RAR-related orphan receptor C (RORC), and the production of IL-17A, IL-17F and IL-22 cytokines (Dewi, van de Veerdonk, and Gresnigt 2017). IL-17A and IL-17F cytokines can trigger the recruitment and activation of neutrophils as well as production of pro-inflammatory cytokines IL-6, IL-1β, TNF-α and G-CSF (van de Veerdonk et al. 2009; Way, Chen, and Kolls 2013; Werner et al. 2009; Dewi, van de Veerdonk, and Gresnigt 2017). As mentioned previously, neutrophils can produce ROS, proteolytic enzymes and anti-microbial peptides to eliminate the fungus. In addition, T_H17 response can also activated upon interaction of dectin-1 by β-glucans (Rivera et al. 2011; Dewi, van de Veerdonk, and Gresnigt 2017).

Regulatory T cells (Treg) play an important role in host defense against the fungus by regulating the inflammatory response and controlling inflammation by releasing anti-inflammatory cytokines such as IL-10 and TGF-β (Vignali, Collison, and Workman 2008). Treg cells include the natural Treg (nTreg) and induced Treg (iTreg) cells. nTreg cells regulate the early infection by limiting neutrophil activity, and iTreg cells limit inflammation in the later stages of infection (Montagnoli et al. 2006). In addition, *Aspergillus*-specific Type (1) regulatory T-cells (Tr1) have been found in the peripheral blood of human and mice, showing *Aspergillus*-specific response by the host (Bedke et al. 2014).

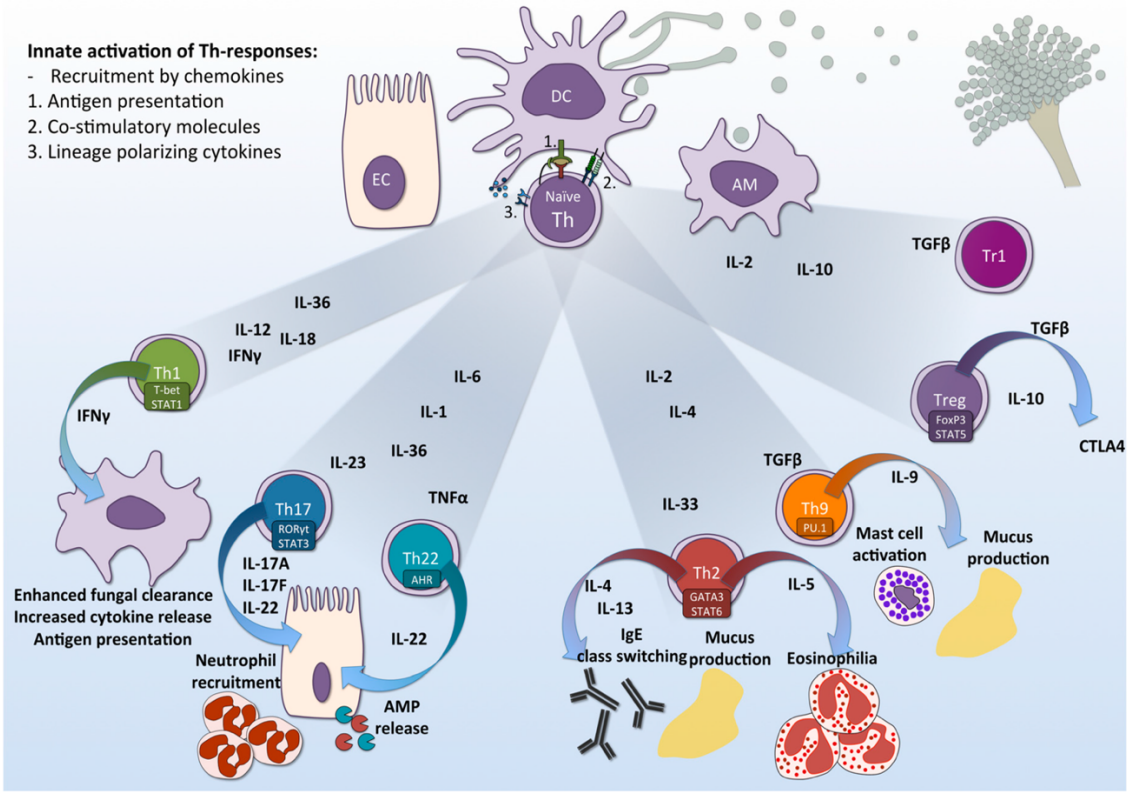

Figure 1.5 Innate activation of T-helper responses to *A. fumigatus.*
Production of distinct cytokines by innate immune cells upon recognition of PPRs, antigen presentation by via MHC-II, and binding of co-stimulatory molecules results in activation and differentiation of naïve CD4+ T-helper cells to distinct lineages: T_H1, T_H17, T_H22, T_H9, T_H2, Treg and Tr1. Figure adapted from van de Veerdonk, and Gresnigt 2017

1.3 Overview of experimental goals of the present research

A. fumigatus can cause a spectrum of lung diseases; the particular manifestation of disease symptoms depends on the immune status of the host. Hence, the initial interaction between conidia and the environment of the lung is important. Upon inhalation, the first cell encountered by conidia is most likely to be a type of airway epithelial cell, either bronchial or alveolar.

The overall aim of my project was to investigate the early molecular response of human bronchial epithelial cells upon interaction with *A. fumigatus* conidia. We hypothesize that novel

insights into the host response to *A. fumigatus* conidia can be obtained by using a multi-OMIC molecular approach. The specific objectives of my study were:

1. to develop a co-culture interaction model of *A. fumigatus* conidia with primary human bronchial epithelial cells (HBECs) that better recapitulates the *in-vivo* airway epithelium,
2. to use a multi-OMIC molecular approach to measure gene expression changes in host upon exposure to *A. fumigatus* conidia using this model,
3. to evaluate the applicability of this model for studying other host-pathogen interactions.

This work is presented in the following chapters. In Chapter 3, a co-culture model was developed using primary human bronchial epithelial cells (HBECs) grown for 21-28 days as air-liquid interface (ALI) cultures that contained basal, mucus-secreting goblet and ciliated cells, to better recapitulate the *in-vivo* bronchial epithelium. Using this model, the early molecular response was analyzed using transcriptomics and proteomics to measure gene expression changes in host upon exposure to *A. fumigatus* conidia. In Chapter 4, I describe comparative analyses that I used to evaluate the applicability of this model to other host-pathogen systems. Specifically, gene expression profiles of ALI cultures were compared to an *in-vitro* model that uses submerged monolayer cultures of the human airway epithelial cell line (1HAEo-), and the specificity of response in ALI cultures was assessed by comparing the response to the immune response of primary HBECs upon exposure to a mutant strain of *A. fumigatus* conidia as well as to Respiratory Syncytial Virus (RSV). In Chapter 5, I present the overall conclusions of my studies and provide some ideas for future directions.

1.4 Strengths and limitations of the chosen cell culture models

In general, *in-vitro* cell culture models of human lung can involve submerged monolayer cultures from immortalized respiratory cell lines, such as 1HAEo- used in Chapter 4, or primary cells isolated from lung tissue, used in Chapter 3. Even though cell lines are transformed and cancerous, and less representative of the airway epithelium (Bhowmick and Gappa-Fahlenkamp 2016), they are easily accessible, cost-effective and can be used at high passages compared to primary cells (Kaur and Dufour 2012). However, when grown as submerged monolayer cultures, both lack the physiological features of the *in-vivo* airway epithelium, such as the mucocililary barrier of the pseudostratified *in-vivo* epithelium (Kaur and Dufour 2012; O'Boyle et al. 2017). Formation of robust tight junctions and trans-epithelial electrical resistance (TEER) values varies within both cell types and is dependent on culture conditions as well (Bhowmick and Gappa-Fahlenkamp 2016).

In Chapter 3, a more complex primary cell based ALI model was used to generate polarized cells. These ALI cultures can differentiate into mucus-producing goblet cells, ciliated cells as well as comprise the ciliary activity, form tight junctions and produce mucus (Karp et al. 2002; Lopez-Souza, Avila, and Widdicombe 2003). However, unlike the intact host epithelium, these ALI cultures used in our study lack both continuous clearance of mucus and other innate immune effector cells, such as dendritic cells, macrophages and neutrophils. Nevertheless, we have used combination of cell culture models to study the molecular response of the host in bronchial epithelium upon exposure to *A. fumigatus* in our study. Further details on both cell culture models are provided in Chapter 3 and Chapter 4.

Chapter 2 Methods

2.1 *A. fumigatus* strain and growth conditions

All experiments were performed using a green fluorescent protein (GFP) expressing strain of *A. fumigatus* derived from ATCC 13073 (American Type Culture Collection, Manassas, VA) (Julie A. Wasylnka and Moore 2002), unless otherwise stated. The conidia from this strain are referred to as wild-type (WT) *A. fumigatus* conidia in Chapter 4. Briefly, the strain was transformed by electroporation with a plasmid containing the codon-optimized *sgfp* gene and the construct yielded stable, high expression of GFP in both conidia and hyphae (Julie A. Wasylnka and Moore 2002).

To obtain fresh conidia for each experiment, the GFP-transformed *A. fumigatus* strain was grown on yeast-agar-glucose (YAG) media at 30 °C until sporulation. Mature conidia were harvested by gently scrubbing the plates using sterile cotton swabs with phosphate-buffered saline plus 0.05% Tween-20 (PBS-T). The conidial suspension was filtered through sterile glass wool, vortexed, pelleted and re-suspended in 1 ml PBS. The suspension was washed twice with PBS to remove any trace of PBS-T prior to quantification using a hemocytometer.

2.2 *Δkdnase A. fumigatus* strain and growth conditions

Kdnase is an *exo*-sialidase identified in *A. fumigatus* (Telford et al., 2011). The *A. fumigatus kdnase* knockout strain was prepared as described in Nesbitt et al. (2018), and is referred to as the *Δkdnase A. fumigatus* strain . Briefly, the strain was transformed by a disruption construct, containing 1000 bp sequences of DNA encoding the upstream and

downstream regions of the *kdnase* gene, which was introduced into the WT strain using *Agrobacterium*-mediated transformation (Nesbitt et al. 2018).

To obtain fresh conidia for an experiment, the *⊿kdnase A. fumigatus* strain was grown on yeast-agar-glucose (YAG) media supplemented with 100 µg/mL hygromycin at 30 °C until sporulation. Mature conidia were harvested by gently scrubbing the plates using sterile cotton swabs with phosphate-buffered saline plus 0.01 % Tween-20 (PBS-T). The conidial suspension was filtered through sterile glass wool, vortexed, pelleted and re-suspended in 1 ml PBS. The suspension was washed twice with PBS to remove any trace of PBS-T prior to quantification using a hemocytometer.

2.3 Overview of experiments

The research presented here is primarily from three different experiments (Figure 2.1). Air-Liquid Interface cultures (ALIs) of primary human bronchial epithelial cells (HBECs) (details below) in experiment #1 consisted of 6 samples (control (n=3) and infected (i.e., exposed to *A. fumigatus* conidia) (n=3)) and experiment #2 consisted of 12 samples (control (n=3), infected (n=3), *Δkdnase*-infected (n=3) and Respiratory Syncytial Virus (RSV)-infected (n=3)). The control samples were incubated with PBS alone, infected samples with *A. fumigatus* conidia suspended in PBS, *Δkdnase*-infected samples with *Δkdnase A. fumigatus* conidia suspended in PBS, and RSV-infected with RSV suspended in PBS for 6 hours at 37 °C.

Experiment #3 was conducted with 1HAEs (details below) incubated with DMEM + 10% FBS (control, n=3) and *A. fumigatus* conidia suspended in DMEM + 10% FBS (infected, n=3) for 6 hours at 37 °C.

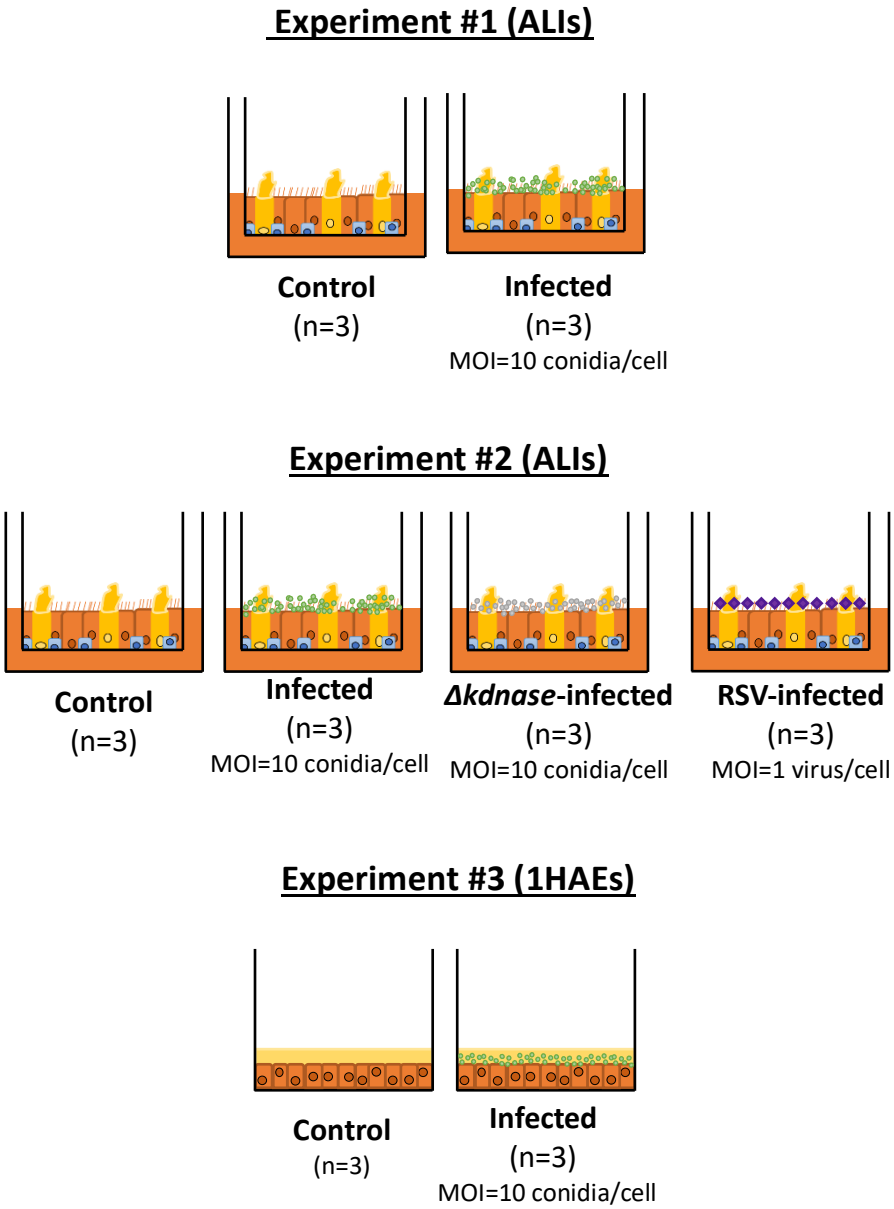

Figure 2.1 Overview of experiments.
Two separate experiments (experiment #1 and #2) were conducted using ALI cultures of human bronchial epithelial cells (HBECs) and corresponding analyses are presented in Chapters 3 and 4. Analyses from the 1HAEs experiment (experiment 3) are also presented in Chapter 4. The number of replicates per treatment in each experiment were 3 (n=3).

2.4 ALI cultures of primary HBECs

Human lungs of de-identified healthy donors, deemed unsuitable for transplantation and donated to medical research, were obtained from the International Institute for the

Advancement of Medicine (Edison, NJ) for primary cell isolation as per approval by the Research Ethic Board (REB) of University of British Columbia / Providence Healthcare (REB# H00-50100). Bronchial epithelial cells were isolated by protease digestion as described by Gray and colleagues, and cultured in bronchial epithelial growth medium (Lonza, Mississauga, ON, CC-3170) at 37 °C in 5% CO_2 (Gray et al. 1996). ALI cultures of primary HBECs were generated using cells at passage one or two in ALI PneumaCult medium (Stemcell Technologies, Vancouver, BC, Catalog# 05001). The cultures were grown on inserts for 21-28 days on 12-(Griener Bio-One, Catalog# 665180) or 24-well (Greiner Bio-One, Catalog# 662160) plates to generate a pseudostratified epithelium. The differentiated ALI cultures contained basal, mucus-producing goblet and ciliated cells. Barrier function of epithelial cells was assessed by measuring Trans-Epithelial Electrical Resistance (TEER) values.

2.5 Submerged monolayer cultures of 1HAEs

SV40-transformed normal human airway epithelial cell line, 1HAEo-, was used for experiments (Cozens et al. 1992). Cells were grown in a 5% CO_2 atmosphere at 37 °C as submerged monolayer cultures in Dulbecco's Modified Eagle Medium (DMEM) supplemented with 10% Fetal Bovine Serum (FBS). Subcultures were routinely performed before cells reached 80% confluency. Cells grown on 12-well plates (Griener Bio-One, Catalog# 665180) were used for experiments.

2.6 Visualizing interaction of *A. fumigatus* conidia with primary HBECs grown in ALI at 2, 6, 12 or 24 hours by confocal microscopy

The apical side of ALI cultures of primary HBECs (21-28 days old) grown in a 24-well plate (Greiner Bio-One, Catalog# 662160) were co-incubated with *A. fumigatus* conidia

suspended in PBS at a multiplicity of infection (MOI) of 10 conidia/cell. ALI PneumaCult medium (Stemcell Technologies, Vancouver, BC, Catalog # 05001) was added to the basal side for 2, 6, 12 or 24 hours at 37 °C. For each time point, culture medium from the apical and basal side were removed. Both apical and basal sides of the inserts were then washed three times with sterile PBS and fixed in 4% paraformaldehyde (PFA) in PBS for 20 minutes at room temperature (RT). Cells were washed and re-hydrated for 10 mins in PBS at RT.

The apical side was incubated with monoclonal mouse anti-*A. fumigatus* antibody (Thermo Fisher Scientific, Catalog# MA174434), diluted 1:300 in PBS, overnight at 4 °C. Following two washes with PBS, the apical side of each insert was incubated with goat anti-mouse IgG highly cross-adsorbed secondary antibody conjugated with Alexa Fluor 594 (Thermo Fisher Scientific, Catalog# A-11032), diluted 1:200 in PBS, for 1hr at RT. The inserts were washed with PBS twice. ALI membranes were removed from the inserts and transferred to a chamber slide prior to mounting with ProLong™ Gold Antifade Mountant with DAPI (Thermo Fisher Scientific, Catalog# P36935).

Cover-slipped slides were visualized with Zeiss LSM-800 inverted confocal microscope system using a 63x/1.4NA oil immersion lens (Carl Zeiss Inc, plan-apochromat 63x/1.4 NA Oil DIC M227), collected with the Zen Black software. The laser lines used were 405 nm (DAPI), 488 nm (GFP) and 594 nm (Alexa 594), fired sequentially to avoid cross-talk, and detected at 410-508 nm, 490-606 nm and 605-734 nm, respectively (Table 2.1).

Table 2.1 Confocal microscope settings for acquired images after 6 and 24 hours.

Zeiss LSM-800 inverted confocal microscope settings	ALI cultures of primary HBECs exposed to *A. fumigatus* conidia for 6 hours (Figure 3.2)	Figure 2.3: ALI cultures of primary HBECs exposed to *A. fumigatus* conidia for 24 hours (Figure 3.3)
Lens	63x/1.4NA Oil	63x/1.4NA oil
Dimension size	512 x 512 pixels, 16-bit	1912 x 1912 pixels, 12-bit
Image size	67.48 x 67.48 µm	134.95 x 134.95 x 104.25 µm
Lasers	Track 1 594 nm : 70% Track 2 488 nm : 6.0% Track 3 405 nm : 2.0%	Track 1 594 nm : 60% Track 2 488 nm : 8.0% Track 3 405 nm : 3.0%
Filters	Track 1 Ch2 : 599-734 Track 2 ChS1 : 490-606 Track 3 Ch1 : 410-508	Track 1 Ch2 : 599-734 Track 2 ChS1 : 490-606 Track 3 Ch1 : 410-508
Master gain	Track 1 Ch2: 666 Track 2 ChS1: 716 Track 3 Ch1: 652	Track 1 Ch2: 708 Track 2 ChS1: 750 Track 3 Ch1: 670
Pinhole	Track 1 Ch2: 68 µm Track 2 ChS1: 90 µm Track 3 Ch1: 41 µm	Track 1 Ch2: 58 µm Track 2 ChS1: 48 µm Track 3 Ch1: 41 µm
Digital gain	Track 1 Ch2: 1.00 Track 2 ChS1: 1.00 Track 3 Ch1: 1.00	Track 1 Ch2: 1.00 Track 2 ChS1: 1.00 Track 3 Ch1: 1.00

2.7 Visualizing interaction of *A. fumigatus* conidia with submerged monolayer cultures of 1HAEo- cells at 6 hours by confocal microscopy

1HAEo- cells grown in a 24-well plate were co-incubated with *A. fumigatus* conidia (MOI=10 conidia/cell) suspended in DMEM + 10% FBS for 6 hours at 37 °C. After 6 hours, cells were washed once with sterile PBS prior to the addition of 0.25% Trypsin. The plate was incubated for 5 minutes at 37 °C after which DMEM + 10% FBS was added to neutralize the trypsin. The cells were collected in a microcentrifuge tube and centrifuged for 5 mins at 1000 *g* to generate a cell pellet. The supernatant was removed and the pellet washed twice with RT PBS . The pellet was fixed with 4% PFA for 20 minutes at RT. The fixative was removed and cells

were re-hydrated for 10 mins in PBS at RT. Another PBS wash (5 minutes) was conducted and the cell pellet was incubated with monoclonal mouse anti-*A. fumigatus* antibody (Thermo Fisher Scientific, Catalog# MA174434), diluted 1:300 in PBS, overnight at 4 °C. Following washing twice with PBS, cells were incubated with goat anti-mouse IgG highly cross-adsorbed secondary antibody conjugated with Alexa Fluor 594 (Thermo Fisher Scientific, Catalog# A-11032), diluted 1:200 in PBS for 1hr at RT. The cell pellet was washed twice with PBS and 1 µg/µl of DAPI in PBS (1:1000 dilution) was added and incubated for 5 minutes at RT. After two washes with PBS, 10 µl of cell pellet was transferred to a chamber slide before cover-slipping. Cover-slipped slides were visualized with Zeiss LSM-800 inverted confocal microscope system using a 63x/1.4NA oil immersion lens (Carl Zeiss Inc, plan-apochromat 63x/1.4 NA Oil DIC M227), collected with the Zen Black software. The laser lines used were 405 nm (DAPI), 488 nm (GFP) and 594 nm (Alexa 594), fired sequentially to avoid cross-talk, and detected at 410-508 nm, 490-606 nm and 605-734 nm, respectively.

2.8 DNA, RNA and protein preparation from ALI cultures

DNA, RNA and proteins were extracted from ALI cells from experiment #1 and experiment #2. As shown in Figure 2.1, experiment #1 consisted of 6 ALI samples: ALI cultures of primary HBECs were incubated with PBS alone (n=3) and *A. fumigatus* conidia suspended in PBS, MOI= 10 conidia/cell (n=3), on the apical side, for 6 hours at 37 °C. Experiment #2 consisted of 12 ALI samples: ALI cultures of primary HBECs were incubated with PBS alone (n=3), *A. fumigatus* conidia in PBS (MOI= 10 conidia/cell (n=3)), Δ*kdnase A. fumigatus* conidia suspended in PBS (MOI= 10 conidia/cell (n=3)), and RSV suspended in PBS (MOI=1 RSV/cell (n=3)), on the apical side for 6 hours at 37 °C.

The basal sides of ALI cultures in both experiments were incubated with ALI PneumaCult medium (Stemcell Technologies, Vancouver, BC, Catalog #05001). For each experiment, 6 hours post-exposure to PBS, conidia in PBS, or RSV in PBS, the culture supernatants from both apical and basal sides were removed. Both sides of the membrane were washed three times with sterile PBS to remove any unbound conidia. The membrane of each insert was detached with a sterile pipette tip, by gently pushing on the edge, and collected in a microcentrifuge tube. Lysis Buffer Q (300 µl) was added to each tube according to the standard operating protocol of the RNA/DNA/Protein Purification Plus Micro Kit (Norgen Biotek Corp, Item# 51600). Membranes were stored at -80 °C until DNA, RNA and proteins extractions were performed (according to the protocol provided by RNA/DNA/Protein Purification Plus Micro Kit (Norgen Biotek Corp, Item# 51600).

2.9 DNA, RNA and protein preparation from 1HAEs cultures

DNA, RNA and Protein were also extracted from experiment #3 conducted using 1HAEs cultures (Figure 2.1). Prior to exposure to *A. fumigatus* conidia, DMEM+10% FBS was aspirated using a sterile glass pipette from 1HAE cells grown in a 12-well plate. 1HAE cell cultures were incubated with DMEM+10% FSB alone (n=3) or *A. fumigatus* conidia suspended in DMEM+10% FBS (MOI= 10 conidia/cell (n=3)) for 6 hours at 37 °C. The culture supernatants were removed after 6 hours. Each well was washed with sterile PBS three times to remove any unbound conidia. To each well, 0.25% trypsin was added and the plate was incubated at 37 °C for 5 mins. DMEM+ 10% FBS was added to neutralize the trypsin. The cell suspension from each well was collected in 2 ml microcentrifuge tubes and centrifuged at 1000 *g* for 5 mins. Cell pellet was washed twice with PBS and Lysis Buffer Q was added to each tube according to the standard

operating protocol of the RNA/DNA/Protein Purification Kit (Norgen Biotek Corp, Item # 51600). The cell pellets suspended in Lysis Buffer Q were stored in -80 °C until extractions were performed (according to the protocol provided by RNA/DNA/Protein Purification Plus Micro Kit (Norgen Biotek Corp, Item# 51600).

2.10 NanoString nCounter RNA transcript expression analysis

RNA yield from each sample in all three experiments were determined using a NanoDrop ND-100 spectrophotometer (Thermo Scientific, Wilmington, DE) and RNA integrity was determined using a 2100 Bioanalyzer (Agilent Technologies, Santa Clara, CA).

2.10.1 nCounter Immune Profiling Panel

The RNA transcript abundance was analyzed using the NanoString nCounter Immune Profiling panel (NanoString Technologies, Seattle, WA) from 100 ng of extracted RNA from ALI cultures (n=6 for experiment #1 and n=12 for experiment #2) and 1HAEs cultures (n=6 for experiment #3) (Figure 2.1). Twelve samples were analyzed using the nCounter Immune Profiling Panel each time: 6 ALI samples from experiment #1 plus 6 1HAE cultures in experiment #3, and 12 ALI samples from experiment #2 were assessed, respectively.

The Immune Profiling panel consisted of 770 genes (730 well-annotated immune genes and 40 housekeeping genes). Briefly, 70 µl of hybridization buffer was added to Reporter CodeSet (XT Formulation, Lot# RC4887X1 and Lot# RC5148X1) to prepare the master mix. To set up the hybridization reactions, each sample tube contained 8 µl of master mix and 5 µl of extracted RNA sample. Capture ProbeSet (2 µl) (XT Formulation, Lot# CP4887X1 and Lot# CP5148X1) was added to each tube. Samples were hybridized at 65 °C for 19 hours. The hybridized samples were analyzed using FLEX system's nCounter Prep Station using the high

sensitivity protocol, and the cartridge was scanned using Maximum resolution (Max FOV) in the nCounter Digital Analyzer to generate RCC files.

2.10.2 nCounter Asthma Elements Panel

The RNA transcript abundance was analyzed from 100 ng of extracted RNA using the nCounter Asthma Elements Panel (NanoString Technologies, Seattle, WA) using ALI samples from experiment #1 (n=6) and 1HAEs samples from experiment #3 (n=6) (Figure 2.1). The Asthma Elements panel consisted of 180 genes (Singh et al. 2018).

To set up the hybridization reactions, each sample tube consisted of 10 µl of hybridization buffer, 5 µl of TagSet Master mix (TagSet-168, Lot #TS4004), 5 µl of Extension TagSet (TagSet-ex24, Lot #TS4004), 1 µl of 30x working probe A pool (inactive probe was added), 1 µl of 30x working probe B pool, 3 µl of DNAase/RNAase free water and 5 µl of RNA Sample (20 ng/µl), for a total volume of 30 µl. The samples were hybridized at 67 °C for 16 hours. The hybridized samples were analyzed FLEX system's nCounter Prep Station using the high sensitivity protocol, and the cartridge was scanned using Maximum resolution (Max FOV) in the nCounter Digital Analyzer to generate RCC files.

2.11 Shotgun proteomics analysis using Liquid chromatography-tandem mass spectrometry (LC-MS/MS) of ALI and 1HAE cultures

Extracted proteins from ALI samples in experiment #1 (n=6) and 1HAEs samples in experiment#3 (n=6) were assessed using liquid chromatography-tandem mass spectrometry (LC-MS/MS). The 6 samples of both ALIs and 1HAEs experiment consisted of control (PBS alone, n=3) and infected samples (*A. fumigatus* conidia suspended in PBS, n=3), which were solubilized in a small volume of 6 M urea/2 M thiourea (in 10mM Hepes, pH 8.0). Proteins were then

precipitated using ethanol-acetate method (Foster, de Hoog, and Mann 2003). The protein concentrations of the samples were measured by the Bradford assay, followed by digestion in solution using Trypsin and Lys-C according to reference (Foster, de Hoog, and Mann 2003). Digested peptides were purified and concentrated on C18 STAGE-tips, eluted in 80% acetonitrile, 0.5% acetic acid, and dried in a vacuum concentrator (Eppendorf).

Dried peptides were re-suspended in 100 mM triethylammonium bicarbonate and chemical di-methylation labeling was performed using light ($^{12}CH_2O$) or heavy ($^{13}CD_2O$) isotopologues of formaldehyde. The light label was used for control samples and the heavy label for the infected samples. Light sodium cyanoborohydride solution (1M) was added to the light labeled samples and 1 M heavy sodium cyanoborodeuteride to the heavy labeled samples. The samples were vortexed and incubated at ambient temperature in the dark for 90 minutes. NH_4Cl (3 M) was added to the samples after which they were incubated at ambient temperature in the dark for 10 minutes. Samples were acidifed to pH < 2.5 by adding 1% trifluoroacetic acid (TFA). After full sodium cyanoborohydride degradation, each heavy labeled sample was combined with the light labeled sample (n=3 for each experiment) and STAGE-tip purified. Eluted samples were dried and re-suspended in 20% acetonitrile and 0.1% formic acid for subsequent fractionation. Peptides were separated offline using basic reverse phase fractionation as described previously (Udeshi et al. 2013).

Peptides fractions were analyzed by a quadrupole–time of flight mass spectrometer (Impact II; Bruker Daltonics) coupled to an Easy nano LC 1000 HPLC (ThermoFisher Scientific) using an analytical column that was 40–50 cm long, with a 75-µm inner diameter fused silica with an integrated spray tip pulled with P-2000 laser puller (Sutter Instruments) and packed

with 1.9 µm diameter Reprosil-Pur C-18-AQ beads (Maisch, http://www.Dr-Maisch.com). The columns were operated at 50 °C using an in-house built column heater. Buffer A consisted of 0.1% aqueous formic acid, and buffer B consisted of 0.1% formic acid and 80% (vol/vol) acetonitrile in water. A standard 90-min peptide separation was performed, and the column was washed with 100% buffer B before re-equilibration with buffer A.

The Impact II was set to acquire in a data-dependent auto-MS/MS mode with inactive focus fragmenting the 20 most abundant ions (one at the time at rate of 18-Hz) after each full-range scan from m/z 200 to m/z 2,000 at 5 Hz rate. The isolation window for MS/MS was 2–3 depending on the parent ion mass to charge ratio, and the collision energy ranged from 23 to 65 eV depending on ion mass and charge. Parent ions were then excluded from MS/MS for the next 0.4 min and reconsidered if their intensity increased more than five times. Singly charged ions were excluded from fragmentation.

Raw mass spectrometry data was analyzed using MaxQuant 1.5.1.0. The search was performed against a database comprised of the protein sequences from Uniprot's human and *A. fumigatus* entries plus common contaminants with cysteine carbamidomethylation and methionine oxidation, protein N-acetylation as fixed and variable modifications, respectively. Light and heavy dimethylation at lysine side chains and peptide N-termini were used for quantitation. Peptides and proteins identified with false discovery rate (FDR) ≤1% were retained for further analyses.

2.12 Statistical analyses of RNA transcript abundance in ALIs and 1HAEs cultures

2.12.1 Pre-processing

The following pre-processing guidelines were applied to 6 ALI samples from experiment #1, 12 ALI samples from experiment #2, and 6 1HAEs samples from experiment #3, respectively.

RCC files generated by NanoString were imported to R Studio to assess quality of all samples using the following quality control (QC) parameters:

a) Imaging QC- Each lane is imaged in discrete units called Fields of View (FOVs). All samples had FOV registration (FOV Count (number of FOVs for which imaging was attempted)/ FOV Counted (number of FOVs successfully imaged)) more than 75%.

b) Binding Density QC- Binding density is the measure of the number of optical features per square micron. If too many codes overlap, binding density is high. All samples had the binding density between 0.005-2.25.

c) Positive Control Linearity QC- There are six positive control corresponding to six different concentration in 30 µl hybridization- 128 fM, 32 fM, 8 fM, 2 fM, 0.5 fM and 0.125 fM. All samples had correlations greater than r=0.9 for the positive controls.

d) Positive Control Limit of Detection QC- This is an estimate of systemic background controls within any single hybridization reaction. All samples had counts for 0.5 fM positive control above the mean of negative controls.

e) Positive Control Scaling Factor QC- All lanes had positive control scaling factor within a range of 0.3-3 (If outside the range, it may indicate under-performance of the lane).

All samples were normalized using the positive controls to normalize for all platform associated sources of variation in each experiment. To do this, geometric mean of positive controls for all samples was calculated, which was then divided by geometric mean of each sample, to generate a positive control normalizing factor. The raw counts were multiplied by the positive control normalization factor.

Genes with positive control normalized counts for at least 2 samples less than the maximum value of negative controls were excluded in each experiment. All samples from each experiment were then normalized separately using total sum normalization. To do this, counts of all genes were summed for each sample. Total sum normalizing factor for each sample was then calculated by dividing the mean sum of all samples by the sum of each sample. All genes in each sample were multiplied by total sum normalization factor.

2.12.2 Differential abundance analysis

2.12.2.1 Differential abundance analyses results in Chapter 3

Chapter 3 reports differential RNA transcript abundance analyses of ALI cultures using Immune Profiling Panel and Asthma Elements Panel. ALI cultures incubated with PBS alone and *A. fumigatus* conidia suspended in PBS from both experiment #1 and experiment #2 were analyzed using the Immune Profiling Panel. These samples were combined together after total sum normalization was performed for differential abundance analysis (total n=12, n=6 for control (PBS alone) and n=6 for infected (PBS+ *A. fumigatus* conidia). All 12 samples were

adjusted for batch effects using ComBat function in the Surrogate Variable Analysis (sva) package [version 3.22.0] in R statistical computing program.

ALI cultures incubated with PBS alone and *A. fumigatus* conidia suspended in PBS from experiment #1 were analyzed using Asthma Elements Panel.

Differential abundance of RNA transcripts in ALI cultures of primary HBECs upon exposure to *A. fumigatus* was determined using least squares regression in the Linear Models for MicroArrays (LIMMA) [version 3.30.13] package. TEER values were added as a co-variate to the linear model. A p-value < 0.05 was considered statistically significant and the Benjamini-Hochberg False Discovery Rate (BH-FDR) of 30% was applied as well. All software packages used to perform differential expression analyses were accessed through The Comprehensive R Archive Network (CRAN) (https://cran.rproject.org/).

2.12.2.1 Differential abundance analysis results in Chapter 4

Chapter 4 reports differential RNA transcript abundance analyses of 1HAEs cultures incubated with PBS alone (control, n=3) and *A. fumigatus* conidia suspended in PBS (infected, n=3), analyzed using Immune Profiling Panel and Asthma Elements Panel. Differential abundance analysis of RNA transcripts in submerged monolayer cultures of 1HAEs upon exposure to *A. fumigatus* conidia for 6 hours was determined using least squares regression in the Linear Models for MicroArrays (LIMMA) [version 3.30.13] package in R statistical computing program. A p-value < 0.05 was considered statistically significant and the BH-FDR of 30% was also applied.

In addition, 12 ALI samples from experiment #2 were also assessed using Immune Profiling Panel. Differential abundance analysis was conducted by comparing ALI cultures

incubated with PBS alone (control, n=3) to ALI cultures incubated with *Δkdnase A. fumigatus (Δkdnase* infected*, n=3)* or RSV (RSV infected, n=3). Similarly, least squares regression in the Linear Models for MicroArrays (LIMMA) [version 3.30.13] package in R statistical computing program was used. A p-value < 0.05 was considered statistically significant and the BH-FDR of 30% was also applied.

Lastly, differential abundance analysis was also conducted between 4 High TEER samples and 2 low TEER samples in experiment #1, without accounting for the addition of conidia.

2.13 Statistical analysis of protein expression

2.13.1 Pre-processing of ALI samples

In all three samples from experiment #1, 2875 proteins were quantified. Protein ratios were log2 transformed. To confirm for MaxQuant normalized ratios, median had to be zero for the log2 transformed ratios in each sample. Proteins with at least 2 out of 3 samples with quantification events were included in the analysis. Of the 2875 proteins, 1793 proteins remained after filtering.

2.13.2 Pre-processing of 1HAEs cultures

In all three samples, 1247 proteins were quantified. Protein ratios were log2 transformed. Since MaxQuant normalized ratios did not have a median of zero, log2 transformed data distributions of all samples were shifted to the median of zero. Proteins with at least 2 out of 3 samples with quantification events were included in the analysis. Of the 1247 proteins, 553 proteins remained after filtering.

2.13.3 Differential abundance analyses

Differential abundant analysis was conducted in (LIMMA) [version 3.30.13] in R for both experiment #1 of ALIs and experiment #3 of 1HAEs. Model matrix was created to test if ratios were different from 1 using moderated t-test in LIMMA. A p-value < 0.05 was considered statistically significant. A BH-FDR of 30% was also applied.

2.14 Bioinformatics analysis

Pathway enrichment analyses of differentially abundant RNA transcripts and proteins were conducted in Enrichr (http://amp.pharm.mssm.edu/Enrichr/) (E. Y. Chen et al. 2013; Kuleshov et al. 2016). Data were also analyzed using Ingenuity Pathway Analysis (IPA) (QIAGEN Inc., https://www.qiagenbioinformatics.com/products/ingenuity-pathway-analysis) to assess the top networks associated with differentially abundant proteins (Krämer et al. 2014).

The Cytoscape plug-in, ClueGo [Version 2.5.0] + CluePedia [Version 1.5.0] (Bindea et al. 2009; Bindea, Galon, and Mlecnik 2013) was used to generate functionally grouped networks of enriched gene ontology (GO) terms associated with biological processes, molecular function and cellular components for differentially abundant RNA transcripts (p-value < 0.01).

Gene Ontology Consortium's PANTHER Overrepresentation Test (http://www.geneontology.org/page/go-enrichment-analysis) was also used to generate enriched GO terms for biological processes, molecular functions and cellular components of differentially abundant proteins (The Gene Ontology Consortium 2017; Ashburner et al. 2000). *Homo sapiens* was used as a reference list and Fisher's Exact with FDR multiple test correction was used (BH-FDR < 0.05).

Chapter 3 Host response to *Aspergillus fumigatus* conidia in an air-liquid interface model of human bronchial epithelium

3.1 Introduction

Cell culture model systems have been important for studying basic cell biology, replicating disease mechanisms and for testing novel drug compounds over the past decades (Segeritz and Vallier 2017). Substantial work has been conducted using cell culture models to understand the interaction between the airway epithelium and the airborne fungal pathogen, *Aspergillus fumigatus (A. fumigatus)*. However, most of these studies have utilized submerged monolayer cultures to model the airway epithelium; in particular, using bronchial epithelial cells and type II alveolar epithelial cells. Studies have yet to be conducted using type I alveolar cells. (Croft et al. 2016). The human bronchial epithelial cell lines such as BEAS-2B (Albright et al. 1990; Balloy et al. 2008; Fekkar et al. 2012) and 16HBE14o- (Forbes et al. 2003; Gomez et al. 2010), have been primarily used to model bronchial epithelial infections, such as those occurring in individuals with allergic bronchopulmonary aspergillosis (ABPA), a disease that affects asthmatics and patients with cystic fibrosis (Knutsen and Slavin 2011; Tracy et al. 2016). 16HBE14o- cells have been shown to internalize 30-50% of bound conidia within 6 hours of co-incubation (Gomez et al. 2010). To investigate *A. fumigatus* infections of the lower airways, e.g., invasive aspergillosis (Dagenais and Keller 2009; Espinosa and Rivera 2016),submerged monolayer cultures of A549o-, a type II pneumocyte cell line derived from human lung carcinoma, have been extensively used (Julie A. Wasylnka and Moore 2002; Alekseeva et al. 2009). A549 cells internalize 30% of bound conidia (Julie A. Wasylnka and Moore 2002). In

addition, one study employed a co-culture model of the human alveolus with primary human pulmonary artery endothelial cells and A549 epithelial cells to model IA (Gregson, Hope, and Howard 2012). The advantages of these cell line are their cost-effectiveness, ease to use and indefinite growth; however, as these cells are transformed, their responses to pathogens may differ from the intact host (Kaur and Dufour 2012).

Some investigators have used submerged monolayer cultures of primary human airway epithelial cells to gain insights into the host-pathogen interaction (Oguma et al. 2011; Oosthuizen et al. 2011). In contrast to cell lines, primary cells are not transformed and, at least during early passages, are a better model of the physiological state of the cells *in-vivo*. Key experiments conducted using cell lines are usually repeated with primary cells (Kaur and Dufour 2012). However, conventional submerged monolayer cultures of primary cells still have limitations such as they allow only one cell type to be cultured in a monolayer; consequently, they do not possess the varied cell types and complex functionality of the *in-vivo* epithelium (O'Boyle et al. 2017).

A few studies have analyzed the interaction of lung epithelial cells and *A. fumigatus in-vivo* using animal models (Kurup and Grunig 2002); however, the molecular response is complex, and it is difficult to collect data from a single epithelium. Furthermore, there are also quantitative and qualitative differences between the anatomy, physiology and molecular responses of humans and other animals (Kheradmand et al. 2002; Porter et al. 2009). As an alternative to submerged cultures, others have successfully grown bronchial epithelial cells at an air-liquid interface (ALI) for 21-28 days to generate polarized epithelial cells that possess tight junctions and form a pseudo-stratified epithelium that contains basal cells, mucus-

secreting goblet cells and ciliated cells. For example, phagocytosis of *A. fumigatus* conidia by epithelial cells has been shown using 14-day old ALI cultures of human primary nasal epithelial cells (Botterel et al. 2008) and porcine tracheal epithelial cells (Khoufache et al. 2010). However, to our knowledge, there have been no studies of the early molecular response of the host airway cells to *A. fumigatus* conidia that use well-differentiated ALI cultures (21-28 days old) of human bronchial epithelial cells.

Submerged cell culture models have been used to assess conidial internalization by cells upon exposure to *A. fumigatus* (Paris et al. 1997; Julie A. Wasylnka and Moore 2003, 2002; Botterel et al. 2008; Han et al. 2011; Rammaert et al. 2015). Other studies quantified the *A. fumigatus*-induced release of cytokines (Zhang et al. 2005; W.-K. Sun et al. 2012; Tomee et al. 1997; Borger et al. 1999; Kauffman et al. 2000; Bellanger et al. 2009) or activation of signaling proteins and pathways (Han et al. 2011; Sharon et al. 2011; Balloy et al. 2008). To date, there have been few studies that utilize high-throughput "omics" techniques to study the early molecular response of human bronchial epithelial cells to *A. fumigatus*. Over the past decades, "omics" techniques have emerged as effective tools in basic, translational and clinical research that provide a better understanding of the complex host response and reveal novel molecular mechanisms in host-pathogen interactions (Culibrk, Croft, and Tebbutt 2016; Jean Beltran et al. 2017).

The transcriptomic response of cultured lung epithelial cells, 16HBE14o- and A549, to *A. fumigatus* has been studied using genome-wide microarray analysis (Gomez et al. 2010; Sharon et al. 2011). Oosthuizen et al. (2011) used a dual-organism transcriptomic approach to profile both host and *A. fumigatus* responses in parallel. More recently, the transcriptome of the

transformed human lung epithelial cell line (A549) interacting with *A. fumigatus* was assessed using RNA-sequencing (Chen et al. 2015). Proteomic analyses include a secretome analysis of cultured human bronchial epithelial cells (BEAS-2B) in response to *A. fumigatus* using differential in-gel electrophoresis (Fekkar et al. 2012). Since previous studies have primarily utilized submerged monolayer cultures, more work needs to be conducted using differentiated cultures of primary cells.

The aims of the research outlined in this chapter were to investigate the uptake of *A. fumigatus* conidia by primary human bronchial epithelial cells (HBECs) grown as ALI cultures that contained basal, mucus-secreting goblet and ciliated cells, and analyze the early molecular response of HBECs upon exposure to *A. fumigatus* conidia using transcriptomic and proteomic analyses. The immune response of the host upon interaction with *A. fumigatus* was assessed by analyzing the transcriptomics, and an unbiased approach was used to study the molecular response using proteomics. The hypothesis for this chapter is that a multi-OMIC molecular approach in a co-culture model that closely mimics the *in-vivo* airway epithelium will provide novel insights into the early molecular response by the host upon interaction with *A. fumigatus* conidia.

3.2 Overview of experimental design for transcriptomic and proteomic studies

To determine the early molecular response of ALI cultures of primary HBECs to exposure to *A. fumigatus* conidia, two separate experiments were conducted (each using cells from a different donor) (Figure 3.1). For each experiment, ALI cultures of primary HBECs were incubated with PBS alone (control , n=3) or *A. fumigatus* conidia suspended in PBS, MOI=10 conidia/cell (infected, n=3). The basal sides of ALI cultures were incubated with ALI PneumaCult

medium (Stemcell Technologies, Vancouver, BC, Catalog #05001). The transcriptome was analyzed using nCounter Immune Profiling Panel (n=12, control (n=6) and infected (n=6)) and nCounter Asthma Elements Panel (n=6, control (n=3) and infected (n=3)). Shotgun proteomics was conducted using Liquid Chromatography Tandem Mass Spectrometry (LC-MS/MS). Differentially abundant RNA transcripts and proteins upon exposure to *A. fumigatus* were identified.

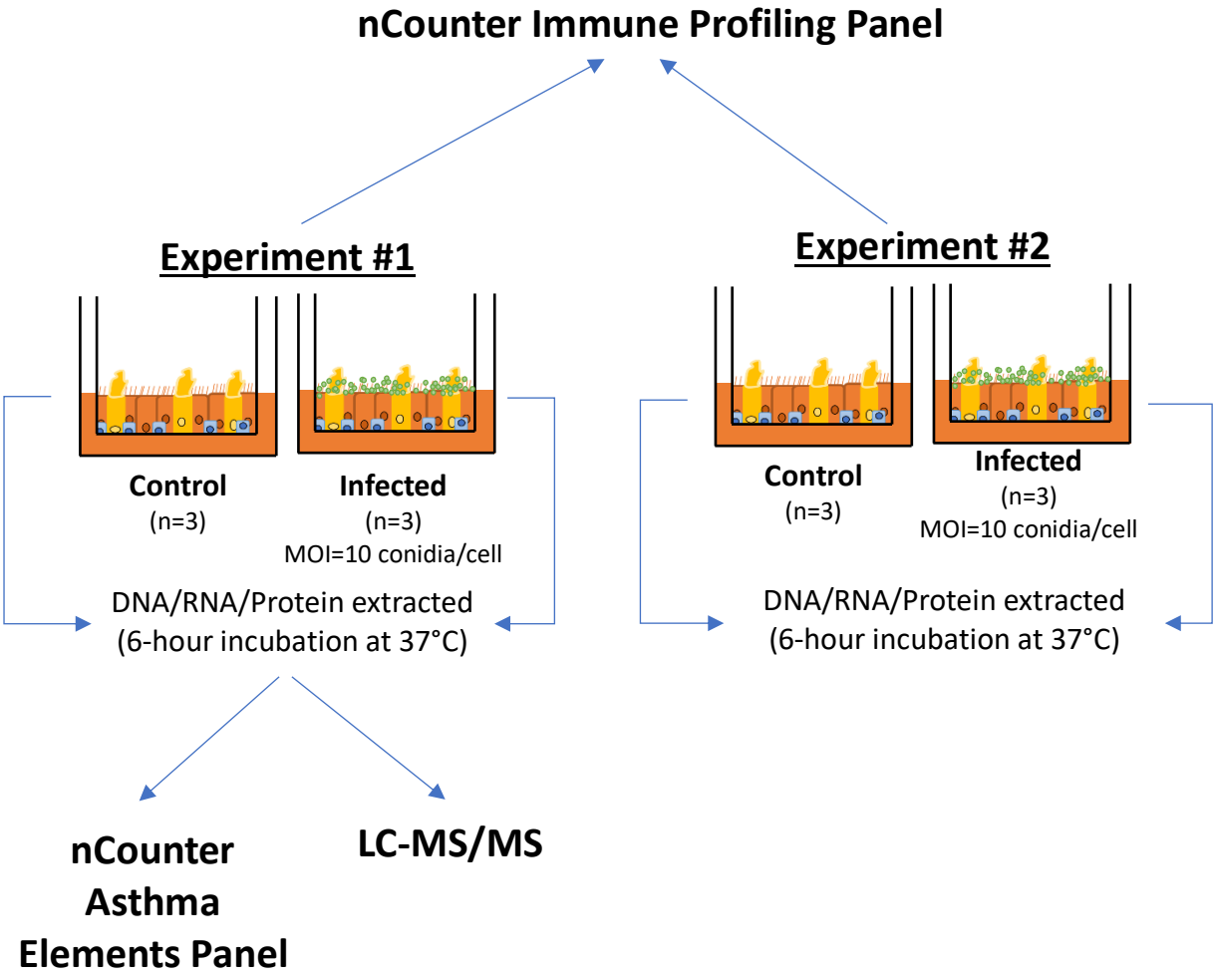

Figure 3.1: Experimental design for transcriptomics and proteomics analyses.
Two separate experiment were performed, each with 3 control and 3 infected samples. The control samples were incubated with PBS alone and infected samples with *A. fumigatus* conidia suspended in PBS for 6 hours at 37 °C. The 6 samples from experiment #1 were analyzed using nCounter Asthma Panel and LC-MS/MS. For nCounter Immune Profiling Panel, 6 samples from experiment #1 and 6 samples from experiment #2 were analyzed.

3.3 Results

3.3.1 Visualizing interaction of *A. fumigatus* conidia in well-differentiated ALI cultures of primary HBECs using confocal microscopy

Well-differentiated ALI cultures were exposed to GFP-expressing *A. fumigatus* conidia for 2, 6, 12 or 24 hours to investigate how primary HBECs interact with *A. fumigatus* conidia. The extent of conidial internalization was assessed by visualizing differentially stained conidia using confocal microscopy.

After 2 hours, ALI cultures of primary HBECs had a small number of conidia bound but no internalization was observed. After 6 hours, only few conidia were bound, and less than 1% of bound conidia were estimated to be internalized as shown in Figure 3.2.

After 12 hours, the number of conidia internalized appeared to be similar to that after 6 hours. However, after 24 hours, hyphae formation was observed from the bound conidia (Figure 3.3). Increased mucus production was observed when supernatants were removed from the apical side of ALI cultures after each time-point; this was only observed in the samples containing conidia. It is likely that the mucus production reduced conidial access to the epithelial surface.

Therefore, gene expression and proteomic studies were conducted using cultures at 6 hours post-exposure to elucidate the early molecular response of the airway epithelium, prior to significant fungal growth. This time-point is also consistent with the previously published studies using submerged monolayer cultures (Gomez et al. 2010; Oosthuizen et al. 2011).

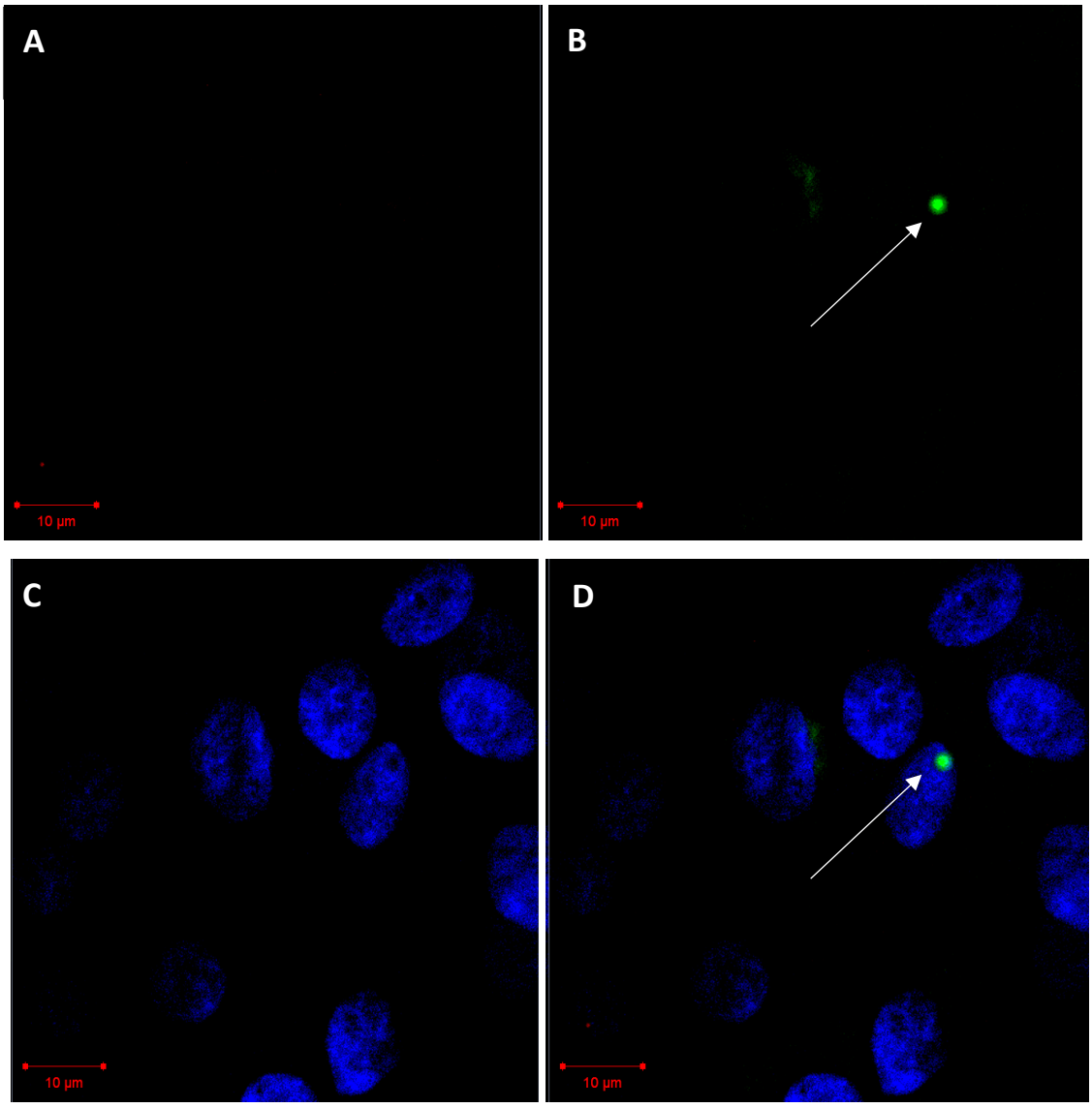

Figure 3.2 Differential staining of extracellular and internalized conidia by anti-*A. fumigatus* antibody using confocal microscopy at 6 hours post-infection.
GFP-expressing *A. fumigatus* conidia and primary HBECs grown in ALI were co-incubated for 6 hours, fixed and stained with DAPI to label cell nuclei, and a monoclonal anti-*A. fumigatus* antibody was used to label extracellular conidia, before visualization using confocal microscopy. One representative field is shown in the following channels: A) wavelength 594nm for anti-*A. fumigatus* antibody (red); B) wavelength 495nm for GFP (green); C) wavelength 405nm for DAPI (blue); D) merged GFP, anti-*A. fumigatus* antibody and DAPI image. Conidia not labeled by the anti-*A. fumigatus* antibody and only visible in the green but not the red channel were considered to be internalized by ALI cultures of primary HBECs (shown with arrows). Field of view is 1912x1912 pixels, and scale bar is 10 µm.

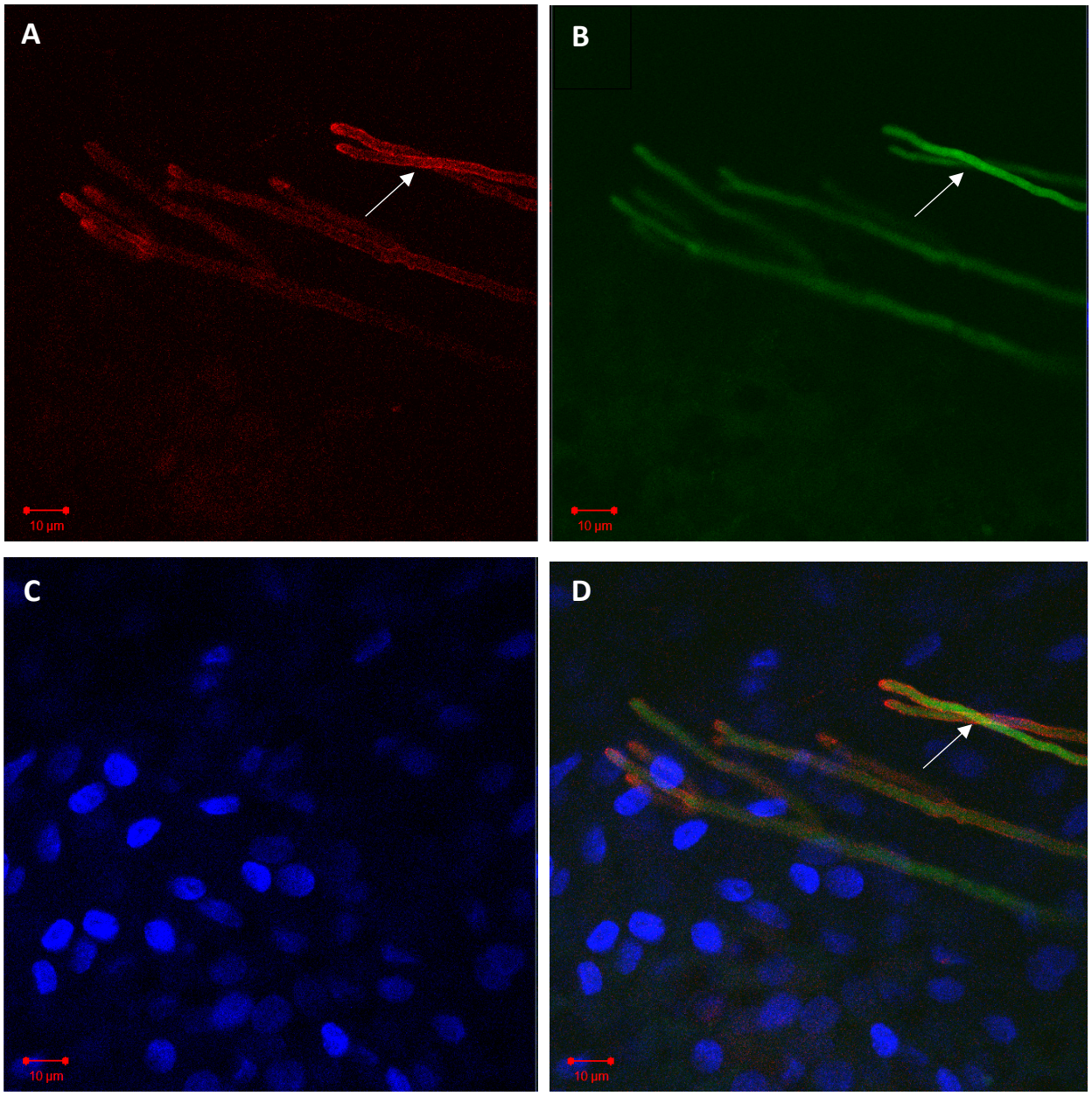

Figure 3.3: Differential staining of extracellular and internalized conidia by anti-*A. fumigatus* antibody using confocal microscopy after 24 hours of co-incubation.
GFP-expressing *A. fumigatus* conidia and primary HBECs grown in ALI were co-incubated for 24 hours and processed as described in Figure 3.2 legend. A) wavelength 594nm for anti-*A. fumigatus* antibody (red); B) wavelength 495nm for GFP (green); C) wavelength 405nm for DAPI (blue); D) merged GFP, anti-*A. fumigatus* antibody and DAPI image. Hyphae (white arrows) germinated from the bound conidia are shown; all hyphae were extracellular as evidenced by the green and red fluorescence. Field of view is 512x512 pixels with a zoom of 2x, and the scale bar is 10 µm.

3.3.2 Quantification and quality assessment of RNA samples

The concentrations of RNA extracted from experiment #1 and experiment #2 are shown in Table 3.1. RNA integrity was also assessed to ensure that the RNA was not degraded and of good quality. The RIN scores of all samples were acceptable (typically, values >8.0) (Table 3.1), except that sample infected-2 from experiment #1 was not quantified. However, further inspection of the specific chromatogram peaks for 18S and 28S indicated that total RNA for this sample was intact (data not shown).

Table 3.1: Trans-Epithelial Electrical Resistance (TEER) Values of 12 ALI cultures exposed to *A. fumigatus* conidia.

Experiment #1 12-well plate format				Experiment #2 24-well plate format			
Sample	**TEER Value (ohms)**	**RNA concentration (ng/µl)**	**RIN**	**Sample**	**TEER Value (ohms)**	**RNA concentration (ng/µl)**	**RIN**
Control-1	360	251.08	7.60	**Control-1**	1030	74.54	8.40
Control-2	440	150.00	10	**Control-2**	1029	75.9	8.50
Control-3	130	92.91	10	**Control-3**	1022	66.25	8.10
Infected-1	405	245.22	9.60	**Infected-4**	1268	71.69	9.30
Infected-2	380	195.86	N/A	**Infected-5**	1056	106.1	9.40
Infected-3	115	64.93	8.20	**Infected-6**	1197	80.32	8.10

3.3.3 Analysis of RNA transcript response to *A. fumigatus*

Preliminary analysis of samples from experiment #1 using principal component analysis (PCA) plot showed that majority of variation between control and infected samples was due to the differences between the TEER values of the samples, rather than due to the presence of the *A. fumigatus* conidia (Figure 3.4). Hence, in experiment #2, ALI cultures with approximately similar TEER values, as shown in Table 2.1, were selected to reduce variation associated with differences between TEER values. In addition, TEER values were included as a co-variate in the

linear models, as previously mentioned. The two samples with low TEER values (control-3 and infected-3) were also grouped together, separately from the other ten samples of well-differentiated ALIs.

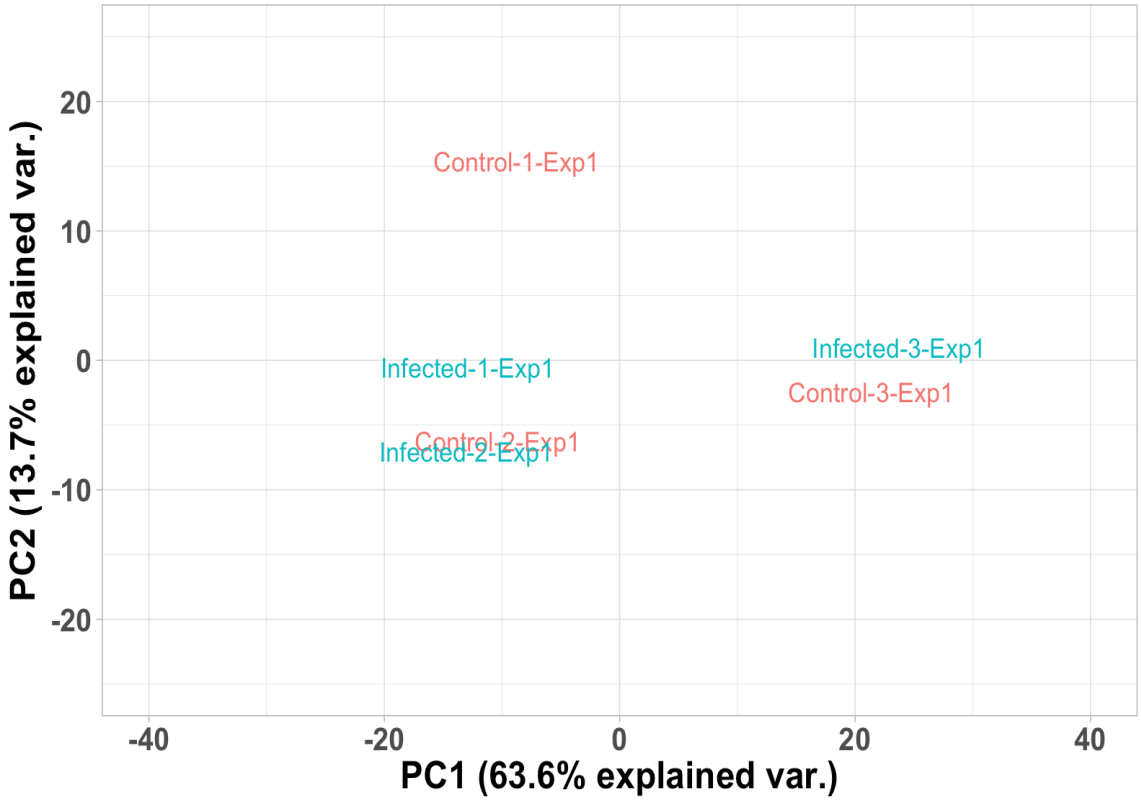

Figure 3.4: Principal Component Analysis of 6 ALI samples from experiment #1.
As shown, principal component 1 (PC1) is describing 63% of variation between 4 samples (control-1-Exp1=360, infected-1-Exp1=405, control-2-Exp1=440, infected-2-Exp1=380) with high TEER values and 2 samples (control-3-Exp1=130, infected-3-Exp1=115) with low TEER values. Hence, majority of variation between control and infected samples is due to the differences in TEER value.

3.3.3.1 nCounter Asthma Elements Panel

Transcriptomics of immune related genes associated with Asthma in ALI cultures of primary HBECs grown were analyzed upon interaction with *A. fumigatus* conidia. Differential abundance analysis of control (n=3) and infected (n=3) samples showed 7 RNA transcripts to be differentially abundant (P-value < 0.5) (Appendix 1). We used a MA plot, a Bland-Altman plot

where data was transformed onto M (log2 ratio) and A (mean average) scales, to compare control ALI cultures with infected cultures. Figure 3.5 shows that 3 RNA transcripts were up-regulated and 4 were down-regulated (Figure 3.5). None of the RNA transcripts were significant under BH-FDR < 0.30.

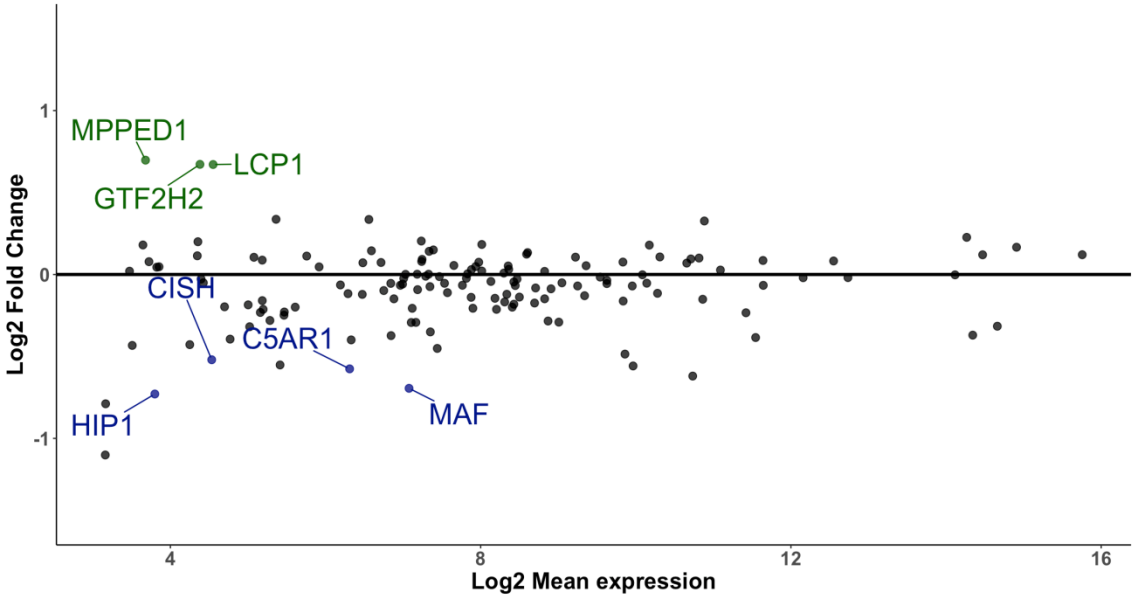

Figure 3.5: MA plot of RNA transcript analysis using NanoString's Element's Asthma Panel. MA plot of RNA transcripts differentially abundant in primary HBECs grown in ALI upon exposure to *A. fumigatus* for 6 hours. 7 genes were differentially abundant (P-value < 0.05). Of these, 3 genes were up-regulated (labeled in green) and 4 genes were down-regulated (labeled in blue) upon exposure to conidia.

The 3 up-regulated RNA transcripts were Metallophosphoesterase Domain Containing 1 (MPPED1), Lymphocyte Cytosolic Protein 1 (LCP1) and General Transcription Factor IIH Subunit 2 (GTF2H2). The 4 down-regulated RNA transcripts were Cytokine Inducible SH2 Containing Protein (CISH), Complement C5a Receptor 1 (C5AR1), MAF BZIP Transcription Factor (MAF) and Huntingtin Interacting Protein 1 (HIP1).

3.3.3.2 nCounter Immune Profiling Panel

Transcriptomics of immune related genes of primary HBECs grown in ALI were analyzed. ALI cultures of both control and infected samples were treated identically, except for the addition of PBS to control and *A. fumigatus* conidia suspended in PBS to the infected samples. Principal Component Analysis (PCA) plot showed separation between control and infected samples upon batch correction (Figure 3.6B), compared to samples without batch correction (Figure 3.6A).

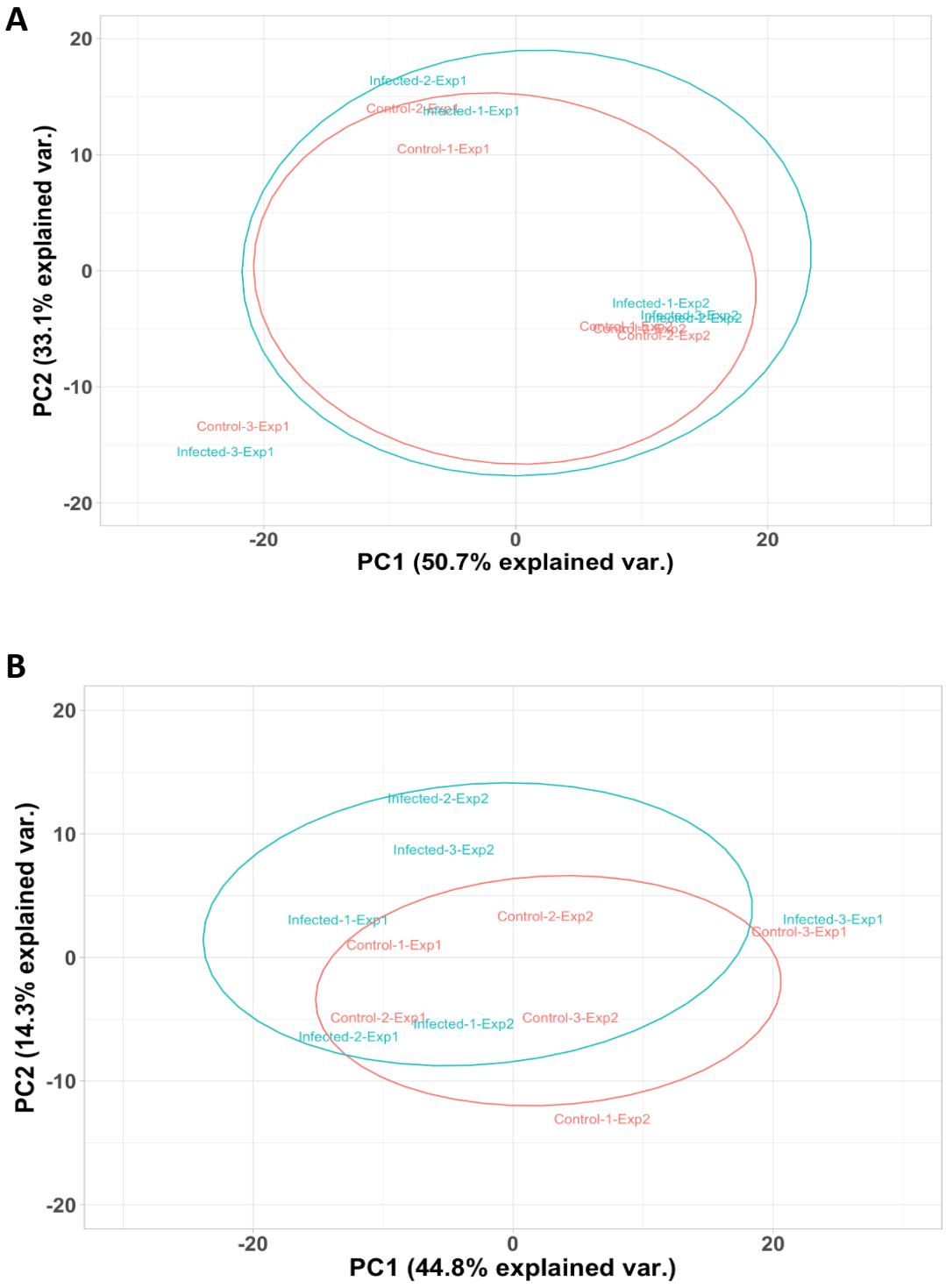

Figure 3.6: Principal Component Analysis (PCA) plot before and after batch correction of all samples.

A) PCA plot of all 12 samples before batch correction. B) PCA plot of all 12 samples after batch correction was performed using ComBat function in SVA package.

Of the 359 RNA transcripts assessed for differential abundance analysis, 41 RNA transcripts were differentially abundant (P-value < 0.05) at 6 hours post-exposure to *A. fumigatus* conidia (Figure 3.7) (Appendix 2). Of these 41, 11 RNA transcripts were significant under BH-FDR < 0.30, labeled in Figure 3.7A. Compared to control ALI cultures, 28 RNA transcripts were up-regulated and 13 RNA transcripts were down-regulated. The up-regulated RNA transcript with maximum Log2 fold change (Log2 fold change=0.9027, p-value= 0.0092, BH-FDR= 0.2998) was CCL15 (C-C Motif Chemokine Ligand 15). For the down-regulated differentially abundant RNA transcripts, CXCL5 (Chemokine (C-X-C motif) Ligand 5) had the maximum Log2 fold change (Log2 fold change=-1.1465, p-value= 0.0320, BH-FDR=0.3315).

KEGG pathway enrichment analysis was conducted in Enrichr (http://amp.pharm.mssm.edu/Enrichr/) to determine major biological themes associated with differentially abundant RNA transcripts (E. Y. Chen et al. 2013)(Kuleshov et al. 2016). KEGG pathways related to apoptosis, natural killer cell mediated cytotoxicity, JAK-STAT signaling pathway and NF-kappa B signaling pathway were associated with the 28 up-regulated RNA transcripts in the infected ALI cultures (Figure 3.7B). The 13 down-regulated RNA transcripts were mainly enriched for cytokine-cytokine receptor interaction and genes involved in the complement and coagulation cascades (Figure 3.7B).

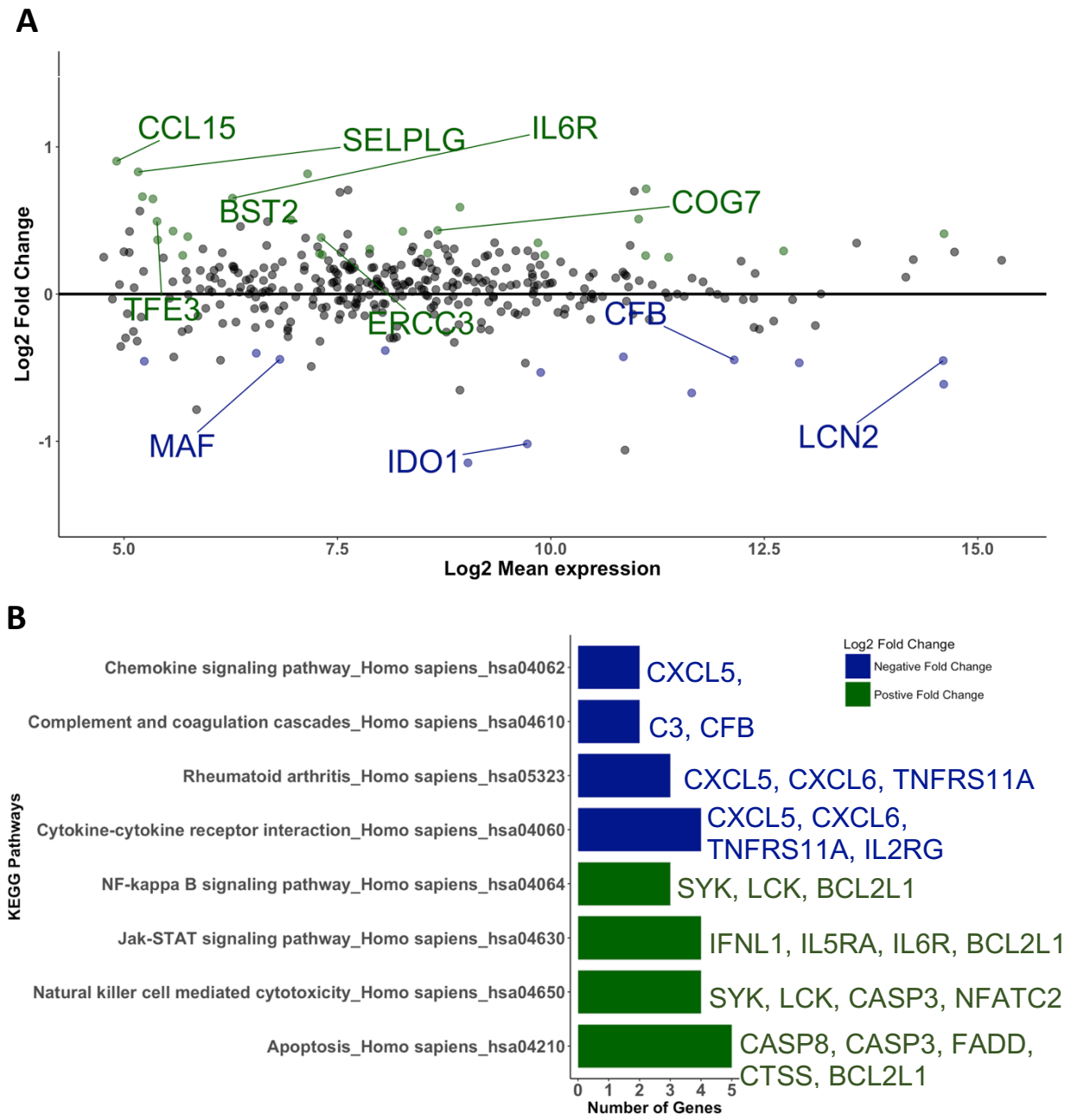

Figure 3.7: MA plot and pathway enrichment analysis of RNA transcripts differentially abundant in Immune Profiling Panel

A) MA plot of RNA transcripts abundant by primary HBECs grown in ALI upon exposure to *A. fumigatus* 6 hours post-exposure. 41 genes were differentially abundant (P-value < 0.05). Of these, 28 genes were up-regulated (green) and 13 genes were down-regulated (blue) upon exposure to conidia. 11 genes were significant under BH-FDR < 0.30 (labeled genes). B) Enrichr identified enriched KEGG pathways for upregulated (green) and downregulated (blue) RNA transcripts upon exposure to *A. fumigatus* conidia (Adjusted P-value > 0.05).

Gene Ontology (GO) enrichment analysis using the Cytoscape plug-in, CLUEGO, showed that differentially abundant RNA transcripts were enriched for death-inducing signaling cellular component, and icosanoid secretion, monocyte chemotaxis, myeloid leukocyte migration were the major biological processes (Figure 3.8).

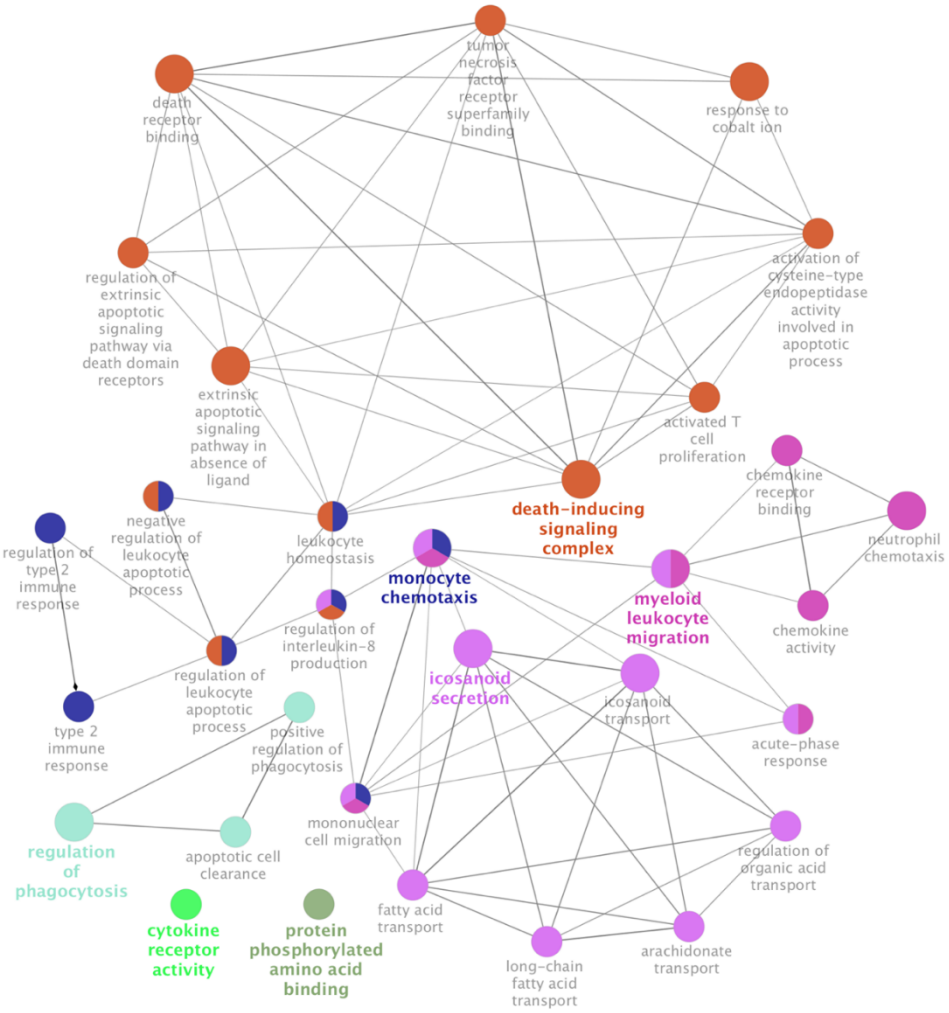

Figure 3.8: Gene ontology enrichment analysis of differentially abundant RNA transcripts in Immune Profiling Panel.

A) Functionally Grouped network of Gene Ontology enrichment analysis of differentially abundant RNA transcripts in ClueGO App (P-value < 0.1). The differentially abundant RNA transcripts were enriched in death-inducing signaling complex, myeloid leukocyte migration, monocyte chemotaxis, icosanoid secretion, regulation of phagocytosis, cytokine receptor activity, and protein phosphorylated amino acid binding.

3.3.4 Analysis of the proteomic response to *A. fumigatus*

LC-MS/MS was used to assess the proteomic response of primary HBECs in ALI to conidial exposure. Untargeted protein differential abundance analysis 6 hours post-exposure to *A. fumigatus* conidia was assessed in control (n=3) and infected (n=3) samples.

Differential abundance analysis of 1793 proteins in LIMMA using normalized ratios of Heavy (infected) to Light (control) protein samples showed that 153 proteins were differentially abundant 6 hours post-exposure to *A. fumigatus* conidia in infected samples (Figure 3.9A) (Appendix 3). Of these 153, 22 proteins were significant under BH-FDR < 0.30. Compared to control samples, 73 proteins were up-regulated and 80 proteins were down-regulated. Three proteins, CALR (Calreticulin), NUCB2 (Nucleobindin 2) and SET (SET nuclear proto-oncogene), had fold-changes greater than 2 (Figure 3.9). Of these 3 proteins, CALR had the highest fold change of 5.723.

Ingenuity pathway analysis was conducted to analyze the top networks associated with differentially abundant proteins (Krämer et al. 2014); cell cycle, gene expression and tissue morphology was the top network with a score of 53 (Figure 3.10). IPA score is based on the fit of a network to the input of genes. It is generated from the p-value and represents the likelihood of finding the input of genes together in the network. For example, a score of 53 indicates that there is 1E-53 chance that the input genes are together in a particular network due to random chance. Overall, the top 5 networks were associated with cell death, protein synthesis and post-translational modification (Table 3.2).

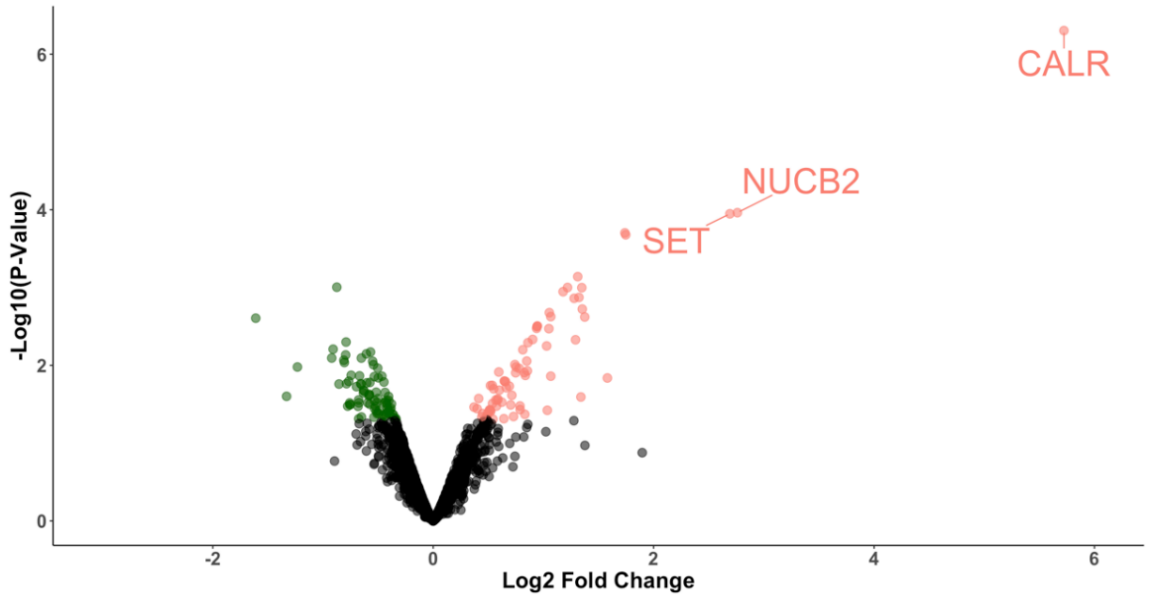

Figure 3.9: Volcano plot and network analysis of differentially abundant proteins identified using shotgun proteomics.

Volcano plot of 1793 quantified proteins. Differential abundance analysis showed that 153 proteins were differentially abundant upon 6 hours post-exposure to *A. fumigatus* (P-Value < 0.05). Of these 153, 73 were upregulated (pink) and 80 were down-regulated (green). Three proteins, SET, NUCB2 and CALR, had a fold-change greater than 2.

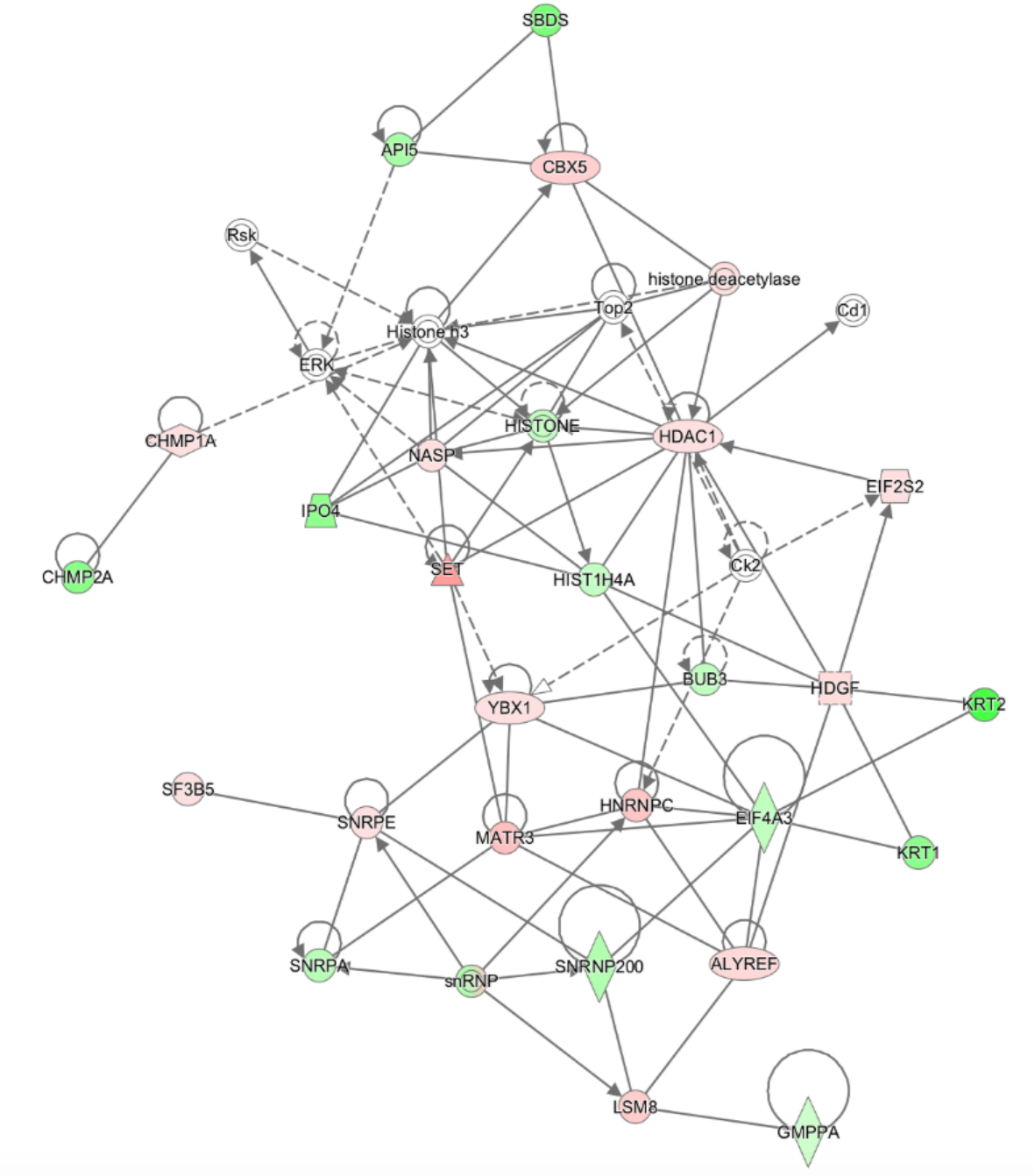

Figure 3.10 Network analysis of 153 proteins using Ingenuity pathway analysis (IPA). Genes in the top network was related to cell cycle, gene expression and tissue morphology (Score =53). The up-regulated proteins upon exposure to *A. fumigatus* are shown in green and down-regulated genes are shown in red.

Table 3.2*:* Top 5 networks identified using Ingenuity pathway analysis (IPA).

Network	Score
Cell Cycle, Gene Expression, Tissue Morphology	**53**
Cancer, Cell Death and Survival, Organismal Injury and Abnormalities	44
Cellular Development, Protein Synthesis, Gene Expression	34
Post-Translational Modification, Protein Degradation, Endocrine System Disorders	27
Drug Metabolism, Protein Synthesis, Renal Damage	23

I also conducted a pathway enrichment analysis for differentially abundant proteins in Enrichr using the Reactome database (http://amp.pharm.mssm.edu/Enrichr/) (E. Y. Chen et al. 2013)(Kuleshov et al. 2016). The enriched pathways for differentially abundant proteins were: Translation, Metabolism of proteins, 3`-UTR mediated translational regulation, Nonsense mediated decay, Major pathway of rRNA processing in the nucleolus and Metabolism of amino acids and derivatives (Table 3.3).

Table 3.3: Enriched Reactome pathways for differentially abundant proteins identified using Enrichr.

ID	Term	Overlap	P-value	Adjusted P-value
R-HSA-72766	**Translation**	22/151	3.90703E-22	2.53566E-19
R-HSA-392499	**Metabolism of proteins**	43/1074	7.60833E-20	2.4365E-17
R-HSA-157279	**3' -UTR-mediated translational regulation**	18/106	1.57142E-19	2.4365E-17
R-HSA-168255	**Influenza Life Cycle**	17/136	3.60394E-16	1.7992E-14
R-HSA-1799339	**SRP-dependent co-translational protein targeting to membrane**	16/107	1.47713E-16	8.71507E-15
R-HSA-927802	**Nonsense-Mediated Decay (NMD)**	16/106	1.26443E-16	8.20614E-15
R-HSA-6791226	**Major pathway of rRNA processing in the nucleolus**	14/166	3.73975E-11	8.66821E-10
R-HSA-71291	**Metabolism of amino acids and derivatives**	17/335	8.42701E-10	1.82304E-08
R-HSA-72163	**RNA Splicing - Major Pathway**	10/134	8.2771E-08	1.6787E-06
R-HSA-597592	**Post-translational protein modification**	14/521	4.86567E-05	0.0007702
R-HSA-199977	**ER to Golgi Anterograde Transport**	7/131	6.75186E-05	0.001043323
R-HSA-381038	**XBP1(S) activates chaperone genes**	4/53	0.000720512	0.009543107

To determine functional processes associated with 73 up-regulated proteins and 80 down-regulated proteins, gene ontology (GO) enrichment analysis was conducted using Enrichment analysis tool in the Gene Ontology Consortium (http://geneontology.org) (Ashburner et al. 2000; The Gene Ontology Consortium 2017). Some of the enriched terms for up-regulated proteins were cadherin binding, spliceosomal complex, endoplasmic reticulum-Golgi intermediate compartment and translation initiation factor activity (BH-FDR < 0.05) (Table 3.4). The down-regulated proteins were associated with extracellular exosome, nonsense-mediated decay, rRNA processing, structural constituent of ribosome, extracellular matrix, oxidation-reduction process (Table 3.5). Some terms related to translation and splicing were enriched in both up- and down-regulated proteins.

Table 3.4*:* Enriched Gene Ontology (GO) terms for 73 up-regulated differentially abundant proteins identified using Gene Ontology Consortium. (MF=Molecular Function; CC=Cellular Component; BP=Biological Processes)

GO	Term	Overlap	P-Value	FDR
MF	**cadherin binding (GO:0045296)**	11/295	9.19E-09	2.12E-05
CC	**cell-cell adherens junction (GO:0005913)**	5/92	2.31E-05	2.11E-03
CC	**ruffle (GO:0001726)**	6/165	3.03E-05	2.24E-03
MF	**protein complex binding (GO:0032403)**	13/796	4.19E-06	2.42E-03
CC	**spliceosomal complex (GO:0005681)**	6/188	6.14E-05	3.46E-03
CC	**endoplasmic reticulum-Golgi intermediate compartment (GO:0005793)**	5/115	6.42E-05	3.51E-03
CC	**U12-type spliceosomal complex (GO:0005689)**	3/27	1.57E-04	7.70E-03
CC	**precatalytic spliceosome (GO:0071011)**	3/29	1.90E-04	8.90E-03
CC	**peptidase complex (GO:1905368)**	4/93	3.76E-04	1.53E-02
MF	**translation initiation factor activity (GO:0003743)**	4/52	4.45E-05	1.86E-02
MF	**cytoskeletal protein binding (GO:0008092)**	12/884	6.14E-05	2.18E-02
CC	**centriolar subdistal appendage (GO:0120103)**	2/9	6.53E-04	2.45E-02
CC	**centriole (GO:0005814)**	4/127	1.16E-03	3.78E-02
MF	**protein homodimerization activity (GO:0042803)**	11/811	1.29E-04	4.27E-02
CC	**spliceosomal snRNP complex (GO:0097525)**	3/63	1.61E-03	4.55E-02
CC	**cell cortex part (GO:0044448)**	4/139	1.61E-03	4.60E-02

Table 3.5*:* Enriched Gene Ontology (GO) terms for 80 down-regulated differentially abundant proteins identified using Gene Ontology Consortium. (MF=Molecular Function; CC=Cellular Component; BP=Biological Processes)

GO	Term	Overlap	P-Value	FDR
CC	**extracellular exosome (GO:0070062)**	43/2757	4.67E-17	8.94E-14
BP	**nuclear-transcribed RNA catabolic process, nonsense-mediated decay (GO:0000184)**	14/119	1.40E-16	2.17E-12
BP	**SRP-dependent cotranslational protein targeting to membrane (GO:0006614)**	12/92	8.61E-15	4.46E-11
BP	**translational initiation (GO:0006413)**	13/143	3.96E-14	7.70E-11
BP	**rRNA processing (GO:0006364)**	14/261	3.42E-12	3.12E-09
MP	**structural constituent of ribosome (GO:0003735)**	12/169	6.19E-12	2.85E-08
CC	**cytosolic large ribosomal subunit (GO:0022625)**	7/65	1.34E-08	1.22E-06
CC	**cytosolic small ribosomal subunit (GO:0022627)**	5/47	1.86E-06	1.15E-04
MP	**protein binding (GO:0005515)**	67/11523	1.16E-06	1.34E-03
MP	**rRNA binding (GO:0019843)**	5/59	5.27E-06	4.05E-03
CC	**spliceosomal complex (GO:0005681)**	6/188	1.17E-04	6.03E-03
CC	**focal adhesion (GO:0005925)**	8/394	1.82E-04	8.95E-03
CC	**extracellular matrix (GO:0031012)**	9/549	3.40E-04	1.42E-02
BP	**oxidation-reduction process (GO:0055114)**	13/949	9.16E-05	1.85E-02
CC	**integral component of membrane (GO:0016021)**	9/68	4.55E-04	1.86E-02
BP	**carbohydrate metabolic process (GO:0005975)**	9/472	1.13E-04	2.25E-02
CC	**nuclear lumen (GO:0031981)**	28/3938	1.06E-03	3.97E-02

3.4 Discussion

The research outlined in this chapter investigated the early molecular response of differentiated primary human bronchial epithelial cells to *A. fumigatus* conidia using both transcriptomic and proteomic approaches. Confocal microscopy was used to visualize the

interaction of the bronchial epithelium with *A. fumigatus*. Two separate panels were used to analyze the transcriptional response of primary HBECs grown in ALI to *A. fumigatus*: the Asthma Elements Panel was used to test the applicability of NanoString in detecting the expression of 180 asthma-related genes in bronchial epithelial cells; the Immune Profiling Panel, (770 immune-related genes) was used to assess the immune response of primary HBECs grown in ALI to *A. fumigatus*. Finally, we used an untargeted approach using Liquid Chromatography-Tandem Mass Spectrometry to assess the proteomic response.

3.4.1 Visualizing interaction of *A. fumigatus* conidia in well-differentiated ALI cultures of primary HBECs

We demonstrated that although primary HBECs grown in ALI cultures are capable of phagocytosing conidia, even after 6 hours post-exposure, the proportion of bound conidia internalized was estimated to be less than 1%. Multiple studies have reported internalization of conidia by immortalized and primary airway epithelial cells *in-vitro* and *ex-vivo* using variety of infection systems and cultures models (Julie A. Wasylnka and Moore 2003, 2002; Paris et al. 1997; Zhang et al. 2005). Cultured bronchial epithelial cells and type II alveolar cells have been shown to internalize approximately 30-50% of bound conidia in both a concentration and time-dependent manner. However, no studies have reported *in-vivo* internalization of conidia by airway epithelial cells. Furthermore, no data has been published on phagocytosis of conidia by fully-differentiated ALI cultures of primary HBECs (21-28 days of growth). Two previous studies have quantified uptake of *A. fumigatus* conidia by 14-day old ALI cultures: Botterel et al. (2008) showed that human nasal epithelial cells internalized $21.8 \pm 4.5\%$ of bound conidia after 4 hours, and a study by Khoufache et al., (2010) found that $21.9 \pm 1.4\%$ of conidia were

internalized by porcine tracheal epithelial cells after 8 hours (Botterel et al. 2008)(Khoufache et al. 2010). Another study by Beisswenger et al. (2012) reported that primary HBECs grown in ALI are activated by resting conidia resulting in activation of IFN-β signaling pathway, but no phagocytosis results were reported using live *A. fumigatus* conidia (Beisswenger, Hess, and Bals 2012).

In differentiated ALI cultures of primary HBECs, negligible phagocytosis of conidia was observed up to 12 hours post-exposure, and after 24 hours, bound conidia had germinated and formed hyphae. The lower rate of conidial internalization in our study may have been due to the more differentiated state of ALI cultures; in particular, the presence of goblet cells that secreted mucus. Infected cells contained significantly more mucus than ALI cultures exposed to PBS alone; this was observed during the staining process for confocal microscopic analysis. We speculate that mucus secretion along with ciliated cells may have prevented the level of phagocytosis, reported in un-differentiated, submerged monolayer cultures. Hence, further research needs to be conducted to better understand the role of ciliated and mucus-goblet cells present in differentiated cultures of primary HBECs upon exposure to *A. fumigatus* in healthy and diseased individuals.

These results are supported by those of Rammaert et al, who measured internalization of fungal conidia by the bronchial epithelium of mice *in-vivo* using transmission electron microscopy. These authors found no phagocytosis of either *A. fumigatus* or *Lichtheimia corymbifera* spores in the first 18 hours post-exposure (Rammaert et al. 2015). Despite the low rate of phagocytosis, we observed significant changes in the transcriptome and proteome of ALI cultures exposed to conidia. Thus, the bronchial epithelium of healthy individuals does not

require phagocytosis of conidia in large numbers to initiate an immune response, and the effect of fungal conidia on the early host response is mediated either by *A. fumigatus* conidia binding to host bronchial epithelia, or alternatively, by interaction with molecules secreted by germinating conidia.

We used a relatively high MOI of 10 to assess conidial phagocytosis to ensure that a maximum number of cells interacted with conidia. Although this MOI likely overestimates normal levels of exposure of the *in-vivo* bronchial epithelium, it is consistent with previous *in-vitro* studies conducted using cell lines (Julie A. Wasylnka and Moore 2003, 2002; Gomez et al. 2010; Oosthuizen et al. 2011).

For transcriptomic and proteomic studies, we exposed ALI cultures to conidia for 6 hours because our confocal microscopy analysis revealed that phagocytosis did not increase with increasing incubation times, and germination of *A. fumigatus* conidia occurred at 24 hours. Previous studies from our laboratory have also used 6 hours of conidial exposure (Gomez et al. 2010; Oosthuizen et al. 2011) so we were able to compare the results between the previous submerged culture systems and primary HBECs grown in ALI cultures.

3.4.2 Analysis of primary HBECs ALI cultures transcriptomics to *A. fumigatus* conidia

The NanoString nCounter platform was used to assess host gene expression in differentiated cultures of primary HBECs upon exposure to *A. fumigatus* conidia. Initial analysis of gene expression changes from experiment #1 indicated that majority of the variation between samples was due to differences between TEER values instead of due to the presence of fungal conidia. Therefore, a strict filtering was used to exclude genes with low expression and to avoid false positives.

Of the 770 genes on the Immune Profiling Panel (n=12) and 180 genes on Asthma Elements Panel (n=6), 73 genes overlapped. Hence, Asthma Elements Panel allowed profiling of additional 107 genes as well. The MAF bZIP Transcription Factor (MAF), was among the differentially abundant RNA transcripts in both panels; compared to control samples, MAF was down-regulated in both analyses upon exposure to *A. fumigatus*, and it was the most significant differentially abundant RNA transcript in the Immune Profiling Panel analysis. MAF is a T_H2 associated proto-oncogene, involved in the production of IL-4, a T_H2 associated cytokine that promotes differentiation of naïve CD4+ T cells into IL-4 producing T_H2 cells (i.e., positive feedback) (J. I. Kim et al. 1999). In cultures of HBECs, IL-4 has been shown to up-regulate the production of monocyte chemoattractant protein-1 (MCP-1) (Ip, Wong, and Lam 2006), which mediates the activation and recruitment of monocytes, mast cells, basophils, eosinophils and T_H2 cells from the vascular compartment to bronchoalveolar space (Romagnani 2002). Increased expression of MCP-1 has also been observed in bronchial tissues of asthmatic patients (Sousa et al. 1994). In addition, it has been shown that *A. fumigatus* elicits a strong T_H2 response in ABPA patients (Becker et al. 2015) who have skewed pulmonary immune responses. Hence, downregulation of MAF upon exposure to *A. fumigatus* in primary HBECs from healthy individuals, may indicate a protective response to the fungus.

RNA transcripts related to complement and coagulation cascades were also differentially abundant in both panels. For example, C3 (Complement C3) and CFB (Complement Factor B) in the Immune Profiling Panel, and C5AR1 (Complement C5a Receptor 1) in the Asthma Elements Panel were down-regulated upon exposure to *A. fumigatus*. This is

consistent with previous findings that showed that *A. fumigatus* binds to complement regulators to evade host attack mediated by the complement system (Behnsen et al. 2008).

Along with MAF, the Immune Profiling Panel revealed differential abundance of RNA transcripts regulating T cell proliferation and the T_H1/ T_H2 responses as well. These included Interferon-Lamba 1 (IFN-λ1 or IL-29), Indoleamine 2,3-dioxygenase (IDO-1) and Interleukin 5 Receptor Subunit Alpha (IL-5RA). IFN-λ was up-regulated upon exposure to *A. fumigatus* conidia. Along with having anti-viral properties, IFN-λ is an inhibitor of T_H2 responses, limiting the secretion of IL-4, IL-5 and IL-13 cytokines (Koltsida et al. 2011). Reduced expression of IFN-λ was also reported in bronchial epithelial cells of asthmatic individuals upon infection with rhinovirus, indicating that it could play an immune-protective role in lower airways. (Bullens et al. 2008). IDO-1, down-regulated upon exposure to *A. fumigatus*, is known to catalyze the first step in the degradation of tryptophan (Schmidt et al. 2009). High expression of IDO-1 is thought to be associated with down-regulation of immune response as degradation of tryptophan results in inhibition of T cell proliferation and apoptosis. IL-5RA was up-regulated in ALI cultures of primary HBECs upon exposure to *A. fumigatus*. IL-5RA is a receptor for Interleukin-5 (IL-5), a T_H2 cytokine that promotes eosinophil differentiation, and results in mucus metaplasia and airway eosinophilia upon induction of allergic airway disease in bronchial epithelia of mice (C. A. Wu et al. 2010). Hence, transcriptomics of primary HBECs grown in ALI exposed to *A. fumigatus* for 6 hours show differential abundance of RNA transcripts regulating both T_H1 and T_H2 responses.

The genes encoding the neutrophil chemoattractants, such as CXCL5 and CXCL6, were down-regulated upon exposure to *A. fumigatus* whereas Annexin-1 (ANXA1) was up-regulated

upon exposure to *A. fumigatus*. ANXA1 is known to limit neutrophil recruitment and production of pro-inflammatory mediators (Sugimoto et al. 2016). Hence, this may be a protective response in the immunocompetent host to avoid tissue damage from prolonged inflammatory responses. These genes are likely to play an important role in IA, since neutrophils have been shown to control germination of A. fumigatus *in-vivo* (Feldmesser 2006).

The differentially abundant RNA transcripts in the Immune Profiling Panel were also enriched in pathways and gene ontologies related to the innate immune response. These findings are consistent with the previous results from our lab of cell-spore submerged co-cultures using primary airway epithelial cells but not transformed cell lines (Gomez et al. 2010; Oosthuizen et al. 2011). RNA transcripts associated with apoptosis, such as CASP3 (Caspase 3), CASP8 (Caspase 8), FADD (Fas-associated protein with death domain), LCN2 (Lipocalin 2), and BCL2L1 (BCL2 Like 1), were up-regulated in the Immune Profiling Panel suggesting that the interaction of conidia with epithelial cells may promote apoptosis. Apoptosis is non-inflammatory programmed cell death that occurs during cellular homeostasis and morphogenesis, as well as in response to intracellular infections (Thompson 1995). Other forms of cell death include necrosis and pyroptosis. Necrosis is a consequence of physical damage, ROS production or danger signals that results in the release of intracellular contents into the extracellular environment upon cytoplasmic swelling and osmotic lysis. In contrast, pyroptosis results in inflammasome mediated caspase-1 activation and results in release of pro-inflammatory cytokines (Thompson 1995). It has been shown that pathogenic *Candida* sp. can induce apoptosis in epithelial cells, and pro- and anti-apoptotic genes are activated as early as 6 hours post-infection, followed by necrosis (Villar and Zhao 2010; Moyes et al. 2014). Little is

known about the fungal components of *A. fumigatus* that may induce apoptosis or other forms of cell death. Differential abundance of up-regulated RNA transcripts associated with apoptosis may be due to a secondary metabolite produced by *A. fumigatus* called gliotoxin. It is known to induce pathways associated with apoptosis in human bronchial epithelial cells by the Bcl-2 pathway (extrinsic pathway) as well as *via* a caspase-dependent mechanism (intrinsic pathway) (Geissler et al. 2013)(Zheng et al. 2017). Genes upregulated in our study such as CASP8, BCL2L1 are involved in such pathways, and these have been shown to have a role in promoting autophagy as well as apoptosis (Gurung and Kanneganti 2015). Autophagy is a pro-survival mechanism that allows cell to survive prolonged stress caused by infectious agents or nutrient deprivation by clearing damaged proteins, organelles or by providing the cell with energy and anabolic building blocks (Gump and Thorburn 2011). Hence, increased expression of genes associated with apoptosis and autophagy in the presence of *A. fumigatus* indicates that HBECs may be undergoing cell stress and/or nutrient deprivation, resulting in apoptosis or/and autophagy to prevent fungal invasion of the host. More studies need to be conducted to elucidate the role of defense systems such as apoptosis and autophagy in order to advance our knowledge regarding interaction of *A. fumigatus* and epithelial cells.

3.4.3 Analysis of primary HBECs ALI cultures proteomics to *A. fumigatus* conidia

We also quantified changes to the proteome of primary HBECs upon exposure to *A. fumigatus* conidia. The data revealed proteins regulating the secretory pathway to be significantly up-regulated in the infected samples after 6 hours. Recent studies have also implicated the role of autophagy in the secretory pathways; specifically, autophagy deficiency has been associated with decreased mucus secretion by decreasing generation of ROS, which

reduces calcium release from ER. Therefore, up-regulation of RNA transcripts associated with autophagy may be associated with excessive mucus production observed during confocal analysis in primary HBECs upon exposure to *A. fumigatus* compared to control samples.

The top three proteins, CALR, NUCB2 and SET had the highest fold change of all the proteins; these proteins are involved in protein folding and quality control as well as calcium metabolism. CALR, an intracellular chaperone, has been shown to mediate phagocytosis of *A. fumigatus* conidia by forming a calreticulin-CD91 complex (Wong and Aimanianda 2017). Up-regulation of CALR has also been associated with increased Ca^{2+} storage capacity in the endoplasmic reticulum (ER) as well as increased sensitivity to apoptosis (Mery et al. 1996; Johnson et al. 2001). NUCB2 is a calcium binding protein (Kalnina et al. 2009), whereas, SET is a multi-tasking protein involved in processes such as apoptosis, transcription, nucleosome assembly and histone chaperoning (Beresford et al. 2001). Up-regulation of proteins related to calcium metabolism and binding, such as CALR and NUCB2, indicates ER stress, which can promote cell-death (apoptosis) or cell-survival (autophagy), and release of Ca^{2+} from the ER (Sano and Reed 2013). Features of ER stress include high protein demand, infection, inflammatory cytokines and mutant protein expression in the ER. As a response, the unfolded protein response (UPR) is activated (Hetz 2012). Enrichment of pathway and gene ontologies associated with UPR confirms the existence of ER stress in the infected samples.

Activation of UPR can result in the up-regulation of molecular chaperones to assist in protein folding, a halt to protein translation and degradation of misfolded proteins (Hetz 2012). Cell death results when UPR fails to restore ER homeostasis (Oslowski and Urano 2011). In our study, other than CALC, heat shock protein 90α (HSP90AA1 or HSP90α) was also up-regulated

upon exposure to *A. fumigatus*. HSP90α is an isoform of molecular chaperone Hsp90, and has been shown to be up-regulated in the presence of stress (Zuehlke et al. 2015). Furthermore, elevated levels of HSP90α were reported in the serum of individuals with chronic obstructive pulmonary disease (COPD) (Hacker et al. 2009). HSP90AA1 was one of the 8 differentially abundant genes from the current study that was also differently abundant in our previous study (Gomez et al. 2010); however, using the submerged cultures, HSP90AA1 was down-regulated upon exposure to *A. fumigatus* conidia. Nevertheless, this gene appears to play an important role in the host-pathogen interaction.

Along with UPR, ER stress can result in release of Ca^{2+} from the lumen into the cytosol. High levels of cytosolic Ca^{2+} have been shown to attenuate nonsense mediated decay (NMD) (Nickless, Bailis, and You 2017). The results from our gene ontology analysis are in agreement with this report: the majority of proteins associated with NMD were down-regulated upon exposure to conidia. Inhibition of NMD can also result from phosphorylation of EIF Factor 2 Subunit Beta (EIF2S2) (Nickless, Bailis, and You 2017). Interestingly, EIF2S2 protein was up-regulated upon exposure to conidia in our study.

We also found that proteins that regulate other translational processes were both up-regulated and down-regulated in primary HBECs upon exposure to *A. fumigatus,* as indicated by enriched pathways and gene ontologies. For example, proteins associated with eukaryotic translation initiation (EIF) such as EIF factor-3 Subunit J (EIF3J), EIF Factor 2 Subunit Beta (EIF2S2) (as noted above) were up-regulated upon exposure to *A. fumigatus* conidia. The majority of ribosomal proteins including those from the 60S large subunit (RPL) and 40S small subunit (RPS), such as RPL3, RPS8 , RPS5, were down-regulated upon exposure to A*. fumigatus*

in our study. Ribosomal proteins can play a role in regulating apoptosis, cell cycle and cell proliferation (X. Xu, Xiong, and Sun 2016). Moreover, down-regulation of ribosomal protein synthesis could serve to lower the overall protein traffic into the ER during ER stress.

Proteins regulating cellular processes such as cell cycle progression were also up-regulated upon exposure to *A. fumigatus* in our study. These included SET and HSP90AA1, as previously mentioned. However, other proteins that we found to be up-regulated upon exposure to *A. fumigatus* and that were essential for cell cycle progression and formation of cilia included Cenexin (ODF2), Dynactin (DCTN1), FGFR1 Oncogene Partner (FGFR1OP or FOP), Histone deacetylase 1 (HDAC1) and Tumor Protein P53 Binding Protein 1 (TP53B1). HDAC1 is known to be important for cell cycle progression and is associated with chronic lung disease in human. Inhibition of HDACs results in cellular growth arrest, differentiation and apoptosis (Shakespear et al. 2011). TP53B1 binds to tumor suppressor protein p53 and is involved in DNA-damage signaling pathways (Rappold et al. 2001). ODF2 is known to be important component of centrosome and basal body and is necessary for the formation of primary cilia. It is also reported to be up-regulated in quiescent cells (Pletz et al. 2013). DCNT1, is also involved in mitotic spindle assembly and primary cilia formation (Ayloo et al. 2014; T.-Y. Chen et al. 2015). FGFR1OP is known to be essential for ciliogenesis as well (Mojarad et al. 2017). Hence, upregulation of genes regulating cell cycle and formation of cilia in primary HBECs upon exposure to *A. fumigatus* may be important to prevent fungal invasion of host tissue.

Another key process that was enriched in the down-regulated proteins in our study was cellular iron homeostasis (Ferritin Light Chain (FTL), Superoxide Dismutase (SOD1), ATPase H+ Transporting V0 Subunit D1 (ATP6V0D1)). In a previous study using submerged cultures of 1HAE

cells, we found that genes associated with iron-uptake were up-regulated in *A. fumigatus* conidia (Oosthuizen et al. 2011). Moreover, a number of studies have shown that iron acquisition is important for *A. fumigatus* virulence (Hissen et al. 2005; Schrettl et al. 2004). Specifically, FTL was up-regulated in 16HBE14o- cells upon exposure to *A. fumigatus* conidia (Gomez et al. 2010). However, down-regulation of proteins such as FTL, an iron-binding protein, increases the amount of free iron available to the fungus (Theil 2004). Since free iron is a catalytic agent for the Fenton reaction that generates free radicals, it can result in oxidative damage in epithelial cells (Antosiewicz et al. 2007).

3.5 Summary

The research presented in this chapter demonstrated that, unlike submerged monolayers, primary HBECs grown in ALI internalize less than 1% of bound *A. fumigatus* conidia. ALI models mimicking the bronchial epithelial barrier in the conductive zone of the respiratory tract can be used to study transcriptomics and proteomics of bronchial epithelial cells upon exposure to *A. fumigatus* conidia. The major pathways that were enriched in the up-regulated genes upon exposure to *A. fumigatus* conidia included apoptosis/autophagy, translation, unfolded protein response, and cell cycle. In contrast, complement and coagulation pathways, iron homeostasis, non-sense mediated decay and rRNA binding pathways were down-regulated upon conidial exposure. Stress responses such as autophagy, unfolded response and non-sense mediated decay may protect the host against infection and promote cell-survival.

Chapter 4 General applicability of ALI cultures for studying host-pathogen interactions at the molecular level

4.1 Introduction

Due to the extensive costs and time involved in using *in-vivo* models, there is a need to identify and validate appropriate *in-vitro* models for studying host-pathogen interactions. Over the past decades, submerged monolayer cultures of continuous cell lines and primary cells have been primarily used to understand immune and molecular responses of the host upon exposure to the fungus, *Aspergillus fumigatus (A. fumigatus).* However, submerged cultures do not fully represent the complexity of cell types and morphology of human lung epithelia. Furthermore, many investigators use immortalized cell lines that may possess significant genetic and biochemical changes from normal tissue (Kaur and Dufour 2012).

In Chapter 3, we used well-differentiated air-liquid interface (ALI) cultures of primary human bronchial epithelial cells (HBECs) to determine the early molecular response of the host to *A. fumigatus*. To determine whether there is a wide applicability of this system for studying host-pathogen interactions, we compared the molecular response of ALI cultures of HBECs (ALI-HBECs) to submerged monolayer cultures of the human airway epithelial cell line (1HAEo-). Host response was evaluated by changes to the transcriptome and the proteome. We also assessed the specificity of response to pathogens by exposing ALI-HBECs to two different strains of *A. fumigatus* conidia as well as respiratory syncytial virus (RSV). Finally, to examine the changes in RNA transcripts associated with differentiation and development of ALI cultures, we compared the transcriptomes of low-TEER versus high-TEER samples from experiment #1.

Most studies of conidial internalization have been conducted using submerged monolayer cultures of immortalized cell lines (Paris et al. 1997; Julie A. Wasylnka and Moore 2003, 2002; Botterel et al. 2008; Han et al. 2011). Interestingly, unlike ALI cultures of primary HBECs (see Chapter 3), it has been reported that submerged monolayer cultures of airway epithelial cells internalize 30-50% of bound conidia after 6 hours (Gomez et al. 2010). The low rate of internalization by ALI-HBECs is consistent with observations of negligible internalization of *A. fumigatus* conidia in airway epithelial cells *in-vivo* (Rammaert et al. 2015). Thus, submerged monolayer cultures may not be representative of the host response to fungal conidia. The significant differences in phagocytosis as well as physiological differences between differentiated ALI cultures of HBECs and un-differentiated submerged monolayer cultures led us to hypothesize that the host response to pathogen exposure in these two model systems would be different.

For comparative gene expression profiling, we used submerged cultures of 1HAEo-, a Simian Virus (SV)-40 T antigen-transformed epithelial cell line. To evaluate how well the HBECs-ALI model mimics the *in-vivo* epithelium and whether it provides a pathogen-specific molecular response, we measured the specificity of response to different pathogens. To do this, we compared the immune responses to wild type strain (WT) of *A. fumigatus* conidia (reported in Chapter 3), to a mutant strain of *A. fumigatus* conidia and to the well-studied pathogenic virus, respiratory syncytial virus (RSV). The mutant stain of *A. fumigatus* has a deletion of the sialidase gene and is referred as the *⊿kdnase* strain. Kdnase is an *exo*-sialidase that prefers 2-keto-3-deoxy-D-glycero-D-galacto-nononic acid (Kdn) over *N*-acetylneuraminic acid (Neu5Ac) as a

substrate. Kdnase has been shown to contribute to *A. fumigatus* cell wall integrity and virulence (Nesbitt et al. 2018).

We used the viral pathogen, respiratory syncytial virus (RSV) to assess the specificity of response in HBECs-ALI cultures. RSV belongs to the genus *Pneumovirus* and is an enveloped virus with negative sense single-strand RNA (ssRNA). The genome is reported to be 15kb nucleotides in length, and encodes eleven proteins, nine structural and two non-structural proteins. Of the nine, five are involved in nucleocapsid structure and/or RNA synthesis, and the remaining four form the viral envelope (T. H. Kim and Lee 2014; Collins and Graham 2008). It can inhibit type 1 interferon host response by interrupting the JAK-STAT signaling pathway. Even though it is a major cause of respiratory infection in young children, there is no licensed vaccine against RSV yet (T. H. Kim and Lee 2014).

4.2 Overview of experiment design for comparative transcriptomic and proteomic studies

To investigate the early molecular response elicited by submerged monolayer cultures of 1HAEo- cells upon exposure to *A. fumigatus*, 1HAE cells were incubated without (control, n=3) or with (infected, n=3) *A. fumigatus* for 6 hours at 37 °C (Figure 4.1). nCounter Asthma Elements Panel and nCounter Immune Profiling Panel were used to profile transcriptomics, and LC-MS/MS was used to profile proteomics of 1HAE cells upon exposure to *A. fumigatus* conidia. Differentially abundant RNA transcripts and proteins were identified and compared to differentially abundant RNA transcripts and proteins identified in ALI cultures upon exposure to A*. fumigatus* conidia.

To assess the specificity of response, ALI cultures of primary HBECs were exposed to *Δkdnase A. fumigatus* conidia (infected, n=3) or RSV (infected, n=3) (Figure 4.1). Differential abundance analysis was conducted by comparing the control samples from experiment #2 (n=3) to the infected *(Δkdnase*- or RSV-infected, n=3 each) samples.

To assess *A. fumigatus* specific response in ALI cultures, differential abundance analysis was also conducted between ALI cultures exposed to WT *A. fumigatus* conidia (experiment #2, infected n=3) and *Δkdnase A. fumigatus* (*Δkdnase*-infected n=3).

The PCA plot in Chapter 3 (Figure 3.4) showed that majority of the variation between ALI samples in experiment #1 was due to the differences between differentiation of cultures. Hence, to further investigate these differences, RNA transcripts of genes assessed using nCounter Immune Profiling Panel were used to conduct differential abundance analysis between 4 High TEER samples and 2 low TEER samples.

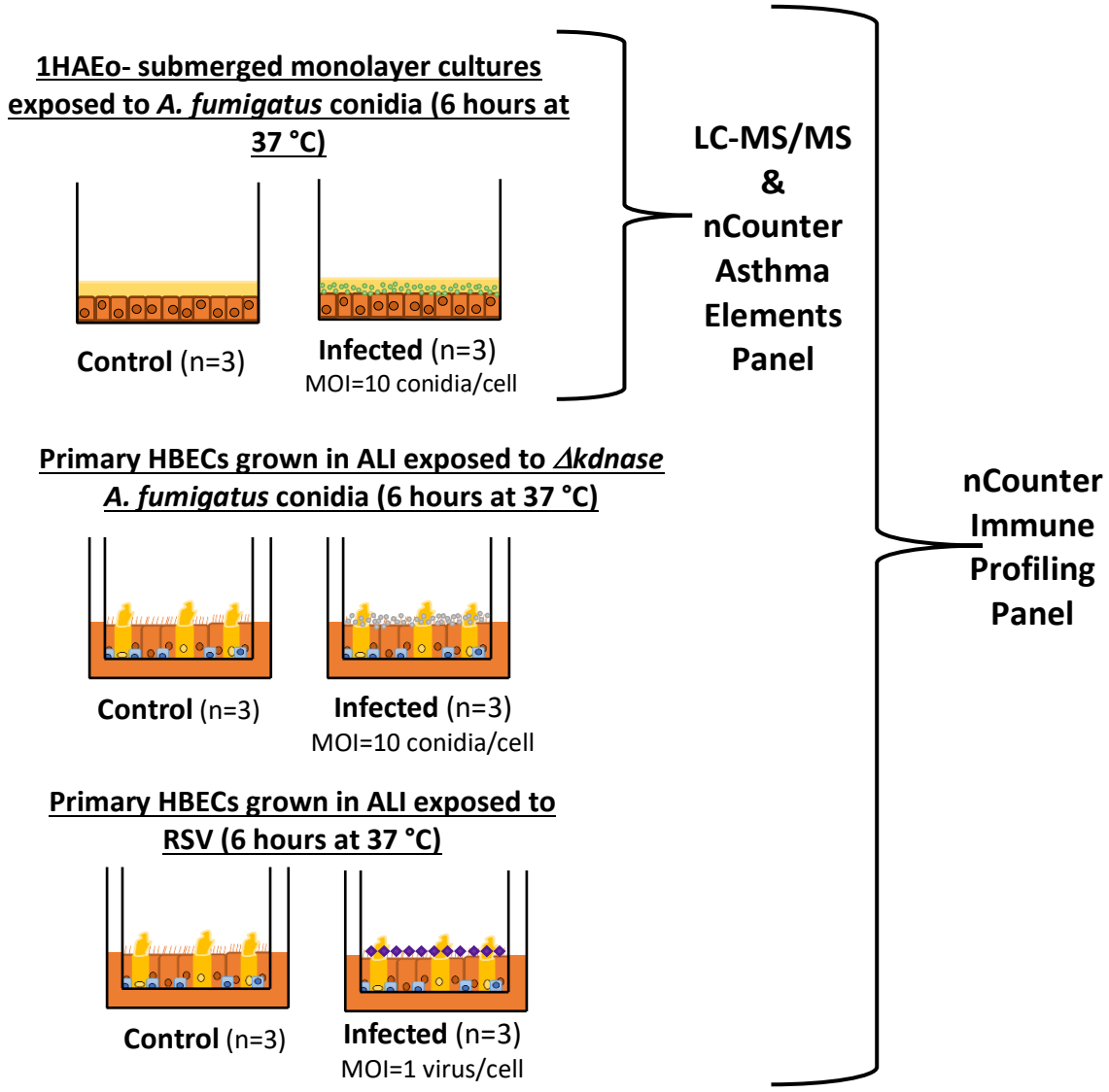

Figure 4.1: Experimental design for comparative analyses.
Submerged monolayer cultures of 1HAE cells were used to compare transcriptomics and proteomics to that of ALIs from Chapter 3. Control (n=3) and infected (n=3) samples were analyzed using nCounter Asthma Elements Panel and nCounter Immune Profiling Panel, previously used to assess transcriptomics of ALIs in Chapter 3 as well. Proteomics were analyzed using LC-MS/MS. To assess the specificity of response in these differentiated cultures, ALI cultures were exposed to *Δkdnase A. fumigatus* conidia (*Δkdnase*-infected, n=3), and RSV (RSV-infected, n=3), along with ALI cultures incubated with PBS (control, n=3).

4.3 Results

4.3.1 Visualizing interaction of *A. fumigatus* conidia in submerged monolayer cultures of 1HAEo- cells using confocal microscopy

Submerged monolayer cultures of 1HAE cells were exposed to GFP-expressing *A. fumigatus* conidia for 6 hours to investigate how submerged monolayer cultures interact with *A. fumigatus* conidia, compared to ALI cultures. The extent of conidial internalization was assessed by visualizing differentially stained conidia using confocal microscopy. As shown in the representative image in Figure 4.2, 6 hours post-exposure, more conidia were bound to submerged monolayer cultures of 1HAEs than differentiated ALI cultures of primary HBECs (Chapter 3, Figure 3.1). In addition, more bound conidia were internalized by submerged monolayer cultures of 1HAEs than differentiated ALI cultures of primary HBECs as well.

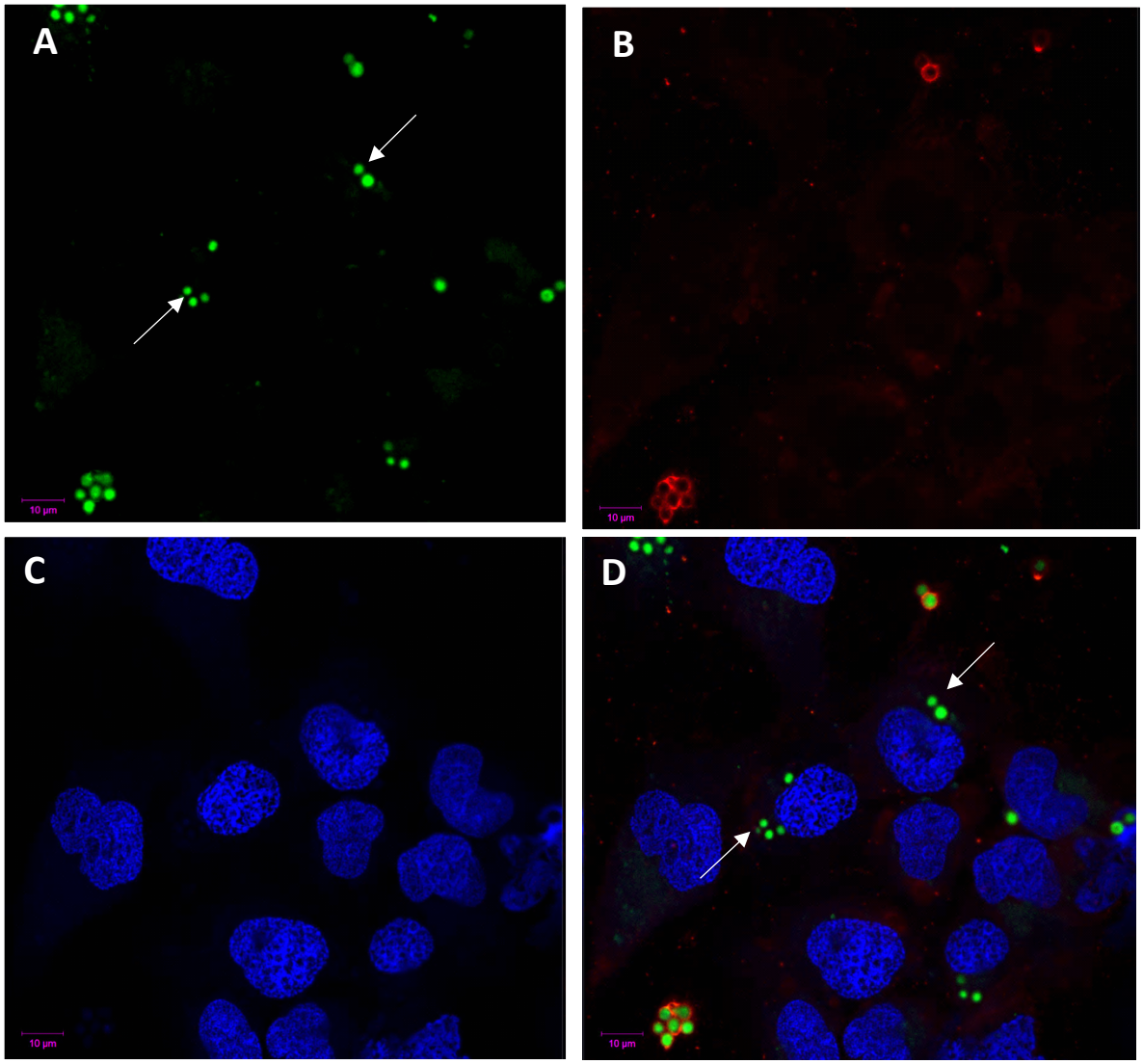

Figure 4.2: Differential staining of extracellular and internalized conidia by anti-*A. fumigatus* antibody using confocal microscopy at 6 hours post-exposure in submerged monolayer cultures of 1HAEs.

GFP-expressing *A. fumigatus* conidia and 1HAEo- cells grown in submerged monolayer cultures were co-incubated for 6 hours, fixed and stained with DAPI to label cell nuclei, and a monoclonal anti-*A. fumigatus* antibody was used to label extracellular conidia, before visualization using confocal microscopy. One representative field is shown in the following channels: A) wavelength 495nm for GFP (green); B) wavelength 594nm for anti-*A. fumigatus* antibody (red); C) wavelength 405nm for DAPI (blue); D) merged GFP, anti-*A. fumigatus* antibody and DAPI image. Conidia not labeled by the anti-*A. fumigatus* antibody and only visible in the green but not the red channel were considered to be internalized by 1HAEo- cells (as indicated by the white arrows).

4.3.2 Quantification and quality assessment of RNA samples

The concentrations of RNA extracted from all 1HAE samples, along with RNA integrity number (RIN) is reported in Table 4.1. TEER values, RNA concentration and RIN are reported for ALI samples in Experiment #2 are reported in Table 4.2. RNA integrity was assessed to ensure that the RNA was of good quality (RIN>8). RIN was not reported for Sample infected-3-RSV; however, further inspection of the specific chromatogram peaks for 18S and 28S indicated that total RNA for this sample was intact (data not shown).

Table 4.1: RNA concentrations and RIN for control and infected 1HAE cultures.

Submerged monolayer cultures of 1HAEs 24-well plate format		
Sample	**RNA concentration (ng/µl)**	**RIN**
Control-1	92.27	9.50
Control-2	89.34	9.60
Control-3	165.09	9.10
Infected-1-Wildtype *A. fumigatus* conidia	60.41	8.30
Infected-2-Wildtype *A. fumigatus* conidia	35.35	7.80
Infected-3-Wildtype *A. fumigatus* conidia	61.17	8.90

Table 4.2: Trans-Epithelial Electrical Resistance (TEER) values, RNA concentrations and RIN for 12 ALI cultures in Experiment 2.

Experiment #2 (ALI cultures of primary HBECs) 24-well plate format			
Sample	**TEER (ohms)**	**RNA concentration (ng/µl)**	**RIN**
Control-1	1030	74.54	8.40
Control-2	1029	75.9	8.50
Control-3	1022	66.25	8.10
Infected-1-Wildtype *A. fumigatus* conidia	1268	71.69	9.30
Infected-2-Wildtype *A. fumigatus* conidia	1056	106.1	9.40
Infected-3-Wildtype *A. fumigatus* conidia	1197	80.32	8.10
Infected-1-*Δkdnase A. fumigatus* conidia	1018	135.3	9.60
Infected-2-*Δkdnase A. fumigatus* conidia	947	79.94	9.10
Infected-3-*Δkdnase A. fumigatus* conidia	940	83.93	9.60
Infected-1-RSV	1754	71.12	8.40
Infected-2-RSV	1611	90.77	9.20
Infected-3-RSV	1990	69.01	N/A

4.3.3 Analysis of transcriptomic and proteomic response to *A. fumigatus* in submerged monolayer cultures of 1HAEs

4.3.3.1 Analysis of RNA transcripts in submerged monolayer cultures of 1HAEs upon exposure to A. fumigatus *conidia*

The transcriptome of 1HAEs grown in submerged monolayer cultures were analyzed using the nCounter Immune Profiling Panel and the nCounter Asthma Elements Panel to assess

the similarities and differences in the early molecular response to that of ALI cultures upon exposure to *A. fumigatus*. Samples of both control (n=3) and infected (n=3) were treated identically, except for the addition of *A. fumigatus* conidia suspended in PBS to the infected samples and PBS alone to the control samples.

4.3.3.1 nCounter Asthma Elements Panel

The PCA plot showed that most of the variation between samples was due to exposure to *A. fumigatus* conidia (Figure 4.3.A). Of the 123 genes assessed for differential RNA transcript abundance analysis, 63 RNA transcripts were differentially abundant upon exposure to *A. fumigatus* conidia (P-value < 0.05) (Figure 4.3.B) (Appendix 4). In addition, 100 RNA transcripts were significant under BH-FDR < 0.3. Compared to control samples, 4 RNA transcripts were up-regulated and 59 were down-regulated 6 hours post-exposure to *A. fumigatus* conidia in submerged monolayer cultures of 1HAEs. The 4 RNA transcripts that were up-regulated in infected samples compared to control samples included Complement C5a Receptor 1 (C5AR1), Mitochondrially Encoded Cytochrome B (MT-CYB), Contactin Associated Protein Like 3 (CNTNAP3) and Cytochrome B isoform (CYTB_comp5).

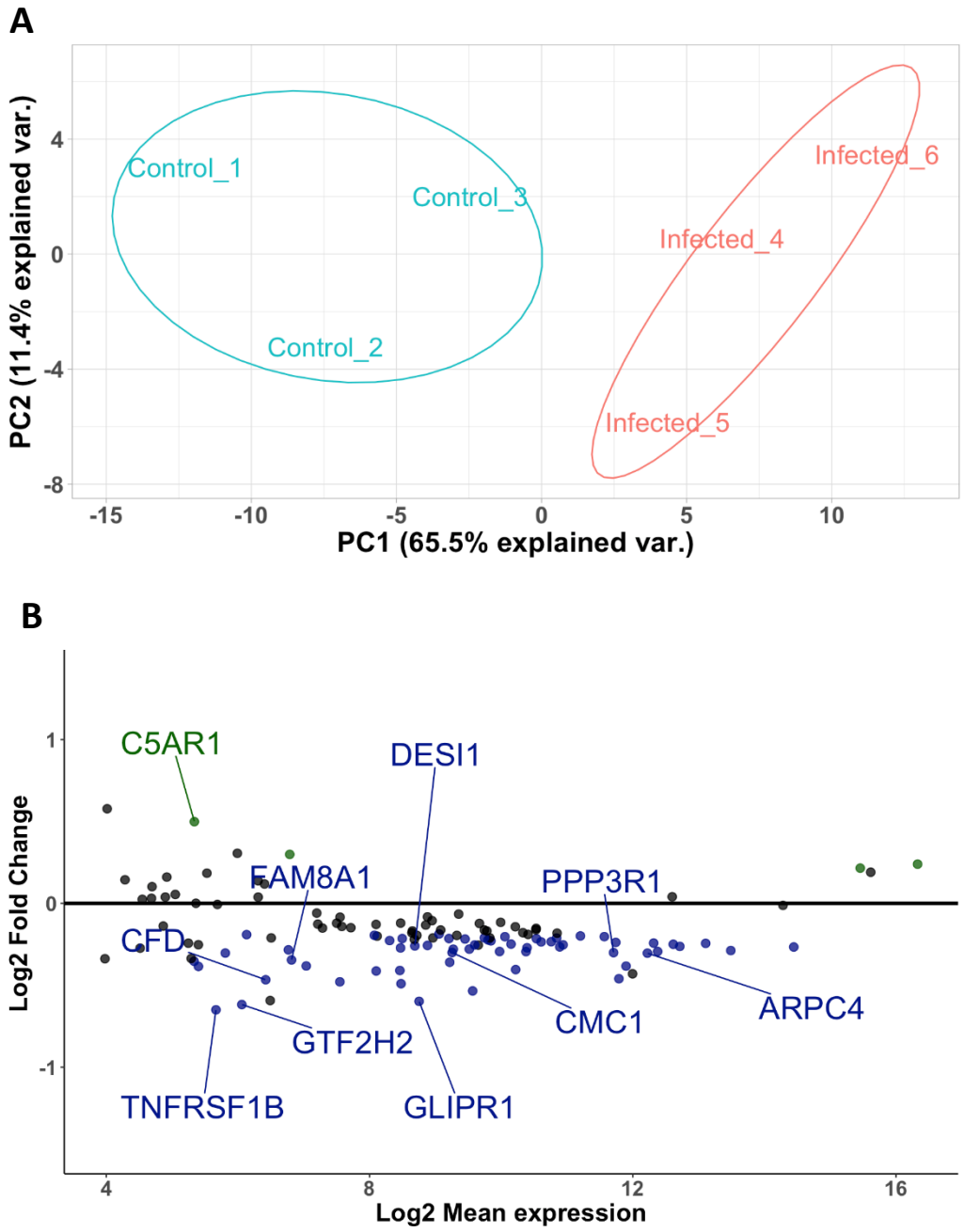

Figure 4.3: Principal Component Analysis (PCA) and MA Plot of 1HAEs exposed to *A. fumigatus* conidia for 6 hours (Asthma Elements Panel).
A) PCA plot showing that PC1 is explaining 65.5% of variation between control (Blue) and infected (Red) samples. B) MA plot of 63 RNA transcripts differentially abundant in 1HAEs upon exposure to *A. fumigatus* for 6 hours. The top 10 genes are labeled, these included GTF2H2 and C5AR1 that were also differentially abundant in ALI cultures upon exposure to *A. fumigatus*.

Pathway enrichment analysis for differentially abundant RNA transcripts was conducted in Enrichr using the Reactome database (http://amp.pharm.mssm.edu/Enrichr/) (E. Y. Chen et al. 2013)(Kuleshov et al. 2016) (Table 4.3). Innate Immune system, TLR3/TLR4 signaling, Dectin-1 signaling, Endosomal/Vacuolar pathway and C-type lectin receptors were some of the enriched pathways (Table 4.3).

Table 4.3: Enriched Reactome pathways for 63 differentially abundant RNA transcripts identified in Asthma Elements Panel in 1HAEs upon exposure to *A. fumigatus* conidia, as identified by Enrichr.

Term	P-value	Adjusted P-value	Combined Score	Genes
Innate Immune System_Homo sapiens_R-HSA-168249	1.702E-08	7.900E-06	43.493	CFD;MAP2K2;C5AR1;HLA-B; UBE2D1; ARPC4;DUSP6;NFKB1;CTSS;NFKBIA;PPP3R1;CD59;PSMF1;FADD;CD46
Immune System_Homo sapiens_R-HSA-168256	1.160E-07	2.692E-05	35.512	CFD;MAP2K2;C5AR1;HLA-B; UBE2D1; ARPC4; HLA-A; TNFRSF1B; DUSP6; NFKB1; CTSS; IL17RA;NFKBIA;PPP3R1;CD59;PSMF1;FADD;CD46;ATG7
Toll-Like Receptors Cascades_Homo sapiens_R-HSA-168898	4.706E-06	7.097E-04	26.281	NFKBIA;UBE2D1;FADD;NFKB1;DUSP6;CTSS
MyD88-independent TLR3/TLR4 cascade_Homo sapiens_R-HSA-166166	1.257E-05	8.056E-04	23.805	NFKBIA;UBE2D1;FADD;NFKB1;DUSP6
TRIF-mediated TLR3/TLR4 signaling_Homo sapiens_R-HSA-937061	1.257E-05	8.056E-04	23.709	NFKBIA;UBE2D1;FADD;NFKB1;DUSP6
Toll Like Receptor 3 (TLR3) Cascade_Homo sapiens_R-HSA-168164	1.257E-05	8.056E-04	23.602	NFKBIA;UBE2D1;FADD;NFKB1;DUSP6
CLEC7A (Dectin-1) signaling_Homo sapiens_R-HSA-5607764	1.389E-05	8.056E-04	23.162	NFKBIA;PPP3R1;UBE2D1;PSMF1;NFKB1
Endosomal/Vacuolar pathway_Homo sapiens_R-HSA-1236977	6.118E-06	7.097E-04	22.335	HLA-B;HLA-A;CTSS
Activated TLR4 signaling_Homo sapiens_R-HSA-166054	2.526E-05	1.302E-03	21.074	NFKBIA;UBE2D1;FADD;NFKB1;DUSP6
C-type lectin receptors (CLRs)_Homo sapiens_R-HSA-5621481	3.964E-05	1.672E-03	21.065	NFKBIA;PPP3R1;UBE2D1;PSMF1;NFKB1

Of the 63 differentially abundant RNA transcripts for 1HAEs and 7 differentially abundant for ALIs upon exposure to *A. fumigatus* conidia obtained using the nCounter Asthma Elements Panel, 2 RNA transcripts overlapped; however, these showed opposite direction of change: General Transcription Factor IIH Subunit 2 (GTF2H2) and C5AR1 (Complement C5a Receptor 1). GTF2H2 was up-regulated in ALIs and down-regulated in 1HAEs, and C5AR1 is down-regulated in ALIs and up-regulated in 1HAEs, upon exposure to *A. fumigatus* conidia.

4.3.3.1.2 nCounter Immune Profiling Panel

Principal component analysis (PCA) plot of control and infected samples analyzed using nCounter Immune Profiling Panel is shown in Figure 4.4A. Control and infected samples were separated with a small overlap between samples, indicating that majority of variation between samples was due to the presence of *A. fumigatus* conidia. Differential abundance analysis of 353 RNA transcripts showed 41 RNA transcripts to be differentially abundant in submerged monolayer cultures of 1HAEs upon exposure to *A. fumigatus* conidia for 6 hours (Figure 4.4B) (Appendix 5). Of these 41, 2 RNA transcripts were significant under BH-FDR < 0.30 (labeled in Figure 4.4B).

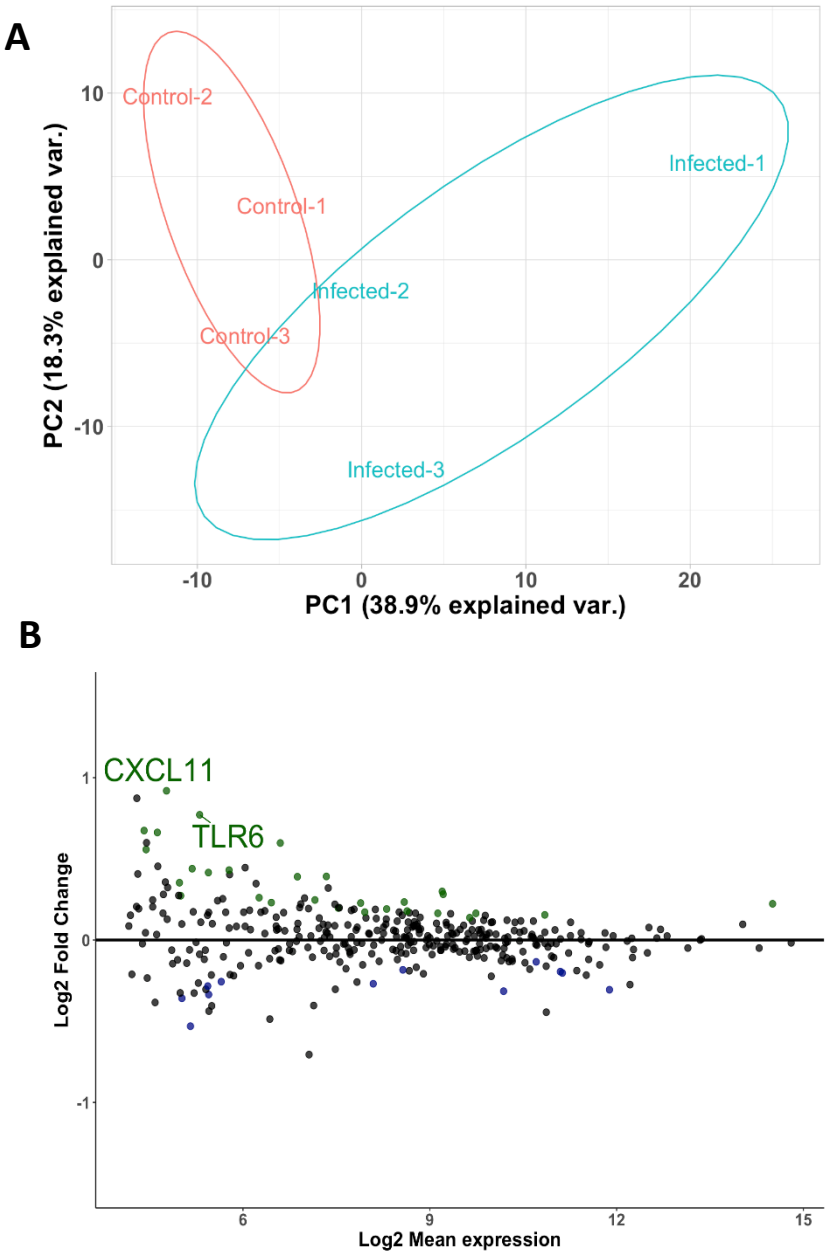

Figure 4.4: Principal Component Analysis (PCA) and MA Plot of 1HAEs exposed to *A. fumigatus* conidia for 6 hours (Immune Profiling Panel).
A) PCA plot showing separation between control (Blue) and infected (Red) samples. B) MA plot of 41 RNA transcripts differentially abundant in 1HAEs upon exposure to *A. fumigatus* for 6 hours. 2 genes were significant under BH-FDR < 0.3 (labeled).

GO enrichment analysis using the Cytoscape plug-in, CLUEGO, showed that up-regulated differentially abundant RNA transcripts were enriched for postive regulation of tumor necrosis factor production, positive regulation of tyrosine phosphorylation of STAT protein, positive regulation of leukocyte migration, regulation of regulatory T-cell differentiation, negative regulation of reproductive process and megakaryocyte differentiation (Figure 4.5). The down-regulated RNA transcripts were mainly enriched for negative regulation of T-cell proliferation and dendritic cell differentiation (Figure 4.5).

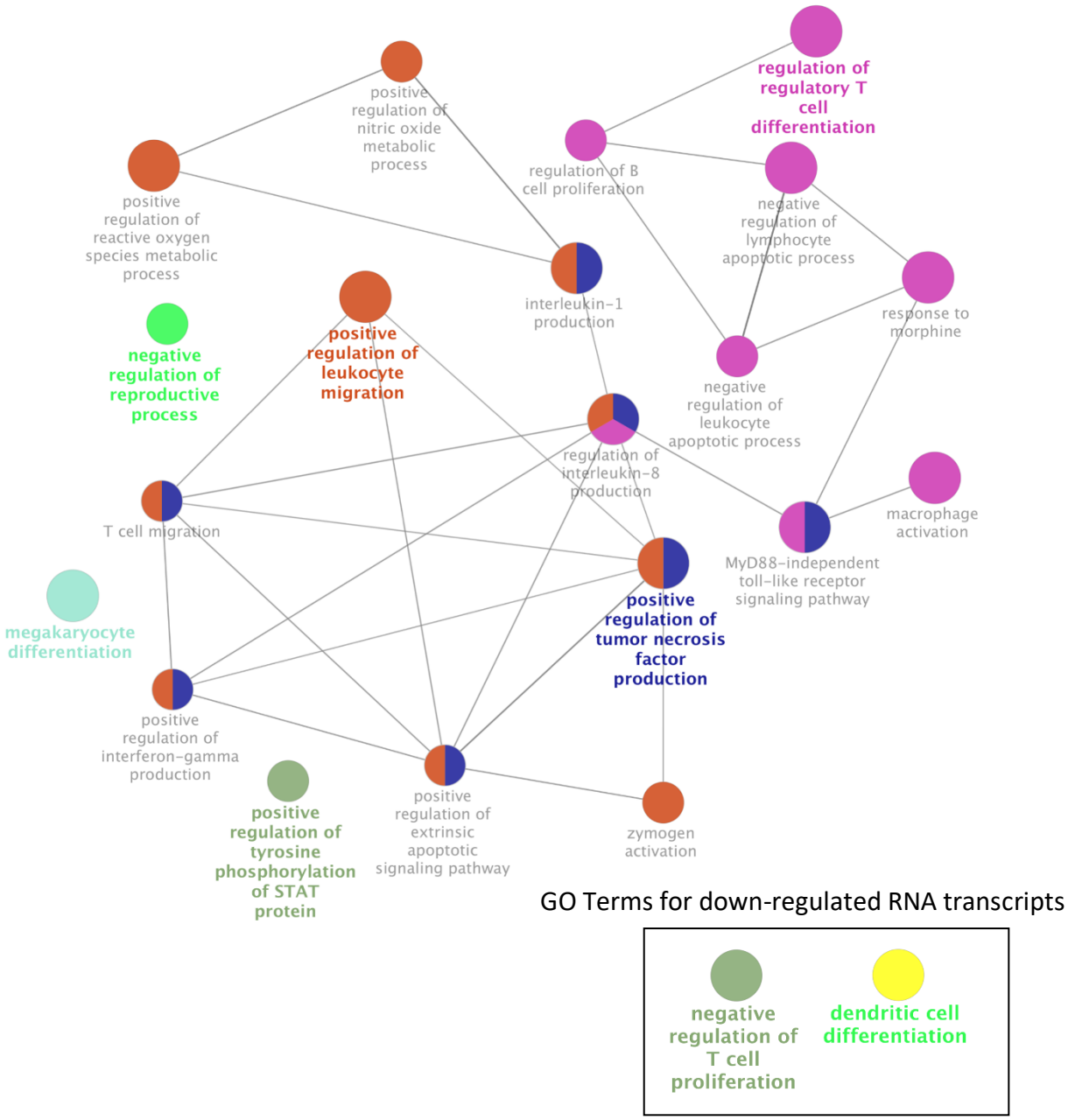

Figure 4.5: Gene ontology enrichment analysis of differentially abundant RNA transcripts identified using Immune Profiling Panel in submerged monolayer cultures of 1HAEs upon exposure to *A. fumigatus*.

Functionally-grouped network of Gene Ontology enrichment analysis for differentially abundant RNA transcripts in ClueGO App is shown (P-value < 0.1). The up-regulated RNA transcripts, compared to control samples, were enriched in positive regulation of leukocyte migration, positive regulation of tumor necrosis factor production, regulation of regulatory T cell differentiation. Boxed terms: The down-regulated RNA transcripts were enriched for negative regulation of T-cell proliferation and dendritic cell differentiation.

Of the 41 RNA transcripts differentially abundant for ALIs (Chapter 3, Appendix 2) and 41 RNA transcripts differentially abundant for 1HAEs upon exposure to *A. fumigatus* for 6 hours (P-value < 0.05), 6 RNA transcripts overlapped, reported in Table 4.4; however, only 4 of the 6 changed in the same direction.

Table 4.4: RNA transcripts (6) that were differentially expressed in both HBECs-ALI cultures and 1HAE submerged monolayer cultures upon exposure to *A. fumigatus* conidia using the Immune Profiling Panel.

ALI cultures of HBECs			Submerged monolayer cultures of 1HAEs	
Average Expression (Log2)	**Log2 FC**	**Overlapping RNA transcripts**	**Log2 FC**	**Average Expression (Log2)**
11.649	-0.672	**CXCL6- C-X-C Motif Chemokine Ligand 6**	0.272	4.999
5.339	0.646	**IFNL1-Interferon Lamba 1**	0.430	5.776
5.575	0.428	**NFATC2-Nuclear Factor Of Activated T-Cells 2**	0.299	9.198
9.929	0.265	**CASP3- Caspase 3**	-0.316	10.185
11.116	0.715	**SPA17-Sperm Autoantigenic Protein 17**	0.178	8.635
5.394	0.368	**FADD- Fas Associated via Death domain**	0.230	6.454

4.3.3.2 Analysis of the proteome of submerged monolayer cultures of 1HAEs in response to A. fumigatus conidia

In total, 1247 proteins were identified of which 558 proteins were quantified (at least 2 out of 3 quantification events). Differential abundance analysis using normalized ratios of Heavy (infected, n=3) to Light (control, n=3) labeled protein samples showed that 54 proteins were differentially abundant 6 hours post-exposure to *A. fumigatus* conidia (Figure 4.6) (Appendix 6). Of these 54, 4 proteins were significant under BH-FDR < 0.30, labeled in Figure 4.6. These 4

proteins included, Albumin (ALB), Ral GTPase Activating Protein Catalytic Alpha Subunit 1 (RALGAPA1), Keratin 10 (KRT10) and Splicing Factor 3a Subunit 2 (SF3A2).

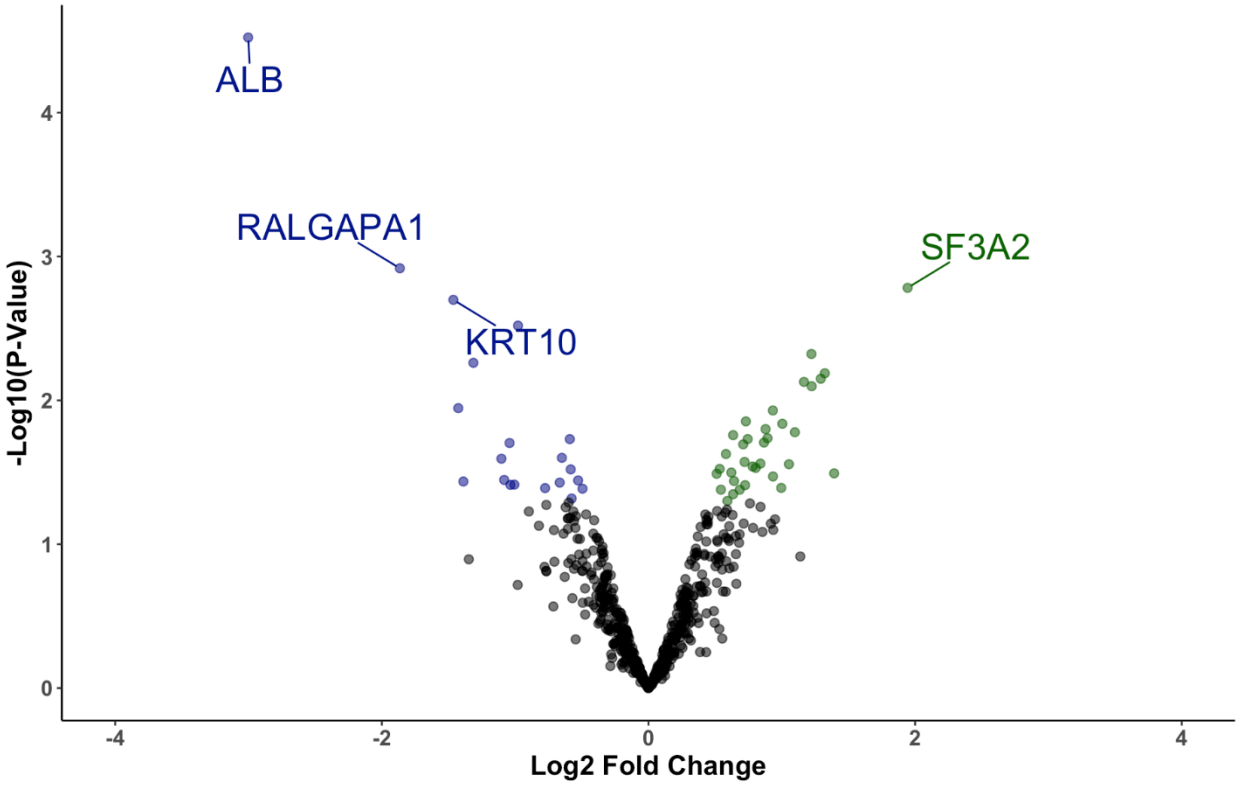

Figure 4.6: Volcano plot of 558 quantified proteins identified using shotgun proteomics in submerged monolayer cultures of 1HAEs upon exposure to *A. fumigatus* conidia. Differential abundance analysis showed that 54 proteins were differentially abundant 6 hours post-exposure to *A. fumigatus* (P-Value < 0.05). 4 proteins were differentially abundant at BH-FDR < 0.3 (labeled). Of the 54, 34 were up-regulated (green) and 20 were down-regulated (blue) upon exposure to *A. fumigatus* conidia.

Compared to control samples, 34 were up-regulated and 20 were down-regulated upon exposure to *A. fumigatus*. The up-regulated proteins were associated with nonsense mediated decay, gene expression, eukaryotic translation initiation, influenza infection, RNA splicing and rRNA processing (Table 4.5). The down-regulated proteins were associated with platelet

degranulation, response to elevated platelet cytosolic Ca2+, disease and vesicle mediated transport (Table 4.6).

Table 4.5: Enriched Pathways for up-regulated proteins in 1HAEs upon exposure to *A. fumigatus*.

Term	P-value	Adjusted P-value	Combined Score	Genes
Nonsense Mediated Decay (NMD) independent of the Exon Junction Complex (EJC)_Homo sapiens_R-HSA-975956	3.915E-07	3.149E-05	28.761	RPL4;RPS4X;RPS16;RPL10A;EIF4G1
Gene Expression_Homo sapiens_R-HSA-74160	1.222E-06	3.149E-05	28.720	YWHAE;RPL4;SF3A2;RPS27L;HNRNPR;RPL10A;YWHAZ;RPS4X;HNRNPK;RPS16;HNRNPC;HNRNPA0;EIF4G1
Eukaryotic Translation Initiation_Homo sapiens_R-HSA-72613	1.343E-06	3.149E-05	26.000	RPL4;RPS4X;RPS16;RPL10A;EIF4G1
Influenza Infection_Homo sapiens_R-HSA-168254	4.695E-06	8.255E-05	24.453	RPL4;RPS4X;RPS16;KPNA2;RPL10A
RNA Splicing - Major Pathway_Homo sapiens_R-HSA-72163	2.982E-06	6.291E-05	24.388	HNRNPK;SF3A2;HNRNPR;HNRNPC;HNRNPA0
Major pathway of rRNA processing in the nucleolus_Homo sapiens_R-HSA-6791226	8.493E-06	1.280E-04	22.694	RPL4;RPS4X;RPS16;RPS27L;RPL10A

Table 4.6: Enriched Pathways for down-regulated proteins in 1HAEs upon exposure to *A. fumigatus.*

Term	P-value	Adjusted P-value	Combined Score	Genes
Platelet degranulation_Homo sapiens_R-HSA-114608	1.502E-04	1.551E-02	16.939	TF;HSPA5;ALB
Response to elevated platelet cytosolic Ca2+_Homo sapiens_R-HSA-76005	1.724E-04	1.551E-02	16.435	TF;HSPA5;ALB
Disease_Homo sapiens_R-HSA-1643685	5.219E-03	1.518E-01	12.440	RBP4;NPM1;RPL18A;ALB
Vesicle-mediated transport_Homo sapiens_R-HSA-5653656	1.235E-02	1.518E-01	9.090	LMAN1;YWHAB;ALB

Of the 2875 proteins identified in the HBECs-ALIs experiment and 1247 proteins identified in 1HAEs experiment, 1008 proteins overlapped. For the 153 proteins differentially abundant in the HBECs-ALIs experiment and 54 proteins differentially abundant in the 1HAEs experiment, 8 proteins overlapped with 7 of 8 showing changes in the same direction (Table 4.7).

Table 4.7: 8 proteins overlapped between ALI cultures and 1HAEs submerged monolayer cultures upon exposure to *A. fumigatus* conidia.

ALI cultures of HBECs		Submerged monolayer cultures of 1HAEs
Log2 FC	**Overlapping Proteins**	**Log2 FC**
-3.002	**ALB-Albumin**	-1.611
1.323	**SF1- Splicing Factor1**	-0.757
-1.426	**KRT1-Keratin 1**	-0.791
1.098	**MATR3-Matrin 3**	1.739
0.866	**CAST-Calpastatin**	1.035
0.878	**LMNA-Lamin A/C**	0.370
0.934	**RRBP1-Ribsome Binding Protein 1**	1.029
-1.388	**KRT2-Keratin 2**	-1.232

4.3.4 Analysis of RNA transcripts in ALI cultures of primary HBECs upon exposure to *Δkdnase A. fumigatus* conidia

The PCA plot showed overlap between control and infected samples, indicating that the majority of the variation between samples may not be due to whether or not ALI cultures were exposed to *Δkdnase A. fumigatus* conidia (Figure 4.7A)**.** Differential RNA transcript analysis showed 52 RNA transcripts to be differentially abundant upon exposure to *Δkdnase A. fumigatus* conidia in ALI cultures of primary HBECs for 6 hours (P-value < 0.05) (Figure 4.7B) (Appendix 7). Of the 52 RNA transcripts, 40 were up-regulated and 12 were down-regulated in *Δkdnase A. fumigatus* conidia exposed ALI cultures compared to control ALI cultures. 31 RNA transcripts were significant under BH-FDR < 0.30.

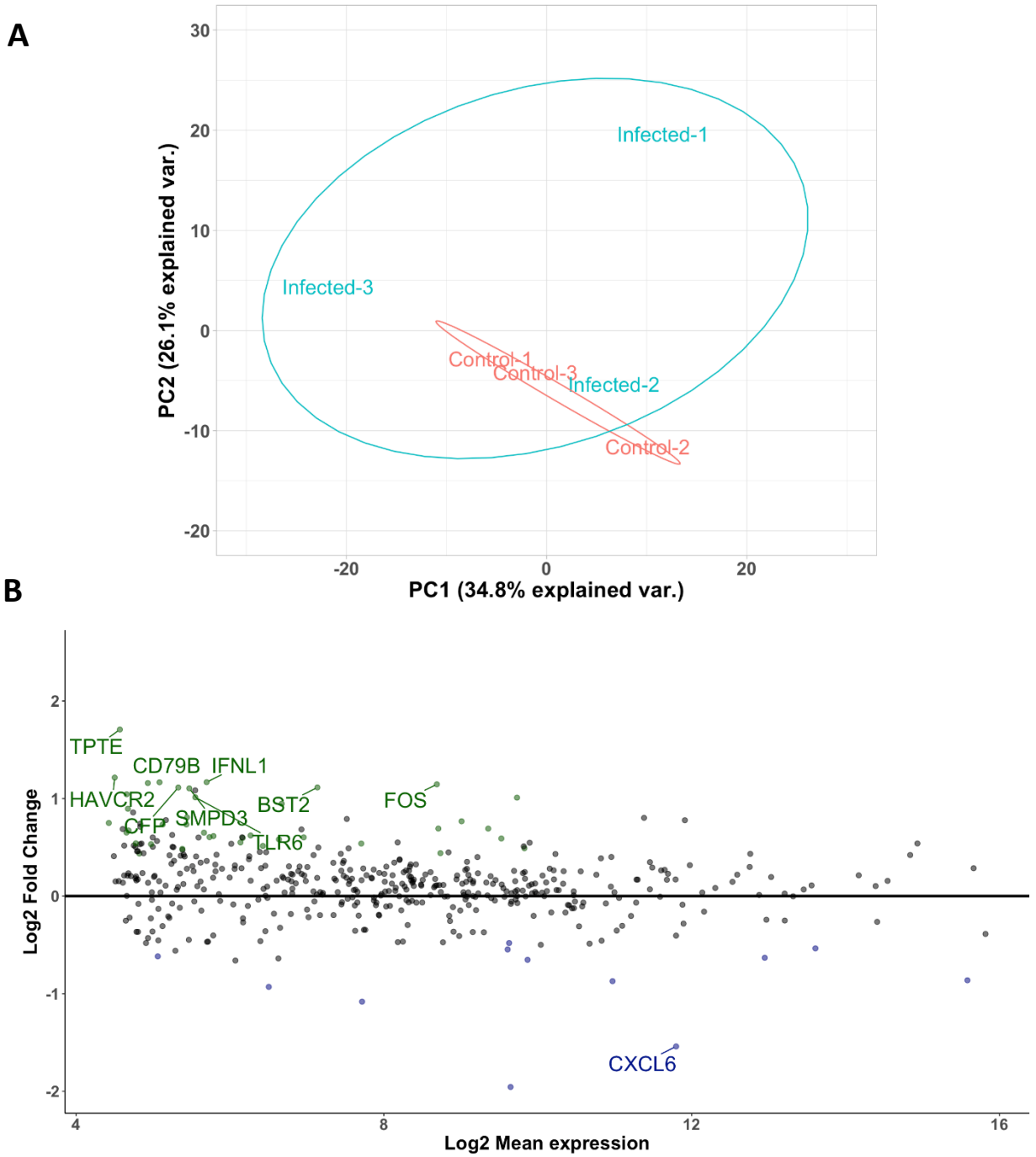

Figure 4.7 PCA plot and MA Plot of ALI cultures exposed to *Δkdnase A. fumigatus* conidia for 6 hours using Immune Profiling Panel.

A) PCA plot did not show separation between control (Blue) and infected (Red) samples. B) MA plot showed 52 RNA transcripts to be differentially abundant upon exposure to *Δkdnase A. fumigatus* conidia in ALI cultures of primary HBECs for 6 hours (P-value < 0.05). Top 10 RNA transcripts are labeled.

Gene ontology enrichment analysis showed enrichment of negative regulation of cytokine production, heterophilic cell-cell adhesion via plasma membrane cell adhesion molecules, regulation of osteoclast differentiation, type 1 interferon signaling pathway to be enriched for up-regulated RNA transcripts (Figure 4.8A), and positive regulation of granulocyte chemotaxis to be primarily enriched in down-regulated RNA transcripts in ALI cultures upon exposure to *Δkdnase A. fumigatus* conidia for 6 hours (Figure 4.8B).

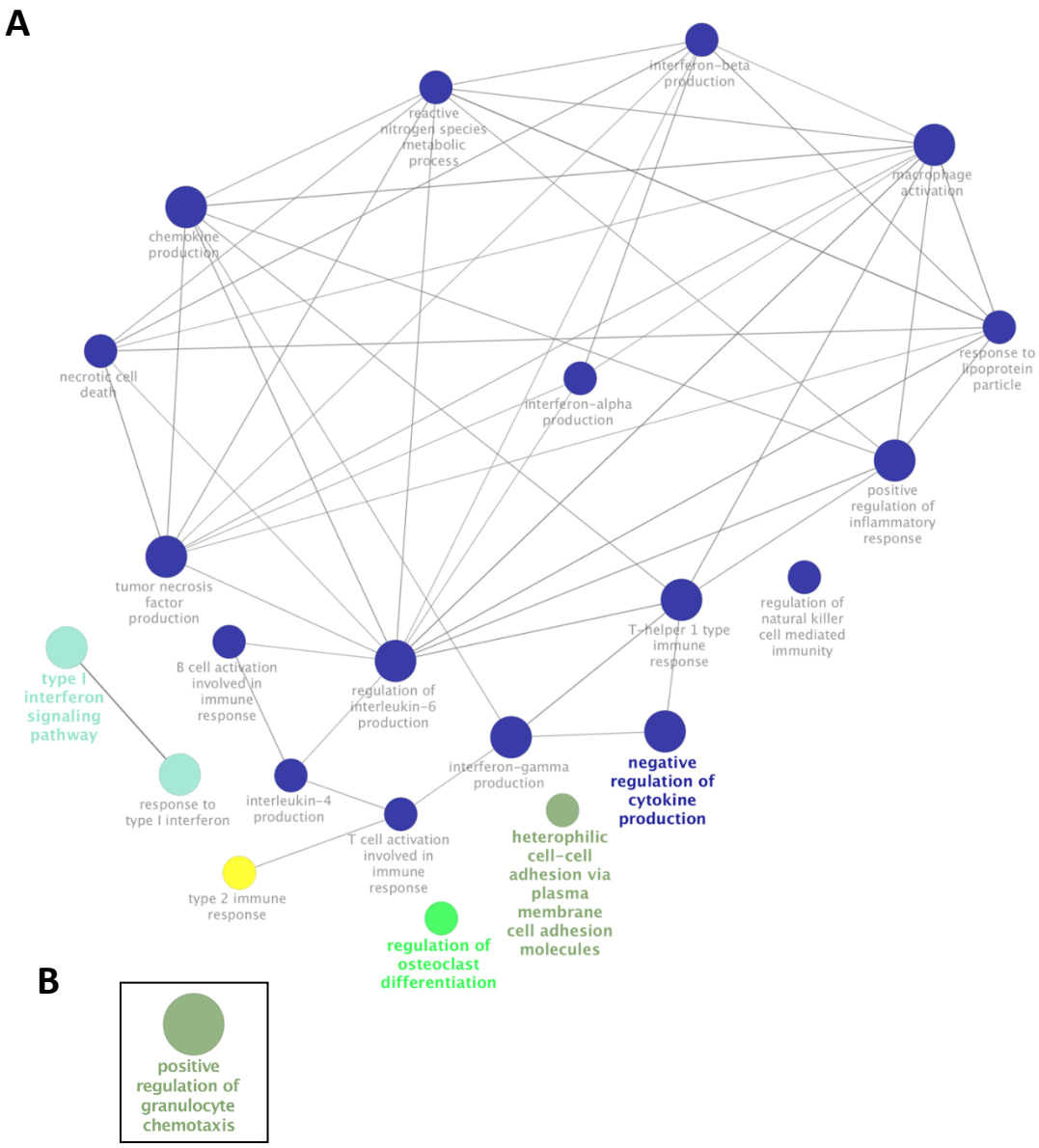

Figure 4.8: Gene ontology enrichment analysis of differentially abundant RNA transcripts identified using Immune Profiling Panel in ALI cultures upon exposure to *Δkdnase* A. *fumigatus*.

A. Functionally grouped network of gene ontology enrichment analysis of differentially abundant RNA transcripts in ClueGO App is shown (P-value < 0.1). The up-regulated RNA transcripts upon exposure to *Δkdnase A. fumigatus conidia* were enriched in type I interferon signaling pathway, negative regulation of cytokine production, regulation of osteoclast differentiation etc. B. The down-regulated RNA transcripts were enriched for positive regulation of granulocyte chemotaxis.

Of the 52 RNA transcripts differentially abundant in response to *Δkdnase A. fumigatus* conidia and 41 RNA transcripts differentially abundant in response to WT *A. fumigatus* conidia, 11 RNA transcripts overlapped (Table 4.8). These 11 included Bone Marrow Stromal Cell Antigen 2/Tetherin (BST2), Interferon Lambda 1/IL-29 (IFNL1), C-X-C Motif Chemokine Ligand 6 (CXCL6), C-X-C Motif Chemokine Ligand 5 (CXCL5), Serum Amyloid A1 (SAA1), Complement Factor B (CFB), Indoleamine 2,3-Dioxygenase 1 (IDO1), Transcription Factor Binding to IGHM Enhancer 3 (TFE3), Complement C3 (C3), LCK Proto-Oncogene, Src Family Tyrosine Kinase (LCK), and Fas Associated Via Death Domain (FADD), shown in Table 4.8. All RNA transcripts changed in the same direction upon exposure to either *Δkdnase A. fumigatus* conidia or WT *A. fumigatus* conidia (same Log2 Fold Change).

Table 4.8: Overlapping RNA transcripts between 52 differentially abundant RNA transcripts of Δ*kdnase A. fumigatus* conidia infected ALI cultures and 41 differentially abundant RNA transcripts of WT *A. fumigatus* conidia infected ALI cultures

Control vs. *Δkdnase A. fumigatus* conidia infected ALI cultures			Control vs. Wild type *A. fumigatus* conidia infected ALI cultures	
Average Expression	**Log2 FC**	**Overlapping Genes**	**Log2 FC**	**Average Expression**
7.136	1.113	**BST2**	0.503	6.960
5.696	1.167	**IFNL1**	0.646	5.339
11.798	-1.540	**CXCL6**	-0.672	11.649
9.647	-1.956	**CXCL5**	-1.147	9.029
15.583	-0.862	**SAA1**	-0.613	14.601
12.949	-0.632	**CFB**	-0.447	12.147
10.972	-0.871	**IDO1**	-1.018	9.724
5.733	0.605	**TFE3**	0.494	5.387
13.608	-0.535	**C3**	-0.467	12.909
4.655	0.651	**LCK**	0.662	5.216
5.380	0.484	**FADD**	0.368	5.394

4.3.5 Analysis of RNA transcript abundance in ALI cultures of primary HBECs upon exposure to *Δkdnase A. fumigatus* conidia and WT *A. fumigatus* conidia for 6 hours

To further assess differences between the immune response associated with mutant strain of *A. fumigatus* conidia compared to WT strain, differential abundance analysis was conducted between ALI cultures exposed to WT *A. fumigatus* conidia and *Δkdnase A. fumigatus* conidia. PCA plot showed overlap between samples upon exposure to WT *A. fumigatus* conidia and *Δkdnase A. fumigatus* conidia. Of the 446 genes assessed for differential RNA transcript abundance analysis, 17 RNA transcripts were differentially abundant upon exposure to *Δkdnase A. fumigatus* conidia compared to WT *A. fumigatus* conidia (P-value < 0.05) (Figure 4.9) (Appendix 8). None were significant under BH-FDR < 0.3.

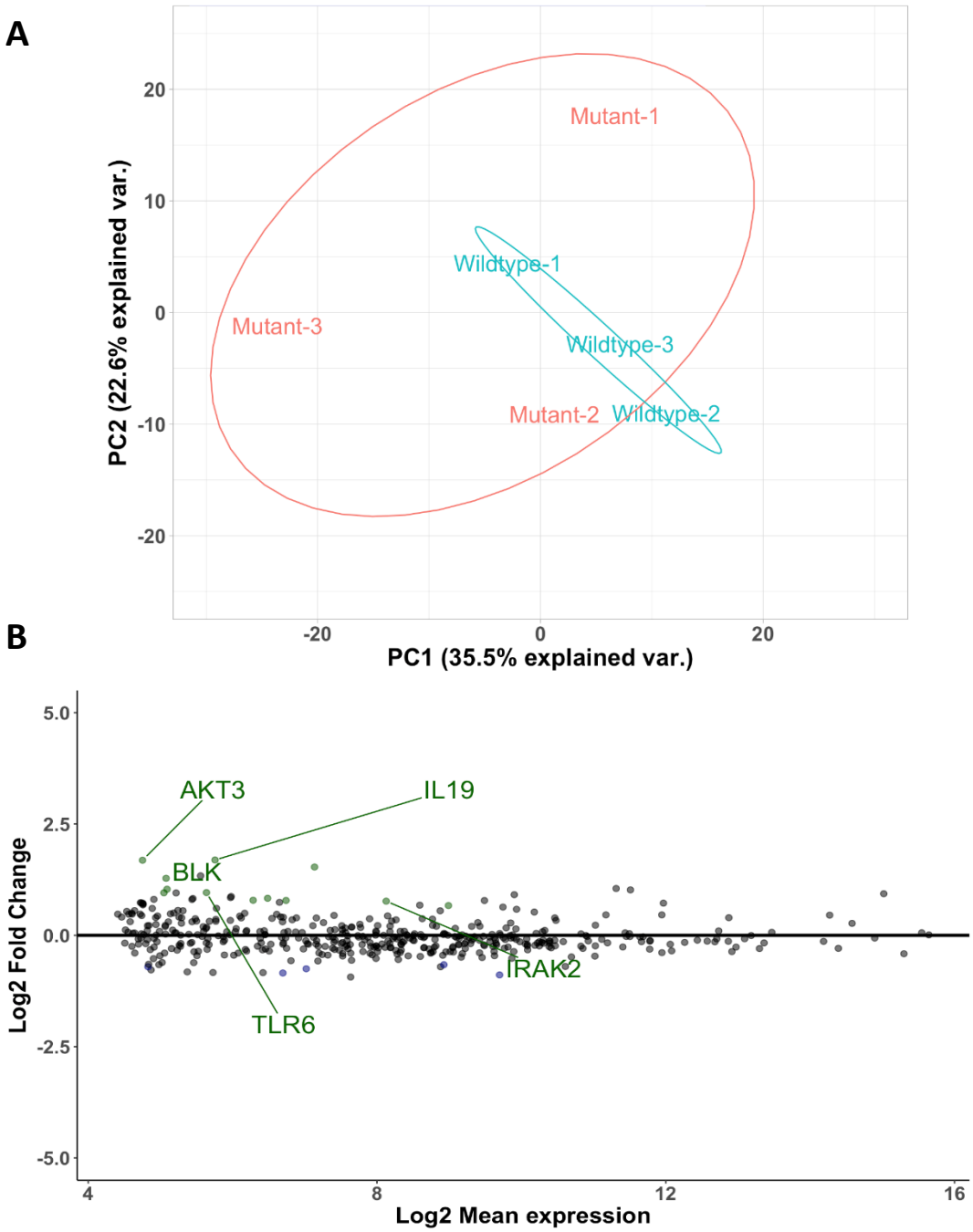

Figure 4.9: PCA plot and MA Plot analyses of ALIs exposed to *Δkdnase* A. fumigatus conidia for 6 hours using Immune Profiling Panel.
A) PCA plot did not show separation between WT-infected (Blue) and *Δkdnase*-infected (Red) samples. B) MA plot showed 17 RNA transcripts to be differentially abundant upon exposure to *Δkdnase A. fumigatus* conidia compared to WT *A. fumigatus* conidia in HBECs for 6 hours (P-value < 0.05). Top 5 RNA transcripts are labeled.

Compared to Wild-type *A. fumigatus* conidia exposed ALI cultures, 12 RNA transcripts were up-regulated (Table 4.9) and 5 were downregulated (Table 4.10).

Table 4.9: 12 RNA transcripts were up-regulated upon exposure to *Δkdnase A. fumigatus* conidia compared to WT *A. fumigatus* conidia in ALI cultures of primary HBECs.

Gene	Gene Name	Log2 FC	P.Value
BLK	**B Lymphoid Tyrosine Kinase**	1.280	0.003
IL19	**Interleukin 19**	1.692	0.007
TLR6	**Toll like receptor 6**	0.960	0.016
AKT3	**AKT Serine/Threonine Kinase 3**	1.686	0.019
IRAK2	**Interleukin 1 Receptor Associated Kinase 2**	0.767	0.019
NT5E	**5'-Nucleotidase Ecto**	0.784	0.024
CD14	**CD 14 Molecule**	1.035	0.026
STAT4	**Signal Transducer And Activator Of Transcription 4**	0.832	0.037
MICA	**MHC Class I Polypeptide-Related Sequence A**	0.788	0.040
DMBT1	**Surfactant Pulmonary-Associated D-Binding Protein**	1.534	0.041
IL32	**Tumor Necrosis Factor Alpha-Inducing Factor**	0.668	0.044
CDH5	**Cadherin 5**	0.955	0.046

Table 4.10: 5 RNA transcripts were down-regulated upon exposure to *Δkdnase A. fumigatus* conidia compared to WT *A. fumigatus* conidia in ALI cultures of primary HBECs.

Gene	Gene Name	Log2 FC	P.Value
TFRC	**Transferrin Receptor**	-0.889	2.498E-02
IL6R	**Interleukin 6 Receptor**	-0.750	2.909E-02
CCL28	**Mucosae-Associated Epithelial Chemokine**	-0.846	3.099E-02
HLA-DMA	**Major Histocompatibility Complex, Class II, DM Alpha**	-0.660	4.208E-02
KIT	**KIT Proto-Oncogene Receptor Tyrosine Kinase**	-0.706	4.817E-02

4.3.6 Analysis of RNA transcript abundance in ALI cultures of primary HBECs upon exposure to RSV

The PCA plot showed that the majority of the variation between control and infected samples was due to exposure to RSV (Figure 4.10A). Differential RNA transcript analysis showed

82 RNA transcripts to be differentially abundant upon exposure to RSV in ALI cultures of primary HBECs (Figure 4.10B) (Appendix 9). Of the 82, 30 were up-regulated and 52 were down-regulated upon exposure to RSV, compared to control ALI cultures. 132 RNA transcripts were significant under BH-FDR <0.30.

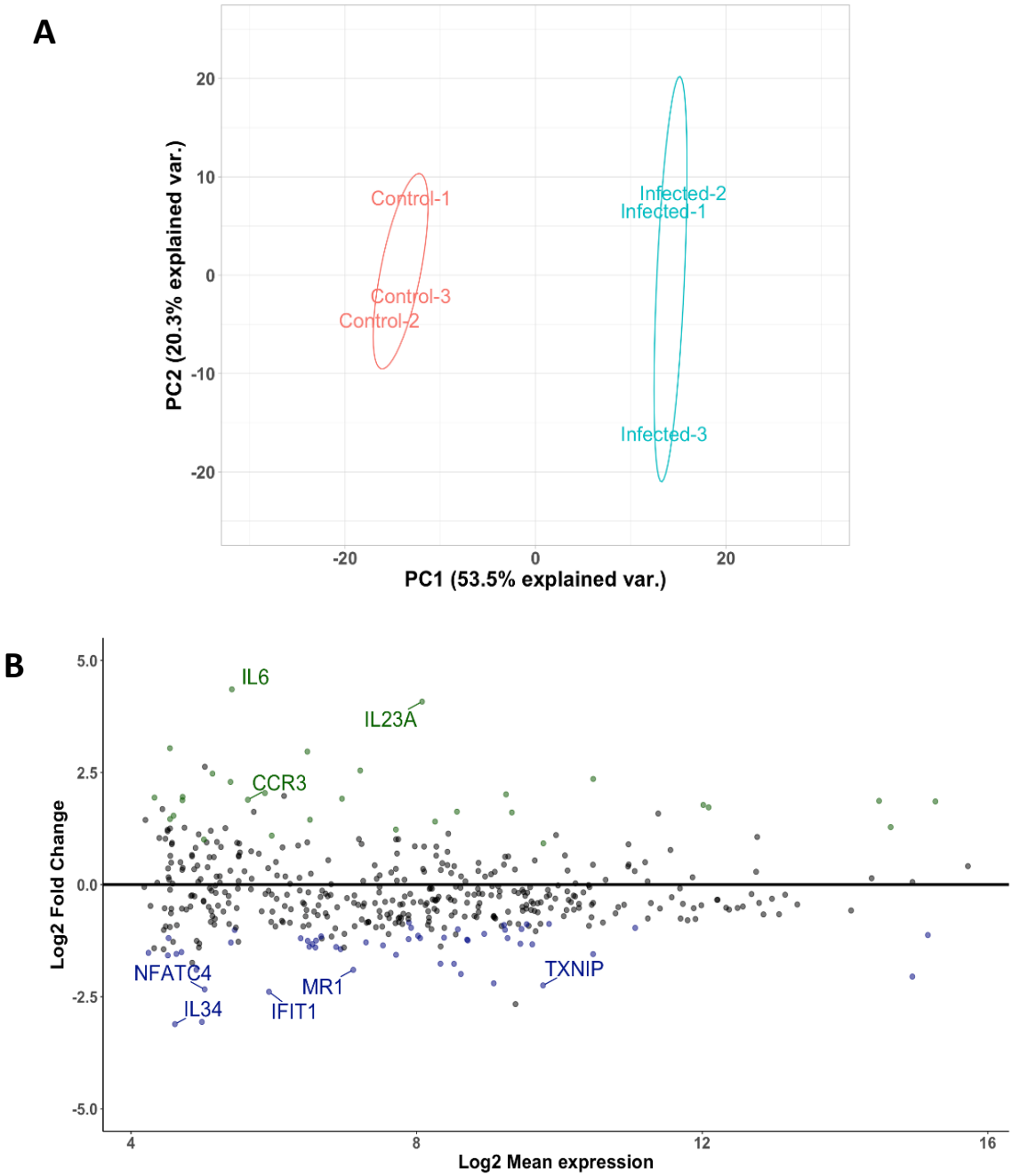

Figure 4.10: PCA plot and MA Plot analyses of ALIs exposed to RSV for 6 hours using Immune Profiling Panel.

A) PCA plot showed separation between control (Blue) and infected (Red) samples. Hence, most of the variation between samples could be explained due to the presence of RSV. B) MA plot showed 82 RNA transcripts to be differentially abundant upon exposure to RSV. Compared to control samples, 30 RNA transcripts were up-regulated (green) and 52 RNA transcripts were down-regulated (blue) (P-value < 0.05). RNA transcripts significant under BH-FDR < 0.1 are labeled.

Enrichment analysis in Enrichr identified Reactome pathways associated with chemokine receptors, immune system, class A/1 (Rhodopsin-like-receptors), cytokine signaling, peptide ligand-binding receptors and signaling by interleukins to be enriched among up-regulated RNA transcripts in ALI cultures upon exposure to RSV (Table 4.11). For the down-regulated RNA transcripts, immune system, cytokine signaling, innate immune system, signaling by interleukins and anti-viral mechanism by IFN-stimulated genes were among some of the enriched Reactome pathways (Table 4.12).

Table 4.11: Enriched Reactome pathways for up-regulated RNA transcripts upon exposure to RSV in ALI cultures of primary HBECs.

Term	Overlap	P-value	Adjusted P-value	Combined Score	Genes
Chemokine receptors bind chemokines_Homo sapiens_R-HSA-380108	6/56	2.060E-10	2.330E-08	43.833	CXCL8;CXCR1;CCL20;CXCL1;CXCL2;CCR3
Immune System_Homo sapiens_R-HSA-168256	14/1547	1.150E-08	6.520E-07	40.643	CSF3;IL1RN;RIPK2;TNFRSF18;SH2D1B;TICAM1;ISG20;CLEC4A;NFKBIA;IL6;IL23A;IL12A;TLR4;HLA-DOB
Class A/1 (Rhodopsin-like receptors)_Homo sapiens_R-HSA-373076	7/323	3.970E-07	1.120E-05	31.195	CXCL8;CXCR1;ADORA2A;CCL20;CXCL1;CXCL2;CCR3
Cytokine Signaling in Immune system_Homo sapiens_R-HSA-1280215	8/620	2.610E-06	4.910E-05	30.344	ISG20;CSF3;IL1RN;IL6;RIPK2;IL23A;TNFRSF18;IL12A
Peptide ligand-binding receptors_Homo sapiens_R-HSA-375276	6/193	3.660E-07	1.120E-05	28.947	CXCL8;CXCR1;CCL20;CXCL1;CXCL2;CCR3
Signaling by Interleukins_Homo sapiens_R-HSA-449147	6/392	2.180E-05	1.842E-04	25.581	CSF3;IL1RN;IL6;RIPK2;IL23A;IL12A
Diseases of Immune System_Homo sapiens_R-HSA-5260271	3/24	6.030E-06	7.580E-05	23.692	NFKBIA;TICAM1;TLR4
TRIF-mediated TLR3/TLR4 signaling_Homo sapiens_R-HSA-937061	4/97	1.290E-05	1.218E-04	23.262	NFKBIA;RIPK2;TICAM1;TLR4
Toll Like Receptor 2 (TLR2) Cascade_Homo sapiens_R-HSA-181438	3/92	3.495E-04	1.580E-03	14.426	NFKBIA;RIPK2;TLR4

Table 4.12: Enriched Reactome pathways for down-regulated RNA transcripts upon exposure to RSV in ALI cultures of primary HBECs.

Term	Overlap	P-value	Adjusted P-value	Combined Score	Genes
Immune System_Homo sapiens_R-HSA-168256	24/1547	9.074E-14	4.020E-11	67.036	DUSP4;MAP3K1;SYK;TNFRSF12A;STAT1;DDX58;IL34;NOD1;IFIT1;TIRAP;HLA-DMA;MAVS;HLA-DMB;INPP5D;SAA1;TXNIP;MAPK1;KLRD1;IKBKG;IL6R;HRAS;TLR3;JAK1;MAPK3
Cytokine Signaling in Immune system_Homo sapiens_R-HSA-1280215	15/620	3.076E-11	3.406E-09	57.559	DUSP4;TNFRSF12A;SYK;STAT1;DDX58;IL34;NOD1;IFIT1;INPP5D;MAPK1;IKBKG;HRAS;IL6R;JAK1;MAPK3
Innate Immune System_Homo sapiens_R-HSA-168249	16/807	1.133E-10	5.017E-09	53.814	DUSP4;MAP3K1;SYK;DDX58;NOD1;TIRAP;MAVS;SAA1;TXNIP;MAPK1;KLRD1;IKBKG;HRAS;TLR3;JAK1;MAPK3
Signaling by Interleukins_Homo sapiens_R-HSA-449147	12/392	2.768E-10	1.115E-08	52.833	DUSP4;SYK;STAT1;INPP5D;IL34;MAPK1;NOD1;IKBKG;HRAS;IL6R;JAK1;MAPK3
Activated TLR4 signalling_Homo sapiens_R-HSA-166054	9/112	1.175E-11	2.603E-09	51.564	DUSP4;MAP3K1;SAA1;MAPK1;NOD1;IKBKG;TIRAP;TLR3;MAPK3
TRAF6 mediated NF-kB activation_Homo sapiens_R-HSA-933542	5/24	3.993E-09	8.845E-08	35.791	MAVS;MAP3K1;DDX58;SAA1;IKBKG
Interleukin-3, 5 and GM-CSF signaling_Homo sapiens_R-HSA-512988	7/261	4.821E-06	5.209E-05	26.651	DUSP4;SYK;INPP5D;MAPK1;HRAS;JAK1;MAPK3
MAP kinase activation in TLR cascade_Homo sapiens_R-HSA-450294	5/60	4.781E-07	8.472E-06	26.452	DUSP4;MAPK1;NOD1;IKBKG;MAPK3
Antiviral mechanism by IFN-stimulated genes_Homo sapiens_R-HSA-1169410	5/72	1.196E-06	1.963E-05	25.282	STAT1;DDX58;IFIT1;MAPK3;JAK1

4.3.7 Analysis of RNA transcript abundance in high TEER and low TEER HBECs-ALI cultures

Differential RNA transcript analysis was performed on 447 RNA transcripts. Of the 447, 286 RNA transcripts were differentially abundant in high TEER samples compared to low TEER samples (P-Value < 0.05). 250 RNA transcripts were significant under BH-FDR < 0.30. Of the 286, 143 RNA transcripts were up-regulated and 143 were down-regulated in high TEER samples, compared to low TEER samples (Figure 4.11) (Appendix 10). 8 differentially abundant RNA transcripts had log2 fold change greater than 5, labeled in Figure 4.11.

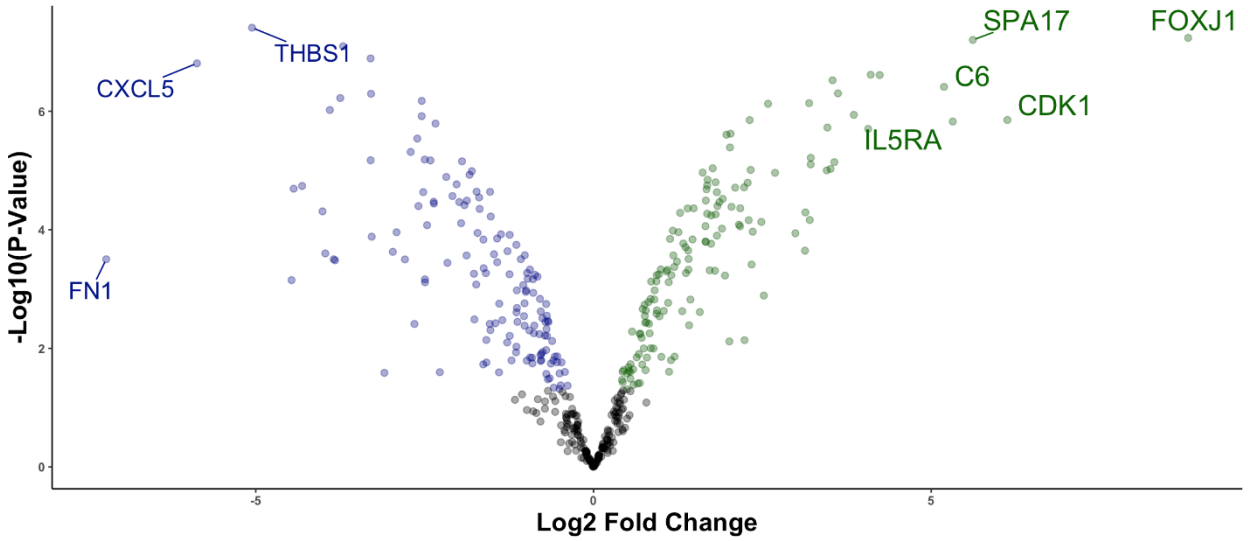

Figure 4.11 Volcano plot of differentially abundant RNA transcripts in high TEER samples compared to low TEER samples.
Volcano plot showing 286 out of 440 RNA transcripts to be differentially abundant in high TEER samples compared to low TEER samples, represented by blue and green dots. Of these 286, 143 were up-regulated (green) and 143 were down-regulated (blue) in high TEER samples compared to low TEER samples. 8 RNA transcripts had a log2 fold change greater than 5 (labeled).

4.4 Discussion

The research outlined in this chapter assessed the applicability of air-liquid interface (ALI) cultures of primary human bronchial epithelial cells (HBECs) for studying the early molecular response of human bronchial epithelium to *A. fumigatus* conidia. We monitored the

extent of conidia internalization and gene expression profiles of primary HBECs-ALI cultures and compared the results to submerged monolayer cultures of 1HAEs after exposure to *A. fumigatus* conidia. The specificity of response in HBECs-ALI cultures upon exposure to different pathogens was also investigated. To assess *A. fumigatus* specific response in HBECs-ALI, response to WT conidia was compared to a mutant fungal strain and to a respiratory syncytial virus (RSV). Differential abundance analysis was also conducted between high TEER and low TEER samples.

4.4.1 Interaction of *A. fumigatus* conidia in submerged monolayer cultures of 1HAEs

We confirmed that submerged monolayer cultures of 1HAEs are capable of phagocytosing conidia. After 6 hours, the proportion of bound conidia internalized was more than 1% (previously estimated for ALI cultures of primary HBECs upon exposure to *A. fumigatus* in Chapter 3*)*. Previous studies from our laboratory and others has shown that submerged monolayer cultures of bronchial epithelial cells or type II alveolar cells, internalize up to 50% of bound conidia (Zhang et al. 2005; Gomez et al. 2010; Julie A. Wasylnka and Moore 2003). Amitani and Kawanami (2009) used an organ culture model of the human bronchial epithelium, which had an air-mucosal interface, to study the interaction of respiratory mucosa with *A. fumigatus*. They showed that 6 hours after infection, the majority of conidia were adhered to damaged epithelial cells, and that conidia also bound to the indentations on the surface of non-ciliated epithelial cells (Amitani and Kawanami 2009). These data indicate that in the presence of mucus and cilia from functional goblet cells and ciliated cells, respectively, only a small number of conidia can bind and be internalized by bronchial epithelium. This was well-

represented by ALI cultures of HBECs since less than 1% of bound conidia were internalized after 6 hours.

4.4.2 Analysis of submerged monolayer culture of 1HAEs upon exposure to *A. fumigatus* conidia after 6 hours

nCounter Asthma Elements Panel and nCounter Immune Profiling Panel were used to assess the gene expression response in submerged monolayer cultures of 1HAEs upon exposure to *A. fumigatus* conidia for 6 hours. Of the 38 overlapping genes between both panels, Fas Associated Via Death Domain (FADD) replicated in the differentially abundant RNA transcripts in both panels. FADD is an adaptor protein for caspase-8 and is involved in inflammasome activation (Gurung et al. 2014). However, it was up-regulated in nCounter immune profiling panel and down-regulated in nCounter Asthma Elements Panel, indicating a need for replicating these experiments using a larger sample size.

nCounter Asthma Elements Panel showed RNA transcripts related to Dectin-1 signaling pathway to be differentially abundant in 1HAEs upon exposure to *A. fumigatus.* These RNA transcripts included NFKB Inhibitor Alpha (NFKBIA), Protein Phosphatase 3 Regulatory Subunit B, Alpha (PPP3Ri), Ubiquitin Conjugating Enzyme E2 D1 (UBE2D1), Proteasome Inhibitor Subunit 1 (PSMF1), and Nuclear Factor Kappa B Subunit 1 (NFKB1). These findings are consistent with the results of Sun et al., who reported that human bronchial epithelial cells recognize *A. fumigatus* through dectin-1 receptors and respond by producing reactive oxygen species, antimicrobial peptides and cytokines (W.-K. Sun et al. 2012). Hence, internalization of large numbers of conidia in 1HAEs may be associated with recognition of bound conidia by dectin-1

signaling pathway, which, in contrast to the HBECs-ALI model, may only be possible in the absence of mucociliary clearance.

Two RNA transcripts, GTF2H2 and C5AR1, overlapped between differentially abundant RNA transcripts identified using nCounter Asthma Elements Panel in 1HAEs and ALIs upon exposure *to A. fumigatus* conidia. Both genes changed in opposite directions in both *in-vitro* models: GTF2H2 was up-regulated in ALIs and down-regulated in 1HAEs, and C5AR1 was down-regulated in ALIs and up-regulated in 1HAEs, compared to control samples. GTF2H2 is a component of TFIIH complex, which is required for transcription, DNA repair and cell cycle control (Gibbons et al. 2012). Previously, it has been shown that cell cycle was down-regulated in submerged monolayer cultures of 16HBE14o- upon exposure to *A. fumigatus* after 6 hours (Gomez et al. 2010). Down-regulation of GTF2H2 in infected samples of 1HAEs compared to control samples may be due to a general stress response resulting from high number of conidia interacting with cells in this *in-vitro* model than the ALI model. Likewise, up-regulation of C5AR1, a receptor of complement system, in infected samples of 1HAEs may also be associated with more conidia binding to the surface of submerged monolayer *in-vitro* model, resulting in the activation of PRRs associated with the complement system in response to fungal conidia.

Of the 41 RNA transcripts differentially abundant in submerged monolayer cultures of 1HAEs, C-X-C Motif Chemokine Ligand 11 (CXCL11) and Toll like receptor 6 (TLR6) passed the BH-FDR < 0.30. Both were up-regulated in 1HAEs upon exposure to *A. fumigatus.* TLR6, along with TLR2 and TLR4, recognizes *A. fumigatus* and has been shown to be up-regulated in mice upon allergenic sensitization to *A. fumigatus* (Kurup, Raju, and Manickam 2005). Activation of TLR6 is known to be important for IL-23 production and the T_H17 response; both cytokines

regulate allergic-inflammatory responses in chronic-fungal induced asthma. Therefore, along with dectin-1 signaling, TLR6 recognizes *A. fumigatus* in 1HAEs and both PRRs may be important for initiating an immune response upon binding and internalization of *A. fumigatus* conidia in HBECs. Genes associated with complement and coagulation pathways were also up-regulated in 1HAEs upon exposure to *A. fumigatus*. These included Complement C1s subcomponent (C1S) in the Immune Profiling Panel and Complement C5a Receptor 1 (C5AR1) in Asthma Element Panel. The expression of complement proteins, along with other PRRs, such as TLRs and Dectin-1, may be associated with conidial binding and internalization in the human bronchial epithelium.

CXCL11, which passed the BH-FDR < 0.30 along with TLR6, is a ligand for CXCR3, and is known to be strongly induced by IFN-γ (Hirota et al. 2006). It can recruit T-cells, natural killer cells and macrophages to the site of infection by binding to CXCR3 (Torraca et al. 2015). IFN-γ is known to play a role in host defense against *A. fumigatus* and promotes fungal clearance in invasive pulmonary aspergillosis (Shao et al. 2005). Other RNA transcripts associated with interferon signaling included Interferon Induced Protein with Tetratricopeptide Repeats 2 (IFIT2) and Interferon Lambda 1 (IFNL1). Both were up-regulated in 1HAEs upon exposure to *A. fumigatus* conidia in our study. IFNL1 was also up-regulated in ALIs upon exposure to *A. fumigatus* conidia, indicating that interferon signaling may play an important role in eliciting appropriate immune response to the fungus.

The majority of GO terms were associated with innate and adaptive immune response for differentially abundant RNA transcripts. For example, regulation of regulatory T cell differentiation was enriched in the up-regulated RNA transcripts in 1HAEs upon exposure to *A. fumigatus*. The RNA transcripts associated with this GO term included B-cell lymphoma 6

(BCL6), Nuclear Factor of Activated T-cells 2 (NFATC2) and Runt Related Transcription Factor 1 (RUNX1). Specifically, NFATC2, along with other NFAT proteins, plays an important role in T cell activation and differentiation by producing cytokines such IL-2, IL-4 and IFN-γ (Gabriel et al. 2016). It was also upregulated in ALIs upon exposure to *A. fumigatu*s conidia. RNA transcripts regulating T cell activation and the T_H1/ T_H2 responses were differentially abundant in ALIs upon exposure to *A. fumigatus* conidia as well, indicating another mechanism which may be important in preventing fungal invasion.

Genes associated with GO term positive regulation of tumor necrosis factor production (Fas Associated Via Death Domain (FADD), Janus kinase 2 (JAK2), PYD and CATD Domain Containing (PYCARD), Thrombospondin 1 (THBS1)) were up-regulated upon exposure to *A. fumigatus* conidia in our study. Along with IFN-γ, Tumor necrosis factor (TNF)-α has shown to play protective roles in invasive aspergillosis in mice, and TNF-α deficient mice are more susceptible to infection with *A. fumigatus* (Nagai et al. 1995).

The down-regulated genes were enriched for negative regulation of T-cell proliferation and dendritic cell differentiation. RNA transcripts with negative regulation of T-cell proliferation included Caspase 3 (CASP3), CD274 Molecule (CD274), and CCAAT/Enhancer Binding Protein Beta (CEBPB). Interestingly, α-(1,3)-glucan on the cell wall of *A. fumigatus* has shown to promote T_H1 responses in dendritic cells upon down-regulation of CD274/PD-L1 pathway (Stephen-Victor et al. 2017). The genes associated with dendritic cell differentiation included AXL Receptor Tyrosine Kinase (AXL), Colony Stimulating Factor 2 (CSF2), and RELB Proto-Oncogene, NF-KB Subunit (RELB). Dendritic cells also play an important role in the initiating T_H2 responses and cytokines, such as CSF2, also known as Granulocyte-macrophage colony-

stimulating factor (GM-CSF), plays an important role in maturation of dendritic cells to promote T_H2 biased differentiation of CD4+ T cells. Elevated levels of GM-CSF in epithelial cells have been demonstrated to increase eosinophil activation and survival in asthmatics. It can recruit circulating neutrophils, macrophages and lymphocytes to the site of infection, and is used to treat neutropenia caused by cytotoxic chemotherapy in cancer patients, AIDs patients and patients after bone marrow transplantation. Even though GM-CSF is an essential pro-inflammatory cytokine that plays an important role in various inflammatory diseases, overexpression of GM-CSF may lead to severe inflammation and tissue damage due to macrophage accumulation and eosinophilia as well (Shi et al. 2006).

In addition to differences in internalization of conidia at 6 hours post-exposure, the differentially abundant RNA transcripts and proteins were also different in submerged monolayer culture of 1HAEs and differentiated ALI cultures of primary HBECs. Of the 41 differentially abundant RNA transcripts identified in both models using the immune profiling panel, 6 RNA transcripts overlapped. CXCL6, neutrophil chemoattractant, was down-regulated in ALIs but was up-regulated in ALIs upon exposure to *A. fumigatus* conidia. Proteins related to nonsense mediated decay, and rRNA processing were up-regulated in 1HAEs upon exposure to *A. fumigatus*. In contrast, these pathways were enriched in the down-regulated proteins in ALIs. These results suggest that the molecular response may be dependent on conidial binding and internalization in each model.

Proteins regulating RNA splicing were among the up-regulated proteins in 1HAEs upon exposure to conidia; these included several proteins from the heterogeneous nuclear ribonucleoproteins (hnRNPs) family: hnRNPR, hnRNPK, hnRNPA0, hnRNPC. hnRNPs are

multifunctional proteins that play an important role in RNA export, localization, translation and stability (Chaudhury, Chander, and Howe 2010). Despite having a high overlap between identified proteins, only 8 differentially abundant proteins overlapped between both models. Thus, differentially abundant genes in both models also varied at the protein-level.

Enrichment of genes associated with interferon signaling pathways, complement and coagulation pathway, nonsense mediated decay and rRNA processing in both models indicates that these pathways may play an important role in early molecular response to *A. fumigatus*. However, genes associated with these pathways were regulated differently in each model, as shown by differentially abundant RNA transcripts in each model. This indicates that the molecular response may be dependent on activation of different PRRs in each model, which in turn is related to the extent of binding of *A. fumigatus* conidia to host epithelia and/or by secretion of molecules from the surface of the conidia. Therefore, ALI cultures, with mucus-producing goblet cells and ciliated cells, may be a better model for studying host response in intact bronchial epithelium to fungal conidia and may more closely mimic the *in vivo* interaction between host and pathogen.

4.4.3 Analysis of pathogen-specific response in ALI cultures

NanoString nCounter platform was used to assess the specificity of response in primary HBECs upon exposure to different pathogens. TEER values were included as a covariate in the linear models during differential abundance analysis to account for variability in differentiation between samples.

Of the 52 RNA transcripts that were differentially abundant upon exposure to *Δkdnase A. fumigatus* conidia and 41 RNA transcripts that were differentially abundant upon exposure

to wild type (WT) *A. fumigatus* conidia in ALI cultures of HBECs, 11 RNA transcripts overlapped. Interestingly, the overlapping genes changed in the same direction (same log2 FC) in both experiments. These included RNA transcripts involved in producing soluble mediators of the innate immune system such as cytokines, chemokines and complement system. Specifically, RNA transcripts involved in cytokine production (FADD, SAA1, BST2, IFNL1, IDO1, C3), regulation of complement and coagulation pathways (CFB, C3) and neutrophil chemotaxis (CXCL5, CXCL6) were differentially abundant. Some of the overlapping genes are involved in T-cell proliferation, such as FADD, LCK, IFNL1, and IDO1. Specifically, FADD and IDO1 are involved in T_H2 type immune response. This indicates that these genes and pathways may play an important role in mediating early immune response against fungal pathogens in human bronchial epithelium.

Gene ontology enrichment analysis of differentially abundant RNA transcripts upon exposure to *Δkdnase A. fumigatus* showed enrichment of type 1 interferon signaling pathway in the up-regulated RNA transcripts. Specifically, interferon-stimulated genes (ISGs) were differentially abundant. These included Interferon alpha-inducible protein 27 (IFI27), Bone Marrow stromal antigen 2 (BST2), Interferon-induced transmembrane protein 2 (IFITM2), Interferon-induced 35kDA protein (IFI35) (Schoggins and Rice 2011). Furthermore, an Interferon Regulatory Factor (IRF), Interferon regulatory factor 5 (IRF5), was differentially abundant upon exposure to *Δkdnase A. fumigatus* conidia (Schoggins and Rice 2011). IRFs are produced upon detection of microbial products by PRRs and cytokines. These IRFs result in activation of interferons (IFNs) through JAK/STAT pathway to induce production of interferon-stimulated genes (ISGs). However, these ISGs can also be induced directly by IRFs in an IFN-independent pathway as well (Schoggins and Rice 2011). Type I IFNs, such as IFN-α and IFN-β, are

polypeptides secreted by infected cells and have been primarily known for anti-viral immune response, but can be expressed upon exposure to non-viral pathogens as well (Malireddi and Kanneganti 2013). The three major functions of type I IFNs include induction of cell-intrinsic antimicrobial states upon infection, modulating innate immune response to promote antigen presentation and natural killer cell functions, and activating adaptive immune system to result in high-affinity antigen-specific T and B cell responses and immunological memory (Ivashkiv and Donlin 2014). However, their role in fungal infections is not well-understood; two studies have indicated that *Candida* spp. stimulate the expression of IFN-β in mouse bone marrow-derived DCs and macrophages (Malireddi and Kanneganti 2013). Interestingly, GO ontologies associated with IFN-α and IFN-β were enriched for up-regulated RNA transcripts upon exposure to *Δkdnase A. fumigatus* conidia as well. None of these RNA transcripts, associated with Type I IFNs, were differentially abundant in ALI cultures upon exposure to WT *A. fumigatus* conidia. However, type III IFN, IFNL1, was differentially abundant upon exposure to both *Δkdnase A. fumigatus* conidia and Wild-type *A. fumigatus* conidia. We speculate that the *Δkdnase*, which has an altered cell wall composition (Nesbitt et al. 2018) may activate both type I and type III interferons by binding PRRs distinct from the ones bound by WT conidia. Further research is required to confirm this hypothesis.

Previously, it has been reported that higher number of macrophages are recruited in mouse lung upon exposure to *Δkdnase A. fumigatus* conidia than WT *A. fumigatus* conidia (Nesbitt et al. 2018). This was supported by enrichment of macrophage activation in GO terms. The RNA transcripts enriched included Hepatitis A virus cellular receptor 2 (HAVCR2/TIM3), Toll like Receptor Adaptor Molecular 1 (TICAM1/TIM1/TRIF), Interleukin-1 receptor like 1 (IL1RL1),

Toll-like receptor 4 (TLR4) and Toll like receptor 6 (TLR6). None of these RNA transcripts were differentially abundant in ALI cultures upon exposure to WT *A. fumigatus* conidia. TLR4 has been previously shown to be involved in recognition of *A. fumigatus* conidia (Netea et al. 2003). It is activated upon binding of two adaptor molecules, myeloid differentiation marker 88 (My D88) and TRIF. Specifically, TRIF- mediated signaling results in less toxic inflammatory response than MyD88-mediated signaling (Kolb et al. 2014). TRIF dependent signaling is also essential for the production of type 1 IFNs (Kolb et al. 2014). TLR signaling can result in production of pro-inflammatory cytokines and antimicrobial small molecules, such as nitric oxide, which can stimulate macrophage activation as well (Kaisho and Akira 2002). Hence, *Δkdnase A. fumigatus* may activate TLR4 signaling via TRIF adaptor molecule to produce type 1 IFNs.

GO terms related to T_H1 and T_H2 type immune response were also enriched in up-regulated RNA transcripts with the *Δkdnase* strain. Specifically, RNA transcripts associated with negative regulation of T_H1 type immune response were among the differentially abundant: Interleukin-1 receptor like 1 (IL1RL1), Hepatitis A virus cellular receptor 2 (HAVCR2), and Tumor necrosis factor ligand superfamily member 4 (TNFSF4). None of these genes were differentially abundant in ALI cultures upon exposure to WT *A. fumigatus*. IL1RL1, receptor for IL-33, can result in induction of T_H2 type immune response by producing pro-inflammatory cytokines (Akhabir and Sandford 2010). Therefore, exposure to *Δkdnase A. fumigatus* conidia in ALI cultures may elicit a T_H2 response

RNA transcripts associated with granulocyte chemotaxis were down-regulated in ALI cultures upon exposure to *Δkdnase A. fumigatus*. These included C-X-C Motif Chemokine Ligand 5 (CXCL5), C-X-C Motif Chemokine Ligand 6 (CXCL6) and S100 Calcium binding protein (S100A7).

CXCL5 and CXCL 6 were also previously down-regulated in ALI cultures upon exposure to WT *A. fumigatus* conidia, indicating that these chemokines may be important for general immune response towards fungal pathogens.

Interestingly, RNA transcripts regulating complement and coagulation cascades were both up-regulated and down-regulated in ALI cultures upon exposure to *Δkdnase A. fumigatus*. These included Complement Factor Properdin (CFP) and Complement C6 (C6) in the up-regulated RNA transcripts as well as Complement Factor B (CFB), Complement C3 (C3), Complement Factor I (CFI) and Complement Component 4B (C4B) in the down-regulated RNA transcripts. *A. fumigatus* has shown to evade complement system by secreting extracellular proteases (Behnsen et al. 2008). However, how *Δkdnase A. fumigatus* regulates different components of complement system is yet to be studied.

Enrichment of genes regulating cytokine production, neutrophil chemotaxis, complement and coagulation cascades and T-cell differentiation in ALI cultures upon exposure to both *Δkdnase* and WT *A. fumigatus* conidia indicates the importance of these pathways in early immune response against fungal pathogens. Up-regulation of PRRs such as complement proteins, TLR6 and TLR4 in ALI cultures upon exposure to *Δkdnase A. fumigatus* but not in WT *A. fumigatus* conidia, indicates pathogen specific response. Hence, in the presence *Δkdnase* in *A. fumigatus*, human bronchial epithelium may activate different PRRs to activate immune response to the mutant strain of *A. fumigatus.*

Differential abundance analysis was conducted between ALI cultures exposed to *Δkdnase A. fumigatus* conidia and WT *A. fumigatus* conidia to assess differentially abundant RNA transcripts between the WT and mutant strain of *A. fumigatus.* The up-regulated RNA

transcripts in the *Δkdnase A. fumigatus* conidia infected ALI cultures compared to WT *A. fumigatus* conidia infected ALI cultures included Toll-like Receptor 6 (TLR6), Cluster of Differentiation 14 (CD 14), Surfactant Pulmonary-Associated D-Binding Protein (DMBT1), Interleukin 1 Receptor Associated Kinase 2 (IRAK2), 5`-Nucleotide Ecto (NT5E) and Interleukin 32 (IL32). TLR-6 recognizes lipoproteins, peptidoglycans, lipotechoic acids, zymosan, and mannan, and CD 14 is also co-receptor with TRL4 for LPS recognition (Kawasaki and Kawai 2014). DMBT1 plays important role in mucosal protection, and has been shown to be up-regulated in inflamed mucosa of Crohn's disease patients (End et al. 2009). IRAK-2 is known to induce NF-kB activation through TLR signaling, and may play an important role in regulating expression of various inflammatory genes (Jain, Kaczanowska, and Davila 2014). IL-32 is also known to be involved in production of various chemokines and inflammatory cytokines such as TNF-α (Khawar, Abbasi, and Sheikh 2016).

CCL28, Mucosae-Associated Epithelial Chemokine, was down-regulated in ALI cultures upon exposure to *Δkdnase A. fumigatus* conidia, compared to WT *A. fumigatus* conidia. Previously, down-regulation of CCL28 has been associated with less inflammatory condition in the intestines (Rashidiani et al. 2017). TFRC, receptor involved in cellular uptake of iron from transferrin, was down-regulated in ALI cultures upon exposure to mutant conidia compared to WT conidia. It is highly expressed in rapidly dividing cells (Ponka and Lok 1999), and down-regulation of TFRC may indicate a quiescent state of cells and down-regulation of cell-cycle progression. Hence, RNA transcripts involved in pathogen recognition and production of inflammatory cytokines were differentially abundant in ALI cultures upon exposure to *Δkdnase A. fumigatus* conidia, compared to WT *A. fumigatus* conidia.

To further assess the specificity of response to different pathogens, differentially abundant RNA transcripts in ALI cultures of primary HBECs upon exposure to RSV for 6 hours were analyzed using Nanostring's nCounter Immune profiling panel. Of the 82 differentially abundant RNA transcripts in RSV exposed ALI cultures and 41 differentially abundant RNA transcripts in WT *A. fumigatus* conidia exposed ALI cultures, only 4 genes overlapped. Of these 4, SAA1 and LCN2 were down-regulated in both experiments. SYK and IL6R were down-regulated in RSV exposed ALI cultures compared to controls, and up-regulated in WT *A. fumigatu*s exposed ALI cultures compared to controls.

Differentially abundant RNA transcripts and enriched pathways indicated virus recognition by TLR4, TLR6, and TLR3. Both extracellular receptors, TLR4 and TLR6, were up-regulated, whereas TLR3, intracellular TLR was down-regulated upon exposure to RSV compared to controls. It was previously reported that F glycoprotein, found on the RSV surface, can activate TLR4, which plays an important role in the activation of innate immune response to RSV infection (Haynes et al. 2001). TICAM1/TRIF was also up-regulated upon exposure to RSV, indicating that activation of Toll-like signaling may be independent of MyD88. TLR4 activation can result in the expression of pro-inflammatory cytokines, such as Interkeukin-6 (IL-6) (Kurt-Jones et al. 2000). IL-6, along with Interleukin 23 Subunit Alpha (IL23A), were among the top two differentially abundant RNA transcripts in ALI cultures upon exposure to RSV. Previously, higher levels of IL-6 during RSV infection have been reported in serum levels and secretions of RSV-infected individuals (Sheeran et al. 1999). IL-6 plays an important role in both innate and adaptive immunity. It can recruit neutrophils to the site of inflammation and can affect macrophage differentiation as well (Liu et al. 1997; Chomarat et al. 2000). IL23A encodes

subunit of Interleukin 23 (IL-23), a cytokine that drives differentiation of human T_H17 cells. Excess secretion of IL-6 is also associated with T_H17 differentiation (Feng et al. 2015). T_H17 cells play an important role in host defense against extracellular pathogens, and recruit neutrophils and macrophages to the site of infection. IL-6 and IL-23 expression has been reported in BEAS-2B cells upon RSV infection by Feng et al. (2015). This shows that the human bronchial epithelium can release inflammatory cytokines upon RSV infection to initiate an immune response resulting in the migration of T_H subsets.

In the RSV-exposed HBECs-ALI cells, up-regulated RNA transcripts included nitric oxide synthase 2 (NOS2A). Nitric oxide has been shown to inhibit replication of other viruses, including rhinovirus (Vareille et al. 2011). Susceptibility to RSV has been associated with single-nucleotide polymorphisms in NOS2A (Janssen et al. 2007). NF-kB Inhibitor Alpha (NFKBIA) was up-regulated upon exposure to RSV; this is known as a major negative regulator of NF-kB activity (Hayden and Ghosh 2008). However, not much is known about its role in RSV infection.

Reactome pathways enriched for up-regulated RNA transcripts upon RSV infection included chemokine receptors bind chemokines. These included RNA transcripts associated with chemokine receptors, CXCR1 and CCR3, and chemokines, CXCL2, CXCL8, CXCL1, and CCL20. CXCR1 is a receptor for CXCL8 and primary RSV infections have been characterized by intense neutrophil recruitment due to high levels of CXCL8, resulting in mucosal inflammation and increased airway secretions, coughing and sneezing (Ugonna et al. 2016). Along with CXCL8, CXCL1 and CXCL2 are involved in neutrophil chemotaxis and activation (Sawant et al. 2016) (W. B. Xu et al. 1995). The receptor CCR3 has been also previously reported to be up-regulated in bronchial biopsies of inflamed asthmatic airways compared to non-diseased (Beck et al. 2006).

The differential abundance of RNA transcripts regulating neutrophil recruitment is supported by studies that showed rapid neutrophil infiltration in severe primary RSV infection: 80% of cells in bronchoalveolar lavage in RSV patients were neutrophils (Stoppelenburg et al. 2013).

Other chemokines such as CCL3, CXCL11 and CXCL10 were down-regulated upon exposure to RSV in ALI cultures compared to control samples. Down-regulation of TLR3 has been previously associated with down-regulation of CXCL10 but not CXCL8 (Rudd et al. 2005). This was supported in the differential abundance results as both TLR3 and CXCL10 were down-regulated, and CXCL8 was up-regulated in ALI cultures upon exposure to RSV. CXCL10 was among the top most highly down-regulated RNA transcripts with Log2 Fold change of -3.06, along with IL-34 (Log2 Fold change -3.11). CXCL10 is known for regulating interferon response and activating T_H1 cells to site of infection. It is also a chemoattractant for monocytes, T cells and NK cells, and increased expression has been associated with advanced human cancers (LIU, GUO, and STILES 2011). Hence, down-regulation of CXCL10 may be associated with host defense against RSV. The two top most significant down-regulated RNA transcripts upon exposure to RSV in ALI cultures were Nuclear Factor of Activated T-Cells 4 (NFATC4) and Interleukin 34 (IL-34). NFAT genes are known to be involved in T-cell activation and differentiation (Gabriel et al. 2016), whereas IL-34 can induce activation of macrophages (Masteller and Wong 2014).

Therefore, activation of PRRs such as TLR4, TLR6, and TLR3 in the presence of RSV but not WT fungal conidia indicates specific detection of viral components by differentiated ALI cultures. The high expression of cytokines genes such as IL-6, IL-23A, along with chemokines and chemokine receptors are critical to prevent viral infection. Overall, our data shows that RSV

infection may result in a more severe early immune response than fungal infection in cultured bronchial epithelial cells.

4.4.4 Analysis of high TEER and low TEER ALI cultures

Previously, TEER values have been used to assess the integrity of tight junctions and cellular barriers in cell culture models of epithelial/endothelial monolayers and ALI cultures. A wide range of TEER values has been reported for pulmonary models in previous studies, ranging from 150 $\Omega.cm^2$ for the transformed human Type 2 epithelial cell line (A549) to 3133 $\Omega.cm^2$ for primary human nasal epithelial cells (Srinivasan et al. 2015). Factors that may affect TEER measurements have been identified in previous studies, and include temperature, cell passage number and cell culture medium composition. Primary cells can have a high degree of variability in TEER values due to differences between donor, cell passage and experiments (Stewart et al. 2012). Therefore, by using TEER value as an assessment of culture differentiation and development in experiment #1, RNA transcripts that were differentially abundant in 4 well-differentiated ALI cultures compared to 2 non-well-differentiated ALI cultures were assessed.

The up-regulated differentially abundant RNA transcripts in high TEER ALI cultures consisted of 5 RNA transcripts with high log2 fold change (greater than 5). These included Forkhead Box J1 (FOXJ1), Cyclin Dependent Kinase 1 (CDK1), Complement Component 6 (C6), Sperm-autoantigenic protein 17 (SPA17), and Interleukin-5 receptor alpha (IL5RA). The FOXJ1 RNA transcript had the highest log2 fold change of 8.81 with the greatest statistical significance (P-value < 0.05). FOXJI is a transcription factor, known to be involved in the formation of motile cilia, and has been shown to be conserved across vertebrates (Choksi et al. 2014). It was also identified to be highly expressed in 28-day old ALI cultures of primary HBECs in a study where

microarray analysis was conducted to assess genes involved in mucociliary differentiation (Ross et al. 2007). FOXJ1 regulates expression of SPA17 in both *Xenopus* and mouse (Thomas et al. 2010). SPA17 was also among the 5 highly expressed RNA transcripts. It was previously shown to be highly expressed in tissues with high number of ciliated cells, such as olfactory sensory neurons, and is important for cilia formation in mouse (McClintock et al. 2008). IL-5RA, a receptor for IL-5, was also among the 5 highly expressed RNA transcripts. IL-5 is known to be involved in eosinophil differentiation and survival. The regulatory factor X (RFX) family DNA-binding proteins can also bind to the *cis* element of IL-5RA (Kouro and Takatsu 2009). Interestingly, RFX transcription factors have been shown to regulate ciliary genes as well (Piasecki, Burghoorn, and Swoboda 2010). RNA transcripts regulating cell cycle and important for cellular proliferation, such as CDK1, were also highly expressed in high TEER samples. CDK1 is known to be a central regulator in cell division and controls cells undergoing G2 phase and mitosis (Diril et al. 2012). C6 was also among the highly expressed RNA transcripts in high TEER ALI cultures compared to low TEER ALI cultures. Overall, RNA transcripts of genes regulating ciliogenesis were highly expressed in high TEER samples compared to low TEER samples, indicating that along with having a more intact cellular barrier, high TEER cultures may have more cilia than low TEER samples.

The down-regulated differentially abundant RNA transcripts with log2 fold change greater than 5 included Fibronectin-1 (FN1), Thrombospondin-1 (THBS1) and Chemokine Ligand 5 (CXCL5). FN1 is a glycoprotein that plays an important role in cell adhesion, migration, growth and differentiation (Pankov and Yamada 2002). It is also a ligand of THBS1, an extracellular molecule that functions by binding to multiple ligands (Resovi et al. 2014). CXCL5, also known

as epithelial cell derived neutrophil attractant 78, is primarily expressed in epithelial cells, and is involved in recruitment and activation of neutrophils by binding to CXCR2. Overexpression of CXCL5 is associated with tumor proliferation, growth and migration (Xia et al. 2015). Other down-regulated differentially abundant RNA transcripts included Transforming growth factor beta-2 (TGFB2), an extracellular glycoprotein involved in cell proliferation and differentiation (M. Wu, Chen, and Li 2016). Therefore, extracellular proteins regulating cell proliferation and differentiation had a lower expression level in high TEER samples compared to low TEER samples.

4.5 Summary

The research presented in this chapter demonstrated that, unlike differentiated ALI cultures of primary HBECs, submerged monolayer cultures of 1HAEs bind and internalize more conidia. This could be due to the absence of ciliated and mucus-producing goblet cells in submerged monolayer cultures, which were present in differentiated ALI cultures of primary HBECs. Even though similar pathways were enriched for differentially abundant RNA transcripts in both *in-vitro* models, the genes regulating these pathways were different in each model. This may be due to the differences in binding of *A. fumigatus* conidia to host epithelia or from secretion of molecules from the surface of the conidia, which can activate different PRRs. Therefore, ALI cultures, with mucus-producing goblet cells and ciliated cells, may be a better model for studying host response in intact bronchial epithelium to fungal conidia. Nevertheless, in damaged epithelia, as may occur in patients with underlying disease (Davies 2009), newly-migrated epithelial cells may behave more like the submerged monolayers. Even ALI cultures may not have consistent levels of differentiation which can affect their response to pathogens.

Therefore, prior to conducting experiments, it is also important to assess the cellular integrity and differentiation of ALI cultures. TEER values are a useful surrogate for differentiation through which the presence of mucus and cilia may also be monitored. Finally, using different fungal strains and a respiratory virus, we showed that the transcriptomic and proteomic responses in ALI cultures of primary HBECs is pathogen specific.

Chapter 5 General conclusions and future directions

The aims of the research presented here were to employ an *in-vitro* model that closely mimics the bronchial epithelial barrier in the conductive zone of the respiratory tract to study the early molecular response of the host to *A. fumigatus*. Hence, an ALI model of primary HBECs with basal cells, ciliated cells and mucus-producing goblet cells, was utilized to study the transcriptomics and proteomics of bronchial epithelial cells upon exposure to *A. fumigatus* conidia. Using this model, we showed that unlike submerged monolayer cultures, differentiated ALI cultures of primary HBECs internalized less than 1% of bound conidia. This could be due to the mucociliary barrier produced by ALI cultures, which is not generated in submerged monolayer cultures. Chapter 4 showed that submerged monolayer cultures of 1HAEs internalized more conidia than ALI cultures. This also shows that intact ALI cultures well-mimic the *in-vivo* host-pathogen interaction where pathogenic fungal spores are efficiently removed from the respiratory tract of healthy individuals without causing an allergic response or infection. Hence, well-differentiated ALI cultures of primary HBECs can be used for studying the early molecular response of intact bronchial epithelium to conidia for future studies.

It was shown using a multi-OMICs approach that interaction of *A. fumigatus* with ALI cultures of primary HBECs elicits molecular response by up-regulating pathways associated with apoptosis/autophagy, translation, unfolded protein response and cell cycle. In contrast, complement and coagulation pathways, iron homeostasis, non-sense mediated decay and rRNA binding pathways were down-regulated upon exposure to *A. fumigatus*. Hence, ALI cultures showed that the effect of fungal conidia on early response could either be mediated by binding

of *A. fumigatus* conidia or the interaction of molecules from the surface of conidia could also initiate the host response.

For the first time, differentiated primary cell cultures along with a multi-OMICs approach was used to study proteomics and transcriptomics in the host-pathogen interaction. Therefore, it was important to further evaluate the applicability of ALI cultures to study host-pathogen interactions for future studies. This was performed by two separate approaches, first by conducting comparative transcriptomics and proteomics studies in submerged monolayer cultures of 1HAEs upon exposure to *A. fumigatus*, and then by assessing pathogen-specific response in ALI cultures.

Even though submerged monolayer cultures of 1HAEs are morphologically different, the pathways enriched were similar to that of ALI cultures upon conidial exposure. These included interferon signaling pathways, complement and coagulation pathway, non-sense mediated decay, and rRNA processing pathways. However, only a small number of differentially abundant RNA transcripts and proteins overlapped between both models. Genes associated with PRR signaling pathways, such as Dectin-1 signaling and TLR signaling, were differentially abundant in 1HAEs upon exposure to *A. fumigatus* conidia. This further supports that in the absence of ciliated and mucus-producing goblet cells, more conidia can bind with bronchial epithelial cells, and may result in the activation of PRRs to elicit an immune response. The research presented here also showed that it may be important to use ALI cultures with approximately similar TEER values in order to ensure that these cultures closely mimic the *in-vivo* epithelium as well as to decrease variability within ALI cultures.

Transcriptomics of *Δkdnase A. fumigatus* conidia identified expression of PRRs, which were not expressed upon exposure to WT *A. fumigatus* conidia. However, further work needs to be conducted to elucidate the importance of Kdnase in fungal virulence upon interaction with host bronchial epithelium. RSV resulted in expression of neutrophil chemoattractants as well as pro-inflammatory cytokines in HBECs. These specific responses upon exposure to different pathogens indicated that response in ALI cultures is pathogen-specific.

One limitation of this study was the small sample size which reflects the exploratory nature of the conducted experiments; however, it resulted in difficulty in obtaining robust significant results. To overcome this and to prioritize biologically significant findings, statistical significance was tested using both nominal (P-value < 0.05) and adjusted P-values (BH-FDR). The small sample size may have yielded a high signal-to-noise ratio, generating high number of false positives in our study. Hence, further analysis is necessary of these exploratory findings.

The results of the present study motivates research in several different avenues. Nevertheless, to increase confidence in these results, it is important to validate them using a larger sample size. NanoString only allowed profiling of a limited number genes associated with the immune response. Therefore, high throughput techniques, such as RNA-sequencing and single-cell sequencing, would be ideal to gain a better understanding of early molecular response of host to *A. fumigatus* in this *in-vitro* model for future studies. Genes of interest from these studies can also be validated using single-cell western platforms to confirm expression levels. Shotgun proteomics was also utilized for the first time to profile host proteomics upon interaction with *A. fumigatus*. Novel proteins and pathways were identified in both *in-vitro* models, which can be also be further investigated in future studies.

ALI cultures of primary HBECs can also be used to understand how host pathology in asthmatic and cystic fibrosis patients may influence the early immune response to *A. fumigatus* conidia as well. The identification of different genes and pathways associated with differentiated ALI cultures of asthmatic cells may help characterize the molecular response involved in *A. fumigatus* induced asthma.

Overall, the research presented here demonstrates that ALI models of primary HBECs can provide novel insights into the mechanisms associated with this opportunistic fungal pathogen. The main significance of this work is three-fold. First, it has shown that differentiated cultures of primary HBECs internalize less conidia than submerged monolayer cultures. This may be better representative of the nature of interaction between inhaled *A. fumigatus* conidia and the bronchial epithelium *in-vivo*. It is likely that in the presence of dysfunctional mucociliary barrier, this interaction can result in a range of diseases associated with *A. fumigatus*. Secondly, this research represents successful application of multi-OMICs approach to identify novel genes and pathways associated with host-pathogen interaction. Finally, it was shown that the response in ALI cultures is pathogen-specific. Even though further experiments need to be conducted to validate these expression patterns, this work shows that an *in-vitro* model of primary HBECs grown in ALI can be used for studying host-pathogen interactions in intact bronchial epithelium.

References

Agarwal, R., A. Chakrabarti, A. Shah, D. Gupta, J. F. Meis, R. Guleria, R. Moss, D. W. Denning, and ABPA complicating asthma ISHAM working group. 2013. “Allergic Bronchopulmonary Aspergillosis: Review of Literature and Proposal of New Diagnostic and Classification Criteria.” *Clinical and Experimental Allergy: Journal of the British Society for Allergy and Clinical Immunology* 43 (8): 850–73. https://doi.org/10.1111/cea.12141.

Aimanianda, Vishukumar, Jagadeesh Bayry, Silvia Bozza, Olaf Kniemeyer, Katia Perruccio, Sri Ramulu Elluru, Cécile Clavaud, et al. 2009. “Surface Hydrophobin Prevents Immune Recognition of Airborne Fungal Spores.” *Nature* 460 (7259): 1117. https://doi.org/10.1038/nature08264.

Akhabir, Loubna, and Andrew Sandford. 2010. “Genetics of Interleukin 1 Receptor-Like 1 in Immune and Inflammatory Diseases.” *Current Genomics* 11 (8): 591–606. https://doi.org/10.2174/138920210793360907.

Albright, C. D., R. T. Jones, E. A. Hudson, J. A. Fontana, B. F. Trump, and J. H. Resau. 1990. “Transformed Human Bronchial Epithelial Cells (BEAS-2B) Alter the Growth and Morphology of Normal Human Bronchial Epithelial Cells in Vitro.” *Cell Biology and Toxicology* 6 (4): 379–98.

Alekseeva, Ludmila, Dominique Huet, Françoise Féménia, Isabelle Mouyna, Mahdia Abdelouahab, Adrien Cagna, Daniel Guerrier, et al. 2009. “Inducible Expression of Beta Defensins by Human Respiratory Epithelial Cells Exposed to *Aspergillus fumigatus* Organisms.” *BMC Microbiology* 9 (February): 33. https://doi.org/10.1186/1471-2180-9-33.

Amitani, R., and R. Kawanami. 2009. “Interaction of Aspergillus with Human Respiratory Mucosa: A Study with Organ Culture Model.” *Medical Mycology* 47 (Supplement_1): S127–31. https://doi.org/10.1080/13693780802558959.

Amitani, R, G Taylor, E N Elezis, C Llewellyn-Jones, J Mitchell, F Kuze, P J Cole, and R Wilson. 1995. “Purification and Characterization of Factors Produced by *Aspergillus fumigatus* Which Affect Human Ciliated Respiratory Epithelium.” *Infection and Immunity* 63 (9): 3266–71.

Antosiewicz, Jedrzej, Wieslaw Ziolkowski, Jan Jacek Kaczor, and Anna Herman-Antosiewicz. 2007. “Tumor Necrosis Factor-α-Induced Reactive Oxygen Species Formation Is Mediated by JNK1-Dependent Ferritin Degradation and Elevation of Labile Iron Pool.” *Free Radical Biology and Medicine* 43 (2): 265–70. https://doi.org/10.1016/j.freeradbiomed.2007.04.023.

Ashburner, M., C. A. Ball, J. A. Blake, D. Botstein, H. Butler, J. M. Cherry, A. P. Davis, et al. 2000. “Gene Ontology: Tool for the Unification of Biology. The Gene Ontology Consortium.” *Nature Genetics* 25 (1): 25–29. https://doi.org/10.1038/75556.

Ayers, M. M., and P. K. Jeffery. 1988. “Proliferation and Differentiation in Mammalian Airway Epithelium.” *The European Respiratory Journal* 1 (1): 58–80.

Ayloo, Swathi, Jacob E. Lazarus, Aditya Dodda, Mariko Tokito, E. Michael Ostap, and Erika L. F. Holzbaur. 2014. “Dynactin Functions as Both a Dynamic Tether and Brake during Dynein-Driven Motility.” *Nature Communications* 5 (September): 4807. https://doi.org/10.1038/ncomms5807.

Balloy, Viviane, and Michel Chignard. 2009. “The Innate Immune Response to *Aspergillus fumigatus*.” *Microbes and Infection* 11 (12): 919–27. https://doi.org/10.1016/j.micinf.2009.07.002.

Balloy, Viviane, Jean-Michel Sallenave, Yongzheng Wu, Lhousseine Touqui, Jean-Paul Latgé, Mustapha Si-Tahar, and Michel Chignard. 2008. “Aspergillus fumigatus-Induced Interleukin-8 Synthesis by Respiratory Epithelial Cells Is Controlled by the Phosphatidylinositol 3-Kinase, p38 MAPK, and ERK1/2 Pathways and Not by the Toll-like Receptor-MyD88 Pathway.” *The Journal of Biological Chemistry* 283 (45): 30513–21. https://doi.org/10.1074/jbc.M803149200.

Bals, Robert, Xiaorong Wang, Michael Zasloff, and James M. Wilson. 1998. “The Peptide Antibiotic LL-37/hCAP-18 Is Expressed in Epithelia of the Human Lung Where It Has Broad Antimicrobial Activity at the Airway Surface.” *Proceedings of the National Academy of Sciences* 95 (16): 9541–46. https://doi.org/10.1073/pnas.95.16.9541.

Barnes, Penelope D., and Kieren A. Marr. 2006. “Aspergillosis: Spectrum of Disease, Diagnosis, and Treatment.” *Infectious Disease Clinics of North America*, Fungal Infections, 20 (3): 545–61. https://doi.org/10.1016/j.idc.2006.06.001.

Barnes, Rosemary A., and P. Lewis White. 2016. “PCR Technology for Detection of Invasive Aspergillosis.” *Journal of Fungi* 2 (3). https://doi.org/10.3390/jof2030023.

Barrios, CS, BD Johnson, JD Henderson, JN Fink, KJ Kelly, and VP Kurup. 2005. “The Costimulatory Molecules CD80, CD86 and OX40L Are Up-Regulated in Aspergillus fumigatus Sensitized Mice.” *Clinical and Experimental Immunology* 142 (2): 242–50. https://doi.org/10.1111/j.1365-2249.2005.02905.x.

Becker, K. L., M. S. Gresnigt, S. P. Smeekens, C. W. Jacobs, C. Magis-Escurra, M. Jaeger, X. Wang, et al. 2015. “Pattern Recognition Pathways Leading to a Th2 Cytokine Bias in Allergic Bronchopulmonary Aspergillosis Patients.” *Clinical & Experimental Allergy* 45 (2): 423–37. https://doi.org/10.1111/cea.12354.

Beck, Lisa A., Brian Tancowny, Mary E. Brummet, S. Yukiko Asaki, Stephanie L. Curry, Margaret B. Penno, Martyn Foster, Ash Bahl, and Cristiana Stellato. 2006. “Functional Analysis of the Chemokine Receptor CCR3 on Airway Epithelial Cells.” *The Journal of Immunology* 177 (5): 3344–54. https://doi.org/10.4049/jimmunol.177.5.3344.

Bedke, Tanja, Rossana G. Iannitti, Antonella De Luca, Gloria Giovannini, Francesca Fallarino, Carsten Berges, Jean-Paul Latgé, Hermann Einsele, Luigina Romani, and Max S. Topp. 2014. “Distinct and Complementary Roles for Aspergillus fumigatus-Specific Tr1 and Foxp3+

Regulatory T Cells in Humans and Mice." *Immunology and Cell Biology* 92 (8): 659–70. https://doi.org/10.1038/icb.2014.34.

Behnsen, Judith, Andrea Hartmann, Jeannette Schmaler, Alexander Gehrke, Axel A. Brakhage, and Peter F. Zipfel. 2008. "The Opportunistic Human Pathogenic Fungus Aspergillus fumigatus Evades the Host Complement System." *Infection and Immunity* 76 (2): 820–27. https://doi.org/10.1128/IAI.01037-07.

Beisswenger, C., C. Hess, and R. Bals. 2012. "Aspergillus fumigatus Conidia Induce Interferon-β Signalling in Respiratory Epithelial Cells." *European Respiratory Journal* 39 (2): 411–18. https://doi.org/10.1183/09031936.00096110.

Bellanger, Anne-Pauline, Laurence Millon, Khaled Khoufache, Danièle Rivollet, Ivan Bièche, Ingrid Laurendeau, Michel Vidaud, Françoise Botterel, and Stéphane Bretagne. 2009. "Aspergillus fumigatus Germ Tube Growth and Not Conidia Ingestion Induces Expression of Inflammatory Mediator Genes in the Human Lung Epithelial Cell Line A549." *Journal of Medical Microbiology* 58 (Pt 2): 174–79. https://doi.org/10.1099/jmm.0.005488-0.

Ben-Ami, Ronen, Russell E. Lewis, and Dimitrios P. Kontoyiannis. 2010. "Enemy of the (immunosuppressed) State: An Update on the Pathogenesis of *Aspergillus fumigatus* Infection." *British Journal of Haematology* 150 (4): 406–17. https://doi.org/10.1111/j.1365-2141.2010.08283.x.

Bennett, Joan W. 2010. "An Overview of Genus Aspergillus." In *In Aspergillus: Molecular Biology and Genomics*, 1–17.

Bercusson, Amelia, Leon de Boer, and Darius Armstrong-James. 2017. "Endosomal Sensing of Fungi: Current Understanding and Emerging Concepts." *Medical Mycology* 55 (1): 10–15. https://doi.org/10.1093/mmy/myw072.

Beresford, Paul J., Dong Zhang, David Y. Oh, Zusen Fan, Eric L. Greer, Melissa L. Russo, Madhuri Jaju, and Judy Lieberman. 2001. "Granzyme A Activates an Endoplasmic Reticulum-Associated Caspase-Independent Nuclease to Induce Single-Stranded DNA Nicks." *Journal of Biological Chemistry* 276 (46): 43285–93. https://doi.org/10.1074/jbc.M108137200.

Bhabhra, R., and D. S. Askew. 2005. "Thermotolerance and Virulence of Aspergillus fumigatus: Role of the Fungal Nucleolus." *Medical Mycology* 43 Suppl 1 (May): S87–93.

Bhowmick, Rudra, and Heather Gappa-Fahlenkamp. 2016. "Cells and Culture Systems Used to Model the Small Airway Epithelium." *Lung* 194 (3): 419–28. https://doi.org/10.1007/s00408-016-9875-2.

Bidula, Stefan, Hany Kenawy, Youssif M. Ali, Darren Sexton, Wilhelm J. Schwaeble, and Silke Schelenz. 2013. "Role of Ficolin-A and Lectin Complement Pathway in the Innate Defense

against Pathogenic Aspergillus Species." *Infection and Immunity* 81 (5): 1730–40. https://doi.org/10.1128/IAI.00032-13.

Bindea, Gabriela, Jérôme Galon, and Bernhard Mlecnik. 2013. "CluePedia Cytoscape Plugin: Pathway Insights Using Integrated Experimental and in Silico Data." *Bioinformatics* 29 (5): 661–63. https://doi.org/10.1093/bioinformatics/btt019.

Bindea, Gabriela, Bernhard Mlecnik, Hubert Hackl, Pornpimol Charoentong, Marie Tosolini, Amos Kirilovsky, Wolf-Herman Fridman, Franck Pagès, Zlatko Trajanoski, and Jérôme Galon. 2009. "ClueGO: A Cytoscape Plug-in to Decipher Functionally Grouped Gene Ontology and Pathway Annotation Networks." *Bioinformatics* 25 (8): 1091–93. https://doi.org/10.1093/bioinformatics/btp101.

Borger, P., G. H. Koëter, J. A. Timmerman, E. Vellenga, J. F. Tomee, and H. F. Kauffman. 1999. "Proteases from *Aspergillus fumigatus* Induce Interleukin (IL)-6 and IL-8 Production in Airway Epithelial Cell Lines by Transcriptional Mechanisms." *The Journal of Infectious Diseases* 180 (4): 1267–74. https://doi.org/10.1086/315027.

Botterel, Françoise, Karine Gross, Oumaïma Ibrahim-Granet, Khaled Khoufache, Virginie Escabasse, André Coste, Catherine Cordonnier, Estelle Escudier, and Stéphane Bretagne. 2008. "Phagocytosis of *Aspergillus fumigatus* Conidia by Primary Nasal Epithelial Cells in Vitro." *BMC Microbiology* 8 (June): 97. https://doi.org/10.1186/1471-2180-8-97.

Bozza, Silvia, Roberta Gaziano, Antonio Spreca, Angela Bacci, Claudia Montagnoli, Paolo di Francesco, and Luigina Romani. 2002. "Dendritic Cells Transport Conidia and Hyphae of *Aspergillus fumigatus* from the Airways to the Draining Lymph Nodes and Initiate Disparate Th Responses to the Fungus." *Journal of Immunology (Baltimore, Md.: 1950)* 168 (3): 1362–71.

Bradding, Peter, Andrew F. Walls, and Stephen T. Holgate. 2006. "The Role of the Mast Cell in the Pathophysiology of Asthma." *The Journal of Allergy and Clinical Immunology* 117 (6): 1277–84. https://doi.org/10.1016/j.jaci.2006.02.039.

Brakhage, Axel A, Sandra Bruns, Andreas Thywissen, Peter F Zipfel, and Judith Behnsen. 2010. "Interaction of Phagocytes with Filamentous Fungi." *Current Opinion in Microbiology*, Host–Microbe Interactions: Fungi/Parasites/Viruses, 13 (4): 409–15. https://doi.org/10.1016/j.mib.2010.04.009.

Brinkmann, Volker, Ulrike Reichard, Christian Goosmann, Beatrix Fauler, Yvonne Uhlemann, David S. Weiss, Yvette Weinrauch, and Arturo Zychlinsky. 2004. "Neutrophil Extracellular Traps Kill Bacteria." *Science (New York, N.Y.)* 303 (5663): 1532–35. https://doi.org/10.1126/science.1092385.

Brown, Neil A., and Gustavo H. Goldman. 2016. "The Contribution of *Aspergillus fumigatus* Stress Responses to Virulence and Antifungal Resistance." *Journal of Microbiology (Seoul,*

Korea) 54 (3): 243–53. https://doi.org/10.1007/s12275-016-5510-4.

Bullens, Dominique M. A., A. Decraene, E. Dilissen, I. Meyts, K. De Boeck, L. J. Dupont, and J. L. Ceuppens. 2008. "Type III IFN-Lambda mRNA Expression in Sputum of Adult and School-Aged Asthmatics." *Clinical and Experimental Allergy: Journal of the British Society for Allergy and Clinical Immunology* 38 (9): 1459–67. https://doi.org/10.1111/j.1365-2222.2008.03045.x.

Cadena, Jose, George R. Thompson, and Thomas F. Patterson. 2016. "Invasive Aspergillosis: Current Strategies for Diagnosis and Management." *Infectious Disease Clinics of North America*, Fungal Infections, 30 (1): 125–42. https://doi.org/10.1016/j.idc.2015.10.015.

Canessa, Paulo, and Luis F. Larrondo. 2013. "Environmental Responses and the Control of Iron Homeostasis in Fungal Systems." *Applied Microbiology and Biotechnology* 97 (3): 939–55. https://doi.org/10.1007/s00253-012-4615-x.

Cenci, E., A. Mencacci, G. Del Sero, A. Bacci, C. Montagnoli, C. F. d'Ostiani, P. Mosci, et al. 1999. "Interleukin-4 Causes Susceptibility to Invasive Pulmonary Aspergillosis through Suppression of Protective Type I Responses." *The Journal of Infectious Diseases* 180 (6): 1957–68. https://doi.org/10.1086/315142.

Chaudhury, Arindam, Praveen Chander, and Philip H. Howe. 2010. "Heterogeneous Nuclear Ribonucleoproteins (hnRNPs) in Cellular Processes: Focus on hnRNP E1's Multifunctional Regulatory Roles." *RNA* 16 (8): 1449–62. https://doi.org/10.1261/rna.2254110.

Chen, Edward Y., Christopher M. Tan, Yan Kou, Qiaonan Duan, Zichen Wang, Gabriela Vaz Meirelles, Neil R. Clark, and Avi Ma'ayan. 2013. "Enrichr: Interactive and Collaborative HTML5 Gene List Enrichment Analysis Tool." *BMC Bioinformatics* 14 (April): 128. https://doi.org/10.1186/1471-2105-14-128.

Chen, Fangyan, Changjian Zhang, Xiaodong Jia, Shuo Wang, Jing Wang, Yong Chen, Jingya Zhao, Shuguang Tian, Xuelin Han, and Li Han. 2015. "Transcriptome Profiles of Human Lung Epithelial Cells A549 Interacting with *Aspergillus fumigatus* by RNA-Seq." *PLOS ONE* 10 (8): e0135720. https://doi.org/10.1371/journal.pone.0135720.

Chen, Ting-Yu, Jhih-Siang Syu, Tsung-Yu Han, Hui-Ling Cheng, Fu-I. Lu, and Chia-Yih Wang. 2015. "Cell Cycle-Dependent Localization of Dynactin Subunit p150 Glued at Centrosome." *Journal of Cellular Biochemistry* 116 (9): 2049–60. https://doi.org/10.1002/jcb.25160.

Choksi, Semil P., Gilbert Lauter, Peter Swoboda, and Sudipto Roy. 2014. "Switching on Cilia: Transcriptional Networks Regulating Ciliogenesis." *Development* 141 (7): 1427–41. https://doi.org/10.1242/dev.074666.

Chomarat, P., J. Banchereau, J. Davoust, and A. K. Palucka. 2000. "IL-6 Switches the Differentiation of Monocytes from Dendritic Cells to Macrophages." *Nature Immunology* 1 (6):

510–14. https://doi.org/10.1038/82763.

Chotirmall, Sanjay H., Mazen Al-Alawi, Bojana Mirkovic, Gillian Lavelle, P. Mark Logan, Catherine M. Greene, and Noel G. McElvaney. 2013. “Aspergillus-Associated Airway Disease, Inflammation, and the Innate Immune Response.” Research article. BioMed Research International. 2013. https://www.hindawi.com/journals/bmri/2013/723129/.

Chotirmall, Sanjay H., Bojana Mirkovic, Gillian M. Lavelle, and Noel G. McElvaney. 2014. “Immunoevasive Aspergillus Virulence Factors.” *Mycopathologia* 178 (5-6): 363–70. https://doi.org/10.1007/s11046-014-9768-y.

Collins, Peter L., and Barney S. Graham. 2008. “Viral and Host Factors in Human Respiratory Syncytial Virus Pathogenesis.” *Journal of Virology* 82 (5): 2040–55. https://doi.org/10.1128/JVI.01625-07.

Cowen, Leah E., and Susan Lindquist. 2005. “Hsp90 Potentiates the Rapid Evolution of New Traits: Drug Resistance in Diverse Fungi.” *Science (New York, N.Y.)* 309 (5744): 2185–89. https://doi.org/10.1126/science.1118370.

Cozens, A. L., M. J. Yezzi, M. Yamaya, D. Steiger, J. A. Wagner, S. S. Garber, L. Chin, E. M. Simon, G. R. Cutting, and P. Gardner. 1992. “A Transformed Human Epithelial Cell Line That Retains Tight Junctions Post Crisis.” *In Vitro Cellular & Developmental Biology: Journal of the Tissue Culture Association* 28A (11-12): 735–44.

Crapo, J. D., B. E. Barry, P. Gehr, M. Bachofen, and E. R. Weibel. 1982. “Cell Number and Cell Characteristics of the Normal Human Lung.” *The American Review of Respiratory Disease* 126 (2): 332–37. https://doi.org/10.1164/arrd.1982.126.2.332.

Croft, Carys A., Luka Culibrk, Margo M. Moore, and Scott J. Tebbutt. 2016. “Interactions of *Aspergillus fumigatus* Conidia with Airway Epithelial Cells: A Critical Review.” *Frontiers in Microbiology* 7 (April). https://doi.org/10.3389/fmicb.2016.00472.

Culibrk, Luka, Carys A. Croft, and Scott J. Tebbutt. 2016. “Systems Biology Approaches for Host–Fungal Interactions: An Expanding Multi-Omics Frontier.” *OMICS: A Journal of Integrative Biology* 20 (3): 127–38. https://doi.org/10.1089/omi.2015.0185.

Dagenais, Taylor R. T., and Nancy P. Keller. 2009. “Pathogenesis of *Aspergillus fumigatus* in Invasive Aspergillosis.” *Clinical Microbiology Reviews* 22 (3): 447–65. https://doi.org/10.1128/CMR.00055-08.

Davies, Donna E. 2009. “The Role of the Epithelium in Airway Remodeling in Asthma.” *Proceedings of the American Thoracic Society* 6 (8): 678–82. https://doi.org/10.1513/pats.200907-067DP.

Del Sero, G., A. Mencacci, E. Cenci, C. F. d'Ostiani, C. Montagnoli, A. Bacci, P. Mosci, M. Kopf, and L. Romani. 1999. "Antifungal Type 1 Responses Are Upregulated in IL-10-Deficient Mice." *Microbes and Infection* 1 (14): 1169–80.

Denning, David W., Kostantinos Riniotis, Richard Dobrashian, and Helen Sambatakou. 2003. "Chronic Cavitary and Fibrosing Pulmonary and Pleural Aspergillosis: Case Series, Proposed Nomenclature Change, and Review." *Clinical Infectious Diseases* 37 (Supplement_3): S265–80. https://doi.org/10.1086/376526.

Dewi, Intan M. W., Frank L. van de Veerdonk, and Mark S. Gresnigt. 2017. "The Multifaceted Role of T-Helper Responses in Host Defense against *Aspergillus fumigatus*." *Journal of Fungi* 3 (4): 55. https://doi.org/10.3390/jof3040055.

Diril, M. Kasim, Chandrahas Koumar Ratnacaram, V. C. Padmakumar, Tiehua Du, Martin Wasser, Vincenzo Coppola, Lino Tessarollo, and Philipp Kaldis. 2012. "Cyclin-Dependent Kinase 1 (Cdk1) Is Essential for Cell Division and Suppression of DNA Re-Replication but Not for Liver Regeneration." *Proceedings of the National Academy of Sciences* 109 (10): 3826–31. https://doi.org/10.1073/pnas.1115201109.

Drummond, Rebecca A, Shinobu Saijo, Yoichiro Iwakura, and Gordon D Brown. 2011. "The Role of Syk/CARD9 Coupled C-Type Lectins in Antifungal Immunity." *European Journal of Immunology* 41 (2): 276–81. https://doi.org/10.1002/eji.201041252.

Dumestre-Pérard, Chantal, Bertrand Lamy, Delphine Aldebert, Catherine Lemaire-Vieille, Renée Grillot, Jean-Paul Brion, Jean Gagnon, and Jean-Yves Cesbron. 2008. "Aspergillus Conidia Activate the Complement by the Mannan-Binding Lectin C2 Bypass Mechanism." *Journal of Immunology (Baltimore, Md.: 1950)* 181 (10): 7100–7105.

End, Caroline, Floris Bikker, Marcus Renner, Gaby Bergmann, Stefan Lyer, Stephanie Blaich, Melanie Hudler, et al. 2009. "DMBT1 Functions as Pattern-Recognition Molecule for Poly-Sulfated and Poly-Phosphorylated Ligands." *European Journal of Immunology* 39 (3): 833–42. https://doi.org/10.1002/eji.200838689.

Espinosa, Vanessa, and Amariliz Rivera. 2016. "First Line of Defense: Innate Cell-Mediated Control of Pulmonary Aspergillosis." *Frontiers in Microbiology* 7. https://doi.org/10.3389/fmicb.2016.00272.

Faro-Trindade, Inês, Janet A. Willment, Ann M. Kerrigan, Pierre Redelinghuys, Sabelo Hadebe, Delyth M. Reid, Naren Srinivasan, et al. 2012. "Characterisation of Innate Fungal Recognition in the Lung." *PLOS ONE* 7 (4): e35675. https://doi.org/10.1371/journal.pone.0035675.

Fekkar, A., V. Balloy, C. Pionneau, C. Marinach-Patrice, M. Chignard, and D. Mazier. 2012. "Secretome of Human Bronchial Epithelial Cells in Response to the Fungal Pathogen *Aspergillus fumigatus* Analyzed by Differential In-Gel Electrophoresis." *Journal of Infectious Diseases* 205

(7): 1163–72. https://doi.org/10.1093/infdis/jis031.

Feldmesser, Marta. 2006. “Role of Neutrophils in Invasive Aspergillosis ▿ .” *Infection and Immunity* 74 (12): 6514–16. https://doi.org/10.1128/IAI.01551-06.

Feng, Jingjing, Yunwen Hu, Zhigang Song, Yi Liu, Xuejun Guo, and Zhijun Jie. 2015. “Interleukin-23 Facilitates Th1 and Th2 Cell Differentiation in Vitro Following Respiratory Syncytial Virus Infection.” *Journal of Medical Virology* 87 (4): 708–15. https://doi.org/10.1002/jmv.24126.

Forbes, Ben, Atiya Shah, Gary P Martin, and Alison B Lansley. 2003. “The Human Bronchial Epithelial Cell Line 16HBE14o− as a Model System of the Airways for Studying Drug Transport.” *International Journal of Pharmaceutics* 257 (1): 161–67. https://doi.org/10.1016/S0378-5173(03)00129-7.

Foster, Leonard J., Carmen L. de Hoog, and Matthias Mann. 2003. “Unbiased Quantitative Proteomics of Lipid Rafts Reveals High Specificity for Signaling Factors.” *Proceedings of the National Academy of Sciences of the United States of America* 100 (10): 5813–18. https://doi.org/10.1073/pnas.0631608100.

Frisvad, Jens C., Christian Rank, Kristian F. Nielsen, and Thomas O. Larsen. 2009. “Metabolomics of *Aspergillus fumigatus*.” *Medical Mycology* 47 Suppl 1: S53–71. https://doi.org/10.1080/13693780802307720.

Fujita, Teizo. 2002. “Evolution of the Lectin-Complement Pathway and Its Role in Innate Immunity.” *Nature Reviews. Immunology* 2 (5): 346–53. https://doi.org/10.1038/nri800.

Gabay, C., and I. Kushner. 1999. “Acute-Phase Proteins and Other Systemic Responses to Inflammation.” *The New England Journal of Medicine* 340 (6): 448–54. https://doi.org/10.1056/NEJM199902113400607.

Gabriel, Christian H., Fridolin Gross, Martin Karl, Heike Stephanowitz, Anna Floriane Hennig, Melanie Weber, Stefanie Gryzik, et al. 2016. “Identification of Novel Nuclear Factor of Activated T Cell (NFAT)-Associated Proteins in T Cells.” *Journal of Biological Chemistry* 291 (46): 24172–87. https://doi.org/10.1074/jbc.M116.739326.

Gafa, Valérie, Maria Elena Remoli, Elena Giacomini, Maria Cristina Gagliardi, Roberto Lande, Martina Severa, Renée Grillot, and Eliana M. Coccia. 2007. “In Vitro Infection of Human Dendritic Cells by *Aspergillus fumigatus* Conidia Triggers the Secretion of Chemokines for Neutrophil and Th1 Lymphocyte Recruitment.” *Microbes and Infection* 9 (8): 971–80. https://doi.org/10.1016/j.micinf.2007.03.015.

Geissler, A., F. Haun, D. O. Frank, K. Wieland, M. M. Simon, M. Idzko, R. J. Davis, U. Maurer, and C. Borner. 2013. “Apoptosis Induced by the Fungal Pathogen Gliotoxin Requires a Triple Phosphorylation of Bim by JNK.” *Cell Death and Differentiation* 20 (10): 1317.

https://doi.org/10.1038/cdd.2013.78.

Gibbons, Brian J., Edward J. Brignole, Maia Azubel, Kenji Murakami, Neil R. Voss, David A. Bushnell, Francisco J. Asturias, and Roger D. Kornberg. 2012. "Subunit Architecture of General Transcription Factor TFIIH." *Proceedings of the National Academy of Sciences* 109 (6): 1949–54. https://doi.org/10.1073/pnas.1105266109.

Gomez, Pol, Tillie L Hackett, Margo M Moore, Darryl A Knight, and Scott J Tebbutt. 2010. "Functional Genomics of Human Bronchial Epithelial Cells Directly Interacting with Conidia of *Aspergillus fumigatus*." *BMC Genomics* 11 (June): 358. https://doi.org/10.1186/1471-2164-11-358.

Gray, T E, K Guzman, C W Davis, L H Abdullah, and P Nettesheim. 1996. "Mucociliary Differentiation of Serially Passaged Normal Human Tracheobronchial Epithelial Cells." *American Journal of Respiratory Cell and Molecular Biology* 14 (1): 104–12. https://doi.org/10.1165/ajrcmb.14.1.8534481.

Gregson, Lea, William W. Hope, and Susan J. Howard. 2012. "In Vitro Model of Invasive Pulmonary Aspergillosis in the Human Alveolus." In *Host-Fungus Interactions*, 361–67. Methods in Molecular Biology. Humana Press. https://link.springer.com/protocol/10.1007/978-1-61779-539-8_24.

Gump, Jacob M., and Andrew Thorburn. 2011. "Autophagy and Apoptosis- What's the Connection?" *Trends in Cell Biology* 21 (7): 387–92. https://doi.org/10.1016/j.tcb.2011.03.007.

Gurung, Prajwal, Paras K. Anand, R. K. Subbarao Malireddi, Lieselotte Vande Walle, Nina Van Opdenbosch, Christopher P. Dillon, Ricardo Weinlich, Douglas R. Green, Mohamed Lamkanfi, and Thirumala-Devi Kanneganti. 2014. "FADD and Caspase-8 Mediate Priming and Activation of the Canonical and Noncanonical Nlrp3 Inflammasomes." *The Journal of Immunology* 192 (4): 1835–46. https://doi.org/10.4049/jimmunol.1302839.

Gurung, Prajwal, and Thirumala-Devi Kanneganti. 2015. "Novel Roles for Caspase-8 in IL-1β and Inflammasome Regulation." *The American Journal of Pathology* 185 (1): 17–25. https://doi.org/10.1016/j.ajpath.2014.08.025.

Hacker, Stefan, Christopher Lambers, Konrad Hoetzenecker, Andreas Pollreisz, Clemens Aigner, Michael Lichtenauer, Andreas Mangold, et al. 2009. "Elevated HSP27, HSP70 and HSP90 Alpha in Chronic Obstructive Pulmonary Disease: Markers for Immune Activation and Tissue Destruction." *Clinical Laboratory* 55 (1-2): 31–40.

Han, Xuelin, Rentao Yu, Dongyu Zhen, Sha Tao, Martina Schmidt, and Li Han. 2011. "β-1,3-Glucan-Induced Host Phospholipase D Activation Is Involved in *Aspergillus fumigatus* Internalization into Type II Human Pneumocyte A549 Cells." *PloS One* 6 (7): e21468. https://doi.org/10.1371/journal.pone.0021468.

Hayden, Matthew S., and Sankar Ghosh. 2008. “Shared Principles in NF-kappaB Signaling.” *Cell* 132 (3): 344–62. https://doi.org/10.1016/j.cell.2008.01.020.

Haynes, Lia M., Deborah D. Moore, Evelyn A. Kurt-Jones, Robert W. Finberg, Larry J. Anderson, and Ralph A. Tripp. 2001. “Involvement of Toll-Like Receptor 4 in Innate Immunity to Respiratory Syncytial Virus.” *Journal of Virology* 75 (22): 10730–37. https://doi.org/10.1128/JVI.75.22.10730-10737.2001.

Hetz, Claudio. 2012. “The Unfolded Protein Response: Controlling Cell Fate Decisions under ER Stress and beyond.” *Nature Reviews Molecular Cell Biology* 13 (2): 89. https://doi.org/10.1038/nrm3270.

Hirota, Yasushi, Yutaka Osuga, Kaori Koga, Osamu Yoshino, Tetsuya Hirata, Chieko Morimoto, Miyuki Harada, et al. 2006. “The Expression and Possible Roles of Chemokine CXCL11 and Its Receptor CXCR3 in the Human Endometrium.” *The Journal of Immunology* 177 (12): 8813–21. https://doi.org/10.4049/jimmunol.177.12.8813.

Hissen, Anna H. T., Adrian N. C. Wan, Mark L. Warwas, Linda J. Pinto, and Margo M. Moore. 2005. “The *Aspergillus fumigatus* Siderophore Biosynthetic Gene sidA, Encoding L-Ornithine N5-Oxygenase, Is Required for Virulence.” *Infection and Immunity* 73 (9): 5493–5503. https://doi.org/10.1128/IAI.73.9.5493-5503.2005.

Ip, W K, C K Wong, and C W K Lam. 2006. “Interleukin (IL)-4 and IL-13 up-Regulate Monocyte Chemoattractant Protein-1 Expression in Human Bronchial Epithelial Cells: Involvement of p38 Mitogen-Activated Protein Kinase, Extracellular Signal-Regulated Kinase 1/2 and Janus Kinase-2 but Not c-Jun NH2-Terminal Kinase 1/2 Signalling Pathways.” *Clinical and Experimental Immunology* 145 (1): 162–72. https://doi.org/10.1111/j.1365-2249.2006.03085.x.

Ivashkiv, Lionel B., and Laura T. Donlin. 2014. “Regulation of Type I Interferon Responses.” *Nature Reviews. Immunology* 14 (1): 36–49. https://doi.org/10.1038/nri3581.

Jain, Ajay, Sabina Kaczanowska, and Eduardo Davila. 2014. “IL-1 Receptor-Associated Kinase Signaling and Its Role in Inflammation, Cancer Progression, and Therapy Resistance.” *Frontiers in Immunology* 5 (November). https://doi.org/10.3389/fimmu.2014.00553.

Janssen, Riny, Louis Bont, Christine L. E. Siezen, Hennie M. Hodemaekers, Marieke J. Ermers, Gerda Doornbos, Ruben van ’t Slot, et al. 2007. “Genetic Susceptibility to Respiratory Syncytial Virus Bronchiolitis Is Predominantly Associated with Innate Immune Genes.” *The Journal of Infectious Diseases* 196 (6): 826–34. https://doi.org/10.1086/520886.

Jean Beltran, Pierre M, Joel D Federspiel, Xinlei Sheng, and Ileana M Cristea. 2017. “Proteomics and Integrative Omic Approaches for Understanding Host–pathogen Interactions and Infectious Diseases.” *Molecular Systems Biology* 13 (3). https://doi.org/10.15252/msb.20167062.

Jeffery, P. K. 1991. “Morphology of the Airway Wall in Asthma and in Chronic Obstructive Pulmonary Disease.” *The American Review of Respiratory Disease* 143 (5 Pt 1): 1152–58; discussion 1161. https://doi.org/10.1164/ajrccm/143.5_Pt_1.1152.

Johnson, Steven, Marek Michalak, Michal Opas, and Paul Eggleton. 2001. “The Ins and Outs of Calreticulin: From the ER Lumen to the Extracellular Space.” *Trends in Cell Biology* 11 (3): 122–29. https://doi.org/10.1016/S0962-8924(01)01926-2.

Kaisho, Tsuneyasu, and Shizuo Akira. 2002. “Toll-like Receptors as Adjuvant Receptors.” *Biochimica et Biophysica Acta (BBA) - Molecular Cell Research* 1589 (1): 1–13. https://doi.org/10.1016/S0167-4889(01)00182-3.

Kalnina, Zane, K. Silina, R. Bruvere, N. Gabruseva, A. Stengrevics, S. Barnikol-Watanabe, M. Leja, and A. Line. 2009. “Molecular Characterisation and Expression Analysis of SEREX-Defined Antigen NUCB2 in Gastric Epithelium, Gastritis and Gastric Cancer.” *European Journal of Histochemistry: EJH* 53 (1): 7–18.

Kaplan, Mark H., Matthew M. Hufford, and Matthew R. Olson. 2015. “The Development and in Vivo Function of T Helper 9 Cells.” *Nature Reviews. Immunology* 15 (5): 295–307. https://doi.org/10.1038/nri3824.

Karp, Philip H., Thomas O. Moninger, S. Pary Weber, Tamara S. Nesselhauf, Janice L. Launspach, Joseph Zabner, and Michael J. Welsh. 2002. “An In Vitro Model of Differentiated Human Airway Epithelia.” In *Epithelial Cell Culture Protocols*, 115–37. Methods In Molecular Medicine™. Humana Press. https://link.springer.com/protocol/10.1385/1-59259-185-X:115.

Kauffman, H. F., J. F. Tomee, M. A. van de Riet, A. J. Timmerman, and P. Borger. 2000. “Protease-Dependent Activation of Epithelial Cells by Fungal Allergens Leads to Morphologic Changes and Cytokine Production.” *The Journal of Allergy and Clinical Immunology* 105 (6 Pt 1): 1185–93.

Kaur, Gurvinder, and Jannette M. Dufour. 2012. “Cell Lines.” *Spermatogenesis* 2 (1): 1–5. https://doi.org/10.4161/spmg.19885.

Kawai, T., and S. Akira. 2006. “TLR Signaling.” *Cell Death and Differentiation* 13 (5): 816–25. https://doi.org/10.1038/sj.cdd.4401850.

Kawamura, S., S. Maesaki, K. Tomono, T. Tashiro, and S. Kohno. 2000. “Clinical Evaluation of 61 Patients with Pulmonary Aspergilloma.” *Internal Medicine (Tokyo, Japan)* 39 (3): 209–12.

Kawasaki, Takumi, and Taro Kawai. 2014. “Toll-Like Receptor Signaling Pathways.” *Frontiers in Immunology* 5 (September). https://doi.org/10.3389/fimmu.2014.00461.

Khawar, Muhammad Babar, Muddasir Hassan Abbasi, and Nadeem Sheikh. 2016. “IL-32: A

Novel Pluripotent Inflammatory Interleukin, towards Gastric Inflammation, Gastric Cancer, and Chronic Rhino Sinusitis." *Mediators of Inflammation* 2016. https://doi.org/10.1155/2016/8413768.

Kheradmand, Farrah, Attila Kiss, Jie Xu, Seung-Hyo Lee, Pappachan E. Kolattukudy, and David B. Corry. 2002. "A Protease-Activated Pathway Underlying Th Cell Type 2 Activation and Allergic Lung Disease." *The Journal of Immunology* 169 (10): 5904–11. https://doi.org/10.4049/jimmunol.169.10.5904.

Khoufache, Khaled, Odile Cabaret, Cécile Farrugia, Danièle Rivollet, Annie Alliot, Eric Allaire, Catherine Cordonnier, Stéphane Bretagne, and Françoise Botterel. 2010. "Primary in Vitro Culture of Porcine Tracheal Epithelial Cells in an Air-Liquid Interface as a Model to Study Airway Epithelium and *Aspergillus fumigatus* Interactions." *Medical Mycology* 48 (8): 1049–55. https://doi.org/10.3109/13693786.2010.496119.

Kim, J. I., I. C. Ho, M. J. Grusby, and L. H. Glimcher. 1999. "The Transcription Factor c-Maf Controls the Production of Interleukin-4 but Not Other Th2 Cytokines." *Immunity* 10 (6): 745–51.

Kim, Tae Hoon, and Heung Kyu Lee. 2014. "Innate Immune Recognition of Respiratory Syncytial Virus Infection." *BMB Reports* 47 (4): 184–91. https://doi.org/10.5483/BMBRep.2014.47.4.050.

Knight, Darryl A., and Stephen T. Holgate. 2003. "The Airway Epithelium: Structural and Functional Properties in Health and Disease." *Respirology (Carlton, Vic.)* 8 (4): 432–46.

Knutsen, Alan P., and Raymond G. Slavin. 2011. "Allergic Bronchopulmonary Aspergillosis in Asthma and Cystic Fibrosis." *Clinical and Developmental Immunology* 2011. https://doi.org/10.1155/2011/843763.

Kolb, Joseph P., Carolyn R. Casella, Shuvasree SenGupta, Paula M. Chilton, and Thomas C. Mitchell. 2014. "Type I Interferon Signaling Contributes to the Bias That Toll-like Receptor 4 Exhibits for Signaling Mediated by the Adaptor Protein TRIF." *Science Signaling* 7 (351): ra108. https://doi.org/10.1126/scisignal.2005442.

Koltsida, Ourania, Michael Hausding, Athanasios Stavropoulos, Sonja Koch, George Tzelepis, Caroline Ubel, Sergei V. Kotenko, et al. 2011. "IL-28A (IFN-λ2) Modulates Lung DC Function to Promote Th1 Immune Skewing and Suppress Allergic Airway Disease." *EMBO Molecular Medicine* 3 (6): 348–61. https://doi.org/10.1002/emmm.201100142.

Kouro, Taku, and Kiyoshi Takatsu. 2009. "IL-5- and Eosinophil-Mediated Inflammation: From Discovery to Therapy." *International Immunology* 21 (12): 1303–9. https://doi.org/10.1093/intimm/dxp102.

Kousha, M., R. Tadi, and A. O. Soubani. 2011. "Pulmonary Aspergillosis: A Clinical Review."

European Respiratory Review 20 (121): 156–74. https://doi.org/10.1183/09059180.00001011.

Kozel, T. R. 1996. “Activation of the Complement System by Pathogenic Fungi.” *Clinical Microbiology Reviews* 9 (1): 34–46.

Kozel, T. R., M. A. Wilson, T. P. Farrell, and S. M. Levitz. 1989. “Activation of C3 and Binding to *Aspergillus fumigatus* Conidia and Hyphae.” *Infection and Immunity* 57 (11): 3412–17.

Krämer, Andreas, Jeff Green, Jack Pollard, and Stuart Tugendreich. 2014. “Causal Analysis Approaches in Ingenuity Pathway Analysis.” *Bioinformatics (Oxford, England)* 30 (4): 523–30. https://doi.org/10.1093/bioinformatics/btt703.

Kuleshov, Maxim V., Matthew R. Jones, Andrew D. Rouillard, Nicolas F. Fernandez, Qiaonan Duan, Zichen Wang, Simon Koplev, et al. 2016. “Enrichr: A Comprehensive Gene Set Enrichment Analysis Web Server 2016 Update.” *Nucleic Acids Research* 44 (W1): W90–97. https://doi.org/10.1093/nar/gkw377.

Kurt-Jones, Evelyn A., Lana Popova, Laura Kwinn, Lia M. Haynes, Les P. Jones, Ralph A. Tripp, Edward E. Walsh, et al. 2000. “Pattern Recognition Receptors TLR4 and CD14 Mediate Response to Respiratory Syncytial Virus.” *Nature Immunology* 1 (5): 398. https://doi.org/10.1038/80833.

Kurup, Viswanath P., and Gabriele Grunig. 2002. “Animal Models of Allergic Bronchopulmonary Aspergillosis.” *Mycopathologia* 153 (4): 165–77. https://doi.org/10.1023/A:1014963600314.

Kurup, Viswanath P., Raghavan Raju, and Pachiappan Manickam. 2005. “Profile of Gene Expression in a Murine Model of Allergic Bronchopulmonary Aspergillosis.” *Infection and Immunity* 73 (7): 4381–84. https://doi.org/10.1128/IAI.73.7.4381-4384.2005.

Kushwah, Rahul, and Jim Hu. 2011. “Complexity of Dendritic Cell Subsets and Their Function in the Host Immune System.” *Immunology* 133 (4): 409–19. https://doi.org/10.1111/j.1365-2567.2011.03457.x.

Lamoth, Frédéric, Praveen R. Juvvadi, Jarrod R. Fortwendel, and William J. Steinbach. 2012. “Heat Shock Protein 90 Is Required for Conidiation and Cell Wall Integrity in *Aspergillus fumigatus*.” *Eukaryotic Cell* 11 (11): 1324–32. https://doi.org/10.1128/EC.00032-12.

Lamoth, Frédéric, Praveen R. Juvvadi, and William J. Steinbach. 2016. “Heat Shock Protein 90 (Hsp90): A Novel Antifungal Target against *Aspergillus fumigatus*.” *Critical Reviews in Microbiology* 42 (2): 310–21. https://doi.org/10.3109/1040841X.2014.947239.

Latgé, Jean-Paul. 1999. “*Aspergillus fumigatus* and Aspergillosis.” *Clinical Microbiology Reviews* 12 (2): 310–50.

Latgé, Jean-Paul. 2001. “The Pathobiology of *Aspergillus fumigatus*.” *Trends in Microbiology* 9

(8): 382–89. https://doi.org/10.1016/S0966-842X(01)02104-7.

Latgé, Jean-Paul, Anne Beauvais, and Georgios Chamilos. 2017. “The Cell Wall of the Human Fungal Pathogen *Aspergillus fumigatus*: Biosynthesis, Organization, Immune Response, and Virulence.” *Annual Review of Microbiology* 71 (September): 99–116. https://doi.org/10.1146/annurev-micro-030117-020406.

Lee, Mark J., and Donald C. Sheppard. 2016. “Recent Advances in the Understanding of the *Aspergillus fumigatus* Cell Wall.” *Journal of Microbiology* 54 (3): 232–42. https://doi.org/10.1007/s12275-016-6045-4.

Lilly, Lauren M., Michaella Scopel, Michael P. Nelson, Ashley R. Burg, Chad W. Dunaway, and Chad Steele. 2014. “Eosinophil Deficiency Compromises Lung Defense against *Aspergillus fumigatus*.” *Infection and Immunity* 82 (3): 1315–25. https://doi.org/10.1128/IAI.01172-13.

Liu, F., J. Poursine-Laurent, H. Y. Wu, and D. C. Link. 1997. “Interleukin-6 and the Granulocyte Colony-Stimulating Factor Receptor Are Major Independent Regulators of Granulopoiesis in Vivo but Are Not Required for Lineage Commitment or Terminal Differentiation.” *Blood* 90 (7): 2583–90.

LIU, MINGLI, SHANCHUN GUO, and JONATHAN K. STILES. 2011. “The Emerging Role of CXCL10 in Cancer (Review).” *Oncology Letters* 2 (4): 583–89. https://doi.org/10.3892/ol.2011.300.

Lopez-Souza, Nilceia, Pedro C. Avila, and Jonathan H. Widdicombe. 2003. “Polarized Cultures of Human Airway Epithelium from Nasal Scrapings and Bronchial Brushings.” *In Vitro Cellular & Developmental Biology. Animal* 39 (7): 266–69.

Madan, T., P. Eggleton, U. Kishore, P. Strong, S. S. Aggrawal, P. U. Sarma, and K. B. Reid. 1997. “Binding of Pulmonary Surfactant Proteins A and D to *Aspergillus fumigatus* Conidia Enhances Phagocytosis and Killing by Human Neutrophils and Alveolar Macrophages.” *Infection and Immunity* 65 (8): 3171–79.

Malireddi, R. K. Subbarao, and Thirumala-Devi Kanneganti. 2013. “Role of Type I Interferons in Inflammasome Activation, Cell Death, and Disease during Microbial Infection.” *Frontiers in Cellular and Infection Microbiology* 3. https://doi.org/10.3389/fcimb.2013.00077.

Margalit, Anatte, and Kevin Kavanagh. 2015. “The Innate Immune Response to *Aspergillus fumigatus* at the Alveolar Surface.” *FEMS Microbiology Reviews* 39 (5): 670–87. https://doi.org/10.1093/femsre/fuv018.

Masteller, Emma L., and Brian R. Wong. 2014. “Targeting IL-34 in Chronic Inflammation.” *Drug Discovery Today* 19 (8): 1212–16. https://doi.org/10.1016/j.drudis.2014.05.016.

McClintock, Timothy S., Chad E. Glasser, Soma C. Bose, and Daniel A. Bergman. 2008. “Tissue

Expression Patterns Identify Mouse Cilia Genes." *Physiological Genomics* 32 (2): 198–206. https://doi.org/10.1152/physiolgenomics.00128.2007.

Mery, Laurence, Nasrin Mesaeli, Marek Michalak, Michal Opas, Daniel P. Lew, and Karl-Heinz Krause. 1996. "Overexpression of Calreticulin Increases Intracellular Ca Storage and Decreases Store-Operated Ca Influx." *Journal of Biological Chemistry* 271 (16): 9332–39. https://doi.org/10.1074/jbc.271.16.9332.

Mezger, Markus, Susanne Kneitz, Iwona Wozniok, Oliver Kurzai, Hermann Einsele, and Juergen Loeffler. 2008. "Proinflammatory Response of Immature Human Dendritic Cells Is Mediated by Dectin-1 after Exposure to *Aspergillus fumigatus* Germ Tubes." *The Journal of Infectious Diseases* 197 (6): 924–31. https://doi.org/10.1086/528694.

Moalli, Federica, Andrea Doni, Livija Deban, Teresa Zelante, Silvia Zagarella, Barbara Bottazzi, Luigina Romani, Alberto Mantovani, and Cecilia Garlanda. 2010. "Role of Complement and Fc{gamma} Receptors in the Protective Activity of the Long Pentraxin PTX3 against *Aspergillus fumigatus*." *Blood* 116 (24): 5170–80. https://doi.org/10.1182/blood-2009-12-258376.

Mojarad, Bahareh A., Gagan D. Gupta, Monica Hasegan, Oumou Goudiam, Renata Basto, Anne-Claude Gingras, and Laurence Pelletier. 2017. "CEP19 Cooperates with FOP and CEP350 to Drive Early Steps in the Ciliogenesis Programme." *Open Biology* 7 (6). https://doi.org/10.1098/rsob.170114.

Montagnoli, Claudia, Francesca Fallarino, Roberta Gaziano, Silvia Bozza, Silvia Bellocchio, Teresa Zelante, Wiswanath P. Kurup, Lucia Pitzurra, Paolo Puccetti, and Luigina Romani. 2006. "Immunity and Tolerance to Aspergillus Involve Functionally Distinct Regulatory T Cells and Tryptophan Catabolism." *Journal of Immunology (Baltimore, Md.: 1950)* 176 (3): 1712–23.

Moore, Margo M. 2013. "The Crucial Role of Iron Uptake in *Aspergillus fumigatus* Virulence." *Current Opinion in Microbiology*, Growth and development: eukaryotes/prokaryotes, 16 (6): 692–99. https://doi.org/10.1016/j.mib.2013.07.012.

Moretti, Silvia, Giorgia Renga, Vasilis Oikonomou, Claudia Galosi, Marilena Pariano, Rossana G. Iannitti, Monica Borghi, et al. 2017. "A Mast Cell-ILC2-Th9 Pathway Promotes Lung Inflammation in Cystic Fibrosis." *Nature Communications* 8 (January): 14017. https://doi.org/10.1038/ncomms14017.

Morton, Charles Oliver, Maria Bouzani, Juergen Loeffler, and Thomas Richard Rogers. 2012. "Direct Interaction Studies between *Aspergillus fumigatus* and Human Immune Cells; What Have We Learned about Pathogenicity and Host Immunity?" *Frontiers in Microbiology* 3. https://doi.org/10.3389/fmicb.2012.00413.

Morton, Charles O., John J. Varga, Anke Hornbach, Markus Mezger, Helga Sennefelder, Susanne Kneitz, Oliver Kurzai, et al. 2011. "The Temporal Dynamics of Differential Gene Expression in

Aspergillus fumigatus Interacting with Human Immature Dendritic Cells In Vitro." *PLOS ONE* 6 (1): e16016. https://doi.org/10.1371/journal.pone.0016016.

Moss, R. B. 2005. "Pathophysiology and Immunology of Allergic Bronchopulmonary Aspergillosis." *Medical Mycology* 43 (Supplement_1): S203–6. https://doi.org/10.1080/13693780500052255.

Mouyna, Isabelle, and Thierry Fontaine. 2009. "Cell Wall of *Aspergillus fumigatus*: A Dynamic Structure," January, 169–83. https://doi.org/10.1128/9781555815523.ch14.

Moyes, David L., Chengguo Shen, Celia Murciano, Manohursingh Runglall, Jonathan P. Richardson, Matthew Arno, Estibaliz Aldecoa-Otalora, and Julian R. Naglik. 2014. "Protection against Epithelial Damage during Candida Albicans Infection Is Mediated by PI3K/Akt and Mammalian Target of Rapamycin Signaling." *The Journal of Infectious Diseases* 209 (11): 1816–26. https://doi.org/10.1093/infdis/jit824.

Nagai, H., J. Guo, H. Choi, and V. Kurup. 1995. "Interferon-Gamma and Tumor Necrosis Factor-Alpha Protect Mice from Invasive Aspergillosis." *The Journal of Infectious Diseases* 172 (6): 1554–60.

Nesbitt, Jason R., Elizabeth Y. Steves, Cole R. Schonhofer, Alissa Cait, Sukhbir S. Manku, Juliana H. F. Yeung, Andrew J. Bennet, et al. 2018. "The *Aspergillus fumigatus* Sialidase (Kdnase) Contributes to Cell Wall Integrity and Virulence in Amphotericin B-Treated Mice." *Frontiers in Microbiology* 8. https://doi.org/10.3389/fmicb.2017.02706.

Netea, Mihai G., Adilia Warris, Jos W. M. Van der Meer, Matthew J. Fenton, Trees J. G. Verver-Janssen, Liesbeth E. H. Jacobs, Tonje Andresen, Paul E. Verweij, and Bart Jan Kullberg. 2003. "*Aspergillus fumigatus* Evades Immune Recognition during Germination through Loss of Toll-like Receptor-4-Mediated Signal Transduction." *The Journal of Infectious Diseases* 188 (2): 320–26. https://doi.org/10.1086/376456.

Nickless, Andrew, Julie M. Bailis, and Zhongsheng You. 2017. "Control of Gene Expression through the Nonsense-Mediated RNA Decay Pathway." *Cell & Bioscience* 7 (May). https://doi.org/10.1186/s13578-017-0153-7.

O'Boyle, Nicky, Erin Sutherland, Catherine C. Berry, and Robert L. Davies. 2017. "Temporal Dynamics of Ovine Airway Epithelial Cell Differentiation at an Air-Liquid Interface." *PLoS ONE* 12 (7). https://doi.org/10.1371/journal.pone.0181583.

Ogden, C. A., A. deCathelineau, P. R. Hoffmann, D. Bratton, B. Ghebrehiwet, V. A. Fadok, and P. M. Henson. 2001. "C1q and Mannose Binding Lectin Engagement of Cell Surface Calreticulin and CD91 Initiates Macropinocytosis and Uptake of Apoptotic Cells." *The Journal of Experimental Medicine* 194 (6): 781–95.

Oguma, Tsuyoshi, Koichiro Asano, Katsuyoshi Tomomatsu, Motohiro Kodama, Koichi Fukunaga, Tetsuya Shiomi, Nao Ohmori, et al. 2011. “Induction of Mucin and MUC5AC Expression by the Protease Activity of *Aspergillus fumigatus* in Airway Epithelial Cells.” *Journal of Immunology (Baltimore, Md.: 1950)* 187 (2): 999–1005. https://doi.org/10.4049/jimmunol.1002257.

Oosthuizen, Jean L., Pol Gomez, Jian Ruan, Tillie L. Hackett, Margo M. Moore, Darryl A. Knight, and Scott J. Tebbutt. 2011. “Dual Organism Transcriptomics of Airway Epithelial Cells Interacting with Conidia of *Aspergillus fumigatus*.” *PLoS ONE* 6 (5). https://doi.org/10.1371/journal.pone.0020527.

Osherov, Nir. 2012. “Interaction of the Pathogenic Mold *Aspergillus fumigatus* with Lung Epithelial Cells.” *Frontiers in Microbiology* 3 (September). https://doi.org/10.3389/fmicb.2012.00346.

Oslowski, Christine M., and Fumihiko Urano. 2011. “Measuring ER Stress and the Unfolded Protein Response Using Mammalian Tissue Culture System.” *Methods in Enzymology* 490: 71–92. https://doi.org/10.1016/B978-0-12-385114-7.00004-0.

Panackal, Anil A., John E. Bennett, and Peter R. Williamson. 2014. “Treatment Options in Invasive Aspergillosis.” *Current Treatment Options in Infectious Diseases* 6 (3): 309–25. https://doi.org/10.1007/s40506-014-0016-2.

Pankov, Roumen, and Kenneth M. Yamada. 2002. “Fibronectin at a Glance.” *Journal of Cell Science* 115 (20): 3861–63. https://doi.org/10.1242/jcs.00059.

Paris, S., E. Boisvieux-Ulrich, B. Crestani, O. Houcine, D. Taramelli, L. Lombardi, and J. P. Latgé. 1997. “Internalization of *Aspergillus fumigatus* Conidia by Epithelial and Endothelial Cells.” *Infection and Immunity* 65 (4): 1510–14.

Parrow, Nermi L., Robert E. Fleming, and Michael F. Minnick. 2013. “Sequestration and Scavenging of Iron in Infection.” *Infection and Immunity* 81 (10): 3503–14. https://doi.org/10.1128/IAI.00602-13.

Patterson, Karen C., and Mary E. Strek. 2014. “Diagnosis and Treatment of Pulmonary Aspergillosis Syndromes.” *Chest* 146 (5): 1358–68. https://doi.org/10.1378/chest.14-0917.

P, Gazendam Roel, Geer Annemarie, Roos Dirk, Berg Timo K, and Kuijpers Taco W. 2016. “How Neutrophils Kill Fungi.” *Immunological Reviews* 273 (1): 299–311. https://doi.org/10.1111/imr.12454.

Piasecki, Brian P., Jan Burghoorn, and Peter Swoboda. 2010. “Regulatory Factor X (RFX)-Mediated Transcriptional Rewiring of Ciliary Genes in Animals.” *Proceedings of the National Academy of Sciences* 107 (29): 12969–74. https://doi.org/10.1073/pnas.0914241107.

Pletz, Nadin, Anja Medack, Eva Maria Rieß, Kefei Yang, Zahra Basir Kazerouni, Daniela Hüber, and Sigrid Hoyer-Fender. 2013. “Transcriptional Activation of Odf2/Cenexin by Cell Cycle Arrest and the Stress Activated Signaling Pathway (JNK Pathway).” *Biochimica et Biophysica Acta (BBA) - Molecular Cell Research* 1833 (6): 1338–46. https://doi.org/10.1016/j.bbamcr.2013.02.023.

Ponka, P., and C. N. Lok. 1999. “The Transferrin Receptor: Role in Health and Disease.” *The International Journal of Biochemistry & Cell Biology* 31 (10): 1111–37.

Pontecorvo, G. 1956. “The Parasexual Cycle in Fungi.” *Annual Review of Microbiology* 10: 393–400. https://doi.org/10.1146/annurev.mi.10.100156.002141.

Porter, P, SC Susarla, S Polikepahad, Y Qian, J Hampton, A Kiss, S Vaidya, et al. 2009. “Link between Allergic Asthma and Airway Mucosal Infection Suggested by Proteinase-Secreting Household Fungi.” *Mucosal Immunology* 2 (6): 504–17. https://doi.org/10.1038/mi.2009.102.

Ramirez-Ortiz, Zaida G., and Terry K. Means. 2012. “The Role of Dendritic Cells in the Innate Recognition of Pathogenic Fungi (A. Fumigatus, C. Neoformans and C. Albicans).” *Virulence* 3 (7): 635–46. https://doi.org/10.4161/viru.22295.

Ramirez-Ortiz, Zaida G., Charles A. Specht, Jennifer P. Wang, Chrono K. Lee, Daniella C. Bartholomeu, Ricardo T. Gazzinelli, and Stuart M. Levitz. 2008. “Toll-like Receptor 9-Dependent Immune Activation by Unmethylated CpG Motifs in *Aspergillus fumigatus* DNA.” *Infection and Immunity* 76 (5): 2123–29. https://doi.org/10.1128/IAI.00047-08.

Rammaert, Blandine, Grégory Jouvion, Fabrice de Chaumont, Dea Garcia-Hermoso, Claire Szczepaniak, Charlotte Renaudat, Jean-Christophe Olivo-Marin, Fabrice Chrétien, Françoise Dromer, and Stéphane Bretagne. 2015. “Absence of Fungal Spore Internalization by Bronchial Epithelium in Mouse Models Evidenced by a New Bioimaging Approach and Transmission Electronic Microscopy.” *The American Journal of Pathology* 185 (9): 2421–30. https://doi.org/10.1016/j.ajpath.2015.04.027.

Rappold, Irene, Kuniyoshi Iwabuchi, Takayasu Date, and Junjie Chen. 2001. “Tumor Suppressor P53 Binding Protein 1 (53bp1) Is Involved in DNA Damage–Signaling Pathways.” *The Journal of Cell Biology* 153 (3): 613–20. https://doi.org/10.1083/jcb.153.3.613.

Rashidiani, Shima, Ali Jalili, Erfan Babaei, Farsad Sheikhesmaeili, Shohreh Fakhari, Pedram Ataee, and Baran Parhizkar. 2017. “The Chemokine CCL28 Is Elevated in the Serum of Patients with Celiac Disease and Decreased after Treatment.” *American Journal of Clinical and Experimental Immunology* 6 (4): 60–65.

Resovi, Andrea, Denise Pinessi, Giovanna Chiorino, and Giulia Taraboletti. 2014. “Current Understanding of the Thrombospondin-1 Interactome.” *Matrix Biology: Journal of the International Society for Matrix Biology* 37 (July): 83–91. https://doi.org/10.1016/j.matbio.2014.01.012.

Rhodes, Judith C. 2006. "*Aspergillus fumigatus*: Growth and Virulence." *Medical Mycology* 44 Suppl 1 (September): S77–81. https://doi.org/10.1080/13693780600779419.

Rivera, Amariliz, Tobias M. Hohl, Nichole Collins, Ingrid Leiner, Alena Gallegos, Shinobu Saijo, Jesse W. Coward, Yoichiro Iwakura, and Eric G. Pamer. 2011. "Dectin-1 Diversifies *Aspergillus fumigatus*-Specific T Cell Responses by Inhibiting T Helper Type 1 CD4 T Cell Differentiation." *The Journal of Experimental Medicine* 208 (2): 369–81. https://doi.org/10.1084/jem.20100906.

Robinet, Pauline, Florence Baychelier, Thierry Fontaine, Capucine Picard, Patrice Debré, Vincent Vieillard, Jean-Paul Latgé, and Carole Elbim. 2014. "A Polysaccharide Virulence Factor of a Human Fungal Pathogen Induces Neutrophil Apoptosis via NK Cells." *The Journal of Immunology* 192 (11): 5332–42. https://doi.org/10.4049/jimmunol.1303180.

Rogers, D. F. 1994. "Airway Goblet Cells: Responsive and Adaptable Front-Line Defenders." *European Respiratory Journal* 7 (9): 1690–1706.

Romagnani, S. 2002. "Cytokines and Chemoattractants in Allergic Inflammation." *Molecular Immunology* 38 (12-13): 881–85.

Ross, Andrea J., Lisa A. Dailey, Luisa E. Brighton, and Robert B. Devlin. 2007. "Transcriptional Profiling of Mucociliary Differentiation in Human Airway Epithelial Cells." *American Journal of Respiratory Cell and Molecular Biology* 37 (2): 169–85. https://doi.org/10.1165/rcmb.2006-0466OC.

Rudd, Brian D., Ezra Burstein, Colin S. Duckett, Xiaoxia Li, and Nicholas W. Lukacs. 2005. "Differential Role for TLR3 in Respiratory Syncytial Virus-Induced Chemokine Expression." *Journal of Virology* 79 (6): 3350–57. https://doi.org/10.1128/JVI.79.6.3350-3357.2005.

Sales-Campos, Helioswilton, Ludmilla Tonani, Cristina Ribeiro Barros Cardoso, and Márcia Regina Von Zeska Kress. 2013. "The Immune Interplay between the Host and the Pathogen in *Aspergillus fumigatus* Lung Infection." *BioMed Research International* 2013. https://doi.org/10.1155/2013/693023.

Sano, Renata, and John C. Reed. 2013. "ER Stress-Induced Cell Death Mechanisms." *Biochimica et Biophysica Acta (BBA) - Molecular Cell Research* 1833 (12): 3460–70. https://doi.org/10.1016/j.bbamcr.2013.06.028.

Sawant, Kirti V., Krishna Mohan Poluri, Amit K. Dutta, Krishna Mohan Sepuru, Anna Troshkina, Roberto P. Garofalo, and Krishna Rajarathnam. 2016. "Chemokine CXCL1 Mediated Neutrophil Recruitment: Role of Glycosaminoglycan Interactions." *Scientific Reports* 6 (September): 33123. https://doi.org/10.1038/srep33123.

Scapini, P., J. A. Lapinet-Vera, S. Gasperini, F. Calzetti, F. Bazzoni, and M. A. Cassatella. 2000. "The Neutrophil as a Cellular Source of Chemokines." *Immunological Reviews* 177 (October):

195–203.

Schaffner, A., H. Douglas, A. I. Braude, and C. E. Davis. 1983. “Killing of Aspergillus Spores Depends on the Anatomical Source of the Macrophage.” *Infection and Immunity* 42 (3): 1109–15.

Schmidt, Silvia K., Anika Müller, Kathrin Heseler, Claudia Woite, Katrin Spekker, Colin R. MacKenzie, and Walter Däubener. 2009. “Antimicrobial and Immunoregulatory Properties of Human Tryptophan 2,3-Dioxygenase.” *European Journal of Immunology* 39 (10): 2755–64. https://doi.org/10.1002/eji.200939535.

Schoggins, John W., and Charles M. Rice. 2011. “Interferon-Stimulated Genes and Their Antiviral Effector Functions.” *Current Opinion in Virology* 1 (6): 519–25. https://doi.org/10.1016/j.coviro.2011.10.008.

Schrettl, Markus, Elaine Bignell, Claudia Kragl, Chistoph Joechl, Tom Rogers, Herbert N. Arst, Ken Haynes, and Hubertus Haas. 2004. “Siderophore Biosynthesis but Not Reductive Iron Assimilation Is Essential for *Aspergillus fumigatus* Virulence.” *The Journal of Experimental Medicine* 200 (9): 1213–19. https://doi.org/10.1084/jem.20041242.

Schweer, K E, C Bangard, K Hekmat, and O A Cornely. 2014. “Chronic Pulmonary Aspergillosis.” *Mycoses* 57 (5): 257–70. https://doi.org/10.1111/myc.12152.

Segal, Anthony W. 2005. “How Neutrophils Kill Microbes.” *Annual Review of Immunology* 23: 197–223. https://doi.org/10.1146/annurev.immunol.23.021704.115653.

Segeritz, Charis-P., and Ludovic Vallier. 2017. “Chapter 9 - Cell Culture: Growing Cells as Model Systems In Vitro.” In *Basic Science Methods for Clinical Researchers*, edited by Morteza Jalali, Francesca Y. L. Saldanha, and Mehdi Jalali, 151–72. Boston: Academic Press. https://www.sciencedirect.com/science/article/pii/B9780128030776000096.

Shakespear, Melanie R., Maria A. Halili, Katharine M. Irvine, David P. Fairlie, and Matthew J. Sweet. 2011. “Histone Deacetylases as Regulators of Inflammation and Immunity.” *Trends in Immunology* 32 (7): 335–43. https://doi.org/10.1016/j.it.2011.04.001.

Shao, C., J. Qu, L. He, Y. Zhang, J. Wang, Y. Wang, H. Zhou, and X. Liu. 2005. “Transient Overexpression of Gamma Interferon Promotes Aspergillus Clearance in Invasive Pulmonary Aspergillosis.” *Clinical and Experimental Immunology* 142 (2): 233–41. https://doi.org/10.1111/j.1365-2249.2005.02828.x.

Sharon, Haim, David Amar, Emma Levdansky, Gabriel Mircus, Yana Shadkchan, Ron Shamir, and Nir Osherov. 2011. “PrtT-Regulated Proteins Secreted by *Aspergillus fumigatus* Activate MAPK Signaling in Exposed A549 Lung Cells Leading to Necrotic Cell Death.” *PLOS ONE* 6 (3): e17509. https://doi.org/10.1371/journal.pone.0017509.

Sheeran, P., H. Jafri, C. Carubelli, J. Saavedra, C. Johnson, K. Krisher, P. J. Sánchez, and O. Ramilo. 1999. “Elevated Cytokine Concentrations in the Nasopharyngeal and Tracheal Secretions of Children with Respiratory Syncytial Virus Disease.” *The Pediatric Infectious Disease Journal* 18 (2): 115–22.

Shi, Yufang, Catherine H. Liu, Arthur I. Roberts, Jyoti Das, Guangwu Xu, Guangwen Ren, Yingyu Zhang, et al. 2006. “Granulocyte-Macrophage Colony-Stimulating Factor (GM-CSF) and T-Cell Responses: What We Do and Don’t Know.” *Cell Research* 16 (2): 126. https://doi.org/10.1038/sj.cr.7310017.

Singh, Amrit, Casey P. Shannon, Young Woong Kim, Chen Xi Yang, Robert Balshaw, Gabriela V. Cohen Freue, Gail M. Gauvreau, et al. 2017. “Novel Blood-Based Transcriptional Biomarker Panels Predict the Late Phase Asthmatic Response.” *American Journal of Respiratory and Critical Care Medicine*, October. https://doi.org/10.1164/rccm.201701-0110OC.

Smet, Kris De, and Roland Contreras. 2005. “Human Antimicrobial Peptides: Defensins, Cathelicidins and Histatins.” *Biotechnology Letters* 27 (18): 1337–47. https://doi.org/10.1007/s10529-005-0936-5.

Soubani, Ayman O., and Pranatharthi H. Chandrasekar. 2002. “The Clinical Spectrum of Pulmonary Aspergillosis.” *CHEST* 121 (6): 1988–99. https://doi.org/10.1378/chest.121.6.1988.

Sousa, A. R., S. J. Lane, J. A. Nakhosteen, T. Yoshimura, T. H. Lee, and R. N. Poston. 1994. “Increased Expression of the Monocyte Chemoattractant Protein-1 in Bronchial Tissue from Asthmatic Subjects.” *American Journal of Respiratory Cell and Molecular Biology* 10 (2): 142–47. https://doi.org/10.1165/ajrcmb.10.2.8110469.

Spina, D. 1998. “Epithelium Smooth Muscle Regulation and Interactions.” *American Journal of Respiratory and Critical Care Medicine* 158 (5 Pt 3): S141–45. https://doi.org/10.1164/ajrccm.158.supplement_2.13tac100a.

Srinivasan, Balaji, Aditya Reddy Kolli, Mandy Brigitte Esch, Hasan Erbil Abaci, Michael L. Shuler, and James J. Hickman. 2015. “TEER Measurement Techniques for in Vitro Barrier Model Systems.” *Journal of Laboratory Automation* 20 (2): 107–26. https://doi.org/10.1177/2211068214561025.

Stephen-Victor, Emmanuel, Anupama Karnam, Thierry Fontaine, Anne Beauvais, Mrinmoy Das, Pushpa Hegde, Praveen Prakhar, et al. 2017. “*Aspergillus fumigatus* Cell Wall α-(1,3)-Glucan Stimulates Regulatory T-Cell Polarization by Inducing PD-L1 Expression on Human Dendritic Cells.” *The Journal of Infectious Diseases* 216 (10): 1281–94. https://doi.org/10.1093/infdis/jix469.

Stewart, Ceri E., Elizabeth E. Torr, Mohd Jamili, Nur H, Cynthia Bosquillon, and Ian Sayers. 2012. “Evaluation of Differentiated Human Bronchial Epithelial Cell Culture Systems for Asthma

Research." Research article. Journal of Allergy. 2012. https://www.hindawi.com/journals/ja/2012/943982/.

Stoppelenburg, Arie Jan, Vahid Salimi, Marije Hennus, Maud Plantinga, Ron Huis in 't Veld, Jona Walk, Jenny Meerding, Frank Coenjaerts, Louis Bont, and Marianne Boes. 2013. "Local IL-17A Potentiates Early Neutrophil Recruitment to the Respiratory Tract during Severe RSV Infection." *PLOS ONE* 8 (10): e78461. https://doi.org/10.1371/journal.pone.0078461.

Sugimoto, Michelle Amantéa, Juliana Priscila Vago, Mauro Martins Teixeira, and Lirlândia Pires Sousa. 2016. "Annexin A1 and the Resolution of Inflammation: Modulation of Neutrophil Recruitment, Apoptosis, and Clearance." Research article. Journal of Immunology Research. 2016. https://www.hindawi.com/journals/jir/2016/8239258/.

Sun, He, Xiao-Yong Xu, Hong-Tao Shao, Xin Su, Xiao-Dong Wu, Quan Wang, and Yi Shi. 2013. "Dectin-2 Is Predominately Macrophage Restricted and Exhibits Conspicuous Expression during *Aspergillus fumigatus* Invasion in Human Lung." *Cellular Immunology* 284 (1-2): 60–67. https://doi.org/10.1016/j.cellimm.2013.06.013.

Sun, He, Xiao-yong Xu, Xiao-li Tian, Hong-tao Shao, Xiao-dong Wu, Quan Wang, Xin Su, and Yi Shi. 2014. "Activation of NF-κB and Respiratory Burst Following *Aspergillus fumigatus* Stimulation of Macrophages." *Immunobiology* 219 (1): 25–36. https://doi.org/10.1016/j.imbio.2013.06.013.

Sun, W.-K., X. Lu, X. Li, Q.-Y. Sun, X. Su, Y. Song, H.-M. Sun, and Y. Shi. 2012. "Dectin-1 Is Inducible and Plays a Crucial Role in Aspergillus-Induced Innate Immune Responses in Human Bronchial Epithelial Cells." *European Journal of Clinical Microbiology & Infectious Diseases* 31 (10): 2755–64. https://doi.org/10.1007/s10096-012-1624-8.

Sutton, P., N. R. Newcombe, P. Waring, and A. Müllbacher. 1994. "In Vivo Immunosuppressive Activity of Gliotoxin, a Metabolite Produced by Human Pathogenic Fungi." *Infection and Immunity* 62 (4): 1192–98.

Telford, Judith C., Juliana H. F. Yeung, Guogang Xu, Milton J. Kiefel, Andrew G. Watts, Stefan Hader, Jefferson Chan, Andrew J. Bennet, Margo M. Moore, and Garry L. Taylor. 2011. "The *Aspergillus fumigatus* Sialidase Is a 3-Deoxy-D-Glycero-D-Galacto-2-Nonulosonic Acid Hydrolase (KDNase) STRUCTURAL AND MECHANISTIC INSIGHTS." *Journal of Biological Chemistry* 286 (12): 10783–92. https://doi.org/10.1074/jbc.M110.207043.

The Gene Ontology Consortium. 2017. "Expansion of the Gene Ontology Knowledgebase and Resources." *Nucleic Acids Research* 45 (D1): D331–38. https://doi.org/10.1093/nar/gkw1108.

Theil, Elizabeth C. 2004. "Iron, Ferritin, and Nutrition." *Annual Review of Nutrition* 24 (1): 327–43. https://doi.org/10.1146/annurev.nutr.24.012003.132212.

Thomas, Joëlle, Laurette Morlé, Fabien Soulavie, Anne Laurençon, Sébastien Sagnol, and Bénédicte Durand. 2010. “Transcriptional Control of Genes Involved in Ciliogenesis: A First Step in Making Cilia.” *Biology of the Cell* 102 (9): 499–513. https://doi.org/10.1042/BC20100035.

Thompson, C. B. 1995. “Apoptosis in the Pathogenesis and Treatment of Disease.” *Science* 267 (5203): 1456–62. https://doi.org/10.1126/science.7878464.

Thywißen, Andreas, Thorsten Heinekamp, Hans-Martin Dahse, Jeannette Schmaler-Ripcke, Sandor Nietzsche, Peter F. Zipfel, and Axel A. Brakhage. 2011. “Conidial Dihydroxynaphthalene Melanin of the Human Pathogenic Fungus *Aspergillus fumigatus* Interferes with the Host Endocytosis Pathway.” *Frontiers in Microbiology* 2: 96. https://doi.org/10.3389/fmicb.2011.00096.

Tomee, J. F., A. T. Wierenga, P. S. Hiemstra, and H. K. Kauffman. 1997. “Proteases from *Aspergillus fumigatus* Induce Release of Proinflammatory Cytokines and Cell Detachment in Airway Epithelial Cell Lines.” *The Journal of Infectious Diseases* 176 (1): 300–303.

Tomee, and Kauffman. 2000. “Putative Virulence Factors of *Aspergillus fumigatus*.” *Clinical & Experimental Allergy* 30 (4): 476–84. https://doi.org/10.1046/j.1365-2222.2000.00796.x.

Torraca, Vincenzo, Chao Cui, Ralf Boland, Jan-Paul Bebelman, Astrid M. van der Sar, Martine J. Smit, Marco Siderius, Herman P. Spaink, and Annemarie H. Meijer. 2015. “The CXCR3-CXCL11 Signaling Axis Mediates Macrophage Recruitment and Dissemination of Mycobacterial Infection.” *Disease Models & Mechanisms* 8 (3): 253–69. https://doi.org/10.1242/dmm.017756.

Tracy, Michael C., Caroline U. A. Okorie, Elizabeth A. Foley, and Richard B. Moss. 2016. “Allergic Bronchopulmonary Aspergillosis.” *Journal of Fungi* 2 (2): 17. https://doi.org/10.3390/jof2020017.

Udeshi, Namrata D., Philipp Mertins, Tanya Svinkina, and Steven A. Carr. 2013. “Large-Scale Identification of Ubiquitination Sites by Mass Spectrometry.” *Nature Protocols* 8 (10): 1950–60. https://doi.org/10.1038/nprot.2013.120.

Ugonna, Kelechi, Konstantinos Douros, Colin D. Bingle, and Mark L. Everard. 2016. “Cytokine Responses in Primary and Secondary Respiratory Syncytial Virus Infections.” *Pediatric Research* 79 (6): 946. https://doi.org/10.1038/pr.2016.29.

Urb, Mirjam, Philippe Pouliot, Fabrice N. Gravelat, Martin Olivier, and Donald C. Sheppard. 2009. “*Aspergillus fumigatus* Induces Immunoglobulin E-Independent Mast Cell Degranulation.” *The Journal of Infectious Diseases* 200 (3): 464–72. https://doi.org/10.1086/600070.

Vandivier, R. William, Carol Anne Ogden, Valerie A. Fadok, Peter R. Hoffmann, Kevin K. Brown, Marina Botto, Mark J. Walport, James H. Fisher, Peter M. Henson, and Kelly E. Greene. 2002. “Role of Surfactant Proteins A, D, and C1q in the Clearance of Apoptotic Cells in Vivo and in

Vitro: Calreticulin and CD91 as a Common Collectin Receptor Complex." *Journal of Immunology (Baltimore, Md.: 1950)* 169 (7): 3978–86.

Vareille, Marjolaine, Elisabeth Kieninger, Michael R. Edwards, and Nicolas Regamey. 2011. "The Airway Epithelium: Soldier in the Fight against Respiratory Viruses." *Clinical Microbiology Reviews* 24 (1): 210–29. https://doi.org/10.1128/CMR.00014-10.

Varki, Ajit, and Roland Schauer. 2009. "Sialic Acids." In *Essentials of Glycobiology*, edited by Ajit Varki, Richard D. Cummings, Jeffrey D. Esko, Hudson H. Freeze, Pamela Stanley, Carolyn R. Bertozzi, Gerald W. Hart, and Marilynn E. Etzler, 2nd ed. Cold Spring Harbor (NY): Cold Spring Harbor Laboratory Press. http://www.ncbi.nlm.nih.gov/books/NBK1920/.

Veerdonk, Frank L. van de, Mark S. Gresnigt, Bart Jan Kullberg, Jos W. M. van der Meer, Leo A. B. Joosten, and Mihai G. Netea. 2009. "Th17 Responses and Host Defense against Microorganisms: An Overview." *BMB Reports* 42 (12): 776–87.

Verdaguer, Virginia, Thomas J. Walsh, William Hope, and Karoll J. Cortez. 2007. "Galactomannan Antigen Detection in the Diagnosis of Invasive Aspergillosis." *Expert Review of Molecular Diagnostics* 7 (1): 21–32. https://doi.org/10.1586/14737159.7.1.21.

Verweij, Paul E., Jianhua Zhang, Alfons J. M. Debets, Jacques F. Meis, Frank L. van de Veerdonk, Sijmen E. Schoustra, Bas J. Zwaan, and Willem J. G. Melchers. 2016. "In-Host Adaptation and Acquired Triazole Resistance in *Aspergillus fumigatus*: A Dilemma for Clinical Management." *The Lancet Infectious Diseases* 16 (11): e251–60. https://doi.org/10.1016/S1473-3099(16)30138-4.

Vignali, Dario A. A., Lauren W. Collison, and Creg J. Workman. 2008. "How Regulatory T Cells Work." *Nature Reviews. Immunology* 8 (7): 523–32. https://doi.org/10.1038/nri2343.

Villar, C.c., and X.r. Zhao. 2010. "Candida Albicans Induces Early Apoptosis Followed by Secondary Necrosis in Oral Epithelial Cells." *Molecular Oral Microbiology* 25 (3): 215–25. https://doi.org/10.1111/j.2041-1014.2010.00577.x.

Volling, Katrin, Andreas Thywissen, Axel A. Brakhage, and Hans Peter Saluz. 2011. "Phagocytosis of Melanized Aspergillus Conidia by Macrophages Exerts Cytoprotective Effects by Sustained PI3K/Akt Signalling." *Cellular Microbiology* 13 (8): 1130–48. https://doi.org/10.1111/j.1462-5822.2011.01605.x.

Walport, M. J. 2001. "Complement. First of Two Parts." *The New England Journal of Medicine* 344 (14): 1058–66. https://doi.org/10.1056/NEJM200104053441406.

Wark, P. A., and P. G. Gibson. 2001. "Allergic Bronchopulmonary Aspergillosis: New Concepts of Pathogenesis and Treatment." *Respirology (Carlton, Vic.)* 6 (1): 1–7.

Warwas, Mark L., Jacqueline N. Watson, Andrew J. Bennet, and Margo M. Moore. 2007. "Structure and Role of Sialic Acids on the Surface of *Aspergillus fumigatus* Conidiospores." *Glycobiology* 17 (4): 401–10. https://doi.org/10.1093/glycob/cwl085.

Wasylnka, J. A., M. I. Simmer, and M. M. Moore. 2001. "Differences in Sialic Acid Density in Pathogenic and Non-Pathogenic Aspergillus Species." *Microbiology (Reading, England)* 147 (Pt 4): 869–77. https://doi.org/10.1099/00221287-147-4-869.

Wasylnka, Julie A., and Margo M. Moore. 2000. "Adhesion of Aspergillus Species to Extracellular Matrix Proteins: Evidence for Involvement of Negatively Charged Carbohydrates on the Conidial Surface." *Infection and Immunity* 68 (6): 3377–84. https://doi.org/10.1128/IAI.68.6.3377-3384.2000.

Wasylnka, Julie A., and Margo M. Moore. 2002. "Uptake of *Aspergillus fumigatus* Conidia by Phagocytic and Nonphagocytic Cells In Vitro: Quantitation Using Strains Expressing Green Fluorescent Protein." *Infection and Immunity* 70 (6): 3156–63. https://doi.org/10.1128/IAI.70.6.3156-3163.2002.

Wasylnka, Julie A., and Margo M. Moore. 2003. "*Aspergillus fumigatus* Conidia Survive and Germinate in Acidic Organelles of A549 Epithelial Cells." *Journal of Cell Science* 116 (8): 1579–87. https://doi.org/10.1242/jcs.00329.

Way, Emily E., Kong Chen, and Jay K. Kolls. 2013. "Dysregulation in Lung Immunity - the Protective and Pathologic Th17 Response in Infection." *European Journal of Immunology* 43 (12): 3116–24. https://doi.org/10.1002/eji.201343713.

Werner, Jessica L., Allison E. Metz, Dawn Horn, Trenton R. Schoeb, Matthew M. Hewitt, Lisa M. Schwiebert, Ines Faro-Trindade, Gordon D. Brown, and Chad Steele. 2009. "Requisite Role for the Dectin-1 Beta-Glucan Receptor in Pulmonary Defense against *Aspergillus fumigatus*." *Journal of Immunology (Baltimore, Md.: 1950)* 182 (8): 4938–46. https://doi.org/10.4049/jimmunol.0804250.

Wong, Sarah Sze Wah, and Vishukumar Aimanianda. 2017. "Host Soluble Mediators: Defying the Immunological Inertness of *Aspergillus fumigatus* Conidia." *Journal of Fungi* 4 (1): 3. https://doi.org/10.3390/jof4010003.

Wu, Carol A., John J. Peluso, Li Zhu, Elizabeth G. Lingenheld, Sharale T. Walker, and Lynn Puddington. 2010. "Bronchial Epithelial Cells Produce IL-5: Implications for Local Immune Responses in the Airways." *Cellular Immunology* 264 (1): 32–41. https://doi.org/10.1016/j.cellimm.2010.04.008.

Wu, Mengrui, Guiqian Chen, and Yi-Ping Li. 2016. "TGF-β and BMP Signaling in Osteoblast, Skeletal Development, and Bone Formation, Homeostasis and Disease." *Bone Research* 4 (April): 16009. https://doi.org/10.1038/boneres.2016.9.

Xia, Jinglin, Xiaojing Xu, Peixin Huang, Mingyan He, and Xiangdong Wang. 2015. “The Potential of CXCL5 as a Target for Liver Cancer - What Do We Know so Far?” *Expert Opinion on Therapeutic Targets* 19 (2): 141–46. https://doi.org/10.1517/14728222.2014.993317.

Xu, W. B., E. B. Haddad, H. Tsukagoshi, I. Adcock, P. J. Barnes, and K. F. Chung. 1995. “Induction of Macrophage Inflammatory Protein 2 Gene Expression by Interleukin 1 Beta in Rat Lung.” *Thorax* 50 (11): 1136–40.

Xu, Xilong, Xiufang Xiong, and Yi Sun. 2016. “The Role of Ribosomal Proteins in the Regulation of Cell Proliferation, Tumorigenesis, and Genomic Integrity.” *Science China. Life Sciences* 59 (7): 656–72. https://doi.org/10.1007/s11427-016-0018-0.

Zhang, Zhihong, Rongyu Liu, Jacobien A. Noordhoek, and Henk F. Kauffman. 2005. “Interaction of Airway Epithelial Cells (A549) with Spores and Mycelium of *Aspergillus fumigatus*.” *Journal of Infection* 51 (5): 375–82. https://doi.org/10.1016/j.jinf.2004.12.012.

Zheng, J, J Zuo, Y Han, L Zhang, L Yan, L Shen, Y Jiang, Y Cao, and J Zhao. 2017. “Gliotoxin Produced by *Aspergillus fumigatus* Induces Apoptosis of Human Bronchial Epithelial Cells via the Bcl-2 Pathway.” *International Journal of Clinical and Experimental Medicine* 10 (June): 8854–65.

Zuehlke, Abbey D., Kristin Beebe, Len Neckers, and Thomas Prince. 2015. “Regulation and Function of the Human HSP90AA1 Gene.” *Gene* 570 (1): 8–16. https://doi.org/10.1016/j.gene.2015.06.018.

Appendix 1: List of differentially abundant mRNA transcripts identified using Asthma Elements Panel in ALI cultures of primary HBECs upon exposure to *A. fumigatus* conidia

	Gene	logFC	AveExpr	t	P.Value	adj.P.Val
1	LCP1	0.67090443	4.55039823	4.2859063	0.00615763	0.34052965
2	HIP1	-0.7292261	3.79930367	-4.1782702	0.006888	0.34052965
3	MPPED1	0.69755766	3.67932166	4.15019285	0.00709437	0.34052965
4	CISH	-0.5202025	4.53258812	-2.9861611	0.02683136	0.83501083
5	C5AR1	-0.575807	6.31062395	-2.7714702	0.03507604	0.83501083
6	GTF2H2	0.67184439	4.38087244	2.76384101	0.03541588	0.83501083
7	MAF	-0.6945296	7.07663281	-2.6565935	0.0405908	0.83501083

Appendix 2: List of differentially abundant mRNA transcripts identified using Immune Profiling Panel in ALI cultures of primary HBECs upon exposure to *A. fumigatus* conidia

	Gene	logFC	AveExpr	t	P.Value	adj.P.Val
1	MAF	-0.4436	6.8257	-4.0697	0.0017	0.2998
2	LCN2	-0.4520	14.5953	-3.6039	0.0039	0.2998
3	TFE3	0.4945	5.3870	3.3656	0.0061	0.2998
4	SELPLG	0.8303	5.1662	3.3349	0.0064	0.2998
5	BST2	0.5030	6.9595	3.2716	0.0072	0.2998
6	IDO1	-1.0180	9.7237	-3.2703	0.0072	0.2998
7	CFB	-0.4470	12.1470	-3.2635	0.0072	0.2998
8	ERCC3	0.3835	7.3092	3.2473	0.0074	0.2998
9	IL6R	0.6520	6.2706	3.2187	0.0079	0.2998
10	COG7	0.4324	8.6739	3.1759	0.0085	0.2998
11	CCL15	0.9027	4.9134	3.1349	0.0092	0.2998
12	IFNL1	0.6464	5.3388	3.0762	0.0102	0.3056
13	IL5RA	0.8170	7.1506	2.9933	0.0119	0.3105
14	CASP8	0.2756	7.2907	2.9055	0.0138	0.3105
15	FADD	0.3682	5.3941	2.8880	0.0143	0.3105
16	SAA1	-0.6128	14.6011	-2.8665	0.0149	0.3105
17	PIN1	0.4260	8.2660	2.8513	0.0154	0.3105
18	FCF1	0.3481	9.8494	2.8109	0.0164	0.3105
19	MFGE8	-0.5326	9.8809	-2.8137	0.0164	0.3105
20	RRAD	0.5903	8.9349	2.7718	0.0177	0.3148
21	NFATC2	0.4277	5.5747	2.7392	0.0188	0.3148
22	CTSS	0.5095	11.0279	2.7252	0.0193	0.3148
23	FEZ1	-0.3836	8.0604	-2.6415	0.0224	0.3166
24	CD164	0.2501	11.3788	2.6347	0.0226	0.3166
25	CD44	-0.4266	10.8492	-2.6106	0.0237	0.3166
26	CXCL6	-0.6718	11.6494	-2.5913	0.0246	0.3166
27	IL2RG	-0.4563	5.2380	-2.5626	0.0259	0.3166
28	SPA17	0.7151	11.1160	2.5533	0.0263	0.3166
29	ALAS1	0.2781	8.5584	2.5398	0.0268	0.3166
30	LCK	0.6621	5.2162	2.5347	0.0272	0.3166
31	C3	-0.4674	12.9094	-2.5320	0.0273	0.3166

32	ANXA1	0.4099	14.6046	2.5143	0.0282	0.3166
33	CXCL5	-1.1465	9.0287	-2.4441	0.0320	0.3315
34	CD24	0.2928	12.7260	2.4390	0.0321	0.3315
35	ATF1	0.3061	7.8794	2.4359	0.0323	0.3315
36	PLA2G6	0.3900	5.7471	2.3602	0.0372	0.3669
37	SYK	0.2668	7.3223	2.3484	0.0378	0.3669
38	BCL2L1	0.2614	11.1098	2.3045	0.0409	0.3776
39	TNFRSF11A	-0.4019	6.5494	-2.3052	0.0410	0.3776
40	CASP3	0.2649	9.9287	2.2454	0.0454	0.3808
41	MERTK	0.2628	5.6880	2.2055	0.0488	0.3808

Appendix 3: List of differentially abundant proteins identified using Immune Profiling Panel in ALI cultures of primary HBECs upon exposure to *A. fumigatus* conidia

	Gene	logFC	AveExpr	t	P.Value	adj.P.Val
1	CALR	5.72296	5.72296	29.47107	0.0000005	0.00089
2	NUCB2	2.76004	2.76004	10.35694	0.00011	0.06737
3	SET	2.69194	2.69194	10.28771	0.00011	0.06737
4	MATR3	1.73914	1.73914	9.19187	0.0002	0.07522
5	TPM3;DKFZp686J1372	1.74663	1.74663	9.08705	0.00021	0.07522
6	CBX5	1.31134	1.31134	7.05672	0.00072	0.19998
7	EEA1	1.2188	1.2188	6.59847	0.001	0.19998
8	EIF4B	1.3481	1.3481	6.59087	0.001	0.19998
9	TMEM205	-0.87489	-0.87489	-5.81094	0.00099	0.19998
10	RDX	1.17865	1.17865	6.42933	0.00113	0.20248
11	ST13;ST13P5;ST13P4	1.32255	1.32255	6.20186	0.00134	0.20541
12	NME1	1.27855	1.27855	6.16663	0.00137	0.20541
13	HMGB3	1.35247	1.35247	5.75821	0.00189	0.26094
14	EIF3J	1.0537	1.0537	5.62692	0.0021	0.26108
15	LSM8	1.37488	1.37488	5.47232	0.00239	0.26108
16	INS;INS-IGF2	1.06686	1.06686	4.92386	0.00236	0.26108
17	ALB	-1.61075	-1.61075	-4.87969	0.00248	0.26108
18	CFAP58	0.94581	0.94581	5.16217	0.00311	0.27517
19	RSPH4A	0.94347	0.94347	5.15343	0.00314	0.27517
20	HDGF	0.94134	0.94134	5.13432	0.00319	0.27517
21	UBXN1	0.93814	0.93814	5.07921	0.00335	0.27517
22	ALYREF	1.04981	1.04981	5.0702	0.00338	0.27517
23	LRRFIP1	0.9023	0.9023	4.71811	0.00464	0.35025
24	KTN1	1.29127	1.29127	4.70766	0.00469	0.35025
25	HDAC1	0.85978	0.85978	4.61618	0.00511	0.35219
26	RRBP1	1.02929	1.02929	4.51269	0.00563	0.37412
27	KRT1	-0.79086	-0.79086	-4.23219	0.00502	0.35219
28	SBDS	-0.90827	-0.90827	-4.41308	0.0062	0.38953
29	SNRPE	0.81285	0.81285	4.39667	0.0063	0.38953
30	ATP6V0D1	-0.79455	-0.79455	-4.23908	0.00736	0.41216
31	AP2M1	-0.56892	-0.56892	-3.97634	0.00674	0.40306

32	CHMP2A	-0.81106	-0.81106	-4.08437	0.00859	0.4293
33	EIF2S2	0.84864	0.84864	4.05977	0.00881	0.4293
34	API5	-0.60699	-0.60699	-3.92988	0.00712	0.41205
35	ODF2	0.74095	0.74095	3.95798	0.00978	0.43992
36	ETF1	-0.92092	-0.92092	-3.82712	0.00805	0.42489
37	HSPE1	-0.65222	-0.65222	-3.82659	0.00806	0.42489
38	YBX1;YBX3;YBX2	0.75167	0.75167	3.88876	0.01052	0.44549
39	PPP1CA	-0.55032	-0.55032	-3.74789	0.00886	0.4293
40	RPL13	-0.80619	-0.80619	-3.71773	0.00919	0.43359
41	PLGRKT	0.8548	0.8548	3.78172	0.01177	0.46411
42	SERPINB4;SERPINB3	-0.54233	-0.54233	-3.6638	0.00981	0.43992
43	SEC11A	0.82671	0.82671	3.73292	0.0124	0.46411
44	NASP	0.74792	0.74792	3.72871	0.01246	0.46411
45	KRT2	-1.23232	-1.23232	-3.60867	0.0105	0.44549
46	EIF4E	-0.74466	-0.74466	-3.65987	0.01342	0.46411
47	NDUFAF2	0.83641	0.83641	3.65533	0.01348	0.46411
48	DHX15	-0.50393	-0.50393	-3.58093	0.01087	0.44549
49	ISYNA1	-0.66913	-0.66913	-3.64376	0.01365	0.46411
50	ESYT2	0.78023	0.78023	3.57616	0.01093	0.44549
51	PRKCSH	1.06681	1.06681	3.63507	0.01378	0.46411
52	CRIP2	0.59493	0.59493	3.48924	0.01218	0.46411
53	IPO4	-0.76666	-0.76666	-3.49703	0.01603	0.46834
54	S100P	0.64847	0.64847	3.49635	0.01605	0.46834
55	C12orf10	0.65603	0.65603	3.4914	0.01614	0.46834
56	STX12	-0.78664	-0.78664	-3.43421	0.0172	0.46834
57	CKMT1A;CKMT1B	-0.46602	-0.46602	-3.39159	0.01377	0.46411
58	CPT1A	-0.85461	-0.85461	-3.4245	0.01738	0.46834
59	RBM47	-0.65321	-0.65321	-3.41848	0.0175	0.46834
60	HEXA	-0.53532	-0.53532	-3.38001	0.01398	0.46411
61	SNRPA	-0.49907	-0.49907	-3.35343	0.01446	0.46547
62	HNRNPC;HNRNPCL1	1.58017	1.58017	3.34906	0.01454	0.46547
63	TP53BP1	0.69088	0.69088	3.36815	0.01852	0.47436
64	ARFGAP2	-0.6967	-0.6967	-3.35522	0.01879	0.47455
65	RELA	0.64402	0.64402	3.27974	0.01588	0.46834
66	BUB3	-0.44757	-0.44757	-3.25582	0.01638	0.46834
67	TMEM14C	0.59921	0.59921	3.26378	0.02085	0.49983
68	POLR2C	-0.6317	-0.6317	-3.26139	0.02091	0.49983
69	RPL7A	-0.57434	-0.57434	-3.24605	0.01659	0.46834
70	RPL13A	-0.60359	-0.60359	-3.23669	0.01679	0.46834

71	RPL28	-0.65822	-0.65822	-3.21726	0.01721	0.46834
72	ACADSB	-0.6338	-0.6338	-3.19468	0.02257	0.51236
73	PGRMC1	0.53587	0.53587	3.17861	0.0181	0.473
74	RPS20	0.51895	0.51895	3.17413	0.0182	0.473
75	COG5	-0.57998	-0.57998	-3.1589	0.02353	0.52736
76	STMND1	0.71323	0.71323	3.13267	0.02426	0.52948
77	RAB10	0.66297	0.66297	3.12472	0.01941	0.4834
78	DNAJC10	-0.58361	-0.58361	-3.11837	0.02467	0.52948
79	ANK3	-1.33082	-1.33082	-3.10577	0.02503	0.52948
80	TXNDC12	0.54822	0.54822	3.10075	0.02003	0.49194
81	CFAP36	0.5854	0.5854	3.04006	0.02704	0.53112
82	GBE1	-0.62675	-0.62675	-3.0482	0.02146	0.50626
83	KIF5B	0.56744	0.56744	3.01499	0.02785	0.53112
84	LMO7	0.58382	0.58382	3.01145	0.02797	0.53112
85	RPL3	-0.51794	-0.51794	-3.02467	0.02213	0.51192
86	GSTT1	-0.43706	-0.43706	-3.02004	0.02227	0.51192
87	ENKUR	0.62207	0.62207	2.95959	0.02975	0.53112
88	H2AFY2	-0.59469	-0.59469	-2.94411	0.0303	0.53112
89	UGGT1	-0.67482	-0.67482	-2.94379	0.03031	0.53112
90	MANF	-0.75803	-0.75803	-2.94025	0.03044	0.53112
91	SOD1	-0.57894	-0.57894	-2.96076	0.02409	0.52948
92	APOO	0.5377	0.5377	2.92769	0.0309	0.53112
93	RPLP0;RPLP0P6	-0.40564	-0.40564	-2.92979	0.0251	0.52948
94	TBCB	-0.75197	-0.75197	-2.9001	0.03194	0.53112
95	PSMA4	0.70297	0.70297	2.8911	0.03229	0.53112
96	HSP90AA1	1.33988	1.33988	2.917	0.02553	0.53112
97	RSPH3	0.57347	0.57347	2.86304	0.0334	0.53351
98	SNX12	-0.68226	-0.68226	-2.85744	0.03362	0.53351
99	UBQLN1	0.41236	0.41236	2.88319	0.02671	0.53112
100	ATP5L	-0.50211	-0.50211	-2.88314	0.02671	0.53112
101	MCU	-0.52275	-0.52275	-2.84919	0.03396	0.53413
102	FTL	-0.67758	-0.67758	-2.85177	0.02786	0.53112
103	ASPH	-0.40332	-0.40332	-2.84071	0.02828	0.53112
104	RPL27	-0.53245	-0.53245	-2.80189	0.03596	0.54158
105	PREP	-0.42289	-0.42289	-2.83877	0.02835	0.53112
106	RPS8	-0.53285	-0.53285	-2.83489	0.0285	0.53112
107	BCCIP	0.5117	0.5117	2.7761	0.03711	0.54158
108	EIF4A3	-0.42784	-0.42784	-2.79937	0.0299	0.53112
109	ABRACL	0.51896	0.51896	2.75658	0.03801	0.54158

110	LDHA	-0.5104	-0.5104	-2.796	0.03003	0.53112
111	DCTN1;DKFZp686E0752	0.50775	0.50775	2.75009	0.03831	0.54158
112	CYFIP1;CYFIP2	-0.44521	-0.44521	-2.79154	0.03021	0.53112
113	MYO6	0.52172	0.52172	2.73328	0.0391	0.54352
114	GLG1	-0.37932	-0.37932	-2.76502	0.03131	0.53112
115	CDK5	-0.57636	-0.57636	-2.75814	0.03161	0.53112
116	PFKP	-0.42249	-0.42249	-2.75309	0.03182	0.53112
117	SF1	-0.75727	-0.75727	-2.74767	0.03206	0.53112
118	EIF1;EIF1B	0.49427	0.49427	2.69085	0.0412	0.55333
119	S100A11	0.78714	0.78714	2.71967	0.0333	0.53351
120	RPL17	-0.77599	-0.77599	-2.71671	0.03343	0.53351
121	TEKT2	0.83154	0.83154	2.66355	0.04261	0.55358
122	LMNA	0.36964	0.36964	2.69458	0.03446	0.53721
123	FGFR1OP	0.48869	0.48869	2.62366	0.04476	0.56923
124	APEH	-0.38335	-0.38335	-2.66966	0.03565	0.54158
125	SF3B5	0.72859	0.72859	2.61077	0.04549	0.57002
126	KRAS	0.39786	0.39786	2.66225	0.03601	0.54158
127	TMED7;TICAM2	-0.41772	-0.41772	-2.66214	0.03601	0.54158
128	HDHD3	-0.65187	-0.65187	-2.60003	0.0461	0.57002
129	SNRNP200	-0.53801	-0.53801	-2.59338	0.04648	0.57019
130	PIR	0.47667	0.47667	2.58879	0.04675	0.57019
131	MYH9	0.78867	0.78867	2.64148	0.03704	0.54158
132	RPS18	-0.39185	-0.39185	-2.64125	0.03706	0.54158
133	CAST	1.0354	1.0354	2.62633	0.03782	0.54158
134	IGFBP3	-0.40502	-0.40502	-2.62031	0.03813	0.54158
135	MAP2K3	-0.67652	-0.67652	-2.55684	0.04865	0.57765
136	UQCRB	-0.49097	-0.49097	-2.61596	0.03836	0.54158
137	SRP14	0.54208	0.54208	2.54755	0.04922	0.58055
138	ALDH1A1	-0.5166	-0.5166	-2.60703	0.03883	0.54352
139	HIST1H4A	-0.41764	-0.41764	-2.57641	0.0405	0.55333
140	RPS6	-0.49713	-0.49713	-2.55926	0.04147	0.55333
141	TMED2	0.44778	0.44778	2.55511	0.0417	0.55333
142	F11R	-0.5095	-0.5095	-2.55407	0.04176	0.55333
143	G6PD	-0.42977	-0.42977	-2.55081	0.04195	0.55333
144	DHRS7	-0.39571	-0.39571	-2.55048	0.04197	0.55333
145	RPS11	-0.36969	-0.36969	-2.54488	0.04229	0.55354
146	RECQL	-0.36164	-0.36164	-2.52953	0.0432	0.55723
147	VWA5A	-0.4533	-0.4533	-2.51851	0.04386	0.56172
148	RPS5	-0.43004	-0.43004	-2.49502	0.04531	0.57002

149	LRPAP1	0.44064	0.44064	2.48498	0.04594	0.57002
150	AARS	-0.35524	-0.35524	-2.46276	0.04737	0.57393
151	GMPPA	-0.34083	-0.34083	-2.45492	0.04789	0.57631
152	CHMP1A	0.64099	0.64099	2.44598	0.04849	0.57765
153	CMAS	-0.33708	-0.33708	-2.42971	0.0496	0.5812

Appendix 4: List of differentially abundant RNA transcripts identified using Asthma Elements Panels in submerged monolayer cultures of 1HAEs upon exposure to *A. fumigatus* conidia

	Gene	logFC	AveExpr	t	P.Value	adj.P.Val
1	GTF2H2	-0.6173758	6.05859516	-5.4298887	0.00084566	0.0571225
2	CFD	-0.4660308	6.4212631	-4.8021953	0.00173971	0.0571225
3	C5AR1	0.49861492	5.33708415	4.47257256	0.00259853	0.0571225
4	GLIPR1	-0.5977106	8.75258603	-4.4555241	0.00265417	0.0571225
5	CMC1	-0.3000108	9.25490306	-4.4030697	0.00283371	0.0571225
6	FAM8A1	-0.3451338	6.81395208	-4.3690468	0.00295725	0.0571225
7	ARPC4	-0.3036772	12.2231276	-3.9573893	0.00502429	0.0571225
8	PPP3R1	-0.3005676	11.7084588	-3.9222804	0.00526279	0.0571225
9	TNFRSF1B	-0.6494562	5.66567677	-3.916591	0.00530258	0.0571225
10	DESI1	-0.2594803	8.68786154	-3.8929128	0.00547173	0.0571225
11	ABHD5	-0.4125353	8.10080624	-3.817691	0.00604907	0.0571225
12	ZNF185	-0.4095381	8.46050578	-3.7277127	0.00682772	0.0571225
13	RPS6	-0.266151	14.4475456	-3.6708817	0.00737489	0.0571225
14	HLA-B	-0.2796081	9.27218399	-3.6367336	0.00772629	0.0571225
15	NFKBIA	-0.3827931	11.8984636	-3.434903	0.01020784	0.0571225
16	GLIPR1_isoform	-0.4901081	8.47856847	-3.4173976	0.01046026	0.0571225
17	CTSS	-0.352995	5.33282352	-3.3936646	0.01081321	0.0571225
18	CARM1	-0.2483937	10.1503974	-3.3843308	0.0109555	0.0571225
19	SF3B1	-0.2654039	10.8905609	-3.3715327	0.01115385	0.0571225
20	RHOA	-0.2494785	12.6161572	-3.3472575	0.01154072	0.0571225
21	HLA-A	-0.2943595	10.377421	-3.346282	0.01155656	0.0571225
22	C9orf78	-0.293774	9.9763331	-3.3351739	0.01173861	0.0571225
23	EWSR1	-0.2380538	11.7419259	-3.3078263	0.01219999	0.0571225
24	NAPA	-0.2152195	10.5358534	-3.2871365	0.01256189	0.0571225
25	NFKB1	-0.3593485	9.2177274	-3.2759501	0.01276231	0.0571225
26	MRPS5	-0.2350307	10.6077023	-3.2757057	0.01276673	0.0571225
27	C1orf27	-0.2720099	8.47091179	-3.268846	0.01289136	0.0571225
28	TMBIM6	-0.2624047	12.7152208	-3.2403343	0.01342344	0.0571225
29	SCARNA5	-0.2877923	13.4904315	-3.1838529	0.01454771	0.0571225
30	FADD	-0.2790219	9.51615975	-3.1793564	0.01464142	0.0571225

31	SERPINA1	-0.5340733	9.5664963	-3.176207	0.01470743	0.0571225
32	CD59	-0.2935295	12.3783736	-3.1653311	0.01493784	0.0571225
33	MT-CYB	0.23935838	16.3294482	3.13380583	0.01562763	0.0571225
34	MAP2K2	-0.2339406	10.7609856	-3.1266014	0.01578996	0.0571225
35	PSMF1	-0.228888	9.843818	-3.0927812	0.01657622	0.05806868
36	UBE2D1	-0.2536149	9.59763965	-3.0641184	0.01727503	0.05806868
37	ACOT9	-0.2707873	10.3939095	-3.0385406	0.01792494	0.05806868
38	TPP1	-0.2103372	9.74482455	-3.0340451	0.01804181	0.05806868
39	MSN	-0.2422125	12.3174396	-3.0142099	0.01856716	0.05806868
40	CD46	-0.2116994	10.8430624	-2.9781255	0.01956468	0.05806868
41	PTPN18	-0.2268256	8.30474756	-2.9579914	0.02014567	0.05806868
42	SH3BGRL3	-0.2440266	13.1083182	-2.9556659	0.02021393	0.05806868
43	FAM133B	-0.2835377	6.76672227	-2.952731	0.02030043	0.05806868
44	IL17RA	-0.3817831	7.03742849	-2.8980806	0.02198426	0.06145601
45	ATG7	-0.2565495	8.88047108	-2.8253868	0.02445425	0.06526207
46	GBE1	-0.214744	8.496586	-2.8200137	0.02464799	0.06526207
47	PLAUR	-0.4596932	11.7895899	-2.8120652	0.02493754	0.06526207
48	TEX261	-0.2529273	10.9415303	-2.7158296	0.02873864	0.07268716
49	EIF2B4	-0.2144785	9.20711883	-2.7107184	0.02895667	0.07268716
50	CNTNAP3	0.29898477	6.78696669	2.69238728	0.02975286	0.07319204
51	CDK5RAP3	-0.1866358	9.05635819	-2.6665715	0.03091286	0.07418068
52	DAP	-0.1986902	11.2048555	-2.6499087	0.0316864	0.07418068
53	IKBIP_isoform	-0.2228666	9.80034687	-2.6440306	0.03196403	0.07418068
54	PABPC1	-0.2030409	11.5680946	-2.608476	0.03369788	0.07675627
55	CHP1	-0.2174015	9.45089435	-2.5920462	0.03453164	0.07722529
56	VPS13A_isoform	-0.3030373	5.80737077	-2.5289801	0.0379346	0.08254448
57	B3GNT5	-0.4040308	10.2208089	-2.5233918	0.03825232	0.08254448
58	CYTB_comp57541_c0_seq1	0.21516976	15.4579184	2.43829437	0.04344209	0.09160571
59	RRAD	-0.3848514	5.39934156	-2.4306694	0.04394095	0.09160571
60	ZNF281	-0.20343	10.057551	-2.4031147	0.0457929	0.09244841
61	DUSP6	-0.4786688	7.54848784	-2.4016333	0.04589468	0.09244841
62	SEMA4D	-0.1907052	6.13127368	-2.3914592	0.04660001	0.09244841
63	COPB1_isoform	-0.1947803	8.07254338	-2.3762801	0.04767287	0.0930756

Appendix 5: List of differentially abundant RNA transcripts identified using Immune Profiling Panel in submerged monolayer cultures of 1HAEs upon exposure to *A. fumigatus* conidia

	Gene	logFC	AveExpr	t	P.Value	adj.P.Val
1	CXCL11	0.9191757	4.77082399	8.76075048	0.00011904	0.0420219
2	TLR6	0.77125351	5.30366308	6.64954605	0.00054691	0.09652877
3	JAK2	0.38990425	6.87353335	4.72035483	0.00321228	0.30924503
4	IFIT2	0.2341136	8.58937646	4.51229898	0.00399876	0.30924503
5	ZNF205	-0.2838895	5.43362231	-4.2371369	0.0053936	0.30924503
6	CXCR1	0.55752541	4.44295954	3.86841863	0.00819806	0.30924503
7	BCL6	0.43916062	5.18307412	3.79740643	0.00890767	0.30924503
8	CXCL6	0.27267483	4.99928735	3.78104568	0.00908068	0.30924503
9	PRKCE	0.17189381	7.95571562	3.65857378	0.01050085	0.30924503
10	RELB	-0.1836117	8.56685631	-3.5722104	0.01165007	0.30924503
11	CD83	-0.269433	8.09121013	-3.5009849	0.01270289	0.30924503
12	STAT2	0.22776945	7.88929967	3.4764449	0.0130896	0.30924503
13	CSF2	-0.3357516	5.4483015	-3.4709246	0.01317837	0.30924503
14	AXL	-0.1948483	11.095775	-3.4644154	0.0132839	0.30924503
15	IFNL1	0.43071411	5.77598355	3.46385418	0.01329304	0.30924503
16	NFATC2	0.29919582	9.19833285	3.40314461	0.01432411	0.30924503
17	TCF7	0.39153791	7.33852886	3.32701628	0.01574329	0.30924503
18	THBS1	0.22307793	14.5052609	3.29808026	0.01632262	0.30924503
19	CASP3	-0.3151583	10.1849158	-3.282466	0.01664492	0.30924503
20	AMMECR1L	0.16467555	9.12788856	3.17125351	0.01915234	0.32037056
21	CYFIP2	0.2608157	6.25863401	3.153515	0.01958914	0.32037056
22	C1S	0.67415996	4.41108307	3.13853702	0.01996644	0.32037056
23	SPA17	0.17818136	8.63483173	2.96015035	0.0251221	0.37752238
24	SMAD3	0.1548152	10.8463914	2.94365447	0.02566724	0.37752238
25	MAP3K1	0.2467808	7.15498836	2.8859566	0.02767685	0.39079712
26	MCAM	0.19112259	8.30661361	2.84359287	0.02926023	0.39726387
27	PYCARD	0.19781912	7.52831629	2.75772178	0.03277669	0.39791924
28	TNFRSF1A	-0.1344485	10.708049	-2.731376	0.03394443	0.39791924
29	MAPK11	0.35303245	4.97911097	2.67798961	0.03644938	0.39791924
30	FADD	0.23056071	6.45451139	2.66866436	0.03690682	0.39791924
31	IL32	-0.2029644	11.1289339	-2.6358316	0.03856674	0.39791924

32	ADA	0.28191558	9.21443942	2.60878105	0.03999401	0.39791924
33	RUNX1	0.1643913	9.74012428	2.57401754	0.04191115	0.39791924
34	CD274	-0.2565487	5.6501759	-2.5732399	0.04195513	0.39791924
35	ITGA2B	0.41552039	5.44403806	2.57306677	0.04196493	0.39791924
36	OSM	0.66243683	4.62430529	2.56257714	0.04256319	0.39791924
37	CCL20	-0.5307588	5.15543735	-2.5223068	0.04494517	0.39791924
38	PDGFRB	0.59764095	6.59857102	2.52153193	0.04499236	0.39791924
39	IFNB1	-0.3588966	5.0186175	-2.5129707	0.04551728	0.39791924
40	CEBPB	-0.3062697	11.8851524	-2.5120692	0.04557292	0.39791924
41	TTK	0.13745984	9.64108202	2.501715	0.04621725	0.39791924

Appendix 6: List of differentially abundant proteins identified using LC-MS/MS in submerged monolayer cultures of 1HAEs upon exposure to *A. fumigatus* conidia

	Gene	logFC	AveExpr	t	P.Value	adj.P.Val
1	ALB	-3.0023602	-3.0023602	-13.315007	3.00E-05	0.01674497
2	RALGAPA1	-1.8647323	-1.8647323	-7.6670734	0.00120714	0.27901937
3	SF3A2	1.94379343	1.94379343	7.08894272	0.00165106	0.27901937
4	KRT10	-1.463663	-1.463663	-5.6812946	0.00200014	0.27901937
5	RPL18A	-0.9788533	-0.9788533	-5.1899689	0.00302282	0.33734714
6	HNRNPK	1.22198134	1.22198134	4.68618962	0.00475885	0.404422
7	KRT9	-1.313281	-1.313281	-4.5357962	0.0054845	0.404422
8	CNBP	1.29234664	1.29234664	4.86025022	0.00707074	0.404422
9	HNRNPA0	1.16643339	1.16643339	4.79433294	0.00743711	0.404422
10	SF1	1.32274783	1.32274783	4.36389071	0.00647513	0.404422
11	RPF2	1.22409529	1.22409529	4.70471235	0.00797248	0.404422
12	KRT1	-1.4264988	-1.4264988	-3.8146008	0.01132782	0.45724709
13	CAPRIN1	1.00421073	1.00421073	3.97831666	0.01454675	0.45724709
14	HNRNPC	0.93325733	0.93325733	3.77948645	0.01175831	0.45724709
15	MATR3	1.09821374	1.09821374	3.82539284	0.01666376	0.45724709
16	NAP1L1	0.73076146	0.73076146	3.61789214	0.01399456	0.45724709
17	RPS27L;RPS27	0.89296627	0.89296627	3.72115607	0.01831693	0.45724709
18	CAST	0.86638623	0.86638623	3.64518246	0.01964455	0.45724709
19	TF	-1.0419985	-1.0419985	-3.6375618	0.01978387	0.45724709
20	LMNA	0.87819679	0.87819679	3.50490435	0.01584464	0.45724709
21	RPL4	0.63505369	0.63505369	3.41825788	0.0174512	0.45724709
22	KPNA2	0.74414419	0.74414419	3.362452	0.01858282	0.45724709
23	HSPA5	-0.5904296	-0.5904296	-3.3616182	0.01860035	0.45724709
24	RBM3	0.71031373	0.71031373	3.28764744	0.02023124	0.45724709
25	HNRNPR	0.83971944	0.83971944	3.29218824	0.02751352	0.45724709
26	BZW1	1.0535723	1.0535723	3.28228405	0.02778273	0.45724709
27	SPTBN1	0.78111988	0.78111988	3.24377522	0.02885907	0.45724709
28	RPS4X	0.58114616	0.58114616	3.15372218	0.02360813	0.45724709
29	YWHAB	-0.649399	-0.649399	-3.1018239	0.02508239	0.45724709
30	EIF4G1	1.39269782	1.39269782	3.13512135	0.03216781	0.45724709
31	RBP4	-1.1029861	-1.1029861	-3.0897753	0.02543914	0.45724709

32	RRBP1	0.93418151	0.93418151	3.08644129	0.03379187	0.45724709
33	YWHAZ	0.72093397	0.72093397	3.04590391	0.02678666	0.45724709
34	PFN2	-1.0821497	-1.0821497	-3.0317114	0.03573243	0.45724709
35	KRT2	-1.3884239	-1.3884239	-3.0067839	0.03665881	0.45724709
36	RPS16	0.80449506	0.80449506	2.96555443	0.0294651	0.45724709
37	YWHAE	0.5339016	0.5339016	2.9508395	0.02998709	0.45724709
38	HGFAC	-1.0060502	-1.0060502	-2.9586144	0.03852867	0.45724709
39	PGD	-0.5832711	-0.5832711	-2.9451758	0.03019073	0.45724709
40	SH3BGRL3	0.99583032	0.99583032	2.907924	0.04061619	0.45724709
41	NONO	0.62139047	0.62139047	2.90297375	0.03175711	0.45724709
42	CHORDC1	-0.7754687	-0.7754687	-2.9050675	0.04073764	0.45724709
43	PHGDH	0.51124895	0.51124895	2.88701481	0.03237267	0.45724709
44	FDFT1	0.68441513	0.68441513	2.88068842	0.0417914	0.45724709
45	NPM1	-0.5276766	-0.5276766	-2.7987124	0.03602543	0.45724709
46	LRRC59	0.64156907	0.64156907	2.79102219	0.0363644	0.45724709
47	2-Sep	-0.6657523	-0.6657523	-2.7704271	0.03728958	0.45724709
48	LMAN1	-1.0350467	-1.0350467	-2.7403729	0.03868634	0.45724709
49	RPL10A	0.72483474	0.72483474	2.73656254	0.03886749	0.45724709
50	ETFB	-0.4950135	-0.4950135	-2.6912792	0.04109283	0.45724709
51	ARHGDIA	0.54328957	0.54328957	2.67807586	0.04176763	0.45724709
52	PPP1CA;PPP1CC	0.63537855	0.63537855	2.61955657	0.04490748	0.48189178
53	HNRNPDL	-0.576268	-0.576268	-2.5645093	0.04809665	0.49398739
54	VIM	0.59229976	0.59229976	2.53379672	0.04998215	0.49398739

Appendix 7: List of differentially abundant RNA transcripts identified using Immune Profiling Panel in ALI cultures of primary HBECs upon exposure to *Δkdnase A. fumigatus* conidia

	Gene	logFC	AveExpr	t	P.Value	adj.P.Val
1	TPTE	1.70687711	4.56904922	6.92829332	0.00025722	0.0729208
2	CD79B	1.16604173	5.08418981	6.21691315	0.00049139	0.0729208
3	BST2	1.11320421	7.13571335	6.14994696	0.00052374	0.0729208
4	CFP	1.11245365	5.32794505	5.72117641	0.00079759	0.0729208
5	HAVCR2	1.21502545	4.50174475	5.71434577	0.00080309	0.0729208
6	IFNL1	1.16722054	5.6962652	5.38478905	0.001127	0.07777562
7	CXCL6	-1.5400571	11.7979496	-5.2089998	0.00135804	0.07777562
8	SMPD3	1.10414054	5.47066744	5.20048872	0.0013705	0.07777562
9	TLR6	1.0123559	5.54920547	4.7514782	0.00225031	0.11351547
10	FOS	1.1460866	8.68855531	4.4375264	0.0032375	0.1469823
11	CXCL5	-1.9555697	9.64655601	-4.3052585	0.00379003	0.15642507
12	MAGEC2	0.74933257	4.4252311	4.06736786	0.00506508	0.17758159
13	SAA1	-0.8621851	15.5833191	-4.0315297	0.00529518	0.17758159
14	S100A7	-1.0809435	7.71638138	-4.0045343	0.00547608	0.17758159
15	C4B	-0.9299218	6.50386333	-3.8361492	0.00676944	0.18716844
16	CFB	-0.6317316	12.949439	-3.828638	0.00683445	0.18716844
17	TNFSF4	1.15853871	4.93218254	3.75598589	0.00749972	0.18716844
18	PLAUR	0.6920706	8.70786915	3.72268626	0.00782799	0.18716844
19	IDO1	-0.8712363	10.9717861	-3.7221862	0.00783304	0.18716844
20	CDH5	0.73404913	5.1250934	3.66547672	0.00842915	0.19134178
21	IFI27	1.00886001	9.72991902	3.5819324	0.0093992	0.20320181
22	TFE3	0.6049885	5.73341369	3.47188531	0.01086653	0.22424556
23	RUNX3	0.80644817	5.44129834	3.42241525	0.01160546	0.22908165
24	ITGAL	1.04368379	4.65698675	3.3739938	0.01238161	0.23208724
25	IL1RN	0.69159911	9.35569966	3.35038974	0.01278013	0.23208724
26	CREB5	0.65007458	5.66172851	3.31187465	0.01346043	0.23503976
27	HLA-DMB	-0.5463503	9.60823682	-3.2567236	0.01450337	0.23575019
28	IL22RA1	0.67245799	4.68236411	3.25488224	0.01453966	0.23575019
29	ITGA5	0.59034459	9.52652113	3.19663403	0.01573947	0.24640412

30	IFI35	0.59683678	6.16526773	3.15999425	0.01654834	0.25043154
31	CXCL11	0.62139683	6.26770858	3.10694831	0.0177993	0.26067358
32	CD40LG	0.54152918	4.77602767	2.95070439	0.02210764	0.30905104
33	ARG2	0.94661546	6.67209186	2.92729867	0.02284329	0.30905104
34	NFATC1	0.58146423	6.6364877	2.91240473	0.0233249	0.30905104
35	IL18R1	-0.6174011	5.06155455	-2.8972649	0.02382552	0.30905104
36	C6	0.76687908	9.00945627	2.81586714	0.02671924	0.33695933
37	TIGIT	0.89521377	4.6735492	2.78419051	0.02794373	0.34287713
38	C3	-0.535071	13.6080562	-2.7521307	0.0292434	0.34938168
39	TFRC	-0.4802386	9.62755042	-2.7179932	0.03069744	0.35734967
40	LCK	0.65130851	4.65533902	2.64110415	0.03425731	0.38866099
41	TRIM39	0.55071549	6.13622918	2.61334604	0.03564641	0.38866099
42	TFEB	0.51391433	6.42742474	2.60732459	0.03595542	0.38866099
43	IL1RL1	0.53239774	4.97401543	2.58892549	0.03691708	0.38916158
44	IRF5	0.60255404	6.95788021	2.57401407	0.0377161	0.38916158
45	IL12A	0.43650649	4.82204056	2.4813743	0.04309993	0.4137631
46	FADD	0.48426287	5.38048704	2.47269255	0.04364373	0.4137631
47	CFI	-0.6524025	9.86701246	-2.4609077	0.04439327	0.4137631
48	TLR4	0.61556428	5.78503702	2.45776111	0.04459564	0.4137631
49	LAG3	0.73393842	5.43376417	2.45656118	0.04467307	0.4137631
50	TICAM1	0.5388668	7.70599657	2.42016786	0.04708838	0.4137631
51	ETS1	0.49063155	9.82631131	2.41697362	0.0473067	0.4137631
52	IFITM2	0.44034986	8.73450578	2.41573894	0.04739137	0.4137631

Appendix 8: List of differentially abundant RNA transcripts identified using Immune Profiling Panel in ALI cultures of primary HBECs upon exposure to *Δkdnase A. fumigatus* conidia and WT *A. fumigatus* conidia

	Gene	logFC	AveExpr	t	P.Value	adj.P.Val
1	BLK	1.2802672	5.07710528	4.47824206	0.00290477	0.95589574
2	IL19	1.69180815	5.75515448	3.79037864	0.00685714	0.95589574
3	TLR6	0.96041687	5.63651953	3.14839539	0.01628435	0.95589574
4	AKT3	1.68630523	4.7508057	3.05460798	0.01856606	0.95589574
5	IRAK2	0.76740658	8.1261155	3.04563997	0.01880142	0.95589574
6	NT5E	0.783637	6.73871381	2.87039714	0.02409596	0.95589574
7	TFRC	-0.8890544	9.69668034	-2.8451814	0.02497903	0.95589574
8	CD14	1.03536161	5.09028543	2.82262024	0.02579804	0.95589574
9	IL6R	-0.7504457	7.01864429	-2.7390025	0.02908832	0.95589574
10	CCL28	-0.8458976	6.69485544	-2.6951612	0.03098653	0.95589574
11	STAT4	0.83199114	6.48377889	2.57269512	0.03700537	0.95589574
12	MICA	0.78757028	6.28322755	2.5155143	0.04021996	0.95589574
13	DMBT1	1.53431968	7.13376405	2.49480416	0.04145433	0.95589574
14	HLA-DMA	-0.6599028	8.92532037	-2.4845518	0.0420798	0.95589574
15	IL32	0.66836048	8.98867756	2.45927349	0.04366387	0.95589574
16	CDH5	0.95529569	5.04705897	2.42832261	0.04568731	0.95589574
17	KIT	-0.7055288	4.82724284	-2.3921767	0.04817276	0.95589574

Appendix 9: List of differentially abundant RNA transcripts identified using Immune Profiling Panel in ALI cultures of primary HBECs upon exposure to RSV

	Gene	logFC	AveExpr	t	P.Value	adj.P.Val
1	IL23A	4.08035799	8.07660769	7.00468529	0.00031314	0.06745488
2	IL6	4.35395494	5.41255498	6.96305517	0.00032408	0.06745488
3	NFATC4	-2.3342263	5.03117799	-6.4272781	0.00051172	0.06745488
4	IL34	-3.1093466	4.61519788	-6.2588908	0.00059432	0.06745488
5	CCR3	1.89265985	5.63609683	5.35429375	0.00140299	0.09995833
6	MR1	-1.8992834	7.1126572	-5.1804617	0.0016739	0.09995833
7	IFIT1	-2.38775	5.93243794	-5.1545222	0.00171917	0.09995833
8	TXNIP	-2.2460912	9.77029717	-5.13102	0.00176138	0.09995833
9	TGFB2	-1.992002	8.62003867	-4.9219618	0.00219265	0.11060706
10	TLR3	-1.7630758	8.33383794	-4.599718	0.00310974	0.1261876
11	CXCL2	1.77669865	12.0141898	4.5802955	0.00317742	0.1261876
12	CXCL8	1.8552697	15.2647988	4.5367178	0.00333535	0.1261876
13	SF3A3	-1.564113	7.7113195	-4.3753437	0.00400133	0.1352695
14	TNFSF10	-1.5485324	10.4716267	-4.2988221	0.00436794	0.1352695
15	INPP5D	-1.4381088	6.93519602	-4.2760218	0.00448429	0.1352695
16	SAA1	-2.050136	14.9423127	-4.2164399	0.00480495	0.1352695
17	IL1RN	2.0121762	9.25248512	4.12340349	0.00535782	0.1352695
18	NFKBIA	1.72339002	12.0894775	4.11644968	0.00540189	0.1352695
19	S100A8	1.62704237	8.56470665	4.03570093	0.00594423	0.1352695
20	ITGB4	-1.3308707	9.61945726	-4.0336156	0.00595901	0.1352695
21	TLR4	2.04167771	5.87539423	3.85291476	0.00740864	0.15630108
22	STAT1	-1.3180121	9.45255463	-3.834816	0.00757406	0.15630108
23	IL12A	1.53679533	4.59567383	3.74972607	0.00840832	0.163275
24	CCL3	-1.5209514	4.24399631	-3.6607187	0.00939059	0.163275
25	PTGS2	2.3561344	10.4728712	3.61117455	0.00999146	0.163275
26	THBS1	-2.1986506	9.07976775	-3.5794437	0.01039837	0.163275
27	EDC3	-1.1917353	8.04900171	-3.5783829	0.01041228	0.163275
28	ATG16L1	-1.3547264	7.52892213	-3.5693267	0.0105319	0.163275
29	ISG20	1.60963361	9.33378939	3.56050279	0.01064989	0.163275

30	CCL20	1.8669129	14.4764331	3.55022954	0.0107891	0.163275
31	HLA-DOB	1.88271175	4.7199322	3.48506227	0.01171985	0.16748967
32	CXCL1	1.28244834	14.6387136	3.47935568	0.01180544	0.16748967
33	NRP1	-1.246277	6.59135888	-3.4371654	0.01245982	0.1682505
34	ADORA2A	2.47524631	5.14147336	3.42818728	0.01260412	0.1682505
35	MAP3K1	-1.214158	7.88718862	-3.4058649	0.01297085	0.1682505
36	DUSP4	-1.1817042	8.38410574	-3.3712747	0.01356231	0.17103578
37	DDX58	-1.3817852	6.49639451	-3.3164252	0.01456123	0.17867023
38	TNFRSF12A	-1.153588	6.66220949	-3.2366198	0.0161602	0.18666237
39	POLR2A	-1.7649297	8.52369831	-3.2260731	0.01638538	0.18666237
40	SH2D1B	2.28999279	5.3932286	3.22325937	0.01644602	0.18666237
41	TNFRSF10C	-1.4007361	6.58238428	-3.1454481	0.01822327	0.19782718
42	DOCK9	-1.0974068	8.94675917	-3.1211379	0.01882027	0.19782718
43	FAS	-1.544692	4.63465532	-3.1137856	0.01900496	0.19782718
44	BATF	1.44631406	6.50637834	3.10717509	0.01917268	0.19782718
45	TIRAP	-1.5039064	4.70597948	-3.0873083	0.01968642	0.19861408
46	TCF7	-1.1960109	6.37631171	-3.0292393	0.02127492	0.20785088
47	CLEC4A	1.95718929	4.72275195	3.02078045	0.0215176	0.20785088
48	SYK	-1.2863558	7.29092671	-2.9430455	0.02389212	0.2259796
49	TNFRSF18	1.00605837	5.02075554	2.91424366	0.02484194	0.23016818
50	TICAM1	1.22842519	7.70913341	2.88330319	0.02590746	0.23523976
51	RIPK2	1.40628197	8.25803445	2.85030442	0.02709787	0.23577001
52	IKBKG	-1.252725	6.47405303	-2.8500522	0.02710719	0.23577001
53	TP53	-1.2432714	8.71609622	-2.8163653	0.02838326	0.23577001
54	BAX	-1.1913696	9.27321823	-2.810971	0.02859347	0.23577001
55	ZC3H14	-0.9607168	7.92257701	-2.8052482	0.02881829	0.23577001
56	MAPK1	-0.9898236	9.46890794	-2.7986018	0.02908176	0.23577001
57	NOS2A	3.04119649	4.54506058	2.77455489	0.03005661	0.23606695
58	HLA-DMB	-1.0071394	9.23823616	-2.7658247	0.03041907	0.23606695
59	HLA-DMA	-1.2249067	8.70633595	-2.7482295	0.03116376	0.23606695
60	LCN2	-1.1236789	15.1595479	-2.7422823	0.03141982	0.23606695
61	IL6R	-1.3260035	6.54048624	-2.7275015	0.03206593	0.23606695
62	KLRD1	-1.1905517	4.52562638	-2.7180685	0.03248561	0.23606695
63	IL10	1.94072598	4.32858938	2.70755014	0.03296046	0.23606695
64	CSF3	2.96634773	6.46944505	2.69207877	0.0336723	0.23606695
65	LAMP1	-0.9640301	11.0606453	-2.6875707	0.03388276	0.23606695
66	ARG2	1.9161097	6.95488449	2.67833894	0.0343181	0.23606695
67	JAK1	-0.8823472	9.54048692	-2.6578029	0.03530785	0.23925021
68	CXCL10	-3.0594129	4.9928707	-2.6268089	0.03685906	0.24608845

69	HRAS	-1.3902739	6.87216773	-2.6055607	0.03796388	0.24979135
70	MAPK3	-0.8995922	9.22507352	-2.5486473	0.04109811	0.26333588
71	NOD1	-1.2910843	5.39889746	-2.547179	0.04118248	0.26333588
72	ETS1	0.921144	9.77507521	2.53443669	0.04192229	0.26434335
73	DNAJC14	1.09239862	5.97069263	2.5190878	0.04283196	0.2644039
74	CXCR1	1.46175083	4.54667945	2.50794458	0.0435053	0.2644039
75	ABCF1	-0.8440083	7.89227663	-2.5008678	0.04393866	0.2644039
76	EPCAM	-0.8753913	9.85450428	-2.4788693	0.0453148	0.2644039
77	CXCL11	-1.0107434	5.45236651	-2.4727882	0.0457031	0.2644039
78	ZKSCAN5	-1.578365	4.51614075	-2.4690069	0.04594629	0.2644039
79	DMBT1	2.54418627	7.21006904	2.46804132	0.04600861	0.2644039
80	GTF3C1	-0.9955002	8.57740042	-2.4527836	0.0470051	0.26571671
81	DPP4	-1.8991842	4.91421389	-2.4467159	0.04740761	0.26571671
82	MAVS	-1.1400472	8.0201358	-2.4216281	0.0491103	0.26995484

Appendix 10: List of differentially abundant RNA transcripts identified using Immune Profiling Panel in high TEER and low TEER ALI cultures of primary HBECs

	Gene	logFC	AveExpr	t	P.Value	adj.P.Val
1	THBS1	-5.0555458	9.32388124	-23.438415	3.89E-08	8.94E-06
2	FOXJ1	8.8057566	9.8618738	22.1881573	5.77E-08	8.94E-06
3	SPA17	5.616669	10.3470116	21.9390433	6.26E-08	8.94E-06
4	TGFB2	-3.7071148	8.3703389	-21.205358	8.00E-08	8.94E-06
5	NT5E	-3.2999999	7.00923775	-19.857492	1.28E-07	1.15E-05
6	CXCL5	-5.8709887	8.195778	-19.334282	1.55E-07	1.16E-05
7	CD4	4.10436651	5.71777256	18.1756403	2.42E-07	1.37E-05
8	RORC	4.23856163	6.04197861	18.1449987	2.45E-07	1.37E-05
9	LCK	3.54041102	5.54135021	17.6370993	3.00E-07	1.49E-05
10	C6	5.19077224	6.17678569	17.019193	3.87E-07	1.73E-05
11	RRAD	3.62078752	8.37471869	16.425964	4.98E-07	1.89E-05
12	NRP1	-3.2931151	6.51651204	-16.387494	5.06E-07	1.89E-05
13	IL32	-3.7488172	8.61415218	-16.008974	5.98E-07	2.06E-05
14	MFGE8	-2.5425339	9.23470292	-15.765488	6.67E-07	2.08E-05
15	CTSS	3.19331161	10.3570114	15.5702991	7.29E-07	2.08E-05
16	LGALS3	2.58512271	12.8988791	15.5202161	7.46E-07	2.08E-05
17	IDO1	-3.9031976	8.5636913	-14.997	9.51E-07	2.50E-05
18	BST1	3.85533971	5.25130267	14.6077033	1.15E-06	2.84E-05
19	CD44	-2.543779	10.4389604	-14.499733	1.21E-06	2.84E-05
20	CDK1	6.1282991	6.55909018	14.2004904	1.40E-06	2.99E-05
21	ISG20	2.31291393	8.32786734	14.1907009	1.41E-06	2.99E-05
22	IL5RA	5.3199854	6.2629278	14.0793296	1.49E-06	3.02E-05
23	CX3CL1	-2.3387463	8.76040066	-13.92286	1.61E-06	3.13E-05
24	CFP	3.46446755	4.23343464	13.6199012	1.88E-06	3.50E-05
25	CCL15	4.06729699	4.26109032	13.518973	1.98E-06	3.54E-05
26	CD9	2.03002337	11.6805046	13.1658459	2.39E-06	4.10E-05
27	SIGIRR	1.96902155	7.50313551	13.0914715	2.48E-06	4.11E-05
28	DUSP6	-2.6082522	8.78095668	-12.817805	2.88E-06	4.60E-05
29	IRF2	2.02159282	9.38167493	12.2005854	4.07E-06	6.28E-05
30	MCAM	-2.7065691	5.20811996	-11.898834	4.85E-06	7.23E-05
31	CD68	3.21744691	6.93594774	11.516782	6.09E-06	8.78E-05

32	FEZ1	-2.4982167	7.86805362	-11.404724	6.52E-06	8.85E-05
33	CSF1	-3.2993755	5.5826769	-11.360478	6.69E-06	8.85E-05
34	VEGFC	-2.413583	6.61316195	-11.351072	6.73E-06	8.85E-05
35	ITGB4	-1.946274	10.627268	-11.292507	6.98E-06	8.91E-05
36	SELPLG	3.5667035	5.05284211	11.241981	7.20E-06	8.94E-05
37	SPINK5	3.21681089	6.62656408	11.1006802	7.86E-06	9.50E-05
38	HLA-DPA1	1.7661062	7.91391771	10.8629695	9.13E-06	0.00010732
39	CD19	3.51047589	4.31387471	10.8236891	9.36E-06	0.00010732
40	BCL6	2.32781805	8.84290216	10.760435	9.75E-06	0.00010811
41	LTK	3.45501238	4.33832741	10.7343494	9.92E-06	0.00010811
42	CD276	-1.8014133	8.51843044	-10.686991	1.02E-05	0.0001088
43	CD74	1.61717298	10.5433834	10.6025774	1.08E-05	0.00011064
44	RORA	2.68857759	6.57427819	10.5894235	1.09E-05	0.00011064
45	AKT3	-1.8351457	5.36816065	-10.471115	1.18E-05	0.0001169
46	CXCL6	-2.1794567	11.4805136	-10.342919	1.28E-05	0.00012448
47	MERTK	1.69021408	5.45916697	10.1806539	1.43E-05	0.00013582
48	LAG3	1.80771343	5.07662938	10.0383072	1.57E-05	0.00014634
49	HLA-DRA	2.28341387	10.6077337	10.0095786	1.60E-05	0.00014634
50	ITGA6	-2.0265007	8.5285077	-9.9198911	1.71E-05	0.00015254
51	TLR1	1.6838806	6.95661813	9.85959508	1.78E-05	0.00015592
52	CCL2	-4.313811	5.23238318	-9.8298442	1.82E-05	0.00015611
53	ARG2	2.23098984	6.46088401	9.7533203	1.92E-05	0.00016042
54	HLA-DRB3	2.09824935	8.50899028	9.73686205	1.94E-05	0.00016042
55	VCAM1	-4.4389026	4.04308937	-9.6781105	2.02E-05	0.00016415
56	COG7	1.67399614	8.07561399	9.64457602	2.07E-05	0.00016508
57	ADA	-1.7305761	6.55440659	-9.516717	2.27E-05	0.00017252
58	C3	-1.5306565	12.3006306	-9.5061126	2.28E-05	0.00017252
59	SAA1	-2.5205066	13.6918879	-9.4904535	2.31E-05	0.00017252
60	MUC1	1.82702459	11.3222977	9.48590669	2.32E-05	0.00017252
61	POU2F2	-2.0881457	4.45949755	-9.2807247	2.69E-05	0.00019689
62	DDX58	-1.6927158	6.43273029	-9.2047396	2.84E-05	0.00020482
63	HLA-DQB1	1.91405058	5.78906684	9.13324655	3.00E-05	0.0002125
64	PNMA1	1.66406774	8.07043	9.0443154	3.20E-05	0.00022063
65	PVR	-1.8760068	7.35883499	-9.0408862	3.21E-05	0.00022063
66	CCL28	-2.3663594	8.14283439	-8.9809395	3.36E-05	0.00022407
67	RUNX3	-1.9868343	4.09869652	-8.9659859	3.39E-05	0.00022407
68	CXCL8	1.8643379	14.5977771	8.96022408	3.41E-05	0.00022407
69	PDGFC	-2.3625977	6.64387599	-8.8888099	3.60E-05	0.00023307
70	AXL	-1.9101428	6.73565895	-8.8067956	3.83E-05	0.00024456

71	FOS	1.83533203	8.87558263	8.7664283	3.95E-05	0.00024652
72	ULBP2	-2.5916177	6.51286376	-8.7596234	3.97E-05	0.00024652
73	IFITM2	2.04334113	8.56299164	8.72260487	4.09E-05	0.00025017
74	BLNK	2.17405465	4.80096442	8.65081656	4.32E-05	0.00025566
75	MAPK3	1.48380997	8.75774569	8.64805827	4.33E-05	0.00025566
76	CNOT10	1.39470723	8.15549591	8.64252129	4.35E-05	0.00025566
77	SLAMF7	-1.6852245	4.38526909	-8.6181187	4.43E-05	0.00025718
78	IL1B	-4.0118905	8.0319027	-8.4969677	4.87E-05	0.00027916
79	TTK	3.13861439	4.77348579	8.44440942	5.08E-05	0.00028732
80	CASP3	1.28334601	9.72688765	8.42226925	5.17E-05	0.00028876
81	ANXA1	1.68428788	14.2935214	8.38093884	5.34E-05	0.00029473
82	IRF5	1.80897059	5.69930203	8.3463906	5.49E-05	0.00029928
83	HLA-DRB4	1.74370826	6.7163015	8.30136486	5.69E-05	0.00030654
84	IGF2R	-1.5208454	7.24472017	-8.2460645	5.95E-05	0.0003167
85	CFD	3.20265692	4.79791788	8.08044936	6.81E-05	0.00035713
86	HLA-DMB	2.29863994	6.8157884	8.06986335	6.87E-05	0.00035713
87	HLA-DMA	2.48619806	6.70521874	7.98852986	7.35E-05	0.00037756
88	IFIT2	-1.9596443	5.89016414	-7.929745	7.72E-05	0.00039199
89	CCL17	2.15361854	4.56705405	7.85862773	8.19E-05	0.00041137
90	CXCL11	-2.4634386	4.92708259	-7.8381921	8.33E-05	0.00041386
91	HLA-DPB1	1.6583895	6.65605312	7.79262581	8.66E-05	0.00042275
92	NFATC2	2.17066457	4.75467629	7.78701374	8.70E-05	0.00042275
93	IL6R	1.90285252	5.63542398	7.68016915	9.53E-05	0.00045805
94	UBC	1.17526361	14.8972411	7.58904637	0.00010307	0.00049015
95	VEGFA	2.35816085	10.3951424	7.54322941	0.00010725	0.00050464
96	RPS6	1.25843178	14.0353664	7.52137198	0.00010931	0.00050543
97	CD274	-2.9155298	4.83337163	-7.5174962	0.00010968	0.00050543
98	TNFRSF10C	-1.7163964	6.60686466	-7.4853369	0.0001128	0.00051451
99	IL1R2	2.98956013	3.80563349	7.47242254	0.00011408	0.0005151
100	F2RL1	-1.3692354	8.22535331	-7.4266086	0.00011876	0.00053087
101	TAP2	-1.239874	7.64389216	-7.4024598	0.00012132	0.00053692
102	ST6GAL1	1.82788582	9.5766261	7.36827735	0.00012504	0.00054796
103	TNFSF14	-3.2835545	3.71723311	-7.322025	0.00013028	0.00056538
104	FYN	-1.427281	5.48747114	-7.2400955	0.00014017	0.00060248
105	STAT6	1.13438398	8.7486708	7.22554507	0.00014202	0.00060459
106	CCR3	1.46667292	4.81982219	7.20109777	0.00014518	0.00060891
107	INPP5D	-1.6294801	7.18735907	-7.1966885	0.00014576	0.00060891
108	FUT7	1.65694639	5.50218683	7.11470285	0.000157	0.00064979
109	HLA-DQA1	1.66620291	6.4982689	7.09450845	0.00015991	0.00065578

110	CD97	1.33041394	9.54137451	7.03086609	0.0001695	0.00068879
111	LYN	1.74185632	7.94325318	7.02057803	0.00017111	0.00068907
112	ITGB1	-1.1421213	12.2415914	-6.9726415	0.00017884	0.00071377
113	PLA2G6	1.36283605	5.39008558	6.87394848	0.00019602	0.00077541
114	REL	1.40263075	6.76148	6.73833121	0.00022272	0.0008718
115	SMPD3	3.13278598	3.97711893	6.73093237	0.00022429	0.0008718
116	CFB	-1.2726754	11.3772408	-6.7103157	0.00022873	0.00088139
117	CXCL10	-2.9707743	4.37107843	-6.6839906	0.00023454	0.00089606
118	PPBP	-3.9701948	3.92646076	-6.6188919	0.00024963	0.00094564
119	ISG15	-1.4727324	7.31279934	-6.5862989	0.00025759	0.0009676
120	IKBKG	-1.0166741	6.07793415	-6.5469498	0.00026759	0.00098993
121	EPCAM	1.18270228	9.44528389	6.5391848	0.00026961	0.00098993
122	C1S	-1.8793452	5.63612068	-6.5370019	0.00027018	0.00098993
123	CD38	1.40871919	5.78148687	6.39916733	0.00030918	0.00110782
124	TUBB	-1.0754493	9.83625931	-6.3892792	0.00031221	0.00110782
125	FN1	-7.2144928	10.1146807	-6.3867094	0.000313	0.00110782
126	CSF2	-3.8458134	4.0165175	-6.3865966	0.00031304	0.00110782
127	LIF	-2.7913833	7.68740515	-6.3810691	0.00031475	0.00110782
128	ITGA1	-3.8260776	5.30175162	-6.3450829	0.00032617	0.00113903
129	HPRT1	1.23625852	8.03180421	6.29593278	0.00034251	0.00118684
130	ICAM1	-1.4250311	9.75013312	-6.2710583	0.00035113	0.00120734
131	ITGB3	-2.1622321	5.7912867	-6.2469882	0.0003597	0.00122737
132	CCL14	2.34104393	3.98448557	6.18195134	0.00038405	0.00130053
133	ALAS1	1.19662434	8.01384149	6.08853107	0.0004223	0.00141932
134	CD3EAP	-1.6258942	4.8707868	-6.0411907	0.00044329	0.00147875
135	ALCAM	0.9966213	10.9863527	5.99693427	0.00046397	0.00153068
136	MYD88	-0.9408786	8.0947153	-5.9920905	0.0004663	0.00153068
137	LAMP3	1.40674069	5.81506203	5.98575189	0.00046937	0.00153068
138	SDHA	1.09399492	7.95626708	5.97920597	0.00047256	0.00153068
139	BIRC5	1.72064448	4.85761937	5.96275215	0.00048068	0.00154579
140	CCL20	1.79972679	11.9137909	5.94652158	0.00048885	0.00156083
141	PRKCD	1.08104153	7.77320595	5.92071912	0.00050215	0.00159194
142	TAP1	-0.9818088	6.92713521	-5.8623783	0.00053375	0.00166739
143	PIN1	1.3694009	8.10171766	5.8593479	0.00053545	0.00166739
144	NOTCH1	-1.5932193	6.60052253	-5.8563294	0.00053715	0.00166739
145	IL1RL1	-1.7701812	5.953072	-5.8340407	0.00054989	0.00169516
146	TNFRSF12A	-1.242782	8.43498934	-5.8134922	0.00056193	0.00171296
147	IRF1	0.96875744	7.69933141	5.81114526	0.00056332	0.00171296
148	IL18	-0.865874	8.56699651	-5.7949469	0.00057305	0.00173062

149	SYK	0.93645485	7.0950374	5.78249224	0.00058065	0.00173062
150	CYFIP2	1.15324693	5.2775834	5.78234152	0.00058075	0.00173062
151	C4B	1.94782542	5.3918407	5.76830151	0.00058946	0.00174494
152	STAT2	-0.8280825	8.40027923	-5.729137	0.00061453	0.0018072
153	CKLF	-0.9739711	8.63673628	-5.6501813	0.00066876	0.00195383
154	TP53	-0.89534	8.2475802	-5.6348991	0.00067986	0.00196492
155	ITGA4	-2.4947084	4.2578274	-5.6328735	0.00068135	0.00196492
156	PDCD1LG2	-4.4704421	3.09625433	-5.6028745	0.00070379	0.00201663
157	TREM1	0.9320258	4.84827665	5.55850812	0.0007385	0.00210261
158	ECSIT	0.85495687	6.98512186	5.55115914	0.00074443	0.00210608
159	FCF1	1.1136413	9.44676023	5.52821604	0.00076329	0.00214426
160	IL6	-2.4944955	5.76028926	-5.5231549	0.00076752	0.00214426
161	IFI27	-1.7361384	9.79016437	-5.4456922	0.00083564	0.00232006
162	TNFRSF10B	-1.0401442	7.94302429	-5.4250381	0.00085491	0.00235893
163	TXNIP	-1.1339157	9.55722049	-5.2440016	0.00104663	0.00284622
164	IRF7	0.90574104	6.36231261	5.24382978	0.00104684	0.00284622
165	IL6ST	-0.9972808	9.466299	-5.2406388	0.00105062	0.00284622
166	LCN2	-1.0011042	13.5200177	-5.1923711	0.00110971	0.00298818
167	IL17RA	-0.8916225	6.08043536	-5.1585762	0.00115326	0.00308688
168	C4BPA	2.52284868	4.15545657	5.06610869	0.00128241	0.00341213
169	LAMP1	-0.7917591	10.3628209	-4.9554216	0.00145845	0.0038432
170	TFRC	0.8460526	9.43067287	4.9535671	0.00146162	0.0038432
171	ZNF143	0.90172342	7.73573306	4.93465742	0.00149436	0.00389669
172	PSMB10	1.43566682	8.40143703	4.93178779	0.0014994	0.00389669
173	ATG5	0.81309586	8.48278623	4.84630859	0.00165843	0.00428509
174	IL2RG	1.10581389	4.75919748	4.82510306	0.00170071	0.00436906
175	ETS1	-1.0201285	8.67984097	-4.8090179	0.00173356	0.00442802
176	IL1A	-1.3949356	9.57381982	-4.7980751	0.00175632	0.00446064
177	BAX	-0.7002691	9.14614906	-4.7876143	0.00177837	0.00449115
178	PRPF38A	0.75808924	8.14179039	4.76299676	0.0018315	0.00459932
179	TLR2	-1.1329579	7.85830249	-4.6595615	0.00207459	0.00518068
180	IFNAR2	0.7283278	8.47667687	4.62724969	0.00215764	0.00535814
181	PRKCE	0.93903948	4.78264772	4.58474958	0.00227249	0.00561217
182	BCL2L1	0.77566384	10.7528001	4.57587477	0.00229731	0.0056423
183	C2	1.04174822	5.70134007	4.56400091	0.00233099	0.00569372
184	CD55	1.31422652	4.53432537	4.55704681	0.00235096	0.0057113
185	TOLLIP	-0.7804515	8.29652981	-4.5490354	0.0023742	0.00573659
186	TNFRSF11A	1.57527245	5.55318593	4.52836951	0.00243533	0.00585266
187	SOCS1	-1.1392336	4.24950155	-4.5187923	0.00246425	0.00589048

188	GPI	0.93454305	9.23543972	4.47658595	0.00259623	0.00617296
189	LAMP2	-0.6895552	8.38748194	-4.412946	0.00281013	0.00664352
190	CFI	0.76073174	8.68887614	4.40904255	0.00282387	0.00664352
191	HLA-DOB	-1.0281661	4.59202514	-4.4006687	0.00285358	0.00667827
192	IFITM1	0.97731126	10.5567994	4.39588865	0.00287069	0.00668333
193	APP	-0.7566278	11.9828304	-4.340335	0.00307805	0.00712896
194	EBI3	-1.7632224	3.03431973	-4.2997618	0.00323984	0.00746499
195	OAS3	-1.3498643	6.18710821	-4.2779644	0.00333058	0.00763471
196	RIPK2	-0.6748318	7.14714542	-4.2535875	0.00343536	0.00783472
197	CD8A	-1.1253141	4.94315959	-4.2254883	0.00356062	0.00803078
198	TNFRSF1A	-0.7110377	9.31379308	-4.2223936	0.00357472	0.00803078
199	PPIA	-0.6667796	7.48189837	-4.2222839	0.00357522	0.00803078
200	CD164	0.78680592	11.0266367	4.20829095	0.00363975	0.00813483
201	CEBPB	0.76585934	10.7136522	4.19988962	0.00367909	0.00818187
202	PTGS2	-1.4521404	9.36071459	-4.1821548	0.00376369	0.00832857
203	ATF1	0.8230818	7.6000251	4.16701396	0.0038376	0.00842526
204	TREM2	-1.5357023	3.93072187	-4.1639456	0.00385276	0.00842526
205	TNF	-2.6502994	4.25512197	-4.1616949	0.00386393	0.00842526
206	IL23A	1.41633013	5.72119604	4.12153889	0.00406924	0.00882986
207	AMMECR1L	-0.8755408	7.36337761	-4.1126872	0.00411608	0.00888835
208	IL18R1	-1.0189276	4.73518627	-4.1074888	0.00414386	0.00890532
209	IFNGR1	-0.6951754	10.5441184	-4.0085652	0.00471338	0.01008076
210	LRP1	-1.5255878	6.66539005	-3.979887	0.004894	0.01041724
211	IL34	-0.9484004	3.91638984	-3.9681681	0.00496997	0.01052879
212	HLA-E	0.57223438	10.0031562	3.93456614	0.00519497	0.01095355
213	IL1R1	-0.8810458	7.50229743	-3.8857431	0.00554184	0.01162047
214	REPS1	0.83227934	9.02599948	3.88283677	0.00556327	0.01162047
215	NOD2	0.69368255	6.03377378	3.87285459	0.00563754	0.01172085
216	TNFRSF14	0.68489287	7.79530284	3.86693038	0.00568213	0.01175886
217	LTBR	-0.799034	8.96750679	-3.8604471	0.00573137	0.01180609
218	IKBKE	-0.7189894	7.43381435	-3.8176722	0.00606803	0.01244225
219	ITGA5	-1.2403207	8.92493303	-3.8086741	0.00614155	0.012479
220	POLR2A	-0.6883828	8.53320886	-3.8086442	0.00614179	0.012479
221	BST2	0.71299782	6.71379981	3.75404993	0.00660901	0.01336756
222	S100A7	-1.5863293	6.66612675	-3.6915793	0.00719127	0.01447972
223	CXCL14	2.2374467	4.40242314	3.68591793	0.00724671	0.01452592
224	MX1	-0.6120037	8.54871961	-3.6619511	0.00748658	0.01493973
225	DMBT1	2.01220274	4.49497391	3.6502311	0.00760698	0.01511253
226	CREB5	-1.2771861	4.85318076	-3.6202637	0.00792444	0.01567356

227	IL11	-1.140949	4.47313589	-3.499625	0.0093544	0.01842034
228	ERCC3	0.84726456	7.15040133	3.45780121	0.00991295	0.0194346
229	CXCL1	0.74385108	13.8183495	3.45174823	0.00999671	0.01945743
230	TCF7	0.88893613	6.32490688	3.45067392	0.01001165	0.01945743
231	JAK3	-0.7007398	4.03391824	-3.4057033	0.01065922	0.02062629
232	MICA	-0.7529527	5.97036691	-3.3502934	0.01151941	0.02219472
233	CD36	-1.1464355	4.96193031	-3.341813	0.01165748	0.02236435
234	CYLD	-0.7730032	8.44031219	-3.3040495	0.01229413	0.02348493
235	PSMB9	0.67269941	8.50633889	3.29527905	0.01244723	0.02367622
236	CXCL3	-0.7844273	9.68164049	-3.2625553	0.01303669	0.02469237
237	SF3A3	-0.5366615	7.48623569	-3.2338137	0.01357897	0.02561096
238	CXCR1	1.20181821	4.88682404	3.22613845	0.01372781	0.02569772
239	TMUB2	-0.5724277	6.99659977	-3.2255166	0.01373994	0.02569772
240	NFATC1	1.00507069	5.52725541	3.21999931	0.01384811	0.0257921
241	ICAM4	0.64007597	5.50174479	3.20667132	0.01411316	0.02616055
242	CARD11	-0.9370703	5.93397337	-3.2038487	0.01416998	0.02616055
243	ITGB2	0.79222897	5.53307798	3.20129934	0.01422151	0.02616055
244	LCP1	-0.9085976	4.36178929	-3.1945008	0.0143599	0.02630687
245	IFNL1	1.14858969	4.94454492	3.13030325	0.01573952	0.02865227
246	MAF	-0.7725887	6.91710978	-3.1290255	0.01576836	0.02865227
247	EGR1	-1.2136418	5.57561555	-3.1222831	0.01592151	0.02874373
248	TAPBP	-0.5935387	9.62238652	-3.1211542	0.0159473	0.02874373
249	PLAU	-0.9876726	12.05267	-3.1172635	0.01603655	0.0287885
250	EP300	-0.7809329	7.88416379	-3.1094934	0.01621636	0.02899486
251	CDH1	-0.5391207	11.5865634	-3.0721561	0.01711069	0.03044639
252	HLA-B	-0.4726275	11.8346921	-3.0699797	0.01716441	0.03044639
253	TLR4	-1.5847796	4.14529479	-3.066092	0.01726081	0.03049637
254	TICAM2	-0.9040445	4.89062528	-3.0434285	0.01783426	0.03138549
255	DUSP4	-0.6310664	8.78464841	-3.0382008	0.01796937	0.03149925
256	TRIM39	0.54968884	5.71134917	3.02140475	0.01841084	0.03214705
257	RAG1	-1.6316789	3.7359914	-3.0149347	0.01858394	0.03231061
258	PYCARD	0.72266476	6.4972952	3.01251652	0.01864908	0.03231061
259	NUP107	0.51831685	7.81233908	2.93762034	0.0207904	0.03588151
260	MAP2K1	0.58902787	9.54482319	2.88241312	0.02253356	0.03874039
261	MST1R	0.44962871	7.35071898	2.86606483	0.02307869	0.03952557
262	FLT3LG	0.77212078	4.14926868	2.86192785	0.02321882	0.03961378
263	CD24	0.52411925	12.6289585	2.83885658	0.02401679	0.04081941
264	ATG7	0.43099845	7.11679014	2.82197573	0.0246188	0.04168411
265	IL1RN	1.1194677	8.76007077	2.8188944	0.02473038	0.04171503

266	PSMB8	0.54714264	9.98667536	2.81489709	0.02487592	0.04174423
267	MAP2K2	-0.4227603	9.94290872	-2.8132959	0.02493447	0.04174423
268	ENG	-2.2750366	3.38916584	-2.8071066	0.02516215	0.04196821
269	THBD	-1.3987143	7.06868854	-2.803815	0.02528411	0.04201486
270	APOE	-3.095447	3.89089208	-2.7900315	0.02580158	0.04271596
271	CDKN1A	-0.5020514	10.3696341	-2.7750301	0.02637736	0.04340923
272	DHX16	0.49966029	7.14161863	2.77407256	0.02641457	0.04340923
273	SERPING1	-0.6980886	6.43839817	-2.7606725	0.02694099	0.04411217
274	ABL1	-0.6476722	7.10092933	-2.6463659	0.03190043	0.05204194
275	HMGB1	0.54616466	9.97699036	2.636933	0.03234992	0.05258332
276	TGFB1	-0.6755	8.10213444	-2.6213117	0.03310875	0.05362177
277	SMAD2	0.42150521	9.19539833	2.60700796	0.03381972	0.0545755
278	USP39	0.43389843	7.43607994	2.54451868	0.03711544	0.05967842
279	MIF	0.68695216	10.974079	2.52342113	0.03830138	0.06136458
280	GPATCH3	0.65532247	6.13796569	2.51063335	0.0390391	0.06232313
281	SBNO2	0.59098071	7.98100487	2.47370991	0.04125207	0.06562161
282	STAT1	-0.4852358	8.82360229	-2.4633889	0.04189334	0.0664054
283	TNFSF10	-0.3825809	11.2162004	-2.4539603	0.04248807	0.06711013
284	JAK1	-0.587534	8.87283453	-2.402573	0.04588445	0.07221954
285	MICB	-0.5038537	4.9129001	-2.3687882	0.04826697	0.07570293
286	IRF3	0.49740046	5.96321051	2.35776821	0.04907099	0.07669487